

SPELEOCHRONOLOGY AND LATE PLEISTOCENE CLIMATES
INFERRED FROM
O, C, H, U AND TH ISOTOPIC ABUNDANCES IN SPELEOTHEMS

By
PETER THOMPSON, B.Sc.

A Thesis
Submitted to the School of Graduate Studies
in Partial Fulfilment of the Requirements
for the Degree
Doctor of Philosophy

McMaster University
May 1973

© Peter Thompson 1973

DOCTOR OF PHILOSOPHY (1973)
(Geochemistry)

McMASTER UNIVERSITY
(Hamilton)

TITLE: Speleochronology and Late Pleistocene Climates Inferred
O, C, H, U and Th Isotopic Abundances in Speleothems.

AUTHOR: Peter Thompson, B. Sc. (University of Bradford, England)

SUPERVISORS: Professor D.C. Ford and Professor H.P. Schwarcz

NUMBER OF PAGES: xv, 352

SCOPE AND CONTENTS:

A karst area in the S.E. part of West Virginia was chosen to assess the usefulness of speleothems, the calcareous stalagmite and stalactite deposits found in caves, for dating by the methods of Uranium Series Disequilibrium. The criteria for accurate age analysis are discussed and the suitability of these deposits is noted. Analyses of speleothems from four different karst areas are used to demonstrate the general applicability of the Th²³⁰/U²³⁴ dating method.

An attempt is made to reconstruct Late Pleistocene climate changes by measuring variations in the ratio of O¹⁸/O¹⁶ and C¹³/C¹² in the CaCO₃. Equilibrium fractionation of the oxygen isotopes between water and calcite, a pre-requisite for paleoclimate analysis, is demonstrated. Variations in the oxygen isotope ratio in West Virginia speleothems are interpreted in terms of regional temperature changes. The problems of interpretation are discussed in detail. The D/H ratio of fluid inclusions trapped within the speleothems is used to help with this interpretation and to calculate approximate temperatures of deposition.

The inferred Late Pleistocene climate changes are compared with other published paleoclimate data, derived mostly from the study of deep-sea sediments and raised coral reefs.

ABSTRACT

The $\text{Th}^{230}/\text{U}^{234}$ and $\text{U}^{234}/\text{U}^{238}$ ratios of speleothems (calcareous deposits) from caves developed in limestones of the Greenbrier Series, S.E. West Virginia, was measured by alpha-particle spectrometry to assess the deficient Th^{230} (ionium) and excess U^{234} dating methods respectively. Pure, non-porous, very coarsely crystalline deposits showing no signs of submersion or re-resolution were found to be suitable for $\text{Th}^{230}/\text{U}^{234}$ dating. This method was used to date deposits between about 2000 and 300,000 years old. The decay of excess U^{234} , which in principle can be used to date deposits 50,000 to 1,500,000 years old, could not be used as a routine method because the initial excess of U^{234} could not be reliably determined. Concordant $\text{Pa}^{231}/\text{Th}^{230}$ and $\text{Th}^{230}/\text{U}^{234}$ ages were measured for two samples from West Virginia.

Norman-Bone Cave and Grapevine Cave, both in Greenbrier Co., were studied in detail. Norman-Bone Cave contains speleothems at least 300,000 years old. Based on the decay of U^{234} , one stalagmite appeared to have been deposited between about 760,000 years and 1,250,000 years B.P. Speleothem ages from caves in the Crowsnest Pass area of Alberta, the Nahanni region of the North West Territories and the Ciudad Valles area of Mexico were also obtained. With the exception of the single Mexican sample, deposition appears to stop during prolonged periods of cold climate; therefore a continuous record of CaCO_3 deposition is not preserved in the northern caves. Based on the gaps in the record, the coldest periods of the Wisconsin, Illinoian and Kansan (?) glacial ages occur between 20-35,000, 135-160,000 and 240-270,000 years B.P. respectively. The inter-

vening periods are times of cool to warm, moist climate which favour speleothem deposition.

The ratio O^{18}/O^{16} (δ_{ct}^O) and C^{13}/C^{12} (δ_{ct}^C) in young and fossil speleothems deposited in isotopic equilibrium with parent waters was measured in an attempt to construct detailed climate curves for the Late Pleistocene. Five young speleothems all appeared to be deposited in isotopic equilibrium: an isotopic temperature of $8.6 \pm 1.6^\circ C$ was calculated, $2.3^\circ C$ lower than the present mean annual surface air temperature. The discrepancy could be real, for cave temperatures are often slightly lower than mean annual surface air temperatures.

Variations in δ_{ct}^O and δ_{ct}^C in two dated stalagmites from Norman-Bone Cave (NB4 and NB10) and a flowstone deposit from Grapevine Cave (GV2) are commonly uncorrelated within individual depositional layers, satisfying Hendy's criteria for $CaCO_3$ deposition in oxygen isotopic equilibrium with water. Parts of NB4 and GV2, which were deposited contemporaneously about 100,000 years ago record the same temperature maximum.

Cyclic secular variations in δ_{ct}^O cannot be interpreted in terms of climate change without knowledge of variations in δ_w^O of waters depositing the $CaCO_3$. An attempt was made to measure these variations directly by extracting water from fluid inclusions in the fossil deposits. The D/H (δ_i^D) ratio of the water was measured and the Craig-Dansgaard relationship ($\delta_i^D = 8\delta_i^O + 10$) applied to calculate δ_i^O ($\equiv \delta_w^O$). Absolute temperatures calculated from δ_w^O and δ_{ct}^O are, in general too low but with further refinements the method may become a valuable tool for paleoclimatologists.

In general, δ_{ct}^O is found to increase in calcite deposited at lower

temperatures. This is attributed to the deposition of CaCO_3 from waters of relatively constant isotopic composition, so that changes in $\delta_{\text{ct}}^{\text{O}}$ are determined by the effect of temperature on the $\text{CaCO}_3\text{-H}_2\text{O}$ fractionation factor. (0.24^o/oo increase per 1^oC temperature drop).

The relative constancy of $\delta_{\text{w}}^{\text{O}}$ values of cave drip-waters is attributed to seasonal CaCO_3 deposition from waters whose isotopic composition is biased toward mean summer values. As mean annual temperatures decrease, CaCO_3 deposition is from waters which are progressively biased in isotopic composition toward the mean July value.

Temperature maxima are recorded in GV2 at 80,000±3000 years B.P. and 100,000±4000 years B.P.; a lower maximum is recorded at 60,000±3000 years B.P. Temperature maxima in NB10 are recorded at 163,000±6800, 170,000±7000 and 180,000±9700 years B.P. An intensely cold period is recorded between 180,000 and 170,000 years B.P. which was inferred to be colder than any event recorded in GV2 between 100,000 and 60,000 years B.P.

$\delta_{\text{ct}}^{\text{C}}$ also increases as regional temperatures decrease, probably as a result of the decreased rate of plant respiration, microbial activity and CO_2 production in the soil during cold periods. The $\delta_{\text{ct}}^{\text{C}}$ variations are not well enough defined to be used as a reliable indicator of climate change.

Good correlation is observed with the time-temperature curve for Wisconsin glaciation and the Sangamon interglacial, as obtained from deep-sea cores and raised coral reefs. Correlation with the penultimate (Illinoian) glaciation and preceding (Yarmouth) interglacial is unclear.

ACKNOWLEDGEMENTS

I would like to thank my supervisors Derek C. Ford and Henry P. Schwarcz for their productive suggestions and continuous support and encouragement throughout the preparation of this thesis. Their faith in speleothem research remained intact despite countless technical and interpretive problems.

On numerous occasions members of the McMaster University Caving and Climbing Club helped collect samples within the caves. Their help is gratefully acknowledged.

I am also indebted to Dr. James O'Neil of the U.S.G.S. at Menlo Park, California for the D/H ratio measurements. Julian Coward helped write and correct the computer program, U DATE II.

Finally, my sincere thanks to Linda Hastie who contributed in many ways to the success of this project, and who undertook the monumental task of typing the final manuscript..

LIST OF CONTENTS

	Page
ABSTRACT	iii
LIST OF CONTENTS	vii
LIST OF FIGURES	xi
LIST OF TABLES	xiv
CHAPTER ONE PROBLEMS OF THE PLEISTOCENE TIME SCALE	
1.1 Introduction	1
1.2 Radiometric Methods of Dating the Quaternary	6
1.2.1 The Potassium-Argon and Fission Track Dating Methods	8
1.2.2 He-U Method of Dating	9
1.2.3 C-14 Dating of Carbonates	10
1.3 The Mechanism of Speleothem Deposition	12
1.4 The Time Scale of the Quaternary Period	15
1.5 Statement of Thesis Objective	18
1.6 Field Areas and Sampling Programme	19
CHAPTER TWO DATING METHODS BASED ON URANIUM SERIES DISEQUILIBRIUM	
2.1 Methods of Dating Carbonates Using Uranium Series Disequilibrium	23
2.1.1 The U-234/U-238 Method (Excess Uranium Method)	23
2.1.2 Th-230/U-234 Method (Deficient Thorium Method)	27
2.1.3 The Pa-231/U-235 Method	31
2.2 The Excess Pa-231/Th-230 Method	35
2.3 Requirements for Reliable Age Determinations	37
2.4 Review of Some Results Obtained with Uranium-Series Disequilibrium Dating	39
2.4.1 Uranium Series Dating of Speleothems	50
CHAPTER THREE DESCRIPTION OF THE PRINCIPAL FIELD AREA, GREENBRIER COUNTY, WEST VIRGINIA	
3.1 The Local Stratigraphy	54
3.2 Description of the Caves Studied	57
3.2.1 The Norman-Bone Cave	60
3.2.2 Grapevine Cave	63
3.2.3 Upper Hughes Cave	67
3.2.4 Overholts Blowing Cave	67
3.3 West Virginia Climate	69
3.4 Relation Between Surface Air Temperature and Cave Temperature	73

	Page	
CHAPTER FOUR THE STABLE ISOTOPIC GEOCHEMISTRY OF SPELEOTHEMS AND		
PALEOTEMPERATURE ANALYSIS		
4.1	Introduction	76
4.2	Isotopic Fractionation in the System $\text{CaCO}_3\text{-CO}_2\text{-H}_2\text{O}$	77
4.3	The Requirements for Paleotemperature Analysis of Speleothems	81
4.4	Factors affecting the Isotopic Composition of Speleothems	85
4.5	Paleotemperature Analysis: Principles	88
4.5.1	Equilibrium Versus Kinetic Fractionation	88
4.5.2	Climate Data from the Isotopic Composition of Speleothems	92
4.6	Previous Work Related to the Isotopic Analysis of Speleothems	93
4.7	Analytical Techniques	
4.7.1	Sampling and Preparation of CO_2 for Mass Spectrometric Analysis	97
4.7.2	Mass Spectrometric Analysis	98
4.7.3	Isotopic Analysis of Water	99
4.7.4	Accuracy and Precision of Mass Spectrometric Analyses	102
4.8	The Case for Equilibrium Deposition in West Virginia	104
4.9	The Isotopic Composition of Meteoric Precipitation	110
4.9.1	Isotopic Composition of W. Va. Precipitation	111
4.10	Effects of Post-Depositional Exchange	114
4.11	Fluid Inclusions in Speleothems and their Applications to Paleotemperature Analysis	115
4.11.1	Principles	115
4.11.2	Notation	115
4.11.3	Extraction and Analysis of Fluid Inclusions	116
4.11.4	Accuracy and Precision	118
4.11.5	The $\delta_w^D - \delta_w^O$ Relationship	120
4.11.6	The $\delta_w^D - \delta_w^O$ Relationship in West Virginia Precipitation and Cave Waters	121
4.11.7	δ_w^D and δ_{ct}^O in Recent Speleothems and Fluid Inclusions	124
4.11.8.	δ_i^D and Temperature of Deposition of Fossil Speleothems	127
4.11.9	The Ability of Speleothems to Retain Fluid Inclusions	137
CHAPTER FIVE RADIOCHEMICAL ANALYTICAL TECHNIQUES		
5.1	Sample Preparation	145
5.2	Analytical Considerations	146
5.2.1	Separation of Thorium from Uranium	147

	Page
5.2.2 Separation of Radium-226 from Uranium and Thorium	148
5.2.3 Separation of Uranium and Thorium from Protactinium	148
5.2.4 Separation of Thorium from Bismuth and Polonium	149
5.2.5 Separation of Uranium from Bismuth and Polonium	149
5.3 Reagents and Reagent Purity	150
5.4 Spike Preparations	
5.4.1 U-232/Th-228 Spike Preparation and Calibration	153
5.4.2 Th-227/U-232 Spike Preparation and Calibration	154
5.5 Preparation and Use of Ion Exchange Columns	158
5.6 Experimental Procedures	160
5.6.1 Carbonate Analysis	162
5.6.2 Water Analysis	164
5.6.3 Laboratory Processing of Fe(OH) ₃ Precipitates	166
5.7 Calculation of Isotope Ratios	166
5.8 Measurement of Uranium Concentrations	169
5.9 Alternative Spiking Procedures	171
5.10 Precision, Accuracy and Sensitivity of the Th-230/U-234 Dating Method	
5.10.1 Precision and Accuracy	171
5.10.2 Sensitivity	174
5.11 Counting Equipment	175
5.12 Data Processing	177
5.13 Leaching Experiments	178
 CHAPTER SIX RESULTS FROM WEST VIRGINIA	
6.1 The Norman-Bone Cave	181
6.1.1 Stalagmites NB1 and NB10 - Two Fossil Deposits from Norman-Bone Cave	181
6.1.2 NB2 and NB11 - Examples of Recent Deposits	195
6.1.3 NB3 and NB12 - Fossil Deposits from Bone Cave	202
6.1.4 Stalagmite NB4 - Analysis of a Drill-core from the Butterscotch Room	207
6.1.5 Stalagmites NB5 and NB9 - Two Neighbouring Deposits from the Butterscotch Room	216
6.2 Grapevine Cave	
6.2.1 GV1- An Ultra Pure Flowstone Sample	219
6.2.2 GVC-1 - Analysis of a Drill Core from Grapevine Cave	221
6.2.3 GV2 - A Layered Flowstone Deposit	223
6.3 Correlation Between the Isotope Records of NB4 and GV2	233
6.4 Results of the Water Sampling Program	235
6.5 Summary	238
 CHAPTER SEVEN APPLICATION OF THE TH ²³⁰ /U ²³⁴ DATING METHOD TO SPELEOTHEMS FROM OTHER KARST AREAS	
7.1 The Crowsnest Pass Area	243
7.1.1 Description of the Samples	244
7.1.1.1 Coulthard Cave Stalagmite	244

	Page
7.1.1.2 Middle Sentry Cave Flowstone	247
7.1.1.3 Eagle Cave Flowstone	247
7.1.1.4 Yorkshire Pot Samples	247
7.1.1.5 Gargantua Cave Samples	248
7.1.2 Results	248
7.2 The Nahanni Region, N.W.T.	252
7.3 Periods of Speleothem Deposition in the Canadian Rockies and N.W.T.	256
7.4 The Ciudad Valles Area, San Luis Potosi, Mexico	259
7.4.1 Tinaja Stalagmite, MT1	259
CHAPTER EIGHT DISCUSSION OF THE EXPERIMENTAL RESULTS	
8.1 Appraisal of the Dating Methods	263
8.1.1 Appraisal of the $\text{Th}^{230}/\text{U}^{234}$ Method	263
8.1.2 Appraisal of the $\text{U}^{234}/\text{U}^{238}$ Method	265
8.1.3 Appraisal of the $\text{Th}^{227}/\text{Th}^{230}$ ($\text{Pa}^{231}/\text{Th}^{230}$) Method	268
8.2 Relation between Uranium Concentrations and Initial $\text{U}^{234}/\text{U}^{238}$ Ratios in Speleothems	270
8.3 Anomalous Results	271
8.4 Criteria for Reliable Speleothem Ages	274
8.5 Speleothem Deposition as an Indicator of Paleoclimate	275
8.6 Interpretation of the Oxygen Isotopic Composition of West Virginia Speleothems	279
8.6.1 Oxygen Isotopic Variations in Grapevine Flowstone, GV2	286
8.6.2 Oxygen Isotopic Variations in Norman-Bone Cave Speleothems	288
8.7 Carbon Isotopic Variations in West Virginia Speleothems	294
8.8 The Late Pleistocene Climate Record Inferred from Phases of Speleothem Deposition and Oxygen Isotopic Abundances	298
8.9 Comparison of the Speleothem Record with other Isotopic Records	304
8.9.1 The Aven d'Orgnac Stalagmites of Southern France	304
8.9.2 The Isotopic Record in Deep-Sea Sediments	308
8.9.3 The Isotopic Record in the Greenland Ice	314
8.10 Considerations for Future Research	315
8.10.1 Geomorphic Rates from Speleothem Age-Data	317
REFERENCES	318
APPENDIX I	336
APPENDIX II	341

LIST OF FIGURES

		Page
2.1	Uranium and Thorium Decay Series	24
2.2	Alpha particle energies of isotopes in the uranium and thorium decay series	25
2.3	Graphical representation of the growth of Th^{230} towards equilibrium with U^{234} in a closed system	29
2.4	Graphical representation of the changing $\text{Pa}^{231}/\text{Th}^{230}$ ratio in a closed system	34
3.1	Generalized stratigraphic section of the Greenbrier Limestone series	55
3.2	Sketch map of the principal field area in West Virginia	59
3.3	Line diagram of Norman-Bone Cave, Greenbrier County, showing the sampling sites	61
3.4	Sampling sites in Grapevine Cave, Greenbrier County	66
3.5	Map of Upper Hughes Cave, Pocahontas County, showing sampling sites	68
4.1	Variations in $\delta_{\text{ct}}^{\text{O}}$ and $\delta_{\text{ct}}^{\text{C}}$ along growth layers in stalagmites NB10, NB11 and flowstone GV2	106
4.2	Variations in the isotopic composition of West Virginia meteoric precipitation with temperature	112
4.3	Exploded view of the apparatus used for extracting fluid inclusions	117
4.4	Relationship between $\delta_{\text{W}}^{\text{D}}$ and $\delta_{\text{W}}^{\text{O}}$ in West Virginia Cave waters and one sample of snow	123
4.5	Location of samples removed from stalagmite NB10 for fluid inclusion extraction and analysis	128
4.6	Sectioning and location of samples for stable isotopic analysis in the Grapevine flowstone GV2	131
4.7	The relationship between $\delta_{\text{i}}^{\text{D}}$ and the calculated isotopic temperature of deposition of recent and fossil speleothems	134
4.8	Location of samples removed from Grapevine Cave flowstone GV2 and heated under vacuum to measure water retention characteristics. (The location of samples removed for fluid inclusion analysis and isotopic temperature calculations is also shown on the extreme right of the figure).	139

	Page
5.1 Alpha-particle energy spectrum of U^{232}/Th^{228} spikes	155
5.2 Alpha-particle spectrum of Th^{228}/Th^{227} mixture	159
5.3 Elution curves for U and Th from Dowex-anion exchange resins	161
5.4 Thorium alpha-particle spectrum	168
5.5 Calibration graph for calculating uranium concentrations from count rates	170
5.6 Schematic diagram of α - particle spectrometer, showing in detail source-detector geometry	176
6.1 Uranium content, Th^{230}/U^{234} and U^{234}/U^{238} isotopic variations in stalagmite NB1, Norman-Bone Cave	182
6.2 Uranium content, Th^{230}/U^{234} and U^{234}/U^{238} isotopic variations in stalagmite NB10, Norman-Bone Cave	185
6.3 Longitudinal section and cross-section of part of NB10	189
6.4 Results for NB1 and NB10 plotted as Th^{230}/U^{234} against U^{234}/U^{238}	191
6.5 Oxygen and carbon isotopic variations along the axis of NB10	193
6.6 Location of analysed samples in speleothems NB2, NB3, NB12 and NB13, Norman-Bone Cave	197
6.7 Oxygen and carbon isotopic variations along a single growth layer and along the axis of stalagmite NB11, Norman-Bone Cave	199
6.8 Th^{230}/U^{234} plotted against Th^{232}/U^{234} for stalagmite NB3	204
6.9 Longitudinal section through stalagmite NB4 showing location of the analysed sample	208
6.10 Cross-section and oxygen and carbon isotopic profile through the upper part of NB4	211
6.11 Oxygen and carbon isotopic profile along the Norman-Bone Cave drill core, NB4	213
6.12 (a) Location of samples for age and stable isotopic analysis in stalagmites NB5 and NB9, Butterscotch Room, Norman Cave. (b) Relationship between δ_{ct}^O and δ_{ct}^C for samples from the base of NB5	217
6.13 Cross-section through flowstone sample GV1, Grapevine Cave	220
6.14 Cross-section through flowstone sample GV2, Grapevine Cave	223

6.15	U^{234}/U^{238} variations along Grapevine Cave Flowstone GV2	229
6.16	Oxygen and carbon isotopic variations along Grapevine Cave Flowstone GV2	231
6.17	Comparison between the oxygen isotopic variations recorded in NB4 and GV2	234
7.1	Sketch map of the alpine karst area south of the Crownest Pass, Southern Alberta, showing the location of the caves studied	246
7.2	Sketch map of the Nahanni Region, NWT, showing the location of the two caves studied	253
7.3	Approximate periods of speleothem deposition (equivalent to interglacial periods) in Western Canada	257
8.1	Initial U^{234}/U^{238} ratios (calculated from the Th^{230}/U^{234} age) of (a) Grapevine Cave samples and (b) Norman-Bone Cave samples, plotted against Th^{230}/U^{234} age of the samples	266
8.2	Initial U^{234}/U^{238} ratios (calculated from the Th^{230}/U^{234} age) plotted against U content of speleothems from (a) West Virginia and (b) the Canadian Rockies	269
8.3	A comparison between periods of coral deposition and speleothem deposition	278
8.4	Schematic diagram showing the effect of decreasing mean annual temperatures on the seasonal periods of speleothem deposition.	283
8.5	Variations in δ_{ct}^O and isotopic temperatures calculated from the fluid inclusion data for part of NB10	292
8.6	δ_{ct}^O plotted against δ_{ct}^C for samples from stalagmites NB4, NB5, NB10 and NB11 (Norman-Bone Cave) and GV2 (Grapevine Cave). The correlation coefficient between δ_{ct}^O and δ_{ct}^C (r) is calculated for each speleothem	296
8.7	Summary of the speleothem data and a time scale for Late Pleistocene climatic events based on these data	301
8.8	A comparison between the speleothem oxygen isotopic records for West Virginia and Southern France (Ardeche Province) between 60,000 and 130,000 years B.P.	305
8.9	A comparison between (a) the speleothem record for West Virginia, (b) the planktonic foraminiferal record from tropical deep-sea cores and (c) the ice record from Greenland	311

LIST OF TABLES

	Page
3.1 Climate Data for Greenbrier and Pocahontas Counties, West Virginia	69
3.2 Response of Cave Temperature to Variations in Surface Air Temperature	73
4.1 Permil Fractionation Factors between CO ₂ Gas and Carbon Species in Solution	81
4.2 Analyses of Isotopic Standards	103
4.3 Isotopic versus Theoretical Temperature of Deposition of Modern Speleothems	108
4.4 Oxygen Isotopic Composition of West Virginia Precipitation	113
4.5 Stable Isotope Data for Recent Speleothems from Norman-Bone Cave	125
4.6 Stable Isotope Data for a Fossil Speleothem from Norman-Bone Cave	129
4.7 Stable Isotope Data for a Fossil Speleothem from Grapevine Cave	132
4.8 Loss of Water from Speleothem Samples when Heated Under Vacuum	141
4.9 Isotopic Temperatures Corrected for Fluid Inclusion Loss	143
5.1 pH for 10, 90 and 100% Extraction of Elements in the Uranium Decay Series into 0.2M TTA in benzene	148
5.2 Summary of Reagent Blank Analyses	151
5.3 Analysis of Granite Standard and Calculation of Spike Ratios	156
5.4 Detector Characteristics	175
5.5 Results of Leaching Experiment on Grapevine Flowstone GV1	178
6.1 Analysis of Stalagmite NB1 (Norman-Bone Cave)	183
6.2 Analysis of Stalagmite NB10 (Norman-Bone Cave)	187
6.3 Analysis of Stalagmites NB2 and NB11 (Norman-Bone Cave)	200

6.4	Analysis of Stalagmites NB3 and NB12 (Norman-Bone Cave)	206
6.5	Analysis of Norman-Bone Drill Core, NB4 and Stalactite NB13	212
6.6	Analysis of Stalagmites NB5 and NB9 (Norman-Bone Cave)	218
6.7	Analysis of Flowstone GV1 and Drill Core GVC-1 (Grapevine Cave)	222
6.8	Analysis of Flowstone GV2 (Grapevine Cave)	227
6.9	U^{234}/U^{238} Ratios in Cave Waters	237
6.10	Summary of the Petrology and Environment of Deposition of Speleothems Chosen for Isotopic Analysis	239 -241
7.1	Analysis of Crowsnest Area Speleothems	249
7.2	Analysis of Speleothems from the Nahanni Region	254
7.3	Analysis of the Tinaja Stalagmite, Cuidad Valles, S.L.P., Mexico	261
8.1	Isotopic Temperature of Deposition and δ_i^o of Warm Climate Speleothems	288
8.2	Late Pleistocene Climate and Chronology Based on δ_{ct}^o and Periods of Speleothem Deposition	301

CHAPTER ONE

PROBLEMS OF THE PLEISTOCENE TIME SCALE

1.1 Introduction

The time scale of the Pleistocene epoch has been, and is currently, one of the most disputed topics in Pleistocene geology. A second, perhaps equally controversial problem concerns the regional and global temperature fluctuations which occurred throughout the period. In both cases the lack of quantitative techniques of observation and measurement has contributed to the current confusion. With the advent of quantitative methods such as radiometric dating and geothermometry based on stable isotopic abundances the confusion can, in theory, be resolved. However, these quantitative methods which are elegantly simple in theory are not easily applied in natural environments due to the complicated nature of geologic processes. The modern methods of dating Pleistocene deposits, for example those based on uranium series disequilibrium, and isotopic thermometry methods must still be considered to be in an experimental stage. Results obtained using these methods must therefore be accepted with caution. Even the well-established C^{14} method of dating late Pleistocene events poses problems when attempts are made to convert radiocarbon years to sidereal years.

To obtain a complete record of Pleistocene climate changes it is necessary to find deposits which are protected from the destructive forces of erosion. An ideal material would give paleoclimate

information, or would be associated with such material, and would give absolute ages. Few deposits meet these requirements. Coastal, shallow water and lacustrine carbonate deposits, whilst datable, can indicate only general, qualitative climatic trends. The classically studied glacial deposits such as loess, tills, peat bogs, etc. though containing abundant climatic information in the form of pollen profiles are rarely datable beyond the range of C^{14} . Where datable interstratified volcanics and glacial deposits occur the chronology is often in dispute due to limitations of the K-Ar method of dating the volcanics (discussed in Section 2.1).

The most promising materials which can be dated and which can provide quantitative climatic information are the undisturbed deep-sea pelagic sediments which are mostly protected from the destructive forces of erosion. Radiometric dating, principally by uranium series disequilibrium, is combined with micropaleontologic analysis and stable isotope analysis of foraminiferal tests to give detailed paleoclimatic information. The method of dating is only applicable to about 250,000 years B.P. at best, but it has already contributed substantially towards an understanding of the Pleistocene climatic fluctuations. The method is not entirely proven yet due to experimental uncertainties and assumptions which must be made to calculate absolute ages. This is brought out in the literature dispute between Rona and Emiliani (1969) and Broecker and Ku (1969) which is discussed in Section 2.4.

Until recently, little quantitative information on continental Pleistocene temperatures was available and most of this was based on

present and past floral and faunal regimes. Dating was mostly by time-stratigraphic correlation. Terrestrial carbonate deposits are the obvious choice for study because the oxygen isotope method can be applied to paleotemperature analysis and the new methods of uranium-series disequilibrium can be used as a dating tool.

Calcareous deposits from limestone caves, commonly termed speleothems, were considered suitable materials for such a study for several reasons.

1) Speleothems are usually very pure deposits. Because the CaCO_3 is deposited as a result of outgassing of CO_2 and not as a result of evaporation of the cave water most of the potential impurities remain in solution. Water entering a cave has travelled through narrow joints and bedding planes which effectively filter out sediment. If no sediment is trapped in the calcite layers, analytical problems are avoided.

2) For paleotemperature studies it is advantageous to be able to measure mean annual surface air temperatures. The temperature of a cave is approximately equal to the time-weighted mean annual air temperature above the cave (for discussion see Chapter 3, Section 3.3). The temperature of a cave does lag behind secular surface temperature variations. The lag depends upon the depth of the cave and the thermal conductivity of the limestone but is of the order of 1 year at 17 metres (Cropley, 1965). This is insignificant when compared to the resolution of the radiometric dating procedure available to us.

3) The rate of accretion of speleothems is a sufficiently

rapid process that secular variations in temperature of a few years could be resolved. There are numerous instances of artifacts less than 1000 years old being covered with inch thick or greater layers of CaCO_3 and in some instances climatic data could be obtained from the incrustations, though these generally occur in parts of caves unsuitable for paleotemperature work.

4) Caves containing speleothems are commonly fossil landforms and fragments of them tend to survive long after contemporaneous surface landforms have been erased. These natural sediment traps may survive long after all surficial traces of an age have been erased. A detailed example of this situation has been cited by Ford et al. (1972).

5) Caves are found over a wide latitudinal extent. They range from subarctic latitudes both north (eg. Canada and Norway) and south (eg. Patagonia) to equatorial latitudes (eg. Venezuela) and are abundant in between. The majority of caves contain speleothems of one kind or another so a wide spectrum of paleoclimates should be accessible to study.

6) Cave deposits are truly continental in origin. Their record of time and temperature is therefore more relevant to the major continental deposits (drift, loess etc.) than are the paleoclimate records obtained from deep-sea sediments. However, phases of speleothem deposition cannot be directly correlated with other continental deposits. The cave environment is an isolated one and evidence of Pleistocene climate changes is more subtly recorded than the evidence in surficial deposits.

7) Many speleothems are well preserved and do not generally show evidence of re-resolution. This is an important consideration when dating by uranium series disequilibrium methods is attempted.

There are certain disadvantages to the use of cave deposits in Pleistocene studies.

1) Speleothem deposition tends to be sporadic and is only controlled in part by climate changes. No assumptions about rates of growth or continuity of growth can be made because rates of growth have been shown to be highly variable (see references in Warwick, 1962 and section 2.4.1) and discontinuous growth is common. The construction of a continuous climatic record therefore, might prove very difficult, and must be pieced together from records in many stalagmites.

2) The very purity of speleothems make them difficult to date since they contain little uranium, and no potassium or rubidium.

3) Sampling poses problems because caves are difficult to work in. Samples must be collected from beyond the region influenced by diurnal and seasonal temperature changes. Often this region can extend hundreds of metres from the entrance of the cave and many obstacles including climbs, drops, underground streams and crawlways may be encountered.

4) Because of their aesthetically pleasing shape and appearance, removal of speleothems from their natural environment is considered by many to be desecration. The number of speleothems deposited within any cave is limited and because the deposits in situ offer no clue as to their age, extensive sampling might be required to

obtain a complete climate record. This is more a problem of conscience than a practical problem.

5) Many deposits are contaminated by detrital phases and often this is not apparent until the speleothem is removed from the cave and sectioned. Also, evaporation can play a part in the deposition of CaCO_3 on a speleothem surface (particularly in tropical regions) and again this may not be recognised until a speleothem is sectioned and analysed. A speleothem deposited wholly or in part by evaporation of water will not give paleoclimate information by oxygen isotopic analysis.

6) Problems are encountered when attempts are made to interpret changes in the oxygen isotopic composition of the CaCO_3 in terms of climate change. These changes are caused both by changes in cave temperature and by changes in the isotopic composition of cave waters. It is difficult to assess the effect of temperature alone on the isotopic composition. In addition, due to non-equilibrium isotope effects, some speleothems do not record paleoclimate information at all. Fortunately this type of deposit can be recognised.

1.2 Radiometric Methods of Dating the Quaternary Period

The methods that have been proposed to date the events of Quaternary Period can be classed into three broad groups, namely (1) those using the decay of relatively short-lived cosmogenic radionuclides, (2) those using naturally occurring secondary radionuclides with relatively short half-lives, and (3) those using the decay of long-lived parent isotopes with noble gas daughter products.

The first group includes dating based on the activities of C^{14} , $t_{1/2} = 5730$ years; Be^{10} , $t_{1/2} = 2.5 \times 10^6$ years (Merrill et al., 1960); Al^{26} , $t_{1/2} = 7.4 \times 10^5$ years (Amin et al., 1966); and Cl^{36} , $t_{1/2} = 3.1 \times 10^5$ years (Schaeffer and Davis, 1958). In general the methods have not met with much success, except of course for C^{14} , because of the very low terrestrial abundance of these cosmogenic isotopes and uncertainties as to the cosmic ray flux. Though Lal (1963) has demonstrated that the long-term cosmic ray flux is reasonably constant, short-term variations are known to occur. These short-term fluctuations affect the accuracy of radiocarbon ages. The principle and limitations of the C^{14} dating method are discussed in more detail in Section 1.2.3. The use of C^{14} as a Pleistocene dating tool is limited by its short half life to dating materials less than about 30-40,000 years old. Under exceptional conditions the method can be used to date objects up to 60,000 years old. At the limit of the method the effect of inadvertant addition of "young" carbon drastically reduces the measured age.

The second group of methods using the naturally occurring secondary radionuclides U^{234} , Th^{230} , Pa^{231} , and Ra^{226} which belong to the uranium-series decay scheme have met with more success and have been the subject of extensive research in the past 15 years. The principles and some of the results obtained from the study of uranium-series disequilibrium dating are discussed in detail in Chapter 2.

The third group of methods is based upon the accumulation of helium or argon, produced from the radioactive decay of uranium (U) and potassium (K) respectively. Some of these methods are discussed briefly below.

1. 2.1. The Potassium-Argon and Fission Track Dating Methods

In theory the potassium-argon (K-Ar) method of dating can be used to date rocks as young as 10^4 years with a precision of 10-20% using present-day equipment and techniques (Dalrymple, 1968). This author quotes ages, on high-K sanidine of approximately 10^5 years with a precision of 2-3%. Unfortunately, only certain potassium bearing minerals can be dated by this method and only a very few, such as sanidine and anorthoclase are useful for dating late Pleistocene events.

The youngest material to give a K-Ar age was analysed by Curtis and Evernden (1962) who obtained an age of 5600 years on sanidine from a post-glacial rhyolite dome at Mono Lake, California. There is, in theory, no lower limit to the method; so certainly all Pleistocene events could be dated if suitable material existed. When analysing very young rocks a small degree of contamination with detrital feldspar or mica which contain occluded radiogenic argon (<0.1%) will invalidate an age determination.

Most suitable material is in the form of continental volcanics and ejecta (submarine volcanics are mostly too altered) and authigenic glauconite which occurs in marine sediments. The rare occurrence of such deposits closely related to deposits of stratigraphic importance constitutes the most serious limitation to the method. In addition the volcanic layers commonly either overlie or underlie the glacial deposits of interest and so give either an upper limit or a lower limit on the age of the sediments. A classic example of the use of the K-Ar dating method was the study of the hominid-bearing Olduvai deposits in East Africa. This 350 foot thick Pleistocene sequence rests upon basalts and

tuffs which have been dated as $1.57 - 1.91 \times 10^6$ years old, (Evernden et al., 1964; Evernden and Curtis, 1965; and Fleischer et al., 1965). It is significant that of the fifty or so dates listed for Olduvai Gorge only 11 K-Ar ages are considered reliable (Hay, 1967; Isaac, 1969). The successfully dated minerals were plagioclase, anorthoclase and augite. Younger volcanic beds interstratified with the Pleistocene deposits have not yet been successfully dated.

K-Ar dating therefore cannot give a detailed Pleistocene chronology but can give useful "spot" ages particularly for the early Pleistocene.

The density of fission tracks may also be used to date materials of Pleistocene age. The method has been applied successfully to dating young micas and microtektites (eg. see Fleischer et al., 1965). Because of experimental difficulties carbonates have never been successfully dated, though Brito and Lalou (1969) have described a method which successfully etches fission tracks in calcite. Given the low (U) usually found in CaCO_3 the method could not be applied to samples less than approximately 10^5 years old.

1.2.2. He-U Method of Dating

The He-U method of dating relies upon the assumption that all helium (produced when an α -particle gains two electrons) is retained within the mineral being dated. As discussed by Schaeffer (1967) and Bender (1970) this assumption is not valid for the majority of minerals. Helium can be lost by diffusion or excess helium can be introduced by secondary addition of uranium or thorium. If the mineral forms a closed

system then the method will give valuable ages since it can be applied within the range of the deficient ionium method and beyond this range. The youngest samples that can be dated would be approximately 100,000 years old. Account must be taken of disequilibrium in the uranium series when calculating U-He ages.

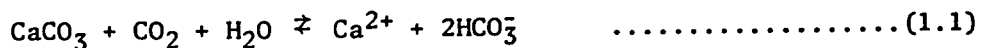
Fanale and Schaeffer (1965) found that aragonitic coral apparently forms a closed system and can be dated at least through the Miocene. Fossil molluscs occasionally give acceptable ages but are reliable only if they agree with uranium-series dating. Bender (1970) supports these conclusions in general but finds that aragonitic corals can have both excess and deficient He even when He loss through "hot-atom" effects is considered. Excess He is probably due to contamination from detritus while samples with deficient He often show disequilibrium in the uranium-series (Rn^{222} leakage). The He-U method can probably be applied to aragonitic speleothems. Since speleothems are in general not as porous as corals corrections due to He loss by the "hot-atom" effect (discussed in detail by Bender) would be expected to be less.

1.2.3 C¹⁴ Dating of Carbonates

The C¹⁴ method of dating, though well established for organic material, is potentially subject to considerable error when applied to dating of fresh-water carbonates. The errors which stem from variations in production rate of C¹⁴, isotopic replacement and contamination by modern or old carbonaceous material are well known and will not be discussed here. A review of such errors was given by Shotton (1967).

More detailed treatment of these errors can be found in the I.A.E.A. Symposium on Radioactive Dating and Methods of Low Level Counting (1967) and in Olssen (1970).

The method can be used to date carbonates if the original proportion of C^{14}/C^{12} in the $CaCO_3$ is known. Some of the carbon in the solution from which $CaCO_3$ is deposited will be "dead" i.e. derived from the limestone, which contains no C^{14} . The remainder will be "live" and is derived from CO_2 of biogenic origin. The original proportion of C^{14}/C^{12} in solution will depend upon the process by which the limestone is dissolved and can vary from approximately 50% to 100% of that of the soil atmosphere. Ideally, calcite dissolves in bicarbonate-bearing ground water according to the equation:



The stoichiometric proportion of "living" to "dead" carbon in solution from equation 1.1 is 1:1. On precipitation of $CaCO_3$ by reversal of equation 1.1, $CaCO_3$ is formed with approximately 50% of the modern C^{14}/C^{12} ratio. This assumes that equimolar quantities of organic and inorganic C are utilized. The actual ratio depends on the pCO_2 of the soil atmosphere (Hendy, 1970, p.423). In the presence of a large excess of HCO_3^- of biogenic origin the C^{14}/C^{12} ratio in solution will approach and even slightly exceed (through isotopic enrichment) the modern atmospheric value. This is the "open system" model of Hendy (1970, p.421). Alternatively, where the solution is quickly isolated from the atmosphere and allowed to exchange with the limestone, the C^{14}/C^{12} ratio may drop to very low values.

Correct choice of the initial C^{14}/C^{12} ratio is vital when

calculating C^{14} ages, particularly when dating young (<10,000 years) carbonates. Hendy (1969, 1970) has attempted to date speleothems using the C^{14} method and assumed that all the carbon was of atmospheric origin. This gave an "apparent" C^{14} age at points in the speleothem. Extrapolation of this "apparent" age to the surface of the speleothem, which was assumed to be modern, gives an "apparent" age at zero time. This "apparent" age at zero time can be subtracted from the other "apparent" ages to give "true" ages. It must be stressed that this method relies upon a constant C^{14}/C^{12} ratio in the solution depositing $CaCO_3$, a constant rate of deposition and the assumption that the surface of the speleothem is modern. These assumptions can be verified in part by other evidence as discussed by Hendy (1970).

Labeyrie et al (1967a) used the C^{14} method for dating speleothems and chose an initial C^{14}/C^{12} ratio 65% of the modern ratio. This ratio was directly measured and assumed constant over the period of deposition. Franke(1965b), Geyh (1970), Franke and Geyh (1971) have also used the C^{14} method to date speleothems. Their measurements give internally consistent results but the absolute accuracy of their measured ages is uncertain.

1.3 The Mechanism of Speleothem Deposition

The mechanism of speleothem deposition has been described in detail by several authors (for example Moore and Nicholas, 1966; Warwick, 1962; Franke,1965a; Roques, 1968 and Wells, 1971). This section briefly summarizes the depositional process; other aspects of the process are introduced at relevant points in the text.

Meteoric waters are capable of dissolving limestone by virtue of the fact that CO_2 , present in the atmosphere and soil air, reacts with water to produce carbonic acid which in turn reacts with CaCO_3 to produce soluble Ca^{++} and HCO_3^- ions. The net reaction is shown by equation 1.1. The forward reaction describes the solution process and the backward reaction the process of (speleothem) deposition. A complex series of equilibria are involved in the solution-deposition process which may be upset by changes in temperature, partial pressure of CO_2 (pCO_2) or the presence of other soluble ions. The most important variable involved in the process is the pCO_2 of the soil air which determines the pH of the solution. This can vary within wide limits (Holland et al, 1964; Enoch and Dasberg, 1971) as a result of changes in the metabolic activity of the plant cover and organisms within the soil.

Water percolating through a soil zone highly charged with CO_2 becomes acidic and dissolves CaCO_3 as it seeps into the bedrock. Ca^{2+} and HCO_3^- ions remain in solution until the water seeps into the cave via a network of vertical joints and horizontal bedding planes. The pCO_2 of the cave air is generally similar to that of the atmosphere (0.03 % Atm) and therefore re-equilibration of the solution with the cave air occurs and CaCO_3 is deposited. Each drop of water entering the cave deposits a small amount of CaCO_3 until large deposits (speleothems) are built up. Deposition continues until seepage stops or is directed to another point in the cave. An increase in flow rates often results in undersaturated waters entering the cave and re-solution of the speleothem surface may occur under these circumstances.

Both calcite and aragonite may be precipitated in caves. Based on the geographic distribution of caves containing predominantly aragonite or calcite speleothems, Moore (1956) suggested that the crystal chemistry of speleothems may be used as a paleoclimate indicator. Moore suggested that in the U.S. speleothems deposited below about 17°C are deposited as calcite and as aragonite when the temperature is above this value.

The internal structure of speleothems is complex and is broadly comparable to the internal structure of trees which exhibit annual growth layers. According to Broecker et al. (1960) the growth layers are annual in some stalagmites. This is based on C¹⁴ dating and counting of growth layers. But Hendy (1969) concludes from C¹⁴ dating studies that each layer represents at least a 10 year period of growth. Dating of speleothems by the counting of consecutive layers would therefore seem to be a dubious method. These layers can be caused either by the inclusion of fine detritus or by changes in the chemistry of the seepage waters which cause trace amounts of iron or manganese to be co-precipitated in the speleothem layers.

The morphology of speleothems is generally quite complex but in most cases the basic shape is dictated by gravitational forces. Horizontal or near-horizontal layers of CaCO₃ are termed flowstones; columnar floor deposits are termed stalagmites and pendant roof deposits, stalactites. The basic shapes of speleothems tend to be modified by changes in the conditions of deposition. For example, a change in the rate of supply of solution or a movement in the centre of deposition will alter the columnar form of stalagmites. A change of climate may

affect the long-term rate of supply of solution to a stalagmite surface. The diameter of a stalagmite has been shown by Franke (1965a) to be dependent on the rate of supply of solution, the diameter increasing as the rate of supply of solution increases. The rate of growth in height according to Franke, is a function of the amount of CaCO_3 dissolved and the partial pressure of CO_2 in the cave air.

1.4 The Time Scale of the Quaternary Period

Before the advent of potassium-argon (K-Ar) and uranium series disequilibrium dating techniques, estimates of the length of the Quaternary Period based on detailed studies of marine sediments varied from 1.8×10^6 years (Ericson et al., 1961) to 3.5×10^5 years (Emiliani, 1955). These represent extreme estimates of the time scale of the Quaternary and intermediate estimates have been proposed (for example by Zeuner, 1959). These widely different estimates were obtained because different criteria were used to recognize changes of climate and time scales were mostly based upon extrapolation of C^{14} ages. The age of the Pliocene/Pleistocene boundary is a matter of definition and in the marine record it is generally recognised as the base of the Calabrian formation (Southern Italy). The terrestrial equivalent is recognised as the Lower Villafranchian deposits of France. The Calabrian stage has been dated at no older than 1.8×10^6 years (Bergren et al., 1967) whilst the Villafranchian stage age has been placed at between 3.4×10^6 and 1.9×10^6 years B.P. (Savage and Curtis, 1970). These ages were obtained by the K-Ar dating method. Apparently

only the upper part of the Villafranchian formation correlates with the Calabrian formation. With the exception of Antarctica the oldest glacial deposits appear to be no older than 2.7×10^6 years and appear to be contemporaneous in the Northern and Southern Hemisphere (Curry, 1966; McDougall and Wensick, 1966; Mathews and Curtis, 1966; Armstrong et al., 1968); again this is based on K-Ar ages. Some glaciation occurred, therefore, in the Pliocene and available evidence indicates that the Pliocene-Pleistocene boundary cannot be recognised as an abrupt deterioration of climate. The pattern of climate change throughout the Late Pliocene and Early Pleistocene was apparently a gradual cooling interspersed with glacial advances. The intensity and frequency of glaciations only increased in the Late Pleistocene ($<1 \times 10^6$ years ago).

The longer time scale of Ericson is supported by the above K-Ar ages but the criteria used by Emiliani to recognize glacial cycles (chiefly the variation in O^{18}/O^{16} ratio in foraminiferal tests) has been shown, by detailed continental and marine comparisons, to be valid. This points to the fact that more than the five glacial cycles originally recognised by Ericson et al. are recorded in the marine sediments over the last 1.8×10^6 years. Kukla (1970) recognised eight complete glacial cycles in loess deposits of Czechoslovakia. These occurred between 0.7 to 1.2×10^6 years ago and the present. It is quite possible that much of the record in continental Quaternary deposits has been erased by the more recent glacial advances.

Much of the current confusion with regard to the Quaternary time scale arose because of the lack of a suitable method to date Middle and Late Pleistocene events. This period of time was not covered

adequately by the C^{14} method and the K-Ar method, though advocates of the latter method would dispute this. However the methods of uranium series disequilibrium dating have been applied with increasing frequency and successes during the last two decades to date these Middle and Late Pleistocene events as well as Recent events. These methods are limited to dating events no older than about 200,000 to 300,000 years and no younger than about 2000 to 5000 years but this conveniently bridges the gap between C^{14} dating and K-Ar (or U-He) dating. Deep-sea sediments, marine and lacustrine carbonates, tufas and travertines have been successfully dated using U series disequilibrium methods. This research was initiated to assess the suitability of speleothems for dating by this method.

An accurate time scale of Quaternary events is required by geologists, climatologists and anthropologists alike. The geologist will be able to correlate regional glacial and interglacial episodes and, by observing general patterns of occurrence test the various hypotheses purporting to explain the causes of Ice Ages. The climatologist will be able to analyse the secular, global climate changes and may eventually produce a generally accepted theory of climate change. The anthropologist will be able to relate man's evolution with glacial/interglacial episodes. Man's past and future is intimately associated with these changes of climate. Should global temperatures decrease in the future and precipitate a new glacial age the consequences for a large part of the world's population would be disastrous. It is, therefore, essential to recognise recurring trends of climate change.

1.5 Statement of Thesis Objective

The present study was undertaken to assess the suitability of carbonate deposits from caves for dating by the methods of uranium-series disequilibrium. In particular a thorough evaluation of the U^{234}/U^{238} or excess uranium method of disequilibrium dating was planned because of the potentially long ($>10^6$ years) time span covered by this method. A further aim of the research was to evaluate the ionium growth or Th^{230}/U^{234} method of dating.

The original research topic was conceived as a dating project and only later did the possibility of using stable isotopic fractionations to obtain paleotemperatures seem a viable proposition. The decision to start stable isotopic (O^{18}/O^{16}) analysis was influenced chiefly by the favourable research of Hendy (1969). The ultimate aim of the research was to combine paleotemperature information with the relevant ages obtained to produce a detailed paleoclimate curve for the part of the Pleistocene period covered by the dating method. It was hoped that speleothems, deposited contemporaneously, in different caves would be found and would exhibit the same stable isotopic fluctuations. This would be considered strong evidence that changes of climate were being measured and not just random or local isotopic fluctuations.

It soon became apparent that construction of a detailed paleoclimate curve was an ambitious project and completion of the project has of necessity been left to others.

1.6 Field Areas and Sampling Programme

A karst area in the southeastern part of West Virginia was chosen as a field area for various reasons. The area was close enough to the front of maximum ice advance to be strongly affected by the advancing and retreating ice sheets. The caves were numerous and so afforded a good chance of finding suitable deposits. Much of the basic field work in the area was already complete when this thesis was started. Many of the caves had been explored and mapped by other students interested in other aspects of the caves such as hydrology and sedimentation. (This proved to be a great advantage since mutual assistance in carrying out work programmes could be anticipated).

A sampling programme was planned to evaluate the U^{234}/U^{238} dating method. Since the method relies upon the assumption that U^{234}/U^{238} ratios in ground waters are constant or vary in a predictable manner an evaluation should take into account the spatial and short-term temporal variations of this ratio in present-day waters. If these were proven to vary in an unpredictable way then the basic premise of the U^{234}/U^{238} dating method would have to be considered unsound. An extensive programme was planned to sample drip-sites in various caves spread over a wide area. Sites were chosen where active deposition was taking place. At the end of the sampling period it was planned to analyse this modern carbonate and compare the U^{234}/U^{238} ratio with the average value in the water. An opportunity arose to sample a karst spring in the Crowsnest Pass area of Alberta during the summers of 1968 and 1969. Though not associated with modern carbonate deposition the results could be expected to show how comparable were U^{234}/U^{238} ratios in

widely different karst areas.

The principal caves investigated were Norman-Bone Cave and Grapevine Cave in Greenbrier County, West Virginia. These caves were chosen for study because of the abundance of speleothem samples. A prime consideration was that the cave should contain a large number of speleothems so that removal of the necessary samples would not deplete the speleothem population noticeably. Wherever possible, broken deposits were collected for analysis.

Some of the caves in the field area contain abundant speleothems but the distribution of these deposits is always localised within them. Many of the caves contain no appreciable secondary mineralization. The type and size of deposit that can be removed from these caves is dictated by the nature of the cave and the sampling programme had to be planned with this restriction in mind. Few "wild" caves allow easy access and egress with heavy samples so the number of specimens that could be collected was limited.

The samples collected were generally stalagmites of uniform cross-sectional area. According to Franke(1965a) these grow slowly under a single, uniform slow drip and thus represent a long period of deposition. A formidable problem encountered in sampling is that the relative age of these deposits within a single cave can rarely be inferred from their appearance or position. Interlayered flowstone and fluvial or fluvio-glacial deposits suggest a relative sequence of deposition but in West Virginia caves such deposits are rarely encountered and are mostly unsuitable for accurate dating due to contamination with detrital phases.

Since stalagmite or stalactite deposits initially offer no clue as to their age (size is definitely no criterion) the basal and top sections must first be analysed to determine the time span of deposition. An unfortunate consequence of this type of sampling programme is that speleothems representing the complete time span of interest may never be encountered. The problem is analogous to that described by Ericson and Wollin (1964) during their search for deep sea cores representing the complete Pleistocene. Unfortunately, speleothems are less abundant and of more aesthetic value in their natural habitat than are deep-sea cores so widespread sampling within a single area was impossible.

There are obvious advantages to working within a commercialized cave. Their attraction usually stems from an abundance of speleothem deposits which are unusually large. Electric lighting invariably illuminates these deposits; the electric power system offers a means of operating a coring device. Long drill cores can, in principle, be obtained without appreciable damage to the appearance of the cored object. Full advantage was taken of an opportunity to obtain drill cores from a West Virginia "show" cave.

Speleothem samples were obtained from other localities to assess the applicability of the dating methods in widely different areas with widely varying climate and ground water chemistry. During the course of this work the research group, of which the author was part, was actively engaged in exploration and other cave research in the Canadian Rockies, N.W.T. and the El Abra range near Ciudad Valles, Mexico. Small sample collections were made in these regions to aid

the regional interpretation. Ages of some of the samples were measured. These are discussed in Chapters 7 and 8.

CHAPTER TWO

DATING METHODS BASED ON URANIUM-SERIES DISEQUILIBRIUM

The methods described in this chapter are based on disequilibrium between U^{238} and its daughter isotopes U^{234} and Th^{230} and on disequilibrium between U^{235} and daughter Pa^{231} . The decay schemes are illustrated in Figure 2.1. The alpha-particle energies of interest are shown in Figure 2.2.

2.1. Methods of Dating Carbonates Using Uranium-Series Disequilibrium

2.1.1. The U^{234}/U^{238} Method (Excess Uranium Method)

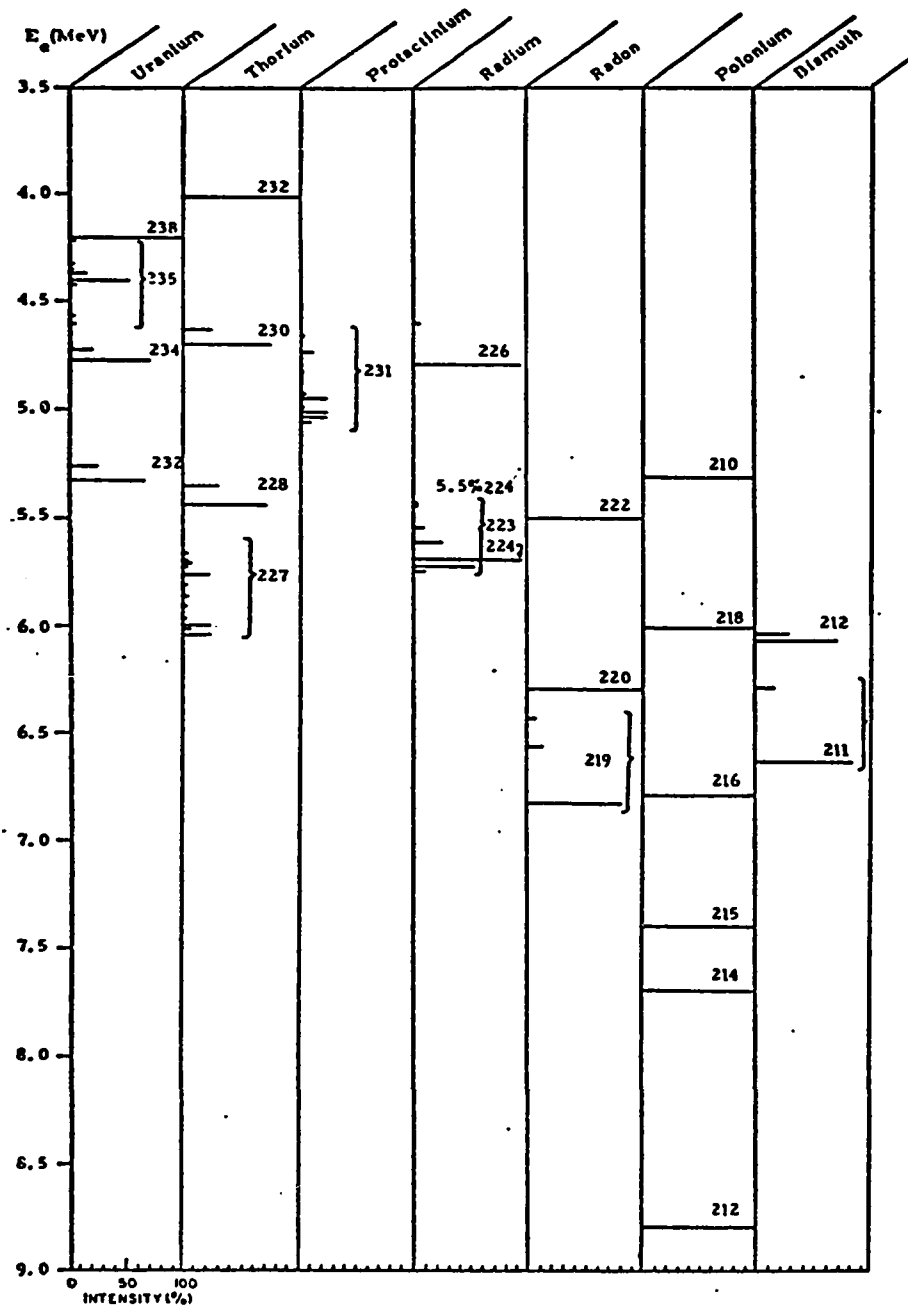
The occurrence of excess U^{234} in natural waters over that required for secular equilibrium with U^{238} was first observed by Cherdynsev (1955). The phenomenon was attributed to the preferential leaching of U^{234} from silicates due to its vulnerable position in a radiation-damaged site and its higher oxidation state due to stripping of electrons during the decay process. This process can lead to fresh waters with U^{234}/U^{238} ratios ranging up to 12.2 (Kronfeld, 1971) though most measured ratios fall between 1.10 and 3.0. Laboratory leaching experiments generally do not explain the high (>1.3) isotope ratios observed but Kigoshi (1971) has demonstrated that considerable Th^{234} may be leached from fine-grained sediments. Thus, both Th^{234} and U^{234} probably contribute to the observed excess of U^{234} in natural waters.

Since one half of this excess uranium will decay in a closed

U ²³⁸ Series	Th ²³² Series	U ²³⁵ Series
U ²³⁸ 4.5x10 ⁹ y	U ²³² 72 y	U ²³⁵ 7.13x10 ⁸ y
↓ α Pa ²³⁴ 1.18 m	↓ α Th ²³² 1.41x10 ¹⁰ y	↓ α Th ²³¹ 25.6 h
↓ β Th ²³⁰ 7.52x10 ⁴ y	↓ β Ac ²²⁸ 6.13 h	↓ β Pa ²³¹ 3.25x10 ⁴ y
↓ α Ra ²²⁶ 1602 y	↓ α Ra ²²⁶ 6.7 y	↓ α Ac ²²⁷ 21.6 y
↓ α Rn ²²² 3.825 d	↓ α Rn ²²⁰ 54.4 s	↓ α Rn ²²³ 11.43 d
↓ α Po ²¹⁸ 3.05 m	↓ α Po ²¹⁶ 0.158 s	↓ α Po ²¹⁵ 1.78x10 ⁻³ s
↓ β Bi ²¹⁴ 19.7 m	↓ β Bi ²¹² 60.5 m	↓ β Bi ²¹¹ 2.15 m
↓ α Po ²¹⁴ 1.6x10 ⁻⁴ s	↓ α Po ²¹² 3.05x10 ⁻⁷ s	↓ α Po ²¹¹ 36.1 m
↓ β Pb ²¹⁴ 26.8 m	↓ β Pb ²¹² 10.6 h	↓ β Pb ²¹⁰ 138.4 d
↓ α Bi ²¹⁴ 5.0 d	↓ α Bi ²⁰⁸ (stable)	↓ α Bi ²¹⁰ 5.0 d
↓ β Pb ²¹⁰ 21 y	↓ β Pb ²⁰⁸ (stable)	↓ β Pb ²⁰⁷ (stable)
↓ α Tl ²⁰⁶ (stable)	↓ α Tl ²⁰⁸ 3.1 m	↓ α Tl ²⁰⁷ 4.79 m

Data from : Table of isotopes, 6th Ed., by C.M. Lederer, J.M. Hollander, and J. Perlman, (Wiley and Sons, 1967)

Figure 2.1 Uranium and Thorium Decay Series



Data from: Table of Isotopes, 6th Ed., Lederer et al editors, 1967

Figure 2.2 Alpha particle energies of isotopes in the uranium & thorium decay series. (The length of each horizontal bar indicates the percent of monoenergetic α -particles emitted from each isotope)

system over a period of 248,000 years (the half-life of U^{234}) it has potential use as a dating tool. Deposition of $CaCO_3$ from U^{234} -enriched waters will result in the excess U^{234} being trapped in the mineral in the same proportion to U^{238} as in the water (provided both uranium isotopes in solution occur in the same oxidation state and provided there is not U-isotope fractionation between any chemical species in solution).

The uranium isotope ratio after time t is a function only of the initial isotope ratio.

$$\text{i.e. } \left(\frac{U-234}{U-238} \right)_t - 1 = \left(\frac{U-234}{U-238} \right)_0 - 1 \cdot e^{-\lambda_{234}t} \quad \dots\dots\dots(2.1)$$

where $\left(\frac{U-234}{U-238} \right)_t$ is the activity ratio after time t .

$\left(\frac{U-234}{U-238} \right)_0$ is the initial activity ratio.

λ_{234} is the decay constant of U-234.

In order to calculate "t", the initial as well as the measured U^{234}/U^{238} ratio must be known. The initial ratio can only be obtained indirectly by comparison with modern samples from the region where mineralization occurred or by comparison with present-day parent waters. The initial ratio must be assumed constant in this location with time. U^{234}/U^{238} activity ratios in continental waters vary over a considerable range which precludes, in most cases, the use of a universal initial U^{234}/U^{238} ratio. The range of measured values is discussed in Section 2.4. Only in the case of the oceans where the residence time of uranium is large (approximately 500,000 years) can a universal initial ratio be assumed.

2.1.2. Th²³⁰/U²³⁴ Method (Deficient Thorium Method)

This method of dating relies upon the fact that calcium carbonate deposited from sea water and from certain surface and ground waters contains uranium but is lacking in thorium (predominantly because Th is quickly removed from solution by other processes). Any Th²³⁰ (ionium) found in the calcium carbonate must therefore have been produced from decay of U and the ratio of Th²³⁰/U²³⁸ will be a function only of the time elapsed since deposition. Since any excess U²³⁴ originally deposited in the calcium carbonate will decay to Th²³⁰ account must be taken of this excess in most cases. The relationship between Th²³⁰/U²³⁸ ratio and the age of the sample is expressed as:

$$\frac{\text{Th-230}}{\text{U-238}} = (1 - e^{-\lambda_{230}t}) + \frac{\lambda_{230}}{\lambda_{230} - \lambda_{234}} (r-1) (1 - e^{-(\lambda_{230} - \lambda_{234})t}) \quad \dots\dots\dots (2.2)$$

where $\frac{\text{Th-230}}{\text{U-238}}$ is the activity ratio after time t (years).

r is the measured $\frac{\text{U-234}}{\text{U-238}}$ activity ratio.

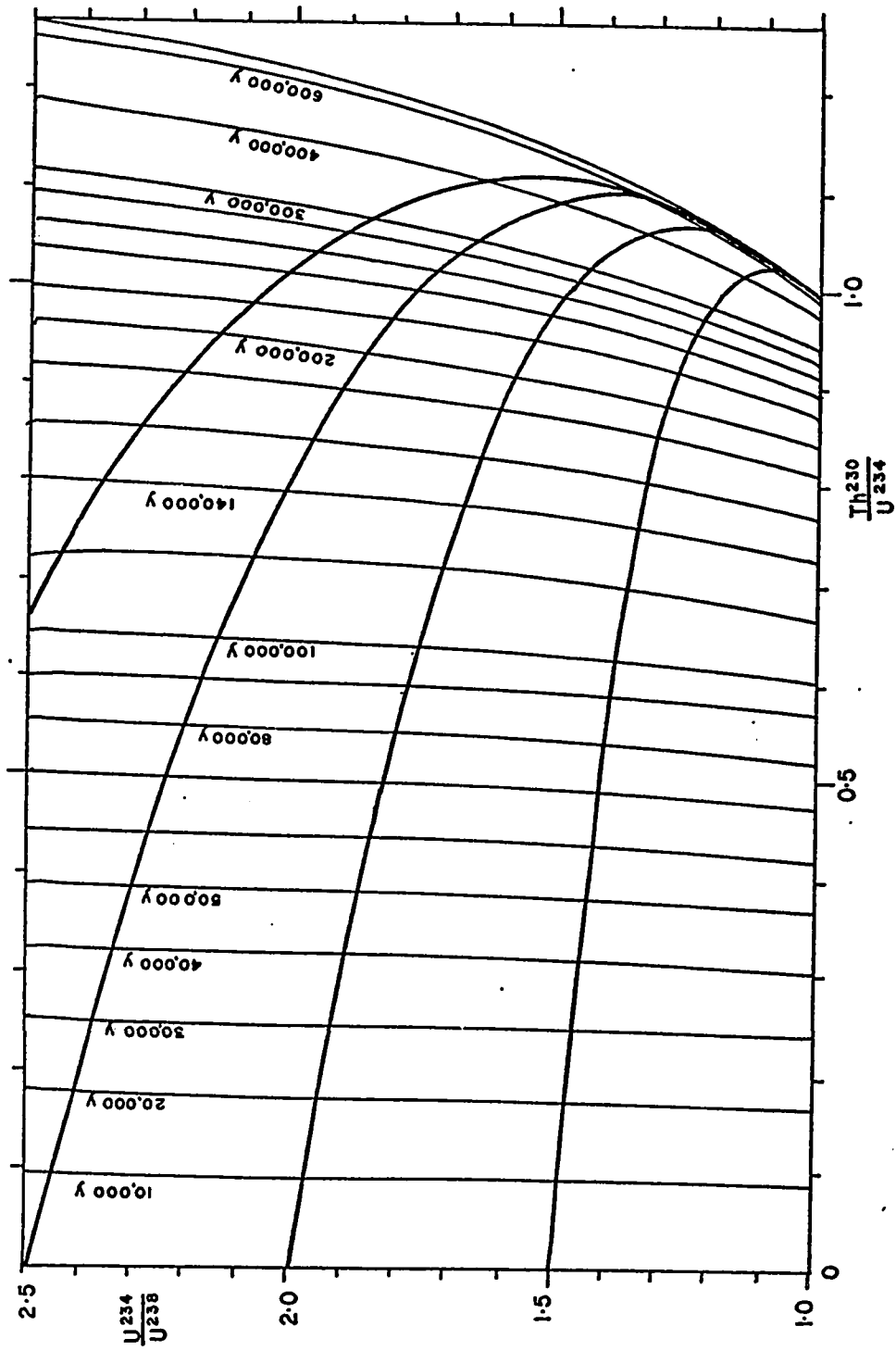
λ_{230} is the decay constant of Th-230

λ_{234} is the decay constant of U-234.

The above equation can also be expressed in terms of Th²³⁰/U²³⁴ ratio:

$$\frac{\text{Th-230}}{\text{U-234}} = \frac{(1 - e^{-\lambda_{230}t})}{r} + \frac{\lambda_{230}}{\lambda_{230} - \lambda_{234}} \left(1 - \frac{1}{r}\right) (1 - e^{-(\lambda_{230} - \lambda_{234})t}) \quad \dots\dots\dots (2.3)$$

Figure 2.3 Graphical representation of the growth of Th^{230} towards equilibrium with U^{234} in a closed system initially containing no Th^{230} . The heavy lines show the development of the system for initial $\text{U}^{234}/\text{U}^{238}$ ratios of 1.5, 2.0, 2.5 and 3.0. The vertical and near-parallel isochrons illustrate the relatively small effect of different initial $\text{U}^{234}/\text{U}^{238}$ ratios on samples less than approximately 100,000 years old.



These equations are derived in Appendix I.

A graphical representation of equation 2.3 is shown in Figure 2.3. The insensitivity of the younger isochrons to changes in initial U^{234}/U^{238} ratios is well illustrated.

For initial ratios of U^{234}/U^{238} close to or equal to one or for small values of t , equations 2.2 and 2.3 reduce to:

$$\frac{\text{Th-230}}{\text{U-238}} = (1 - e^{-\lambda_{230}t}) \dots\dots\dots (2.4)$$

(The activity ratio, the ratio of the decay rates of two isotopes becomes equal to 1.0 when equilibrium is reached. The time taken to reach equilibrium represents the limit of the dating method).

If thorium is present initially (eg. by occlusion or associated with clay and mineral inclusions) then the method can only be used if the non-radiogenic fraction of Th^{230} can be calculated. Since non-radiogenic Th^{230} is inevitably accompanied by Th^{232} ($t_{1/2} = 1.41 \times 10^{10}$ years) which can be considered of constant activity over the life-time of the deposit, the ratio $\text{Th}^{230}/\text{Th}^{232}$ in modern samples can be used to correct the measured Th^{230} activity because:

$$(\text{Th-230})_r = (\text{Th-230})_t - \left[\frac{\text{Th-230}}{\text{Th-232}} \right]_0 \cdot \text{Th-232} e^{-\lambda_{230}t} \dots\dots\dots (2.5)$$

where $(\text{Th-230})_r$ is the authigenic Th^{230} activity

$(\text{Th-230})_t$ is the total measured Th^{230} activity

$\left[\frac{\text{Th-230}}{\text{Th-232}} \right]_0$ is the activity ratio at time zero.

t is the time elapsed since contamination with Th, and is gener-

ally taken to be the time elapsed since deposition.

This approach has been used to correct ages obtained from contaminated carbonates and is discussed in more detail in Section 2.4. Post-depositional contamination is impossible to detect. This makes the removal of surface coatings essential.

Fortunately the ratio of Th to U in sea water and fresh waters is very low (approximately 10^{-4} in sea water according to Somayajulu and Goldberg, 1966). This fact coupled with the crystallographic discrimination (by CaCO_3) against Th suggests that pure carbonates will be essentially free of occluded Th.

Depending upon the material used, the deficient Th method can be used to date samples as young as 400 years (Thurber et al, 1965) and as old as 300,000 - 350,000 years.

2.1.3. The Pa²³¹/U²³⁵ Method

In ground-water systems and in the oceans protactinium (Pa) behaves chemically like Th so carbonates can be expected to form virtually free of Pa. The growth of Pa²³¹ towards equilibrium with its parent U²³⁵ can be monitored and will be a function only of the age of the sample provided the system remains closed. The age of the sample can be computed from the equation:

$$\frac{\text{Pa-231}}{\text{U-235}} = (1 - e^{-\lambda_{231}t}) \dots\dots\dots(2.6)$$

where $\frac{\text{Pa-231}}{\text{U-235}}$ is the activity ratio in the sample.

λ_{231} is the decay constant of Pa-231

t is the age of the sample (in years)

Secular equilibrium is attained after approximately 200,000 years which represents the practical limit of the method. The age calculated from equation 2.6 above and the age calculated from equation 2.2 should be concordant for the same sample. This is a valuable check on the closed system assumption since any perturbation is unlikely to affect both isotopic ratios ($\text{Th}^{230}/\text{U}^{234}$ and $\text{Pa}^{231}/\text{U}^{235}$) to the same extent.

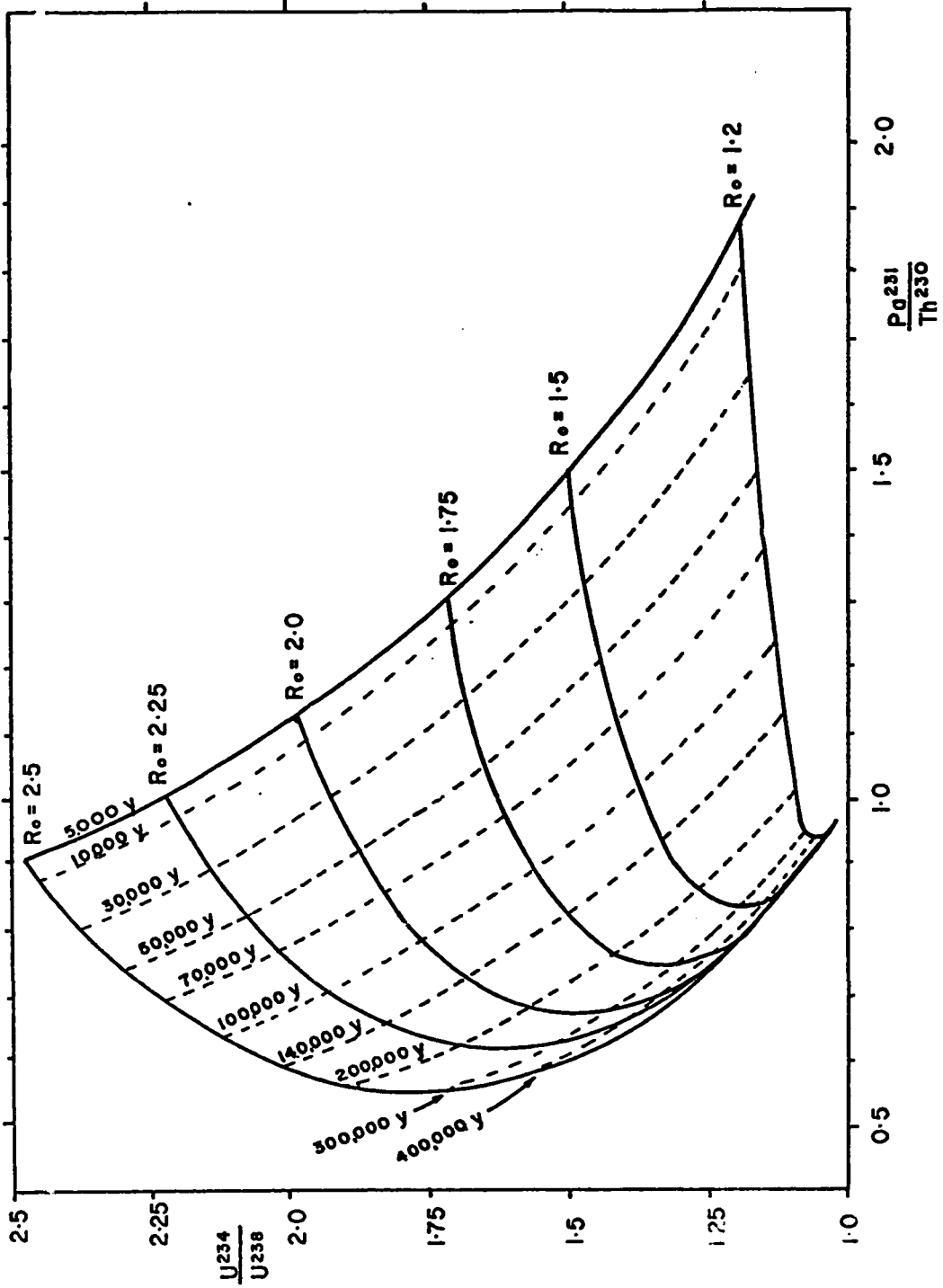
Since the $\text{U}^{238}/\text{U}^{235}$ isotopic abundance ratio is apparently constant in the lithosphere (137.4 : 1) the ratio $\text{Pa}^{231}/\text{Th}^{230}$ will be a measure of the age of the sample also. By dividing equation 2.6 by equation 2.2 $\text{Pa}^{231}/\text{Th}^{230}$ is obtained in terms of t :

$$\frac{\text{Pa-231}}{\text{Th-230}} = \frac{21.7(1-e^{-\lambda_{231}t})}{(1-e^{-\lambda_{230}t}) + (r-1) \frac{\lambda_{234}}{\lambda_{230}-\lambda_{234}} (1-e^{-(\lambda_{230}-\lambda_{234})t})} \dots (2.7)$$

The factor 21.7 is the activity ratio $\frac{\text{U-238}}{\text{U-235}}$.

A graphical representation of this equation is presented in Figure 2.4. From this figure it can be seen that $\text{Pa}^{231}/\text{Th}^{230}$ ratios are potentially quite useful for extending the normal range of $\text{Pa}^{231}/\text{U}^{235}$ dating. When initial $\text{U}^{234}/\text{U}^{238}$ ratios are high (>2.0) as often is the case with continental carbonate deposits it is theoretically possible to resolve age ambiguities arising from $\text{Th}^{230}/\text{U}^{234}$ ages between 200,000 years and approximately 350,000 years. The accuracy of the measured ratios will determine the limit of the method. Pa^{231} can be considered to be essentially in equilibrium with its daughter product Ac^{227} ($t_{1/2}$ =22 years) which is in turn in equilibrium with Th^{227} ($t_{1/2}$ =18.4 days).

Figure 2.4 Graphical representation of the changing $\text{Pa}^{231}/\text{Th}^{230}$ ratio in a closed system initially containing excess U^{234} and no Pa^{231} or Th^{230} . The development of the system is shown for initial $\text{U}^{234}/\text{U}^{238}$ ratios of 1.2, 1.5, 1.75, 2.0, 2.25 and 2.5.



Thus $\text{Th}^{227}/\text{Th}^{230}$ which is measured from the thorium α -spectrum is a direct measure of $\text{Pa}^{231}/\text{Th}^{230}$. The advantage of this approach is that chemical yields do not have to be monitored. Problems arising through the use of spike preparations which are discussed later are therefore avoided.

The principle disadvantage of using $\text{Pa}^{231}/\text{Th}^{230}$ ratios, and in many cases a prohibitive one, arises from the low abundance of Pa^{231} which can only exhibit a maximum activity of 1/21.7 times that of Th^{230} . Unless concentrations of uranium are reasonably high or unless large amounts of sample are available, reasonable statistical accuracy is impossible.

2.2. The Excess $\text{Pa}^{231}/\text{Th}^{230}$ Method

This method, though not applicable to carbonates has been extensively used to date deep sea sediments. Since the results obtained with this method will be used in discussion later, the principles and limitations of the method are discussed here.

Pa and Th exhibit a strong tendency to hydrolyse, form colloids and become attached to sediment particles. The residence time of these two elements in the oceans is therefore low (<300 years) and sediments become enriched in Pa and Th relative to the level supported by U in the sediments. The ratio of excess Pa^{231} to Th^{230} decays in a predictable manner and the age of the sediment can be obtained from the equation (Rosholt et al, 1961):

$$9.03 \frac{(\text{Pa}-231)_s - (\text{Pa}-231)_u}{(\text{Th}-230)_s - (\text{Th}-230)_u} = e^{-(\lambda_{231} - \lambda_{230})t} \dots\dots\dots (2.8)$$

the subscripts s and u refer to the activity of the total sediment and the activity of uranium-supported Th^{230} and Pa^{231} respectively.

λ_{230} is the decay constant of Th^{230}

λ_{231} is the decay constant of Pa^{231}

The factor 9.03 is a measure of the initial $\text{Pa}^{231}/\text{Th}^{230}$ activity ratio in the sediments.

In deriving this equation Rosholt et al. made three assumptions:

(1) That U^{238} , U^{235} and U^{234} are and have been present in normal equilibrium relative abundances in sea water. This assumption is invalid because of the well-documented excess of U^{234} in the oceans. A small correction must be applied to allow for excess Th^{230} produced by U^{234} decay.

(2) That the residence time of Pa in sea water will be very nearly the same as that of Th. The factor 9.03 (Koczy, 1954) is derived from this assumption. Measurements on numerous deep sea cores and manganese nodules have demonstrated that this assumption may not be valid. (Sackett, 1966 ; Ku and Broecker, 1967 ; and Broecker and Ku, 1969). The assumption that Pa and Th are geochemically coherent therefore is open to question.

(3) That the daughter products of U decay will be in radioactive equilibrium so that the activity of U-unsupported Pa^{231} and Th^{230} may be calculated. This assumption is difficult to verify but in general corrections due to U-supported Th and Pa are small and only become appreciable in older sediments when any initial disequilibrium in the uranium-series will be less pronounced.

Results obtained with this method are discussed briefly in Section 2.4.

2.3. Requirements for Reliable Age Determinations

There are three basic requirements that must be met before reliable uranium-series age determinations can be obtained.

(1) There should be sufficient concentration of uranium in the sample and sufficient sample available to give accurate results in a reasonable period of counting.

(2) There should be no migration of the radioelements of interest either into or out of the system after deposition. The isotopic composition of the sample should be altered only by the process of radioactive decay. This is termed the closed system assumption.

(3) The initial state of the system must be known. For the deficient thorium method $\text{Th}^{230}/\text{U}^{234}$ must initially be zero and for the deficient protactinium method $\text{Pa}^{231}/\text{U}^{235}$ must initially be zero. If such is not the case then the initial amount present must be known and allowance made for it when computing the age of the sample.

The first requirement is easily checked by a laboratory survey of typical samples for uranium content.

A check on the closed system assumption is rather difficult if only one dating method is contemplated and if no stratigraphic correlation is possible. However, if another dating method is available which covers the time span of interest this acts as a useful cross-check.

Th^{230} and Pa^{231} are daughters of different uranium isotopes, namely U^{238} and U^{235} respectively. Therefore, the ratios $\text{Th}^{230}/\text{U}^{238}$ and $\text{Pa}^{231}/\text{U}^{235}$

should give identical ages if the closed system assumption holds.

Other members of the two decay chains can be used to cross-check results. A particularly useful one is Ra^{226} which, because of its short half-life (1620 years), will help verify young ages (<8000 years) obtained by Th or Pa dating or will indicate whether open-system conditions occurred less than 8000 yrs ago in a supposedly old sample.

Speleothem samples should preferably be of aragonite because U and Th leaching or exchange might occur on inversion of aragonite to calcite. Calcite samples should be used only if there is no evidence of recrystallisation or if there is a firm indication that the material was deposited as calcite.

Furthermore, speleothem dates should be internally consistent. This is easily checked since the well-defined internal stratigraphy of speleothems in most cases allows an unambiguous assignment of the relative ages of the various layers within the speleothems. Though growth is sometimes discontinuous, the age of a stalagmite always decreases from the base to the top of the column.

The half-lives of the isotopes used in U-series dating are known quite accurately. But since the start of research into the U-series dating methods, the half-lives of Th^{230} and Pa^{231} have been re-evaluated. Attree et al., (1972) suggested a half-life of 75,200 yrs for Th^{230} to replace the value of 80,000 years measured by Hyde (1949). Ku (1968) suggests a value of 34,300 years (cf earlier value of 32,480 years given by Kirby, 1961) be accepted as the half-life of Pa^{231} , based on his measurements of the age of Barbados coral by the $\text{Pa}^{231}/\text{Th}^{230}$ method. The age of these corals have been determined quite accurately by the

$^{230}\text{Th}/^{234}\text{U}$ method and acceptance of the higher half-life brings into agreement the Pa^{231} and the Th^{230} ages.

2.4. Review of Some Results Obtained with Uranium Series Disequilibrium Dating

Early work in uranium series disequilibrium dating was pioneered by Barnes *et al* (1956), Sackett (1958) and Blanchard (1963), the latter two working under the auspices of Prof H.A. Potratz at Washington University, St. Louis. Concurrently, Cherdyntsev, who originally reported the discovery of excess U^{234} in ground waters, developed the deficient ionium and protactinium methods. Most of the research published on U series disequilibrium before mid-1966 is recorded in Cherdyntsev's book, Uranium-234 (1971).

This early research proved that the deficient ionium method, at least, was a reliable method for dating marine carbonates, corals in particular, and some terrestrial carbonates. When disequilibrium between U^{234} and U^{238} was first measured it presented an attractive dating method with a potential for dating terrestrial deposits as old as 1.5×10^6 years. This potential has never been realised because subsequent work has shown that $\text{U}^{234}/\text{U}^{238}$ ratios of terrestrial waters vary unpredictably over a large range. Carbonates deposited from these waters are therefore expected to reflect the same variations.

The $\text{U}^{234}/\text{U}^{238}$ ratio of surface and ground waters varies considerably according to the chemical composition of the rock type being weathered. Isabaev *et al* (1960) measured ratios as high as 7.8 with an average of 3.0 for waters draining off granitic rocks. $\text{U}^{234}/\text{U}^{238}$ ratios as high as

12.25 were measured by Kronfeld (1971) for deep sub-surface waters contained within a Cretaceous sedimentary sequence of Central Texas. Kronfeld was able to use the decay of excess U^{234} to place limits on the rate of ground water flow because the waters were apparently contained in a closed system. Surface waters varied over a relatively narrow range of 1.15 to 1.40. In general, the U^{234}/U^{238} ratio for waters draining sedimentary rocks is low, ranging from 1.0 to 1.36 (Cherdyntsev et al., 1963). However, the ratio can be higher in the vicinity of carbonate rocks (this study and Thurber, 1964). Based on numerous analyses, Cherdyntsev (1971) reports an average U^{234}/U^{238} ratio of 1.25 ± 0.05 for major rivers in the U.S.S.R.

When rocks which have previously lost a large proportion of their U are weathered, the U^{234}/U^{238} isotopic composition of the water may be less than unity. Ground waters from a carbonate aquifer in Florida were found to be depleted in U^{234} by as much as 50% (Kaufmann et al., 1969). However, this deficiency in U^{234} is sufficiently constant in waters sinking at specific sites that Osmond et al. (1968) were able to use U^{234}/U^{238} disequilibria as an aid to the hydrologic study of the same Floridan aquifer. It appears, therefore, that the U^{234}/U^{238} isotopic composition of sub-surface waters is quite constant in a given geologic setting, but that wide variations in this ratio occur from region to region.

As surface waters are channeled into major lakes the U^{234}/U^{238} ratio appears to become more constant. Chalov et al. (1964, 1966, 1970) have used the decay of excess U^{234} in bottom sediments to date no-outflow lakes. The agreement between the radiometric age of these lakes and that inferred from geologic evidence indicates that in some situations the

U^{234}/U^{238} ratio may be constant over periods up to 3.5×10^5 years.

Thurber (1962,1964), Koide and Goldberg (1965), Somayajulu and Goldberg (1966) and others have found the U^{234}/U^{238} ratio in the oceans to be constant at 1.15 ± 0.02 . Even in coastal marine waters where fresh-water with $U^{234}/U^{238} = 1.15$ is quickly diluted to the oceanic value of 1.15 (Blanchard, 1965). Miyake et al., (1966) did find variation of U^{234}/U^{238} ratio with depth in the ocean, finding lower values at depth near the oxygen minimum in bottom layers. However, application of the method is restricted to near-surface carbonate deposits (mostly corals and oolites) and the surface value of the U isotope ratio has been shown to be quite constant. In practise the method is limited by the precision of the experimental procedure. Most uranium activity ratios are measured to (at best) ± 0.01 which represents an error of 30,000 years in a 250,000 year old sample (12% error). To measure activity ratios to better than 1% accuracy would entail a more painstaking approach to measurement and interpretation of the alpha spectra. It is possible that over a long period of time fluctuations of the isotopic composition of parent ocean waters might be appreciable at the less than 1% level.

Better accuracy is promised by analysis of terrestrial deposits which characteristically have higher U^{234}/U^{238} ratios. Larger differences between initial and final ratios measured with the same accuracy as above permit greater precision in age determinations. However, the assumption that initial U^{234}/U^{238} isotope ratios can be estimated in fresh water carbonates is questionable.

An early proponent of the excess U^{234} method of dating, Thurber (1964) verified the 15% excess U^{234} in ocean water and modern corals and used the decay of this excess to date fossil coral from Eniwetok (Thurber et al., 1965). The precision of these analyses was limited by the precision of the equipment used. He also attempted to date terrestrial carbonate deposits of the Great Basin by decay of excess U^{234} . A wide range of U^{234}/U^{238} ratios was measured which did not, in general, decrease in a simple manner with age. The U^{234}/U^{238} ratio of waters from Pyramid Lake (1.46 ± 0.04) compared favourably with the average U^{234}/U^{238} ratio of carbonates from the same lake (1.47, error not calculated). The average U^{234}/U^{238} ratio for some Lake Lahontan Basin waters was 1.47 (range 1.22 to 1.86). However, an inverse relationship between U^{234}/U^{238} and lake level was established for Lake Bonneville. A possible explanation was proposed whereby mixing of rivers that feed the lake (which vary widely in isotopic composition) was restricted as lake level fell leading to variations in the lake water. U^{234}/U^{238} ratio of carbonates of Lake Bonneville varied from 1.74 to 2.30.

Kaufman (1971) has dated carbonates from the Dead Sea Basin by the Th^{230}/U^{234} method, using an isochron method to correct for detrital Th contamination. Based on these ages initial U^{234}/U^{238} ratios can be calculated. The values range from 1.51 to 1.70 with an average value of 1.54. Carbonates falling within the age range 13,000 - 35,000 years have more constant initial ratios (1.51 to 1.58, with an average of 1.54). Older carbonates falling within the age range 40,000 - 60,000 years have higher initial ratios (1.39 - 1.70, average 1.65) but these ratios are subject to higher analytical uncertainties.

Thurber et al. (1965) have suggested various criteria which may be useful for assessing the reliability of coral ages. Since these criteria may be used in part to assess the reliability of speleothem ages they are discussed briefly here. The seven criteria listed by Thurber can be summarized as (1) no recrystallisation, (2) narrow range of U concentration (2 - 3 p.p.m.), (3) $(U^{234}/U^{238})_0$ at zero time should be equal to the present-day oceanic value, (4) Ra^{226}/Th^{230} should be consistent with the age of the sample, (5) Th^{230}/Th^{232} ratio should be high (>50), (6) Th^{230}/U^{234} should be consistent with C^{14} age (for young samples) and (7) ages should agree with stratigraphic position. To these criteria could be added two further ones (8) Pa^{231}/U^{235} should be consistent with the ages of the sample and (9) Th^{232} concentration in the sample should be less than or equal to that in recent corals from the same area where the fossil corals were collected (Omura and Konishi, 1970). This last recommendation stems from measurements on partly calcitized corals which were found to assimilate Th as fine-grained terrigenous material.

It has been demonstrated by Pilkey and Goodell (1964) that cations present in molluscs can migrate even though no apparent recrystallisation has occurred in the sample. Under certain conditions therefore, unrecrystallised aragonitic marine carbonates may lose or gain radiochemical components.

Most aragonitic corals which appear to give reliable ages contain between 2 and 3.5 p.p.m. U (see references with Figure 8.3, Chapter 8.

Recrystallised corals commonly have lower uranium concentrations

than the 2.0 - 3.5 p.p.m. found in most unrecrystallised corals, (Schlanger et al., 1963). Fossil marine molluscs can assimilate up to 25 times the amount of U contained in living molluscs (Broecker, 1963, and Kaufman et al., 1971). This is explained in part by the decay of the organic component of the molluscs after death. A semi-micro reducing environment is formed and U^{6+} (as UO_2^{2+}) may be reduced to U^{4+} and deposited within the organism. If this process is complete shortly after the death of the organism no appreciable error will result, but the process seems to continue after molluscs have been sub-aerially exposed and in contact with ground waters (Kaufman et al., 1971). A constant(U) in cave deposits cannot be expected since ground water compositions and the rock types encountered by surface and ground waters vary considerably. The diagenetic change in (U) of fossils which is associated with organic matter, is not expected in speleothems.

As discussed above, initial U^{234}/U^{238} isotope ratios for checking Th^{230}/U^{234} ages in terrestrial carbonate deposits cannot be estimated until the factors influencing the uranium isotope ratio in surface and sub-surface waters are better understood. Initial isotope ratios calculated from ionium ages for many corals are slightly below the expected value of 1.15 (Thurber et al., 1965). Whether this reflects a true change in the U^{234}/U^{238} isotopic composition of sea water or experimental error is open to question.

Ra^{226}/Th^{230} ratios have been used extensively to check freshwater lucustrine and marine carbonate ages obtained by both C^{14} and Th^{230}/U^{234} dating. Well preserved samples generally gave concordant ages but major discrepancies between the three methods were observed (Kaufman and

Broecker, 1965. These authors found it difficult to determine where the error lies since C^{14} dating is also subject to errors. In general though, high ages seem to be attributable to excess Th^{230} and Ra^{226} and low ages to U addition. Ra^{226} is therefore of limited value as a check on the ionium or U^{234}/U^{238} dating method, particularly since any perturbation of the closed system would not be recorded by the Ra^{226}/Th^{230} ratio after about 8000 years.

In coralline material the ratio Th^{230}/Th^{232} is generally very high (>100). A correction for non-authigenic Th^{230} therefore does not have to be made except for the youngest samples. This applies only to quite pure $CaCO_3$ deposits; any associated detrital material contributes Th. The association of detrital Th with lacustrine deposits (gastropods, ostracods, marls, etc.) and the problems encountered in dissolution of these samples were described by Kaufman (1964). Not only are problems encountered with detrital phases but also non-authigenic Th can be included in the carbonate lattice and will therefore be released regardless of dissolution conditions. Only a fraction of Th in detrital phases is released upon mild acid dissolution. Kaufman chose to dissolve the entire sample and obtain the $(Th^{230}/Th^{232})_0$ ratio from analysis of recent samples. There is no guarantee, and in fact it would be surprising if this ratio were constant over long periods as must be assumed. A further problem arises when the time of addition of this detrital Th is considered. If addition is assumed to have been recent, when in fact thorium was present initially, ages may be too low and vice versa.

An isochron method was proposed by Osmond et al. (1970) to cor-

rect for non-authigenic thorium. If $\text{Th}^{230}/\text{U}^{234}$ is plotted against $\text{Th}^{232}/\text{U}^{234}$ and the data extrapolated to $\text{Th}^{232}/\text{U}^{234} = 0$, this would give the true $\text{Th}^{230}/\text{U}^{234}$ ratio in the sample, that is the ratio which would be measured if no detrital contamination were present. The slope of the straight line through a number of data points representing samples of the same age gives the $\text{Th}^{230}/\text{Th}^{232}$ ratio in the detrital component. If the points do not lie on a straight line then the method cannot be used because the $\text{Th}^{230}/\text{Th}^{232}$ ratio is variable. Osmond et al. dated fossil shells and beach rock from the Cape Kennedy area, Florida. Recent samples analysed fell on a line which could be extrapolated through the origin (that is, $\text{Th}^{230}/\text{U}^{234} = 0$ when $\text{Th}^{232}/\text{U}^{234} = 0$). This is convincing evidence that the method works. The modern samples had a $\text{Th}^{230}/\text{Th}^{232}$ ratio of 5.0. Kaufman (1971) used the technique to date inorganic marls from the Dead Sea Basin which were contaminated with detrital silicates. He found a $\text{Th}^{230}/\text{Th}^{232}$ ratio of approximately 2 for 20,000 to 40,000 year old samples. The spread of the data limited the accuracy of both studies. Fortunately, many speleothems are akin to corals in that they are quite pure and are not associated with detrital material.

The relatively high U content of modern and fossil corals enables them to be dated by the $\text{Pa}^{231}/\text{U}^{235}$ method. This offers an independent check on the ionium dating method since it is an independent age method and has a useful range of less than 1000 years B.P. to approximately 200,000 years B.P. The method has been applied successfully by Ku (1968) to check the well-documented ionium ages of Barbados corals (Broecker et al., 1968; Mesolella et al., 1969). Agreement between the two methods depends on a rather subjective choice of the Pa^{231} half-life. Until a

more precise half-life is measured, ages obtained by this method may be slightly inaccurate. A half-life of 34,300 years is suggested by Ku's data.

Komura and Sakanoue (1967) have also compared $\text{Th}^{230}/\text{U}^{234}$ and $\text{Pa}^{231}/\text{U}^{235}$ ages of aragonite corals and *Tridacna* shells from the Ryukyu Islands. The results of the two methods agree quite well though the use of *Tridacna* shells is limited by the low uranium content (<1 p.p.m.). Pa^{231} ages were generally slightly higher than Th^{230} ages but this can be attributed to too high a correction for initial Pa^{231} or the wrong choice of the Pa^{231} half-life. Acceptance of the higher half-life (34,300 years) would bring the two methods into better agreement.

The problem was encountered by Konishi *et al.* (1968) during a study of Holocene hermatypic corals from Taiwan. Pa^{231} ages were consistently higher than Th^{230} ages which were in turn consistently higher than C^{14} ages of the same material. Though some C^{14} ages were shown to be in error because of contamination with modern carbon, most of the error was assigned to inaccurate initial Th and Pa corrections. Young material is sensitive to the values chosen for the non-authigenic Th^{230} and Pa^{231} deposited in small amounts in the carbonates. This consideration is probably the limiting factor which determines the accuracy of the deficient Pa and Th methods, particularly when used to date very young material.

In summary, unrecrystallised coral seems to be eminently suitable as a material for deficient ionium and protactinium dating. The methods are restricted by incomplete knowledge of the extent of non-authigenic Th^{230} and Pa^{231} contributions, by the low Pa^{231} concentrations and by

the uncertainty as to the half-life of Pa²³¹.

Broecker (1963); Kaufman and Broecker (1965); Szabo and Rosholt (1969); and Szabo and Vedder (1971) have applied the deficient Th²³⁰ and Pa²³¹ methods to dating both fresh-water and marine molluscs. Szabo uses the method of neutron activation to produce U²³² from Pa²³¹ which avoids problems encountered during Pa separation and purification. In general the analysis of molluscs and other fresh-water species has met with little success, even when the material is un-recrystallised. Szabo and Rosholt (1969) proposed an Open System Model to allow for U, Th and Pa migration and obtained apparently reasonable results using this method. Recently, however, Kaufman et al. (1971) have disputed the basic premise of this model and in an analysis of most mollusc results conclude that the mechanism of addition or removal of the isotopes of interest is not well enough known to permit accurate age determinations.

The excess Pa²³¹/Th²³⁰ method, first proposed by Rosholt (1957) was applied to the absolute dating of deep-sea cores by Rosholt et al. (1961). The general validity of the method was proven in this paper but complications and limitations due to reworking of the sediments were recognized. In a later paper Rona and Emiliani (1969) obtained internally consistent ages for two Carribbean cores using the excess Pa²³¹/Th²³⁰ method. These authors still assumed that Pa and Th were geochemically coherent and used the initial value of the Pa²³¹/Th²³⁰ ratio (9.4) derived theoretically by Rosholt et al. (1961). This ratio is slightly modified to take into account the more recent determinations of the half-life of Pa²³¹ (32,480 years) and Th²³⁰ (75,200 years).

Rona and Emiliani's results, which dated the maximum of the penultimate glaciation at approximately 105,000 years B.P. were criticized by Broecker and Ku (1969) as being 25% too low. They criticized the results on two points, namely (1) that the U concentrations, measured by the previous authors were too low (and therefore the correction for U-supported Pa^{231} and Th^{230}) and (2) that the initial $\text{Pa}^{231}/\text{Th}^{230}$ ratio could not be predicted because Pa and Th are not geochemically coherent. Broecker and Ku argue that the log of the $\text{Pa}^{231}/\text{Th}^{230}$ ratio should be plotted against depth and the best straight line fit used to calculate the average sedimentation rate. This assumes that initial $\text{Pa}^{231}/\text{Th}^{230}$ ratios and sedimentation rates are both constant.

A low estimate of the (U) of the core lowers the estimate of the age. Mo et al. (1970), in an independent series of analyses obtained U concentrations on an average 20-30% higher than Broecker and Ku and a factor of 3 higher than Rona and Emiliani. If the values of Mo are correct then even Broecker and Ku's ages are too low and Rona and Emiliani's are even lower. These points have not yet been resolved.

The $\text{Pa}^{231}/\text{Th}^{230}$ method is limited by surface reworking of the sediments to at best a resolution of 2000 years. A further potential source of error, as pointed out by Bonatti et al. (1971), arises from the post-depositional mobility of U in sediments showing evidence of oxidised and reduced zones. U is concentrated in reduced zones whereas Th (and probably Pa) appear to be immobile.

The excess $\text{Pa}^{231}/\text{Th}^{230}$ dating method, though useful in principle, offers considerable analytical problems and has yet to yield unambiguous results.

2.4.1 Uranium Series Dating of Speleothems

Rosholt and Antal (1962) attempted the first analyses of speleothems. They measured the $\text{Th}^{230}/\text{Pa}^{231}$ ratios in a number of stalagmites but did not attempt to measure the $\text{U}^{234}/\text{U}^{238}$ ratio. The uranium content of these deposits varied from 0.012 p.p.m. to 0.8 p.p.m., but in general the (U) was less than 0.1 p.p.m. The authors did not consider the stalagmites to be suitable for dating. Each sample contained excess Pa^{231} and Th^{230} which was attributed to post depositional leaching of U. From the measured daughter activities they calculated that the initial U content was between 1 and 5 p.p.m. indicating that in most cases considerable U leaching had taken place. Samples with low levels of detrital contamination showed low Th^{228} ($=\text{Th}^{232}$) activity indicating that the excess Th^{230} activity at least was not derived from a detrital source.

The deficient ionium method has also been applied to dating speleothems by Cherdyntsev (1965); Fornaca-Rinaldi (1968); Duplessey et al., (1970, 1971) and in a single instance by Komura and Sakanoue (1967).

Cherdyntsev, in a study of calcareous and ferruginous cave travertines concluded that this material was suitable for dating by the deficient ionium method despite considerable amounts of detrital Th. An initial value of 0.54 for the $\text{Th}^{230}/\text{Th}^{234}$ ($=\text{Th}^{230}/\text{U}^{238}$) ratio was measured on the ferruginous travertines whereas the purely calcareous stalactites gave values of <0.01 . The deposits were apparently unsuitable for dating by the excess $\text{U}^{234}/\text{U}^{238}$ method because of large variations (1.10 - 1.41) between modern deposits within the cave (Akhshtyr Cave, Kraznodar region, U.S.S.R.). Cherdyntsev found that in general $\text{U}^{234}/\text{U}^{238}$ ratios in cave-deposited travertines and stalagmites varied from region

to region and even at the same site over a period of tens of thousands of years. In ferruginous travertines from Hungary, Cherdyntsev also found high Th concentrations and in a modern travertine, a high $\text{Th}^{227}/\text{U}^{235}$ ratio (1.40 ± 0.07) which he attributed to excess Ac^{227} ($t_{1/2} = 22$ years). In general $\text{Th}^{230}/\text{Th}^{234}$ and $\text{Th}^{227}/\text{U}^{235}$ ($=\text{Pa}^{231}/\text{U}^{235}$) ages were in agreement for travertines and some cave deposits leading Cherdyntsev (1971) to conclude, "The retention of radioactive elements in travertines is usually satisfactory, except in small layers inside Quaternary deposits. The retention is much poorer in carbonate deposits of karst caves, which often lose uranium (though not as extensively as is believed by Rosholt and Antal); occasionally, an entry of U can be shown to take place." The travertines yielded ages of $95,000 \pm 10,000$ years and $225,000 \pm 35,000$ years and the Akhshtyr cave stalagmites $35,000 \pm 2000$ years.

Fornaca-Rinaldi, working with deposits from Italian caves measured $\text{Th}^{230}/\text{Th}^{234}$ ratios of various speleothems but neglected to measure $\text{U}^{234}/\text{U}^{238}$ ratios, assuming this ratio to be near unity. Appreciable excess U^{234} can occur in speleothems which would result in high $\text{Th}^{230}/\text{U}^{238}$ ages if a unity ratio were assumed. Because Fornaca-Rinaldi dated deposits <80,000 years old the error involved is probably quite small. U concentrations of between 0.2 and 0.5 p.p.m. were measured. The absence of non-authigenic Th was confirmed in very pure speleothems but those same deposits were found to contain high β -activity, attributable to excess Pb^{210} ($t_{1/2} = 22$ years) in rain waters. Po^{210} activity was observed in the Th spectra indicating that separation of Th from Bi was incomplete. In addition, many of the samples contained Th associated with

an insoluble detrital phase. Most of these were considered to be unsuitable for dating purposes.

Duplessey et al. (1970) have dated stalagmites from the Aven d'Orgnac (Ardeche, S. France) by both C^{14} (Labeyrie et al., 1967a) and the deficient ionium methods. The initial U^{234}/U^{238} ratio of the columnar stalagmite analysed in detail by Duplessey et al. varied from 1.09 to 1.25. U concentrations between 0.064 p.p.m. and 0.117 p.p.m. were measured. No regular decrease in U^{234}/U^{238} ratio along the length of the stalagmite was measured as would be expected for a constant U^{234}/U^{238} ratio in the parent water. Water in the cave has a present-day ratio of 1.03 (Nguyen and Lalou, 1969). The Th^{230}/U^{234} ratio varied in a systematic manner though and allowed the time of the start of deposition to be determined as 130,000 years B.P. and the period of growth to be 40,000 years. The rate of growth varied from an average of 3.2 cm/ 10^3 years between 120,000 years and 100,000 years ago to an average of 14.5 cm/ 10^3 years from 100,000 to 93,000 years B.P. A high rate of 60 cm/ 10^3 years appears to have occurred between 93,000 and 92,000 years B.P. The material used met the requirements that Th^{230} be authigenic since Th^{230}/Th^{232} ratios as high as 1000 were measured on samples from the centre of a column from the same cave. Samples from the outside of the same column, however, gave values of 8.4 indicating appreciable detrital Th concentrations on the outer surfaces of the deposit.

Labeyrie measured rates of growth of a modern (6500 years B.P. to present) columnar stalagmite by C^{14} dating. The average growth rate was 32 cm/ 10^3 years though the rate was not constant. Growth was constant over the last 4000 years, but twice as slow in the period 6500-

4000 years B.P. (on average). No instances are reported of dating the same speleothem by C^{14} and Th^{230} .

Komura and Sakanoue reported a single analysis of a stalagmite which yielded inconsistent results, probably due to non-authigenic Th leached from detrital material present as brownish-yellow coloured rings. Again measured U^{234}/U^{238} values were close to and in one case less than, unity. Low U concentrations between 0.09 p.p.m. and 0.13 p.p.m. were measured. Two samples of cave water, one from the entrance and the other from the exit of Yuki cave in Okinawa had U^{234}/U^{238} values of 1.34 and 1.35 respectively. The stalagmite was collected from Ikejima "very near by Okinawa-jima" though the precise locations are not given. The analyses were not precise enough to date its formation but a minimum age of 15,000 years was proposed.

Speleothems, therefore, appear to be quite suitable for dating by the deficient ionium method if care is taken to obtain pure deposits. When errors in dating do occur they can generally be attributed to U loss. Except for ferruginous cave deposits, the (U) of speleothems appears to be uniformly low. The attraction of such deposits for accurate dating is somewhat less in light of this, especially if recent samples are analysed. The results published so far indicate that initial U^{234}/U^{238} ratios in cave waters are variable and therefore the excess- U^{234} method of dating cannot apparently be used.

This concludes the description of the dating methods. Before the principles of stable isotope geothermometry are introduced a chapter is devoted to the description of the West Virginia area and the caves studied. The chapters were organised this way because the discussion of some of the stable isotope results assumes a knowledge of the area in general.

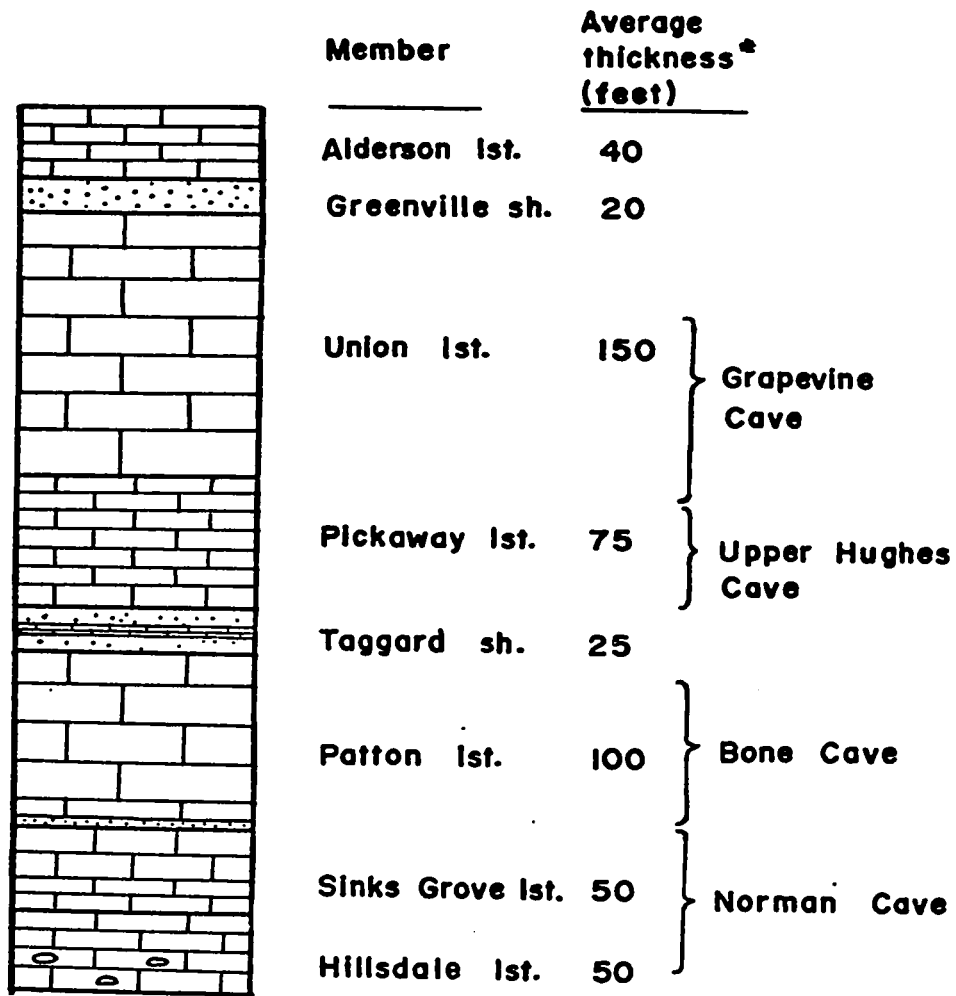
CHAPTER THREE

DESCRIPTION OF THE PRINCIPAL FIELD AREA, GREENBRIER COUNTY, WEST VIRGINIA

3.1 The Local Stratigraphy

The caves encountered in this study are formed in limestones of the Greenbrier Series which are of Lower Mississippian age. The strata dip at a shallow angle to the S.S.W. The Greenbrier river generally follows the strike and is incised to the base of the Greenbrier Series. The caves are formed in the valley and ridge province at the base of the Allegheny Front. The Greenbrier Series is part of a sedimentary sequence ranging from Silurian to Pennsylvanian in age. A generalized section of the series in Greenbrier County, West Virginia is shown in Figure 3.1 (from Price and Heck, 1939). The stratigraphic position of the caves studied are included in the diagram. The Greenbrier Series increases in thickness from about 100 feet (30.4 m) in Monongalia County in the north to 1050 feet (318 m) in Mercer County in the extreme southern part of West Virginia. No unconformities have been recognised in the Series.

The Alderson Limestone is the youngest member of the Greenbrier Series. It is a thick-bedded, crystalline and fossiliferous, dark grey limestone, high in silica. Cave development is usually restricted within this member because the underlying Greenville shale limits downward development. Relatively few caves are known in the Alderson limestone.



* In the area of Renick, Greenbrier Co.

N.B. Thin interbeds are omitted from this generalised section.

Figure 3.1 Generalized stratigraphic section of the Greenbrier limestone series (from Price and Heck, 1939)

The Greenville Shale, a highly calcareous shale acts as an aquiclude but when breached it generally gives access to a large cavern. Grapevine Cave is an example of this. The shale is highly fossiliferous and weathers brown to dark red.

The Union Limestone is a very pure, thick-bedded oolitic limestone, the thickest member of the Series. Extensive cave development has taken place in this member.

The Pickaway Limestone grades almost imperceptibly into the Union limestone. It is a very pure limestone, characterized by very thin shale layers which interdigitate with the limestone beds. Cave development in this member is extensive.

The Taggard Formation is an impervious mixture of limestone and shale beds. A relatively thin limestone is sandwiched between two thicker, red shale beds. The Taggard Formation acts as an aquiclude but it is occasionally breached and often gives rise to subterranean waterfalls. The formation acts as an important marker bed in the local stratigraphy.

The Patton Limestone is also very pure and fossiliferous. Extensive cave development occurs in this member when the Taggard shales are breached.

The Patton Shale is a thin, impervious bed which acts a barrier to percolating, vadose water but not to cave development. It is often breached and can be recognized as forming the lip of an underground waterfall

The Sinks Grove and Hillsdale Limestones, the oldest members,

grade imperceptibly into one unit but both have characteristic features. The Sinks Grove is thick-bedded, dark grey and of uniform texture, whilst the Hillsdale contains an abundance of chert nodules and Lithostrotion corals. A cave passage in the Hillsdale is readily recognised by the nodular protuberances on walls and ceiling. Cave development in both the Sinks Grove and Hillsdale limestones is extensive.

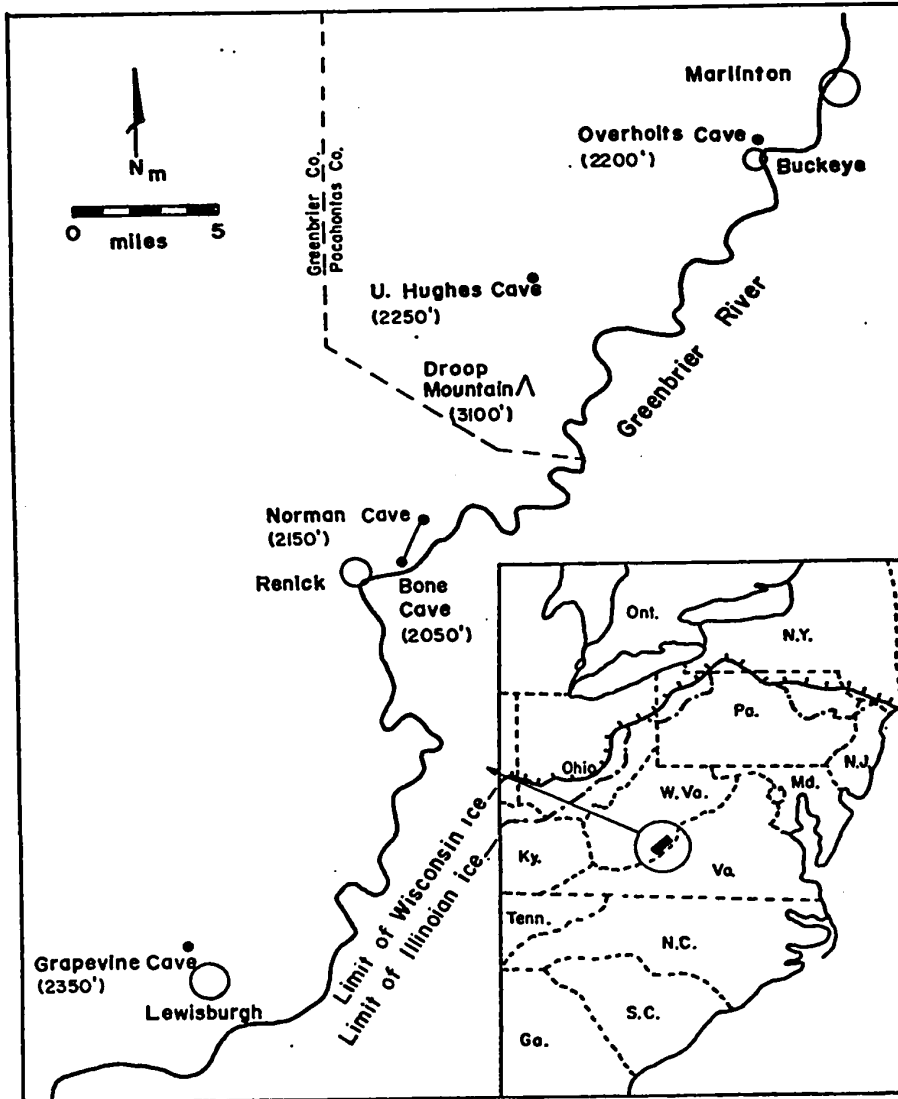
In general, the limestones are non-porous and cave development is along open joints, bedding planes and faults. According to Rutherford (1971) faulting has played an important part in the development of caves in Greenbrier County. For a more detailed description of the area see Wolfe (Ph.D. thesis, to be published).

3.2 Description of the Caves Studied

Of the numerous caves in Greenbrier County the Norman-Bone Cave System and Grapevine Cave (now the commercialized "Lost World") were chosen for intensive study.

Their location is shown in Figure 3.2. The location of two other caves (Hughes Cave and Overholts Blowing Cave) from which samples were obtained is also shown in this figure. Both caves were considered unsuitable for dating or paleotemperature work. Hughes Cave was sampled for present-day uranium-isotopic composition of its waters and Overholts Blowing Cave for stable isotopic composition of present-day drip waters. Some dating work was attempted in Overholts Blowing Cave but was abandoned because of very low uranium concentration in speleothems and in present-day waters. Only one drip-water was obtained from Overholts Cave so a full description of the cave is not relevant here. The sampling

Figure 3.2 Sketch map of the principle field area in West Virginia showing the location and elevation (above msl) of the caves studied. (The maximum limits of the ice advances are from Flint, 1971).



site in Hughes Cave is shown in Figure 3.5.

3.2.1 The Norman-Bone Cave System

A line diagram of the cave showing sampling sites is shown in Figure 3.3. The cave is developed in the lower part of the Greenbrier Series, predominantly in the Patton and Hillsdale limestones. It is a multi-level network with over nine miles (15 km) of passages mapped, but only two entrances to it are known. The upper, or Norman entrance is close to where a stream sinks underground. This stream is encountered a short way into the cave and can be followed for nearly 3.4 km to a point where the passage becomes completely flooded. The water resurges a 100 metres or so further on in the bed of the Greenbrier River. A climb out of the flooded passage leads, via a network of upward trending passages, to the second, downstream entrance of the cave. This portion is Bone Cave, a fossil exit cave which is very dry and dusty.

The cave is a "classical" river cave with linear development and progressive entrenchment which has shifted passages downwards from the initial phreatic conduits. The high levels are therefore the oldest. The uppermost (exit) passage of Bone Cave appears to be the most ancient fragment of the system. These high levels are moderately dry to very dry. Low levels are very damp because of the perennial stream in them.

Both in the low and high level passages there are numerous areas where extensive speleothem deposits are encountered. In the higher levels the deposits are mostly fossil though there are important exceptions. The Butterscotch Room, located close to the Norman entrance, is an abandoned level which contains dozens of fossil, columnar stalag-

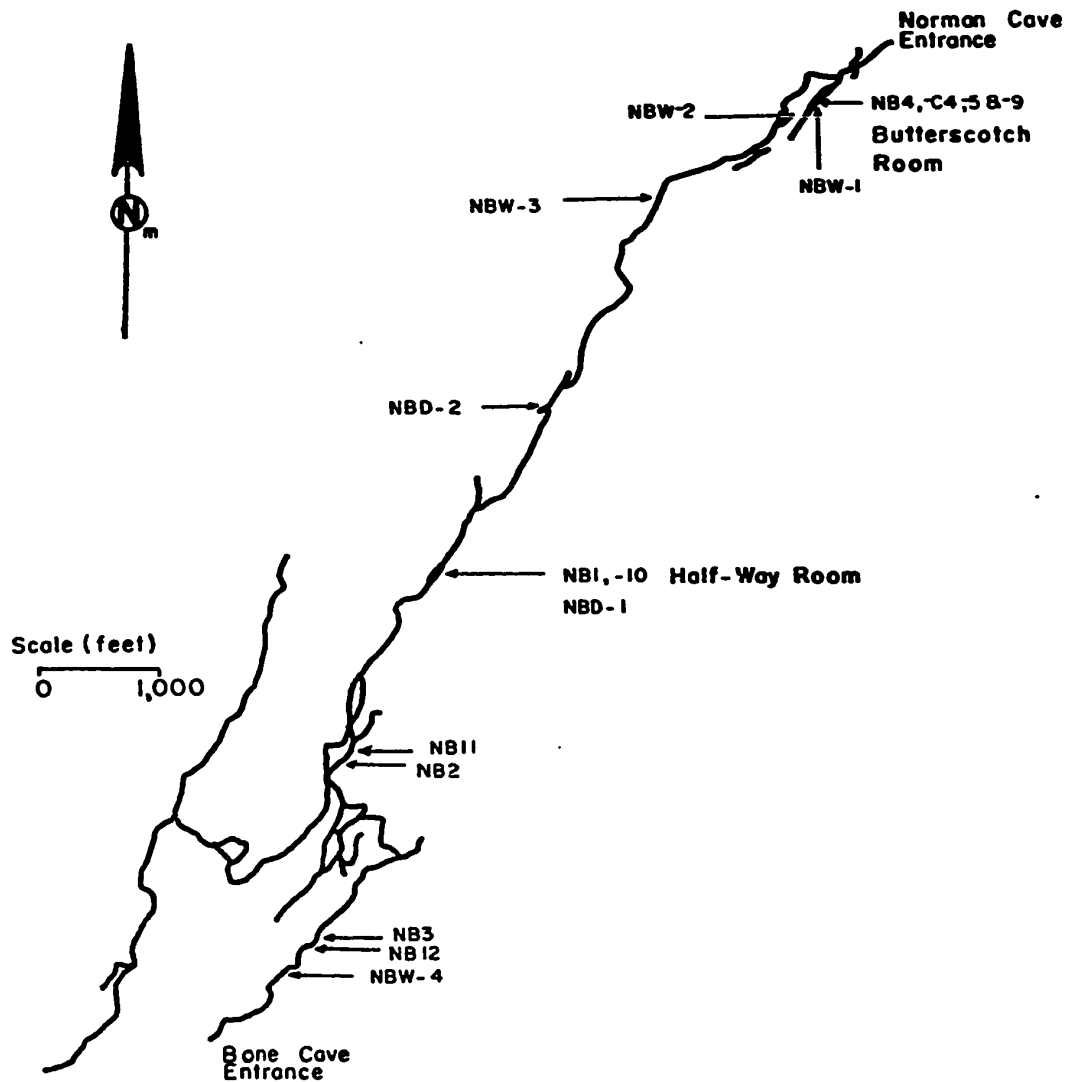


Figure 3.3 Line diagram of the Norman-Bone Cave system showing the collection sites.

NB- = speleothem sample

NEW- = drip-water sample for U isotopic analysis.

NBD- = drip-water sample for stable isotopic analysis.

mites as well as many broken deposits, presumably the result of tectonic activity (though some evidence of vandalism is apparent). Sheets of flowstone cover the floor but these are not very thick (5-10 cm). Some broken stalagmite or stalactite fragments which have been severely eroded by re-resolution are lightly cemented to the floor and offer evidence of a period when vadose waters submerged the fallen deposits. Roof deposits are uncommon in the Butterscotch Room as in other parts of the cave. Where stalactites occur they are as tubular soda-straws or "plugged" soda-straws which have developed into more solid pendant forms. These stalactites are often clustered around ceiling joints and in some cases effectively stop seepage through such joints when the whole mass becomes solidly cemented together.

Other fossil deposits are encountered at higher levels in the form of extensive sheets of flowstone. Sometimes these deposits almost block the passage making further progress impossible. In terms of volume this flowstone probably accounts for the majority of CaCO_3 deposited in the cave.

The Half-Way Room (so named by the author because of its position roughly half-way between the two entrances) is an abandoned high level room enlarged by collapse and subsidence. It contains numerous deposits both modern and fossil. These deposits tend to be of the same type as those encountered in the Butterscotch Room (columnar stalagmites) but in this case recent stalagmites are forming by the side of fossil ones. (It is possible that the new growth is on the surface of old stalagmites but this was not checked). These modern deposits are very pure.

During a traverse of the cave from the Norman Cave entrance to

Bone Cave no other areas of extensive stalagmite deposition are encountered until the upper level of Bone Cave is reached. The speleothems in Bone Cave are, with one exception, completely fossil. The exception is a large flowstone bank which is being dissolved by "aggressive" seepage water. Almost the entire length of this exit passage is floored with flowstone. The flowstone is overlain by a thin layer of very fine dust. The majority of the speleothems are dirt-encrusted and dull in appearance. In general, these deposits are smaller than those of the Butterscotch Room and the Half-Way Room.

Recent speleothems are distinguished from these fossil deposits by their clean, white surfaces. Most of the current deposition is taking place in the stream passage as small tubular stalactites. In general, extensive, present-day speleothem deposition is restricted to only a few sites in the entire cave. Apart from the blockage of seepage outlets by CaCO_3 cementation (mentioned above), it is possible that the relatively small number of active sites is caused by regional de-forestation. It is conceivable, for example, that the surface run-off is increased at the expense of groundwater seepage by clearing of the forest for grazing. It is likely that both soil CO_2 levels and seepage rates were lowered sufficiently to diminish speleothem deposition. This illustrates that non-climatic effects may affect the rate of growth of speleothems.

3.2.2 Grapevine Cave

The cave is located 20 miles (32 km) S.W. of Norman Cave and at approximately the same elevation. It is developed in the Union limestone and upper part of the Pickaway limestone of the Greenbrier Series. A

small amount of the Greenville shale overlies the cave and is apparent near the one natural entrance, a 38 metre pit. A second horizontal entrance was excavated when the cave was opened to the public.

Figure 3.4 is a map of the cave showing the sample sites. It is basically two large rooms separated by breakdown and massive stalagmite columns. Beyond the second room a narrow crawlway leads to a further large passage liberally decorated with speleothems. The cave ends in a high canyon, impassably narrow.

The cave is developed along a joint which pinches out at the downstream end of the cave. Collapse and subsidence has greatly increased the size of the original cave; the floors of the two large rooms are strewn with breakdown blocks. Only a very small stream occupies the cave at present and this is entrenched to a lower, constricted level.

Both fossil and active speleothems are encountered. By far the largest proportion of the speleothems are inactive. These are mostly large stalagmites though some large roof deposits are encountered. The largest of the fossil stalagmites is 12 metres high and 4 metres in diameter. Most of the deposits have a dull, white surface and are, in general, well preserved. Some flowstone deposits are found which partially cover and cement the breakdown.

The modern deposits are also predominantly stalagmites but in one section of the cave a large, complex stalactite-stalagmite pair is active. The modern stalagmites vary in size but are mostly between 50 cm and 3 metres high. These active deposits are confined to two areas; one in the smaller room (GVC-2 and -3 are modern stalagmites) and the other in the unsurveyed passage, beyond the constriction.

Figure 3.4 Sampling sites in Grapevine Cave, Greenbrier County.

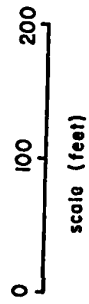
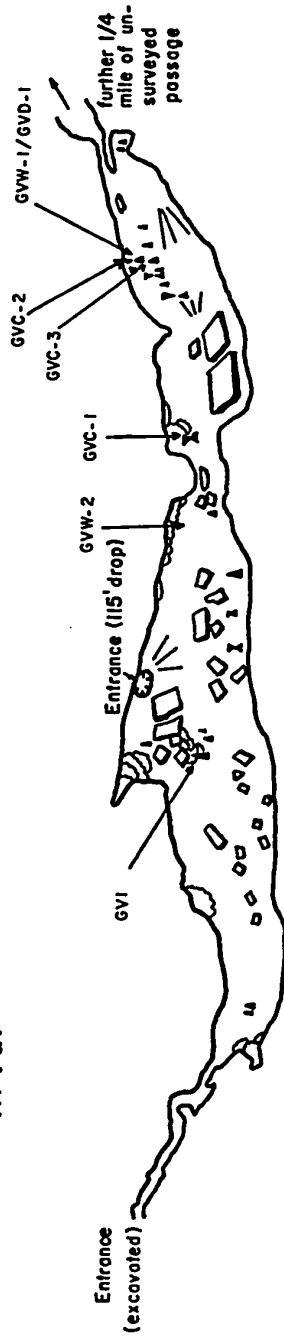
GV- = speleothem sample

GVW- = drip-water sample for U isotopic analysis

GVC- = speleothem drill core

GVD- = drip-water sample for stable isotopic analysis

Grapevine Cave
Greenbrier Co.
W. Va.



- Legend
- ◊ breakdown
 - ▲ prominent stalagmite
 - ▼ " stalactite
 - ⊗ column
 - ⚡ flowstone
 - ▾ slope (down in played direction)

The deposits of Grapevine Cave tend to be much larger than the deposits of Norman-Bone Cave. This is in part due to the abundant supply of seepage water entering Grapevine Cave along a major joint that reaches the surface (the entrance pit is developed along this joint). This water is not interrupted in its downward flow by extensive shale bands as is the case with Norman-Bone Cave.

There are obvious advantages to sampling these large stalagmites which are assumed to be deposited over long periods of time; this is only possible by taking drill cores. Because of the abundance of material, some released by blasting operations during the commercialization of the cave, and the electric power lines which make drilling possible, the cave was studied extensively during the summer of 1969.

3.2.3 Upper Hughes Cave

The cave is developed in the Pickaway limestone near the contact between this and the Taggard Formation. Water from the cave flows over the impervious Taggard shale and sinks again 65 metres downstream in Lower Hughes Cave. The Upper Cave consists of a lower active stream passage and an upper, fossil level. The site was located in a small side room off the upper level. Water samples and a single modern stalagmite were collected for U^{234}/U^{238} isotopic analysis. No other speleothems in the cave were considered worth analysing because of their impure appearance. A map of the Upper Cave is shown in Figure 3.5.

3.2.4 Overholts Blowing Cave

Overholts Cave, located in Pocahontas County, is an extensive river cave which carries a perennial stream. The cave has a single

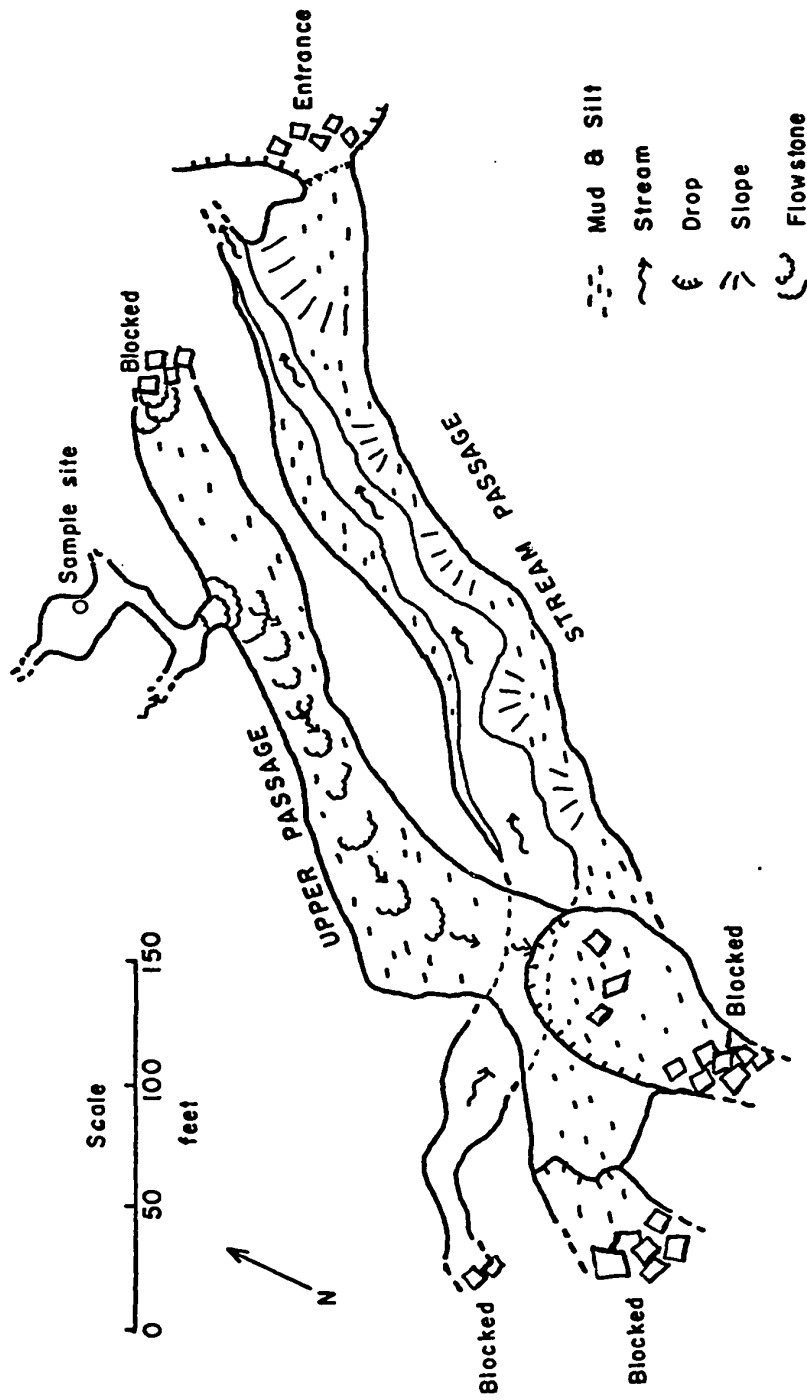


Figure 3.5 Upper Hughes Cave, Pocahontas County, showing location of sample site.

known entrance which, as the name implies, blows cold air most of the year. Because seasonal temperature fluctuations occur throughout the cave it was not considered suitable for paleotemperature studies.

3.3 West Virginia Climate

The climate records of West Virginia in the areas of interest are summarised in Table 3.1. Lewisburg is 5 miles (8 km) S.E. of Grapevine Cave. Buckeye is one mile (1.7 km) east of Overholts Blowing Cave.

Table 3.1

Climate Data for Greenbrier and Pocahontas Counties, West Virginia

Location	Elevation	Average Jan. Temp. (°C)	Average July Temp. (°C)	Average annual Temp. (°C)	Average annual precip. (mm)
Lewisburg*	2250 ft	0.40	21.8	10.9	1010
Lewisburg**	2250 ft	-1.25	22.0	11.0	915
Buckeye**	2100 ft	-3.00	20.5	10.3	1095

* Information based on the period 1900-1935 (Price and Heck, 1939)

** Information based on the period 1967-1971 (U.S. Department of Commerce)

Summer precipitation is derived from moist tropical air which flows northeast from the Gulf of Mexico or northwest from the South Atlantic. Much of the moisture has been lost by the time the air masses reach West Virginia so most of the precipitation occurs as light showers. Heavy thunderstorms occasionally occur in West Virginia when

hurricanes precipitate their remaining moisture. On these occasions very high rainfall has been recorded e.g. in 1969, 22cm of rain fell in one day in Greenbrier County (Hurricane Camille). During the colder half of the year precipitation is derived from frontal storms which move in from the northwest, west or southwest. Again many of these fronts have lost much of their moisture before reaching West Virginia.

The floods resulting from heavy storms can often completely fill even large caves with water and sediment. When the floods subside sedimentary sequences are often completely re-worked. These catastrophic events are quite infrequent though. Norman-Bone Cave is subject to flooding but, except for samples collected in the streamway, all the samples were collected from above any possible high-water level. Fragile, soda-straw stalactites in the stream passage remain unbroken after heavy floods indicating that the stream never fills the cave passage. Grapevine Cave is not influenced by such floods since the only stream in the cave is at a lower, inaccessible level. This stream is very small and fluctuates only slightly in flowrate.

These sporadic storms cause a temporary increase in the rate of seepage into the cave. Under these conditions it may be quite possible that the seepage waters are undersaturated and are dissolving rather than precipitating CaCO_3 on the speleothems. A chemical study has not been carried out to check this assumption.

Past climates in this region have been reconstructed by various disciplinary approaches. Clark (1968) presents evidence for colder climatic conditions in West Virginia during Pleistocene cold phases. This evidence is based on the occurrence of sorted patterned ground in areas

where current climatic conditions are not sufficiently severe to produce such cold-climate forms. The range of elevation within which such forms are found in Greenbrier and neighbouring counties is 2450-3650 feet (747 to 1113 meters). Evidence also comes from the Blue Ridge Province, Roanoke, Virginia. Michalek (1969) studied alluvial fans formed by solifluction in a periglacial environment and concluded that mean annual temperature was reduced by 15°F (8.3°C) during the Wisconsin cold period. He concluded that the snowline was lowered to 6500 feet (1980 m) and the treeline to between 3000 (910 m) and 3500 feet (1065 m).

Additional evidence for climate deterioration has been obtained for the Virginias through palynological studies. Craig (1969) studied pollen profiles in lake sediments of the Shenandoah Valley, Virginia. He concluded that the vegetation was affected by glacial advance in the north though not to a drastic extent. Boreal forest predominated 13,000 years ago and by 9,500 years B.P. vegetation was much the same as at present (mixed hardwood-deciduous forest). However, since this period was a time of climatic amelioration pollen typical of true periglacial climate may not have been present. It is possible that plant species growing during these periods could have been reflecting the availability of water. Also the possibility exists that the pollen species present were transported to the present site from a more southerly latitude. Conclusions drawn from this study were that climate changes were not extreme and that the Shenandoah Valley may have constituted a refugium during cold periods. A pollen profile measured by Cox (1968) near the West Virginia/Maryland border supports the conclusion by Craig that changes in climate were not extreme.

The geomorphic/geologic and palynological studies do not appear to be compatible. Conditions which produce sorted stripes, nets and polygons indicate former frozen ground, and possible permafrost (Flint, p282 1971) Patterned ground occurs at altitudes as low as 2450 feet (745 m) therefore the effect on vegetation should have been extreme. However, the inferred boreal climate from the Shenandoah Valley and Southern Maryland is typical of milder climates. The differences are possibly explained by altitude effects. Hack and Quarles Ponds (Shenandoah Valley) are at elevations of 1540 feet (468m) and 1460 feet (498 m) respectively and the vegetation was possibly not subjected to as low temperatures as the higher elevations in Greenbrier County.

A further factor which should be considered is that the occurrences described above are possibly not of the same age and that gradation of climate is part of a natural sequence. Arctic-type climate which produced the patterned ground could have graded into boreal climate and then into present climate conditions. It seems reasonable to conclude that at some point during the Wisconsin glacial phase much colder climate prevailed in West Virginia even at relatively low altitudes of about 2450 feet (745 m). At higher altitudes permafrost or seasonally frozen-ground prevailed while at lower altitudes a vegetation (including forest) cover occurred throughout at least the latter part of the Wisconsin (13,000 to 10,000 years B.P).

3.4 Relation Between Surface Air Temperature and Cave Temperature

The air and water entering a cave will, after reaching thermal equilibrium, assume the temperature of the surrounding rock. The temperature of the rock at depth will reflect mean annual surface temperatures and so the temperature of air and water within a cave when in thermal equilibrium with the wall-rock should be a measure of mean annual surface air temperature. There is expected to be a lag between a change in the mean annual surface temperature and the response to this change in the cave because of the finite rate of heat transfer through the rock. Cropley (1965) has shown the response time to be small when the cave is of shallow depth (Table 3.2).

Table 3.2

Response of Cave Temperature to Variations in Surface Air Temperature*

Depth (feet)	Annual Temp. Variation (\pm °F)	Time Lag (days)
0	19.3	0
1	16.9	7.04
5	10.5	35.20
10	5.6	70.40
25	1.0	176.00
50	0.05	352.00

* (from Cropley, 1965)

These figures are applied specifically to the Lewisburg area with an average annual temperature of 51.6^oF (10.9^oC) and an average

annual temperature variation of 19.3 °F (10.7 °C).

Thermal equilibrium between the cave air, water and limestone must not be upset by the invasion of large amounts of warm or cold water (or air) into the cave. If a stream of fluctuating volume flows into a cave then the cave must be long enough to allow water, air and rock to achieve thermal equilibrium. Two detailed temperature studies in West Virginia caves have been undertaken to assess the effect of changing surface conditions on cave temperature. Davies (1960) studied an extreme situation where air and water flowed through the 270 metre long Martens Cave (near Droop Mountain). The cave air temperature varied between -2.8°C and 11.7°C in response to seasonal temperature fluctuations and the invasion of large amounts of cold water in winter. Isotopic temperatures of deposition of speleothems from such a cave would clearly not reflect mean annual temperatures. Cropley (1965) undertook a more detailed study of two of the larger caves in West Virginia, namely Greenbrier Caverns and Ludington's Cave near Lewisburg. Both caves contain a perennial stream. Cropley observed that cave temperatures in the stream passages did not become equal to mean annual surface air temperatures until measurements were taken 1500 metres from the respective entrances. In general, cave temperatures were lower than mean annual surface temperatures. This was attributed to the increased volume of the underground streams during the winter. It was noted, however, that relatively dry, draft-free rooms are of constant temperature.

In light of these findings the suitability of Grapevine Cave and Norman-Bone Cave for paleotemperature work can be assessed. There is no evidence that a large stream occupied Grapevine Cave after the breakdown

phase. Most of the speleothems are deposited on breakdown so it can be concluded that temperatures were not affected by external factors other than secular temperature variations. It is possible that the entrance pit acts as a sink for cold, dense air and this might tend to lower cave temperatures slightly. This is not expected to have a significant effect on average cave temperatures.

Norman-Bone Cave is similar to those described by Cropley in that it contains a perennial stream. Therefore significant temperature variations can be expected in the first 1500 metres of the streamway. The Butterscotch Room is close to the streamway but separated from it by a crawlway. It, therefore, can be classed as a dry, draft-free room. The only temperature variations expected are those caused by a change in the amount of heat conducted by the limestone at the surface. The roof of the Butterscotch Room is at least 15 metres below the surface. The Half-Way Room is high above the stream and >1500 metres inside the cave and therefore the rock and air are expected to be in permanent thermal equilibrium. No accurate data on the depth of this room was available but it was estimated to be between 30 and 60 metres beneath the surface. No samples were collected directly from the streamway for stable isotopic analysis.

CHAPTER FOUR

THE STABLE ISOTOPIC GEOCHEMISTRY OF SPELEOTHEMS AND PALEOTEMPERATURE ANALYSIS

4.1 Introduction

The part of this study concerned with stable isotopic analysis of speleothems was undertaken from the start with reservations. It was understood that interpretation of results in terms of paleoclimate change would be difficult. Some promising results obtained by Hendy (1969) on New Zealand speleothems, however, encouraged further work. The theory of the isotopic geochemistry of speleothems has been developed adequately by Hendy in his thesis and later publications (1970, 1971). Consequently this chapter is more concerned with the application of the method and its assessment in a different situation to that encountered by Hendy.

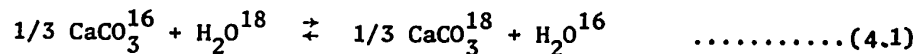
The problem of paleotemperature analysis via oxygen isotopic abundance measurements reduces to one of firstly establishing that CaCO_3 was deposited in isotopic equilibrium and secondly to one of identifying the change in isotopic abundance due to temperature changes. This latter problem involves distinguishing between changes in the isotopic composition of the CaCO_3 due to temperature changes and those due to changes in the isotopic composition of regional precipitation.

Because of the problems involved in interpreting the isotope curves constructed during the course of this study a second, independent

method of temperature analysis was attempted. This method involves analysis of fluid inclusions in the CaCO_3 for Deuterium/Hydrogen (D/H) ratio, an indirect measure of $\text{O}^{18}/\text{O}^{16}$ ratio of the water. These inclusions are considered to represent "paleowaters". An advantage of the method is that actual temperatures of deposition can be measured. This aspect of the study was started at a late date and is incomplete. The results obtained are interesting, though, and are included in this chapter despite their preliminary nature.

4.2 Isotopic Fractionation in the System $\text{CaCO}_3 - \text{CO}_2 - \text{H}_2\text{O}$

The redistribution of the stable isotopes of oxygen and carbon between various coexisting ionic and molecular species in solution can be described in terms of an equilibrium constant. For example in the equilibrium exchange reaction involving CaCO_3 and H_2O :



$$K = \frac{(\text{CaCO}_3^{18})^{1/3} (\text{H}_2\text{O}^{16})}{(\text{CaCO}_3^{16})^{1/3} (\text{H}_2\text{O}^{18})} \quad \dots\dots\dots(4.2)$$

The experimentally measured fractionation factor (α) is defined as:

$$\alpha = (\text{O}^{18}/\text{O}^{16})_{\text{calcite}} / (\text{O}^{18}/\text{O}^{16})_{\text{water}}.$$

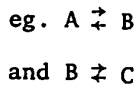
For one atom exchange (as above) $\alpha = K$. In general where the maximum number of exchangeable atoms is n in any one of the molecules under consideration $\alpha = K^{1/n}$. The value of K can be measured experimentally or calculated using the methods of statistical mechanics. It is found

to be temperature dependent, but independent of pressure or activities of other dissolved species. Agreement between experimental and calculated values is generally quite good (Urey, 1947; Urey et al., 1948; Epstein et al., 1953; Clayton, 1959; and O'Neil et al., 1969) over a temperature range 0 to 500°C. The measured fractionation factor for the above exchange reaction is 1.0280 at 25°C and 1.0339 at 0°C (O'Neil et al., 1969). This indicates that CaCO₃ will be slightly enriched in O¹⁸ when equilibrium is reached at 25°C and will become progressively enriched in O¹⁸ at lower temperatures.

Permil fractionation factors (ϵ) are often used in place of α :

$$\text{where } \epsilon = (\alpha - 1) \times 1000 \text{ } \text{‰} \dots \dots \dots (4.3)$$

It is convenient to use ϵ when two consecutive exchange reactions are being considered:



It can be shown that Permil fractionation factors are approximately additive:

$$\text{i.e. } \epsilon_{AC} \approx \epsilon_{AB} + \epsilon_{BC} \quad \text{for } \epsilon \ll 1000 \quad \dots \dots \dots (4.4)$$

The common notation used in measuring isotopic fractionations is the "del" notation. Because absolute changes in isotopic composition are small, samples are compared to a standard and the difference in isotopic composition between the sample and standard is used for comparison between samples. For example in oxygen isotopic analysis:

$$(\text{"del" } O^{18}) \delta O^{18} = \frac{(O^{18}/O^{16})_{\text{sample}} - (O^{18}/O^{16})_{\text{std.}}}{(O^{18}/O^{16})_{\text{std.}}} \times 1000 \text{ } \text{‰} \quad \dots \dots (4.5)$$

Since differences between samples are usually very small, δ^{18} is expressed as parts per thousand or per mil ($^{\circ}/_{\infty}$). The standards used predominantly are P.D.B., a marine belemnite from the Pee Dee formation of Cretaceous age, South Carolina (Craig, 1961) and Standard Mean Ocean Water (SMOW) a synthetic water standard approximating the isotopic composition of sea water (Craig, 1961).

For convenience "del" values will be abbreviated according to the following convention:

$$\delta^{18}(\text{CaCO}_3) = \delta^{\circ}$$

$$\delta^{13}(\text{CaCO}_3) = \delta^{\text{C}}$$

$$\delta^{18}(\text{H}_2\text{O}) = \delta^{\circ}_{\text{w}}$$

Unless otherwise stated CaCO_3 and H_2O isotopic ratios will always be compared to the PDB standard and SMOW respectively. If the "del" value refers to a sample of calcite this will be denoted by a subscript i.e. $\delta^{\circ}_{\text{ct}}$ or $\delta^{\text{C}}_{\text{ct}}$. (When "del" values increase a substance is commonly said to become "heavier"; conversely the same substance is said to become "lighter" when "del" values decrease).

Where equilibrium isotopic exchange is involved between two oxygen-containing species x and y, the relationship between α and the measured $\delta^{\circ}_{\text{x}}$ and $\delta^{\circ}_{\text{y}}$ can be expressed as:

$$10^3 \ln \alpha = \frac{1 + 10^{-3} \delta^{\circ}_{\text{x}}}{1 + 10^{-3} \delta^{\circ}_{\text{y}}} \approx \delta^{\circ}_{\text{x}} - \delta^{\circ}_{\text{y}} \approx \epsilon_{\text{xy}} \quad \dots \dots \dots (4.6)$$

The experimentally obtained temperature dependence of the CaCO_3 - H_2O fractionation can be expressed in terms of $\delta^{\circ}_{\text{w}}$ and $\delta^{\circ}_{\text{ct}}$. One such

equation was proposed by Epstein et al. (1953) and modified by Craig (1965):

$$T^{\circ}\text{C} = 16.5 - 4.3 (\delta'_{\text{C}} - \delta'_{\text{W}}) + 0.14 (\delta'_{\text{C}} - \delta'_{\text{W}}) \dots\dots\dots(4.7)$$

where $\delta'_{\text{C}} = 10.25 + 1.01 \delta^{\circ}_{\text{ct}}(\text{SMOW}) \dots\dots\dots(4.8)$

$$\delta'_{\text{W}} = 40.7 + 1.04 \delta^{\circ}_{\text{W}}(\text{SMOW}) \dots\dots\dots(4.9)$$

A more recent measurement of this relationship was made by O'Neil et al. (1969):

$$T^{\circ}\text{C} = (1.218 + 0.3593 \cdot 10^3 \ln \left\{ \frac{1+10^{-3} \delta^{\circ}_{\text{ct}}}{1+10^{-3} \delta^{\circ}_{\text{W}}} \right\}^{1/2}) 10^3 - 273.15 \dots\dots\dots(4.10)$$

where $\delta^{\circ}_{\text{ct}}$ and $\delta^{\circ}_{\text{W}}$ are taken w.r.t. the same standard (usually SMOW).

Both of the above equations refer to calcite-water equilibrium fractionation. The aragonite-water fractionation factor is slightly different:

$$\epsilon_{\text{ct} - \text{arag}} = 0.8 \text{ } ^{\circ}/\text{oo} \quad (\text{Tarutani } \underline{\text{et al.}}, 1969)$$

Applied to the problem of paleotemperature analysis equation (4.10) indicates that if CaCO_3 is deposited in isotopic equilibrium with water of a known isotopic composition then an absolute temperature of deposition can be measured. In principle such measurements can be made to an accuracy of 0.2°C .

The equilibrium distribution of C isotopes between the various species (CO_2 gas, $\text{CO}_2(\text{aq.})$, HCO_3^- , and CO_3^{2-}) involved in carbonate equilibria can be calculated by reference to Table 3.1 which lists the permil

fractionation factors at various temperatures between the co-existing species. The figures are a best fit to available experimental and theoretical data (Harmon, 1971a). From this table it can be seen that C^{13} is concentrated in $CaCO_3$ relative to CO_2 and that the fractionation is only slightly temperature dependent ($0.10 \text{ }^{\circ}/\text{oo}/^{\circ}\text{C}$). Modern $CaCO_3$ precipitated in equilibrium with atmospheric CO_2 will have a δ^C value of approximately $+1$ to $+2 \text{ }^{\circ}/\text{oo}$ at 25°C because atmospheric CO_2 is depleted in C^{13} ($\delta^C = -7$ to $-8 \text{ }^{\circ}/\text{oo}$, Craig, 1953; Keeling, 1958, 1961). Variations slightly outside of this range have been demonstrated by Galimov (1966).

Table 4.1

Permil Fractionation Factors between CO_2 Gas and Carbon Species in Solution

$T^{\circ}\text{C}$	$\epsilon_{(CO_{2g}-CO_{2aq})}^{\circ}/\text{oo}$	$\epsilon_{(CO_{2g}-HCO_3^-)}^{\circ}/\text{oo}$	$\epsilon_{(CO_{2g}-CO_3^{2-})}^{\circ}/\text{oo}$	$\epsilon_{(CO_{2g}-CaCO_3)}^{\circ}/\text{oo}$
0°	-0.94	+10.26	+8.38	+12.38
10°	-0.95	+ 9.27	+7.48	+11.28
20°	-0.92	+ 8.18	+6.49	+ 9.99
30°	-0.90	+ 7.30	+6.09	+ 9.32

4.3 The Requirements for Paleotemperature Analysis of Speleothems

The criteria for selecting speleothems that are suitable for paleotemperature analysis have been summarized by Hendy (1969):

".....it is essential to have isotopic equilibrium between the carbon dioxide in solution and the bicarbonate ions, if the speleothem is to have calcite deposited on it which is in isotopic equilibrium with the water. If the calcite is not in isotopic equilibrium with the water, the speleothems will not be of use as a paleoclimate indicator. To achieve oxygen isotopic equilibrium between the water and the calcite, the rate of loss of carbon dioxide must not be too great. It is essential that the average isotopic composition of the water passing over the speleothem be the same as the average rain water, and thus evaporation of water within the cave or in the soil above the cave must be avoided. It is also necessary that the temperature within the cave at the site of the speleothem vary as little as possible. If the cave is sufficiently long, and heat transfer by the water and air moving through the cave sufficiently small (eg. does not have a river flowing through it) the extent of temperature fluctuations will depend solely on the depth of the cave and thermal conductivity of the limestone. Thus a deep cave will tend to have a greater dampening effect on the temperature fluctuations of the surface, than will a shallow cave."

The possible effects of evaporative enrichment of water in the soil must be considered. Nearly 60% of the total influx to the continents is evaporated but this is mostly through the process of evapotranspiration. This type of evaporation takes place from capillary systems within the soil or plants and this water does not mix with the

large reservoir of soil and ground water. Consequently, the majority of water percolating into the ground will be unaltered meteoric precipitation. At high temperatures and when the water cannot quickly percolate into the ground evaporation would be expected to alter the bulk isotopic composition of the water. This situation is unlikely to be encountered in a karst area because of the high permeability of karst terrain. When the percolating water reaches the cave, evaporation is unlikely to take place since the humidity of most caves is close to 100%.

To maintain this 100% humidity, water should be continually fed into the cave, preferably as percolation water and the circulation of the cave air should be very slow.

Hendy infers that slow rates of deposition are of prime importance in determining whether or not equilibrium deposition will occur. A slow drip rate and high CO₂ content of the cave air will ensure such a situation. Stalagmites that have formed slowly within a cave can be recognized. They are generally of constant diameter (about 7.5 cm); and upon sectioning the core of the stalagmite will appear to be formed from one continuous crystal lattice, with cleavage indicating the c-axis to be vertical. This has been noted by Schillat (1969).

Slow growth ensures continuous deposition on existing crystal faces and if the rate of supply of solution is slow most of the deposition will take place as a thin layer on the top of the existing stalagmite. This explains the candle-like shape of such stalagmites. Irregular drip rates lead to irregular stalagmite shapes.

Slow deposition from sheets of water moving over bedrock or sediment results in the formation of layered travertines or "flowstone".

Slow deposition is typified by thin, uniform layers deposited from an almost stationary water film. A near horizontal surface is necessary for this type of deposition. When water films flow over steeper slopes, micro-gours are formed and very porous flowstones result. When water flows over steep slopes turbulent mixing will result and CO_2 loss will be more rapid than from a near-stationary water film. Consequently flowstones deposited on slopes are less likely to be useful for paleotemperature analysis.

The rate of CO_2 loss from solution will depend upon the CO_2 content of the cave air as well as on the degree of agitation of the water film. The smaller the concentration gradient between CO_2 in solution and in the cave air the slower will be the rate of loss of CO_2 to the cave air. A situation is therefore required where relatively large quantities of percolation water enter the cave, deposit CaCO_3 and release CO_2 to the cave air. This CO_2 must not be swept away by strong air movements but at the same time it must not increase to such an extent that CaCO_3 deposition stops. The most promising situation, therefore, in which to find equilibrium deposits is a side-room or passage, well-decorated with speleothems and with no perceptible air movement.

In summary, the "ideal cave" should have a single entrance and the cave passages should be at least 15 metres below the surface. The majority of water entering it should be as percolation water. The rooms and passages should be connected by a network of restricted crawlways. The area to be sampled should have a high speleothem density. Columnar stalagmites and horizontal flowstone deposits should be sampled, though, when accessible, stalactites are probably just as suitable.

4.4 Factors Affecting the Isotopic Composition of Speleothems

The equilibrium oxygen isotopic composition of the CaCO_3 of speleothems is determined by a) the temperature of deposition and b) the oxygen isotopic composition of the ground water seeping into the cave. Non-equilibrium processes can also play a role in determining $\delta^{18}\text{O}$. For example, deposition through the process of evaporation will result in CaCO_3 which is progressively enriched in ^{18}O as more water is evaporated. In addition, if decarboxylation of carbonic acid determines the rate at which CaCO_3 is deposited then $\delta^{18}\text{O}$ will be different from the equilibrium value. Hendy (1969) has shown that paleoclimate information can only be obtained from oxygen isotopic analysis of speleothems if neither of the above non-equilibrium processes were involved in the deposition of the CaCO_3 .

The carbon isotopic composition of the CaCO_3 of speleothems is a valuable indicator of whether deposition was an equilibrium process or not. The factors affecting this carbon isotopic composition are numerous. It is worth noting that the temperature dependence of $\alpha_{\text{CO}_2-\text{CaCO}_3}$ is not an important factor. The carbon isotopic composition is primarily determined by the isotopic composition of soil CO_2 and of the limestone being dissolved. The isotopic composition of the resultant carbon species in solution depends on the process by which the limestone is dissolved.

In temperate climates where grasslands and forests predominate, the isotopic composition of soil CO_2 is generally found to lie between -23 ‰ and -24 ‰ (Munich and Vogel, 1959; Broecker and Walton, 1959; Galimov, 1966; Vogel and Ehhalt, 1963; Galimov et al., 1965;

and Wendt, 1968). However, for tropical and sub - tropical grasslands or desertlands soil CO₂ with $\delta C^{13} = -12$ ‰ is found (Bender, 1968). Rightmire and Hanshaw (1971) measured intermediate values of -15.2 ‰ and -19.0 ‰ for the soil CO₂ composition of Floridan grasslands and -20.4 ‰ and -21.3 ‰ for that of forests.

Most limestones have a carbon isotopic composition close to that of P.D.B., that is 0 ‰ (Craig, 1953). The actual isotopic composition of a cavernous limestone will vary according to the depositional environment and diagenesis but most limestones can be expected to fall in the range -4 to +2 ‰. Since the carbon species in a solution entering the cave will be derived both from the limestone and soil CO₂ then these species will have a carbon isotopic composition intermediate between the two. The actual value depends on the nature of the solutional process, in particular whether or not solution takes place in a "closed" or "open" system. In a closed system there is a finite amount of CO₂ capable of reacting and dissolving the limestone. In an open system an unlimited amount of CO₂ is considered to be continuously in contact with the solution until it emerges into the cave. Hendy (1969) has considered the effects of dissolution under these boundary conditions and concluded from his studies on New Zealand speleothems that most karst ground waters originated in a closed system. This conclusion is supported by a study of karst ground waters in Pennsylvania by Harmon(1971b). The first CaCO₃ deposited from waters which evolved in a closed system with δC^{13} of the soil CO₂ = -24 ‰ and δC^{13} of the limestone = +1 ‰ will have a carbon isotopic composition of approximately -11.5 ‰ at 10°C. (Under open system conditions this would approximately be -13.0 ‰ at 10°C.)

More CaCO_3 can be dissolved in an open system for a given partial pressure of CO_2 than can be dissolved in a closed system. It has been shown by Hendy (1969, p.97) that a solution in contact with atmospheric CO_2 ($p\text{CO}_2 = 0.03\% \text{ Atm}$) will dissolve the same amount of CaCO_3 as a solution in a closed system initially in equilibrium with a partial pressure of CO_2 of 1.25% Atm. (at 10°C). Thus, assuming the cave air has the same level of CO_2 as the atmosphere, soil CO_2 levels would have to be greater than 1.25% Atm. if CaCO_3 is to be deposited from a solution which has attained equilibrium in a closed system. Speleothem deposition does occur in areas where soil cover does not even exist (for example, the high rock range in the Southern Canadian Rockies, see Chapter 7) so it cannot be assumed that all speleothem deposition is from a solution which equilibrated in a closed system.

The carbon isotopic composition of the first CaCO_3 precipitated from water entering a cave is determined by the processes described above. The carbon isotopic composition of CaCO_3 subsequently deposited on a speleothem, however, changes according to the nature of processes acting within the cave. These processes are complex but have been described and evaluated by Hendy (1969, 1971). It is this change in isotopic composition which gives the clue as to whether deposition was an equilibrium process or not. Non-equilibrium processes cause a correlated change in $\delta_{\text{ct}}^{\text{O}}$ and $\delta_{\text{ct}}^{\text{C}}$ of calcite precipitated along the surface of a stalactite or stalagmite. Hendy (1969) has shown that when CaCO_3 is deposited as a result of evaporation, $\delta_{\text{ct}}^{\text{C}}$ and $\delta_{\text{ct}}^{\text{O}}$ are related in such a manner that $\Delta_{\text{ct}}^{\text{C}} \approx -2 \Delta_{\text{ct}}^{\text{O}}$. ($\Delta_{\text{ct}}^{\text{O}}$ is the change in $\delta_{\text{ct}}^{\text{O}}$ between two

points on the surface of a speleothem). When kinetic loss of CO_2 is involved in the depletion process, $\Delta_{\text{ct}}^{\text{C}} \approx 4\Delta_{\text{ct}}^{\text{O}}$. However, other functional relationships between $\delta_{\text{ct}}^{\text{O}}$ and $\delta_{\text{ct}}^{\text{C}}$ have been measured for non-equilibrium stalagmite deposition (Fantidis and Ehhalt, 1970) indicating that other processes or a combination of processes may effect the relationship between $\delta_{\text{ct}}^{\text{O}}$ and $\delta_{\text{ct}}^{\text{C}}$. Hendy suggests that no correlation between $\delta_{\text{ct}}^{\text{O}}$ and $\delta_{\text{ct}}^{\text{C}}$ along single growth layers, coupled with constant $\delta_{\text{ct}}^{\text{O}}$, is strong evidence for equilibrium deposition.

4.5 Paleotemperature Analysis: Principles

It has been stressed that paleotemperature analysis of speleothems can only be successful if CaCO_3 deposition is an equilibrium process. It was also stressed that the isotopic composition of the parent waters must be known before the absolute temperatures can be calculated. A third requirement is that the isotopic composition of the CaCO_3 has undergone no post-depositional alteration, e.g. recrystallisation.

These three requirements and the means of assessing the reliability of speleothems for paleotemperature analysis are discussed below.

4.5.1 Equilibrium Versus Kinetic Fractionation

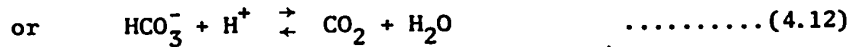
Non-equilibrium or kinetic fractionation during deposition of CaCO_3 may be attributed to (a) evaporation of water from the speleothem surface or (b) rapid loss of CO_2 from solution. The first process can sometimes be recognized from the crystallographic structure of a speleothem. Microcrystalline, randomly oriented porous structures are typically found near cave entrances within the area affected by diurnal temperature changes. However, porous speleothems are also found inside caves, well

out of the range of diurnal temperature fluctuations. Where such deposition is at present taking place flow rates are usually relatively rapid.

The second process giving rise to non-equilibrium fractionation is rapid loss of CO_2 from solution. Under these circumstances equilibrium between dissolved CO_2 and HCO_3^- cannot be maintained with the result that CaCO_3 will be kinetically enriched in C^{13} and O^{18} . The problem reduces to one of calculating how quickly CO_2 may be lost from solution before kinetic effects become significant. The rate of loss of CO_2 from a real system can be compared with these results to assess whether or not an equilibrium situation can theoretically exist. A practical means must also be found for recognising the case of kinetic fractionation in fossil speleothems.

The development of the system $\text{CaCO}_3\text{-H}_2\text{O-CO}_2$ has been treated by Roques (1969), particular emphasis being placed on kinetic effects. Roques considered a relatively simple situation where CO_2 was lost from a droplet of water formed at the end of a tubular stalactite. The response time for 90% exchange of CO_2 with the CO_2 of the cave air is pH dependent. For pH values of 8.0 and 9.0 (the approximate range of observed values in cave waters) the response time varies from approximately 10 minutes to 2 hours respectively. This is a measure of the net rate of diffusion of CO_2 across the air/water interface. It must be shown, therefore, that the slowest reactions taking place in solution are faster than the response time for CO_2 loss to the cave air. The slowest reactions in solution involve CO_2 and HCO_3^-





The rate of each of these reactions is pH dependent. Roques has shown that at pH 8.0 and 9.0 the conversion of HCO_3^- is 90% complete after approximately 5 minutes and 60 minutes respectively. Hendy (1971) has shown that the rate at which isotopic equilibrium is reached between dissolved species is approximately the same as the rate at which chemical equilibrium is reached. For this simple case, therefore, rate of loss of CO_2 would be controlled by diffusion across the liquid/gas interface; equilibrium between the dissolved species will be maintained and CaCO_3 will be deposited in isotopic equilibrium with the HCO_3^- in solution. The situation is complicated when splash effects are considered. The rate of CO_2 loss by diffusion depends upon the thickness of the water layer. (A thick water layer was considered above). The splash of a falling drop rapidly increases the surface area of the liquid and therefore the rate of diffusion of CO_2 across the boundary. Under these conditions the rate of loss of CO_2 could result in the de-hydration reaction being rate-limiting.

Hendy (1971) has developed further the theory of kinetic isotope effects in the $\text{CO}_2\text{-H}_2\text{O-CaCO}_3$ system. He showed that, given the range of observed $p\text{CO}_2$ values in caves and solutions entering caves, a water film thickness of approximately 1 mm is required before loss of CO_2 to the cave atmosphere is sufficiently slow to permit isotopic equilibrium between the dissolved species. On the top of a stalagmite, which is often slightly concave this condition is likely to be met.

A number of studies have indicated that kinetic enrichment of

the heavy isotopes can occur during speleothem deposition. Perhaps the most thorough study to date on this topic was conducted by Fantidis and Ehhalt (1970). Their study of speleothems indicated that $\delta^{18}\text{O}$ and $\delta^{13}\text{C}$ showed parallel variation along a single growth layer. It is possible for $\delta^{13}\text{C}$ to increase along a growth layer in the direction of flow due to preferential loss of "light" CO_2 according to the Rayleigh distillation law and/or exchange with atmospheric CO_2 . A parallel increase in $\delta^{18}\text{O}$ is not expected, except where enrichment in O^{18} is the result of a kinetic process. They describe one example where $\delta^{18}\text{O}$ and $\delta^{13}\text{C}$ became progressively lighter along a single growth layer in the direction of flow. Laboratory simulation of speleothem deposition resulted in analogous variations, the mutual enrichment or depletion of the heavy isotopes along the growth layers depending on the rate of flow of feed solution. This pointed toward the fact that kinetic effects other than evaporation were involved in the fractionation process. The authors concluded that a kinetic isotope effect arose in the loss of CO_2 to the cave atmosphere and in the formation of CO_2 from HCO_3^- . In addition, they conclude that the isotopic composition of the water film flowing over the speleothem surface is heterogeneous and that the kinetic isotope effects probably take place in a sub-layer at the speleothem surface. It is significant that axial samples taken along the kinetically fractionated speleothems showed no correlation between $\delta^{18}\text{O}$ and $\delta^{13}\text{C}$. Such a lack of correlation has been argued as evidence of equilibrium deposition (Duplessey *et al.*, 1970).

The laboratory experiments in Fantidis and Ehhalt's study did not quite simulate deposition of CaCO_3 from actual drip-waters. Deposi-

tion was very fast (of the order of mgm/sec) whereas much longer times are usually required for deposition of CaCO_3 under cave conditions (Roques 1969).

A minimum amount of 5 mgm of CaCO_3 is required for accurate analysis. An approximate rate of deposition of CaCO_3 within the Norman-Bone Cave is 300 ± 100 mgm/year (during warm climate). In principle, therefore, the isotopic composition of seasonally precipitated CaCO_3 within a cave could be easily studied. Such a study would give more pertinent information about the depositional process than a laboratory study. If sampling sites were carefully chosen, temperature, pCO_2 , and humidity would remain constant whilst drip rates could be easily monitored.

4.5.2 Climate Data from the Oxygen Isotopic Composition of Speleothems

Once it has been established that CaCO_3 was deposited in isotopic equilibrium, temperatures of deposition and paleoclimate curves can be calculated from equations 4.7 or 4.10, if the isotopic composition of the parent water (δ_w°) is known. Except for freshly deposited CaCO_3 , δ_w° is not generally known. However, a useful climatic variable can be calculated if the change in δ° of tropical foraminifera ($\delta_{\text{foram}}^{\circ}$) is known over the period of interest. This variable is the temperature gradient between the tropical oceans and the region studied. Hendy (1969) showed that

$$\Delta_{\text{spel}}^{\circ} = \Delta_{\text{foram}}^{\circ} - 0.46(T_x - T)$$

where $\Delta_{\text{spel}}^{\circ}$ = the change in δ° of CaCO_3

$\Delta_{\text{foram}}^{\circ}$ = the parallel change in δ° of tropical forams

T_x = the change in regional temperature

T = the change in temperature of the ocean

surface waters.

and $(T_x - T)$ = the change in thermal gradient between
the region studied and the tropical ocean.

Ilendy used this equation to show that a glacial phase in New Zealand is preceded by an increased thermal gradient. The equation is of limited use if the effect of a change in the temperature gradient on the isotopic composition of meteoric precipitation is not known. (Ilendy assumes a value of -0.7‰ per $^{\circ}\text{C}$ decrease in the temperature gradient but this value is probably not universally valid; see discussion in section 4.9). An alternative approach to the problem was attempted in this study: paleowaters, preserved in the CaCO_3 as fluid inclusions, were extracted and analysed. The advantage of this approach is that, in principle, an absolute temperature of deposition can be calculated which is the ultimate goal of paleoclimate studies. The method is discussed in section 4.11.

4.6 Previous Work Related to the Isotopic Analysis of Speleothems

Labeyrie et al (1967a) measured an oxygen and carbon isotope profile along the axis of a post-glacial stalagmite from the Aven d'Orgnac. The base was C^{14} -dated as 7000 years old. Though growth was not at a constant rate it was continuous to the present. An obvious correlation between δ^{O} and δ^{C} is apparent; nevertheless, the oxygen isotope curve was claimed to reflect climate fluctuations that broadly compared with those deduced from a study of Mediterranean transgressions. These authors concluded that cave deposits became depleted in O^{18} by about 0.5‰ for a 1°C decrease in temperature of deposition.

Duplessey et al (1969) attempted to show that modern cave

deposits from the Aven d'Orgnac (Ardeche Province, Southern France) and Grange Mathieu (Jura Alps, Central France) were being deposited in equilibrium with waters at present entering the caves. Only one of three stalagmites analysed appeared to be deposited in equilibrium. Since the temperature of the caves were different (Aven d'Orgnac = 12.6 °C, $\delta_w^O = -7.13$ ‰; G. Mathieu = 8 °C, $\delta_w^O = -7.76$ ‰) the effect of temperature on the isotopic composition of meteoric waters in these locations can be calculated. A change of -0.14 ‰ for a 1°C decrease in temperature is calculated from the above figures. The calculation depends upon the assumption that the groundwater compositions measured represent average drip-waters and that the cave temperatures measured are average annual temperatures.

A difference (not accounted for by $\epsilon_{\text{HCO}_3^- - \text{CaCO}_3}$) in the carbon isotopic composition of dissolved HCO_3^- and CaCO_3 subsequently deposited was claimed to be evidence for non-equilibrium deposition. This conclusion can only be correct if the carbon isotopic composition of the dissolved HCO_3^- remained unaltered before CaCO_3 deposition occurred. The carbon isotopic composition of HCO_3^- will be continually altered as re-equilibration of the dissolved species with the cave air occurs and therefore the above condition is unlikely to be realised. This limits the usefulness of carbon isotopes to measure the extent of kinetic fractionation.

In a later paper Duplessey et al. (1970) analysed a stalagmite which was active between 130,000 and 90,000 years B.P. Dating was by the $\text{Th}^{230}/\text{U}^{234}$ method. The evidence presented for equilibrium deposition was lack of correlation between δ^O and δ^C along the axis of the stalag-

mite. However, as Fantidis and Ehhalt (1970) pointed out, lack of correlation alone is not evidence for equilibrium deposition. (The results from Aven d'Orgnac are discussed further in Chapter 8).

The search for speleothems showing evidence of equilibrium deposition has also been conducted by Fornaca-Rinaldi et al. (1968). They concluded that the cave concretions they studied were probably not suited for paleoclimate analysis due to kinetic fractionations. These conclusions were based on a definite correlation between $\delta^{18}\text{O}$ and $\delta^{13}\text{C}$ for samples taken along growth layers of stalagmites and stalactites. In addition, certain stalactites appeared to show evidence of enrichment in O^{18} by evaporation of water. However, though the authors do not specifically state from which part of the caves deposits were collected, it is probable that they were near-entrance deposits. (This is based on their statement that some of the deposits were associated with Roman remains which are unlikely to be found deep inside a cave).

Galimov et al. (1965) attributed fluctuations in $\delta^{13}\text{C}$ of calcite deposited in caves of the Crimea to climate fluctuations which affected the pedological environment and the isotopic composition of CO_2 . These authors conclude that lighter calcites (range -8.3 ‰ to -9.9 ‰) are formed during warm periods and that heavier calcites (-4.9 ‰ to -7.3 ‰) form during colder periods. It was inferred that reddish ferruginous layers with lighter $\delta^{13}\text{C}$ values were formed at the same time as tropical or sub-tropical red soils in a warm climate. Later layers, free of iron and with heavier $\delta^{13}\text{C}$ values were inferred to form in the colder Quaternary period when the process of photosynthesis was

modified such that soil became enriched in C^{13} . However since the layers were not dated the conclusions remain open to question.

Hendy (1969) found that caves in New Zealand contained speleothems where $CaCO_3$ was deposited in isotopic equilibrium with waters entering the cave. Some speleothems showed evidence of non-equilibrium deposition which was attributed either to evaporation of water or to rapid CO_2 loss from solution. Most of the speleothems studied were no older than 50,000 years and the isotopic record preserved in four speleothems deposited within the time span 0 - 40,000 years B.P. showed parallel variations in $\delta^{18}O$. During the late glacial period the $CaCO_3$ of the New Zealand speleothems was approximately 1 ‰ heavier than that of recent speleothems.

Geyh (1970) has measured $\delta^{18}O$ and $\delta^{13}C$ variations along the axis of a 60 cm long stalagmite from the Mieru Cave (elevation 821 m) in the lower Tatra mountains (Czechoslovakia). The stalagmite was dated by the C^{14} method (the initial C^{14}/C^{12} ratio was assumed to be 85% of the modern ratio) and found to be deposited between $10,095 \pm 190$ and 2645 ± 125 years B.P. Between 10,095 and 4400 years B.P. the average growth rate was $2 \text{ cm}/10^3$ years and between 4400 and 2645 years B.P. the growth rate increased to $26 \text{ cm}/10^3$ years. Geyh compared the measured $\delta^{18}O$ and $\delta^{13}C$ variations with those measured by Labeyrie *et al.* (1967a) and, over the interval of time covered by both stalagmites, found a broad correlation between both the $\delta^{18}O$ and $\delta^{13}C$ curves. The $\delta^{18}O$ values of the Mieru Cave stalagmite varied over a larger range than those of the Aven d'Ornagac stalagmite (due to larger temperature variations in the "continental" Tatra?). Geyh concluded that variations in both $\delta^{18}O$ and $\delta^{13}C$

are caused by climate changes. In accordance with the findings of Labeyrie et al., Geyh attributed a decrease in both δ^O and δ^C to a lowering of the temperature of deposition. However, according to Labeyrie's arguments $CaCO_3$ should be depleted by 0.46 ‰ for a 1°C decrease in temperature. The temperature of the Mieru Cave is 5-6 °C lower than that of Aven d'Orgnac at present, yet δ^O values of $CaCO_3$ deposited quite recently (2600 years B.P.) in both caves are identical. The remaining δ^O values of the Mieru Cave stalagmite are consistently heavier than those for Aven d'Orgnac. According to Labeyrie et al. (1967) and Duplessey et al. (1970) the heavier $CaCO_3$ is deposited at higher temperatures. Yet this does not seem reasonable considering present-day temperatures in both regions. The results can only be explained by assuming that no simple relationship exists between the isotopic composition of cave deposited $CaCO_3$ and mean annual temperature. Alternatively, one or both of the speleothems is not reflecting climate variations at all but random isotopic variations due to kinetic fractionation effects.

This brief literature review shows that many of the speleothems studied to date have not yielded paleotemperature information due to the predominance of kinetic isotope effects. Those speleothems apparently deposited in isotopic equilibrium present problems when interpretation of the isotopic record in terms of climate change is attempted.

4.7 Analytical Techniques

4.7.1 Sampling and Preparation of CO_2 for Mass Spectrometric Analysis

About 40-50 mgm of sample were obtained by using a 1/8 inch hand

drill. The surface drillings were discarded to avoid contamination. More precision in sampling could have been obtained by collecting scrapings from individual growth layers. In many cases the frequency of sampling could have been increased by a factor of ten but this precision was not thought necessary in this preliminary study. Each of the samples for isotopic analysis was tested to differentiate between calcite and aragonite. Initially this was done by using x-ray diffraction but was discontinued after a short while in favour of specific gravity identification. Bromoform (S.G. = 2.85) is of such critical density that aragonite (S.G. = 2.95) sinks whilst calcite (S.G. = 2.72) floats. All of the West Virginia samples were identified as being calcite.

CO₂ was prepared by reacting 30 mgm samples of CaCO₃ with aged, 100% H₃PO₄ at a temperature of 25°C according to the method of McCrea (1950).

4.7.2 Mass Spectrometric Analysis

A 6 inch, 90° double collecting instrument was used for isotopic analysis. To minimise the effects of instrument instability the sample gas was frequently compared with a standard gas. The working standard was CO₂ produced from the Grenville Calcite Standard (G.C.S.) a low Mg marble from near the Ottawa River.

The raw results from the mass spectrometer are corrected for tailing effects and converted to ‰ w.r.t. P.D.B. using the formula:

$$\delta_x^O(\text{PDB}) = 0.99371 \delta_x^{46}(\text{GCS}) + 0.009 \delta_x^{45}(\text{GCS}) - 11.72 \quad \dots\dots(3.17)$$

where δ_x^O (PDB) is the O isotopic composition of the sample w.r.t.
P.D.B. in ‰.

δ_x^{46} (GCS) is the "raw" O isotopic composition of the sample
w.r.t. G.C.S. in ‰.

δ_x^{45} (GCS) is the "raw" C isotopic composition of the sample
w.r.t. G.C.S. in ‰.

$$\text{and } \delta_x^C(\text{PDB}) = 1.081 \delta_x^{45}(\text{GCS}) - 0.034 \delta_x^{46}(\text{GCS}) + 0.62 \dots\dots\dots(4.18)$$

where δ_x^C (PDB) is the C isotopic composition of the sample w.r.t.
P.D.B.

and δ_x^{45} (GCS) is the "raw" C isotopic composition of the sample
w.r.t. G.C.S.

These conversion formulae are derived by Schwarcz (1971).

To check the stability of the spectrometer freshly prepared CO_2 from the G.C.S. standard was run against the G.C.S. working standard. This operation was carried out after 4 or 5 samples had been processed. In practice the oxygen isotopic ratio of freshly prepared CO_2 from G.C.S. was always slightly lighter than that of the working gas (due to fractionation in the capillary) by 0.19 ± 0.05 ‰ on average. The error is one standard deviation. The freshly prepared CO_2 was also consistently lighter in C^{13} than the working gas by an average of 0.14 ± 0.04 ‰. A correction was made to the observed δ^O values to compensate for this effect.

4.7.3 Isotopic Analysis of Water

$^{18}\text{O}/^{16}\text{O}$ ratios of water are measured by equilibrating CO_2 gas of known isotopic composition with a known volume of water at a constant

SPELEOCHRONOLOGY AND LATE PLEISTOCENE CLIMATES

temperature of 25 °C. After exchanging for 2-3 days at pH = 4, the CO₂ equilibrates with the water and the isotopic composition of the latter can be measured by analysing the CO₂ (Epstein and Mayeda, 1953).

The procedure is outlined in the following steps:

1. 5 ml of water is introduced into the reaction vessel via the side arm.
2. The pH is adjusted to approximately 4.
3. The water is frozen in a chloroform/carbon tet/dry ice bath and the vessel evacuated.
4. The ice is allowed to melt, without heating and allowed to de-gas completely.
5. Step 3 is repeated; then a measured pressure (40-45 cm) of CO₂ gas introduced into the vessel. The lower tap is closed and the ice allowed to melt. Meanwhile the gas pipette is evacuated; then the upper tap closed.
6. Immediately the ice is melted, the vessel is transferred to a constant temperature bath (25°C) and left for 3 days with occasional shaking.
7. Gas is extracted for analysis by allowing CO₂ into the gas pipette (at the same time checking that no water trapped in the neck of the vessel is drawn into the capillary), then freezing this and one further cut in liquid N₂. The condensed gas is treated identically to CO₂ from calcites, but is analysed only for its oxygen isotopic composition.
8. Successive aliquots of CO₂ are removed at intervals of 12 hours until δ° is constant.

LEAF 101 OMITTED IN PAGE NUMBERING.

The raw results are converted to ‰ w.r.t. SMOW using the equation:

$$\delta_w^O(\text{SMOW}) = 1.004 \delta_{\text{CO}_2}^{46}(\text{GCS}) - 11.52 \quad \dots\dots\dots(4.17)$$

where $\delta_w^O(\text{SMOW})$ is the O isotopic composition of the water w.r.t. SMOW and $\delta_{\text{CO}_2}^O(\text{GCS})$ is the O isotopic composition of CO_2 in equilibrium with the water w.r.t. G.C.S.

Equation (4.17) is strictly true only for a fixed volume of water (5 ml) and a fixed CO_2 pressure (0.5 atm). The equation also assumes a constant isotopic composition for the tank CO_2 .

4.7.4 Accuracy and Precision of Mass Spectrometric Analyses

The accuracy of the CaCO_3 analyses and the water analyses were checked by analysing standards of accurately known isotopic composition. NBS-20 (Solenhofen Limestone Standard) was used as a calcite standard and a water close in isotopic composition to SMOW was used as a water standard. Table 4.2 lists the results of these analyses. Both these standards were obtained from the International Atomic Energy Agency, Vienna, Austria.

If allowance is made for the fact that the machine bias gives results which are slightly too "light" (-0.19 ‰ for δ^O and -0.14 ‰ for δ^C) then the agreement between the measured values and the actual values is within the limits of experimental error.

Any short-term loss of accuracy should have been detected by the frequent G.C.S. analyses. Only once, and for a period of one day, were the isotopic analyses seriously in error. The same samples gave

quite acceptable results the following day and the reason for the anomalous results was never found. (On this occasion samples and G.C.S. standard both gave analyses approximately 1 ‰ too light).

It was found that the precision of the isotopic analyses varied from day to day depending on the stability of the mass spectrometer, or more precisely on the stability of the vibrating reed electrometers that were used to measure the intensity of the ion currents. Oxygen isotopic analyses were generally less precise than carbon isotopic analyses. At best, oxygen isotopic ratios could be measured to ± 0.1 ‰ and carbon to ± 0.05 ‰. The precision of each analysis was not calculated and was assumed to be ± 0.15 ‰ on average.

Table 4.2
Analyses of Isotopic Standards

Standard	δ^{O} w.r.t.	δ^{C} w.r.t.
	P.D.B. ‰	P.D.B. ‰
NBS-20 (1)	-4.20	-1.37
NBS-20 (2)	-4.25	-1.32
NBS-20 (3)	<u>-4.28</u>	<u>-1.22</u>
Average	-4.24 \pm 0.15	-1.30 \pm 0.10
Actual value	-4.14	-1.06
$\delta_{\text{w}}^{\text{O}}$ w.r.t. SMOW		
SMOW (1)	+0.05	
SMOW (2)	<u>+0.04</u>	
Average	+0.045	
Actual value	0.00	

4.8 The Case for Equilibrium Deposition in West Virginia

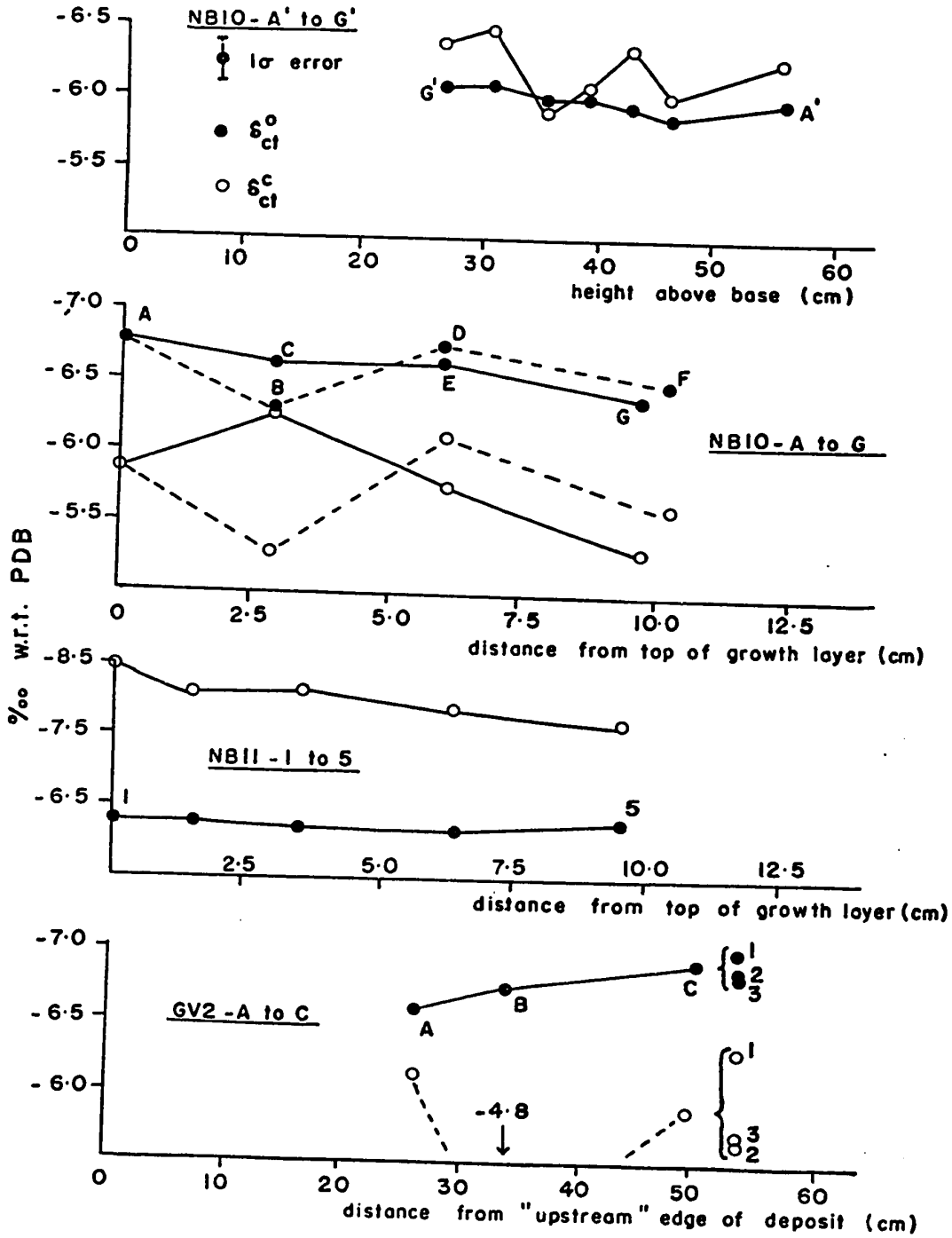
From the previous discussion it is apparent that the most reliable way of confirming equilibrium fractionation during speleothem deposition is to measure δ_{ct}^O and δ_{ct}^C along growth layers. Constant δ_{ct}^O and lack of correlation between δ_{ct}^O and δ_{ct}^C along growth layers in the direction of water flow is strong evidence that fractionation was an equilibrium process. Accordingly, samples were extracted along growth layers of two stalagmites (NB10 and NB11) and one flowstone sample (GV2). In Figure 4.1 δ_{ct}^O and δ_{ct}^C are plotted versus distance from the point where $CaCO_3$ deposition started. Because GV2 was only a fragment of flowstone it could not be determined exactly where deposition started; instead distance is measured from the "upstream" edge of the flowstone block. The three points at C in Figure 4.1(d) represent three samples taken in a line perpendicular to the direction of flow. The precise location of those samples is shown in Figure 4.5.

Within the limits of experimental error δ_{ct}^O is constant along each growth layer for NB10 and NB11. GV2 shows a slight depletion in O^{18} in the direction of water flow. This depletion rules out the possibility of evaporative enrichment of the water. There is no parallel variation in δ_{ct}^O and δ_{ct}^C which rules out the possibility of kinetic isotope effects during deposition. The results are probably explained by the inadvertent inclusion of isotopically heavier $CaCO_3$ from an adjacent growth layer in the samples drilled from the thinner growth layers. (The layers thinned appreciably towards the "upstream" edge of the flowstone block).

7

Figure 4.1 Variations in δ_{ct}^o and δ_{ct}^e along growth layers in stalagmites NB10, NB11 and flowstone GV2. (The precise location of the samples is shown in Figures 6.4, 6.7 and 4.5 respectively).

└



An isotopic temperature of deposition can be calculated for recent speleothems if the isotopic composition of the average cave drip-water is measured. If this calculated temperature is comparable with the measured cave temperature then deposition must have taken place in isotopic equilibrium. Some recent active speleothems were collected to permit such a comparison.

Two active soda-straw stalactites were sampled as well as a stalagmite and stalactite-stalagmite pair. One stalactite was from Grapevine Cave and the remainder of the samples were from Norman-Bone Cave. The isotopic temperatures were calculated using an average value for the drip-water isotopic composition and the equation of O'Neil et al (equation 4.10). The average Norman-Bone drip-water composition is based on three analyses and only one drip-water sample was obtained from Grapevine Cave. Consequently the average drip-water composition may be subject to considerable error. The calculated temperatures of deposition are shown in Table 4.3. The Norman-Bone Cave temperature was 11.2 ± 0.5 °C and that of Grapevine Cave was constant at 11.6 °C. However, based on a 56 year period from 1902-1958 and a 4 year period from 1967-71 the mean annual temperature at Lewisburg, 5 miles from Grapevine Cave, was 10.9 °C. The samples collected would represent a period of deposition of at least 50 years and so an average cave temperature of 10.9 °C is probably a reliable estimate. (The above average temperature of Grapevine Cave is most probably due to the presence of powerful lights and numerous visitors which upset the thermal balance of the cave). The isotopic temperatures are all slightly too low but δ_{ct}^o is quite constant as would be expected if deposition were an

Table 4.3

Isotopic versus Theoretical Temperature of Deposition of Modern Speleothems*

Sample (Date of Collection)	Location	$\delta_{ct}^{18}O$ w.r.t. SMOW	$\delta_w^{18}O$ w.r.t. SMOW	Isotopic Temperature ($^{\circ}C$)	
				$\delta_w^{18}O$ (as measured)	$\delta_w^{18}O$ = -8.66 $^{\circ}/\infty$
Stalactite NC3 (16.7.71)	Norman Cave	23.25	-8.58	9.0	8.8
Stalagmite NC3 (16.07.71)	Norman Cave	23.32	-8.58	8.7	8.6
Stalactite NC1 (? .08.71)	Norman Cave	23.00	-8.99	8.2	9.8
Stalagmite NC2 (16.07.71)	Norman Cave	23.07	-8.33	11.5	9.6
Stalactite LW1	Grapevine Cave	23.39	-8.69	8.3	8.3
Average and error**		23.21 ± 0.17	-8.66 ± 0.24		8.65 ± 1.6

* Theoretical temperature of deposition = mean annual surface temperature = 10.9 $^{\circ}C$

** Error (1 standard deviation) of the mean

equilibrium process.

The relation between cave temperatures and surface temperature was discussed in Section 3.3. It was noted that cave temperatures slightly below mean annual temperature are not uncommon. The isotopic temperatures, therefore, though slightly lower than expected are not grossly inaccurate. It is possible that the value chosen for the average isotopic composition of the drip-waters could be slightly too "light". These results show that some deposits can be found which show no sign of kinetic effects.

Convincing proof of equilibrium deposition would be the construction of identical isotope curves from different speleothems growing over the same period of time. Such a construction was attempted in West Virginia but only two speleothems were analysed which grew over the same period of time. A detailed isotope profile was measured for each speleothem but one of them (NB4, see Section 6.14 p.207) was not suitable for accurate age analysis. Consequently, a detailed comparison between the two curves was impossible. The results of this comparison are discussed in Chapter 6 but it can be noted here that, within the limits of the dating method, the two speleothems appear to record similar isotopic fluctuations. One of the problems which will continue to frustrate such comparisons is the inability of investigators to assign even an approximate age to fossil deposits in situ, and thus to collect suitable material for such comparisons.

4.9 The Isotopic Composition of Meteoric Precipitation

One of the most problematic aspects of paleotemperature analysis is that of assigning an isotopic composition to water from which CaCO_3 was deposited, but which is now no longer available for analysis, or whose isotopic composition has been modified. Dansgaard (1964) has attempted to develop a model which relates the depletion of meteoric water in O^{18} to the temperature gradient between the tropical oceans (the principal source of precipitation) and points on the earth's surface. By treating the precipitation part of the hydrologic cycle as a Rayleigh Distillation Process, Dansgaard predicted that isobaric cooling of water vapour at 20°C would produce precipitation that is progressively depleted in O^{18} by $0.7^\circ/\text{oo}$ per $^\circ\text{C}$ decrease in temperature. In general, this prediction is found to hold in maritime and polar regions.

However, the model does not appear to be valid for Continental North America. Calculations by Stuiver (1968) on the isotopic composition of Chicago precipitation indicates a temperature effect of only $0.3^\circ/\text{oo}$ per $^\circ\text{C}$. Stuiver concluded from a study of the oxygen and carbon isotopic composition of fresh water molluscs and marls in the Great Lakes Region that little change in the isotopic composition of atmospheric precipitation had occurred over the last 11,000 years, despite significant temperature variations. The precise effect of temperature on the isotopic composition of the Lake water could not be calculated because of complicating effects such as evaporation from the Lake surface. Measurements on the isotopic composition of West Virginia precipitation (next section) substantiate these findings and indicate that a universal model cannot be used to predict oxygen isotopic abundances. These

examples show that it may be unwise to attempt to predict changes in the isotopic composition of meteoric precipitation (and therefore cave waters) on the basis of our present knowledge.

4.9.1 Isotopic Composition of West Virginia Precipitation

As a test of the relationship between δ_w^O and temperature a series of rain and snow samples were collected between June 1971 and March 1972. The majority of these samples were collected by Mr. D.G. McKeever of Buckeye, West Virginia immediately after a significant amount of precipitation. The temperature was recorded during the period of precipitation whenever possible. Snow was allowed to melt indoors then immediately bottled and sealed. The plastic bottles were sealed with tape to avoid losses due to evaporation or spillage.

Since time was limited only a fraction of the samples collected were analysed. Eight samples, four representing summer and four representing winter precipitation were processed. The results are presented in Table 4.4 and in Figure 4.2.

The change in isotopic composition of the precipitation represents a decrease of 0.28 ± 0.07 ‰ in δ_w^O for a 1°C decrease in temperature in approximate agreement with a value of 0.3 ‰/°C calculated by Stuiver, but considerably less than Dansgaard's 0.67 ‰/°C. The West Virginia data are based on few measurements and the temperature dependence of the fractionation could be measured much more accurately. But even an accurate knowledge of the temperature factor would not validate its use for paleotemperature studies because of other meteorological factors which may change over long-term periods.

The average isotopic composition of summer precipitation is

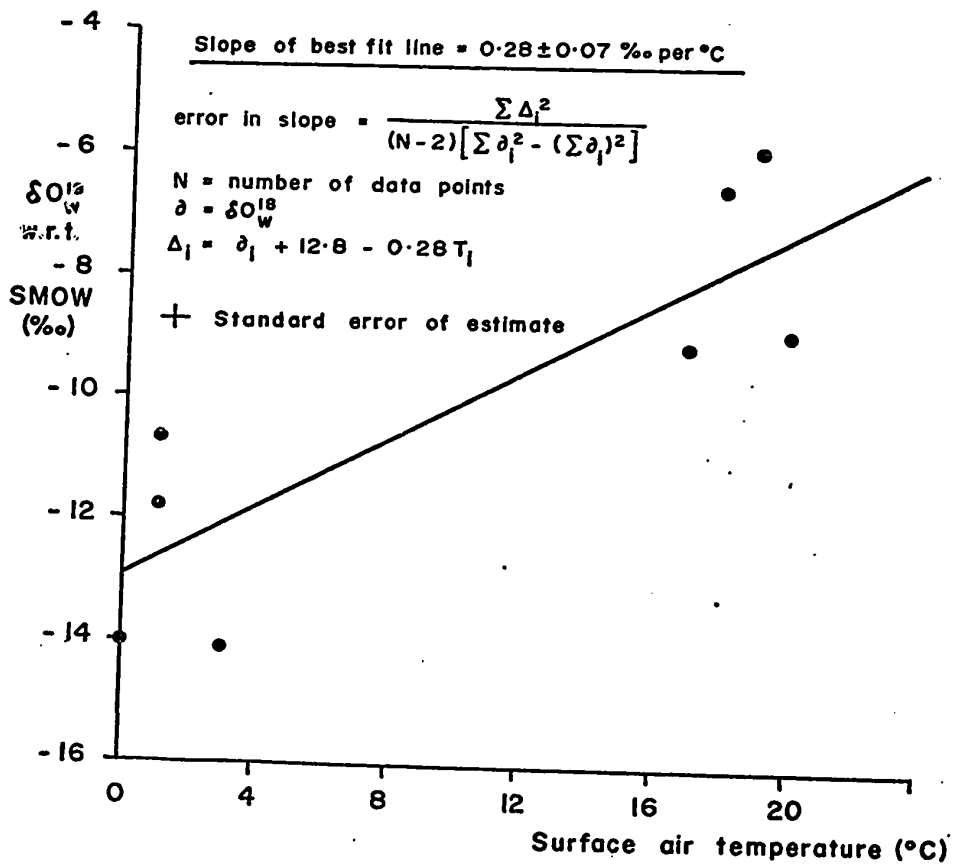


Figure 4.2 Variations in the isotopic composition of West Virginia meteoric precipitation with temperature. (All samples were collected at Buckeye, Pocahontus County).

approximately 1 ‰ heavier than the cave drip-waters which were used for the temperature calculations in Table 4.3 whereas winter precipitation is 4 ‰ lighter than the average drip-water. This suggests that more CaCO_3 is deposited during the summer months than in the winter months in West Virginia. Moore (1962), however, concluded from a study of cave-water chemistry that in Virginia the opposite was true; deposition appeared to be favoured during the winter months.

Table 4.4

Oxygen Isotopic Composition of West Virginia Precipitation

Date of Collection	Form of Precipitation	Measured temperature	$\delta^{18}\text{O}$ H_2O w.r.t. SMOW
10.06.71	Rain	17°C	-9.00
26.06.71	Rain	18°C	-6.49
19.07.71	Rain	19°C	-5.87
21.07.71	Rain	20°C	-8.95
Average		18.5°C	-7.56
21.11.71	Rain	1°C	-10.70
25.11.71	Snow	0°C	-14.00
20.12.71	Snow & Rain	1°C	-11.70
25.01.72	Rain	3°C	-14.10
Average		1.25°C	-12.62

4.10 Effects of Post-depositional Exchange

The changes in isotopic composition of the CaCO_3 of speleothems are approximately the same whether the polymorph is calcite or aragonite because $\epsilon_{\text{ct-w}} \approx \epsilon_{\text{arag-w}}$ (Tarutani *et al.*, 1969). However, if water is present during the inversion of aragonite to calcite, recrystallisation accompanied by isotopic re-equilibration will take place. The resulting isotopic composition of the calcite will reflect only the temperature of transformation and the isotopic composition of the water during re-equilibration. In this situation the apparent age of the calcite may also be affected through migration of the radioisotopes. Therefore, anomalous dating results should reveal changes due to recrystallisation.

In West Virginia (mean annual surface air temperature 10-11°C) both modern and fossil speleothems encountered were entirely composed of calcite. This does not preclude the possibility that recrystallisation has taken place in the past but it does seem to indicate that conditions favouring aragonite deposition are not found in West Virginia caves. Since many of the speleothems studied were essentially single crystals it is probable that the polymorphic form of the first CaCO_3 deposited from solution will determine the form of the remainder of the speleothems.

A further process which should be considered as introducing a source of error is later calcite deposition in the interstices of porous speleothems of either primary or solutional origin. For this reason porous speleothems should be avoided if possible and material removed only from the massively crystalline parts of the deposit.

4.11 Fluid Inclusions in Speleothems and their Applications to Paleotemperature Analysis

4.11.1 Principles

The paleotemperature equations of Epstein or of O'Neil et al. (equations 4.9 and 4.10) require a knowledge of the isotopic composition of the water and of the CaCO_3 deposited from that water. If the isotopic composition of fluid inclusions trapped within speleothems is equivalent to that of waters entering the cave and from which CaCO_3 is deposited (in isotopic equilibrium) then these requirements can be met. However, the oxygen isotopic composition of such fluid inclusions is likely to be altered by isotopic exchange with the CaCO_3 host and therefore cannot, in all probability, be directly measured.

The D/H ratio of atmospheric precipitation, when not affected by kinetic processes, is directly related to the $\text{O}^{18}/\text{O}^{16}$ ratio. Assuming no relative fractionation occurs before atmospheric precipitation ultimately reaches the cave, then the D/H ratio of this water, a measurable parameter, will give directly the $\text{O}^{18}/\text{O}^{16}$ ratio. The oxygen isotopic composition of the host CaCO_3 is easily measured and therefore in principle, an absolute temperature of deposition can be calculated. An evaluation of the method and the assumptions involved follows.

4.11.2 Notation

The usual "del" notation is used as a measure of the D/H ratio. The results are always expressed as ‰ w.r.t. SMOW. Abbreviated notation is as follows:

δ_1^D = hydrogen isotopic composition of fluid inclusions

δ_w^D = hydrogen isotopic composition of cave and surface waters

δ_i^O = oxygen isotopic composition of fluid inclusions (N.B.

which are always calculated from δ_i^D).

4.11.3 Extraction and Analysis of Fluid Inclusions

The water content of speleothems is expected to be quite low. Because only small samples can be analysed (if good resolution of temperature data is to be expected), quantitative recovery of the water is necessary. Isotope fractionation and contamination of the extracted water with atmospheric moisture must also be avoided. Therefore the speleothem samples are crushed in vacuo and the water condensed quantitatively into a breakseal. A photo of the crusher is shown in Figure 4.3. The procedure for extraction is outlined below.

- 1) The weighed sample is placed in the crushing chamber and the apparatus evacuated and left under vacuum overnight. The whole apparatus including the sample is then heated to between 30°C and 40°C to drive off any remaining atmospheric moisture adsorbed on the apparatus or sample.

- 2) The sample is crushed by applying hammer blows to the plunger and the released water is condensed into a break-seal cooled in liquid N₂. Condensed gases are removed by heating the break-seal in a chloroform/carbon tet/ dry ice bath. The crusher apparatus is again heated to 40°C after the crushing operation.

- 3) The break-seal is removed from the line whilst the water is still frozen.

- 4) The CaCO₃ is removed from the crushing chamber, finely

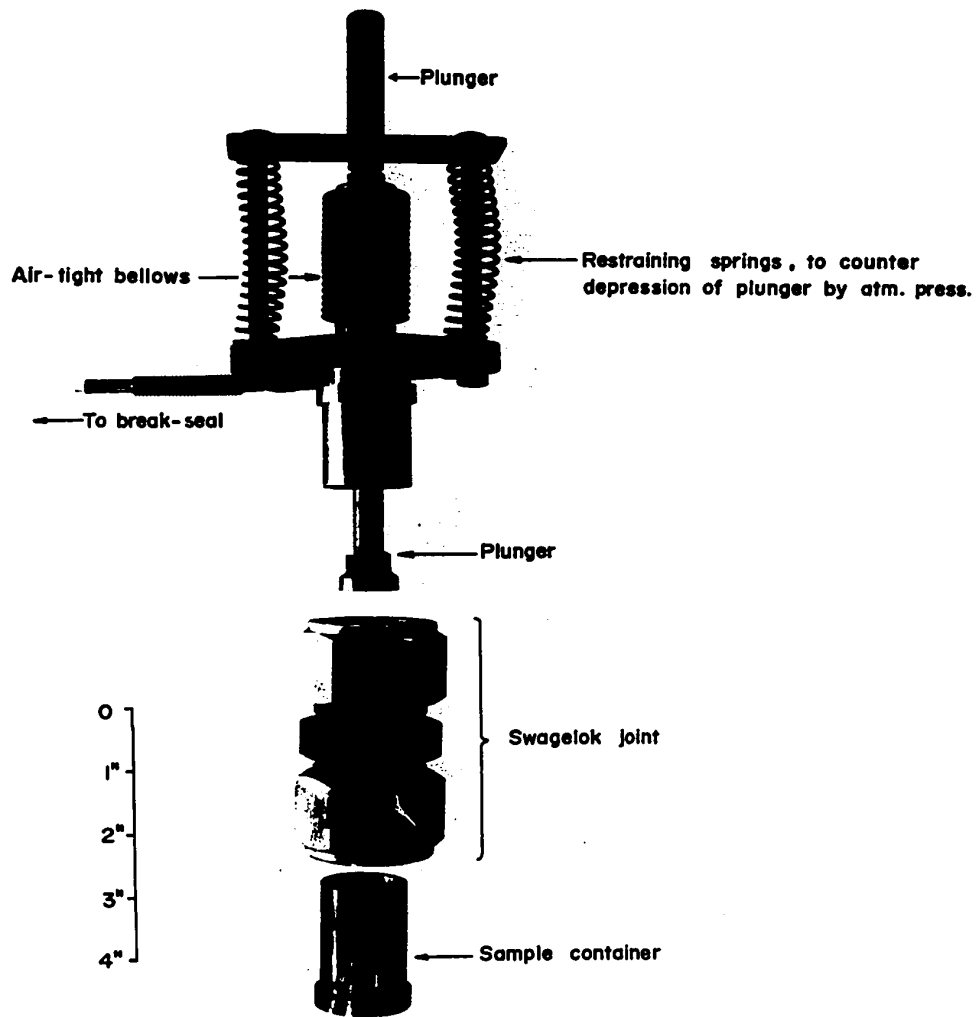


Fig 4.3 Exploded view of the apparatus used for extracting fluid inclusions

ground and homogenised; then an aliquot is analysed for oxygen and carbon isotopic composition.

Since facilities do not exist at McMaster University for carrying out the D/H ratio measurements, Dr. James R. O'Neil of the U.S. Geological Survey in Menlo Park, California kindly analysed most of the samples. (Some early analyses, identified by asterisks in Tables 4.4 to 4.6 were carried out by Dr. K. Hardcastle in Irving Friedman's laboratory at the U.S. Geological Survey in Denver, Colorado).

As little as 0.5 mg of water was successfully analysed using the technique described by Bigeleisen et al. (1952). Briefly, the water is reacted with uranium metal at 800°C and the liberated H₂ is collected on activated charcoal at liquid N₂ temperatures. (Originally the H₂ was collected on finely powdered uranium, but the use of activated charcoal recently supplanted this practice in O'Neil's laboratory). The D/H ratio is determined mass spectrometrically.

4.11.4 Accuracy and Precision

The precision assigned most of the D/H ratio measurements was ± 0.5 ‰. This error combined with an error of ± 0.15 ‰ in $\delta_{\text{Ct}}^{\text{O}}$ results in a precision of $\pm 1^{\circ}\text{C}$ in the isotopic temperature. When either large or very small amounts of water were supplied for analysis the results were probably less precise. A large (>25 mgm) water sample was not entirely converted to H₂ and the process used to obtain a smaller aliquot of the sample may have resulted in errors due to isotopic fractionation. A correction must be applied when very small amounts of H₂ are introduced into the mass spectrometer because the sample is run

at a reduced gas pressure. When either too much or too little water was supplied for an accurate analysis it is noted in the tables of results. These results are not necessarily inaccurate or imprecise, but they should be viewed more critically.

During the course of the analyses the method of H₂ collection was changed. H₂ collected on activated charcoal was consistently found to be 1.5 to 2.0 ‰ lighter than values obtained when a uranium collector was used. It has not yet been resolved if this difference is due to a change in the collecting technique or to changes in the isotopic composition of the working standard gas. Consequently the results obtained may be subject to varying degrees of accuracy but the error involved is not expected to alter the overall trend of the results or the conclusions inferred from them.

Errors introduced during the extraction procedure are expected to be revealed by duplicate analysis of identical samples. A number of "duplicate" analyses were attempted but, by virtue of the fact that unbroken samples of a potentially inhomogeneous material had to be used, true duplicates were impossible to obtain. Increasing experience with the extraction procedure resulted in the successful analysis of smaller and smaller samples. Only these later analyses were considered to represent near-identical samples. These include NB10-3a/b, NB10-8a/b and NB10-9a/b. As can be seen by reference to Table 4.5 there are small but significant differences in the isotopic composition of the extracted water from these duplicates. Whether this is due to instrumental error or to a process of fractionation intrinsic to the extraction procedure could not be resolved in the time available.

4.11.5 The $\delta_w^D - \delta_w^O$ Relationship

Craig (1961) and Dansgaard (1964) have shown that variations in the D/H isotope ratio (δ_w^D) and in the oxygen isotope ratio (δ_w^O) of meteoric precipitation are related in a constant manner. The relationship arises from the process by which water is evaporated and condensed in the hydrologic cycle. For the most common situation, where water is evaporated from the oceans in a non-equilibrium process and fractionally condensed in an equilibrium, isobaric or moist adiabatic process the following linear relation between δ_w^D and δ_w^O is found:

$$\delta_w^D = (8.0 \pm 0.2) \delta_w^O + (10 \pm 1) \quad \dots\dots\dots(4.20)$$

The straight line of slope 8 and δ_w^D intercept of +10 ‰ is usually termed the meteoric water line. Both the slope and intercept (termed the deuterium excess) of this line can vary if other processes are acting. If, through rapid evaporation of falling drops, kinetic isotope effects become significant the relationship becomes:

$$\delta_w^D = (4.6 \pm 0.4) \delta_w^O + (0.1 \pm 1.6) \quad \dots\dots\dots(4.21)$$

In any process involving kinetic isotope effects which induce variations in δ_w^D and δ_w^O , the deuterium component will be much less affected than the oxygen component. This explains the lower slope of the δ_w^D versus δ_w^O plot in 4.21. Similarly, kinetic isotope effects caused by rapid ablation of snow can lead to melt-waters whose isotopic composition is not described by 4.20. Moser and Stichler (1970) find the following relationship in melt waters:

$$\delta_w^D \approx 7 \delta_w^O - 10 \quad \dots\dots\dots(4.22)$$

Equation (4.20) appears to hold for precipitation at middle and high latitudes (Dansgaard 1964; Craig, 1961) and in Greenland ice the relationship appears to be time invariant (Dansgaard et al., 1969) at least to approximately 120,000 years B.P.

Non-equilibrium condensation can result in a linear relationship between δ_w^D and δ_w^O with a slope >8 and, depending upon the thermal history of atmospheric vapour, other deuterium excess values can be measured (Dansgaard, 1964, p.459). The value of the deuterium excess depends on the extent of initial disequilibrium between the vapour phase and the ocean. When the relative humidity is low, and evaporation high, water vapour is depleted more in O^{18} than deuterium and the deuterium excess increases. For example, in the Eastern Mediterranean region the excess is $+22$ ‰ (Nir, 1967).

Duplessey et al. (1971) have measured the $\delta_w^D - \delta_w^O$ relationship in cave waters. The isotopic composition of waters from Southern France (Aven d'Orgnac and La Cave) is almost exactly described by equation 4.20. Waters from the Grange Mathieu (Jura) fell parallel to but slightly displaced from the meteoric water line; the deuterium excess was approximately $+6$ ‰.

4.11.6 The $\delta_w^D - \delta_w^O$ Relationship in West Virginia Precipitation and Cave Waters

Throughout this study equation 4.20 was used as a basis for converting δ_i^D (equivalent to δ_w^D) to δ_i^O . To test the validity of this assumption some cave waters and a surface snow sample (collected in January, 1971) were analysed. Four Norman-Bone cave drip waters were

collected in April, 1971 and the Overholts Blowing Cave sample was collected in September, 1970. The results are plotted in Figure 4.4. Only one of the six samples analysed falls on the meteoric water line and the remainder fall on a line approximately parallel to it. The displacement of these samples from the meteoric water line is not in the direction expected if exchange between the (heavier) limestone and water occurred. Evaporation would also leave the residual water relatively enriched in both deuterium and O^{18} , but the majority of waters are depleted in deuterium and O^{18} relative to "model" waters falling on the meteoric water line. These results are difficult to explain in terms of the conventional isotopic fractionation effects discussion in Section 4.11.5.

A drip-water collected from Overholts Cave in September is probably more representative of summer precipitation than those collected in Norman-Bone Cave in April. From these limited data there appears to be a seasonal effect on the relationship between δ_w^D and δ_w^O . This is not uncommon according to Dansgaard's precipitation survey (1964); for example in the Chicago area the slope of the δ_w^D versus δ_w^O plot for winter precipitation is 7 ± 1 and for summer precipitation is 5 ± 1 whilst for winter precipitation the deuterium excess varies from $+22 \text{ ‰}$ to -15 ‰ .

Because $CaCO_3$ deposition in West Virginia appears to be most active in the summer months it has been assumed that fluid inclusions obey the Craig-Dansgaard relationship. Clearly more evidence is required to support this assumption. Some indirect evidence is cited below.

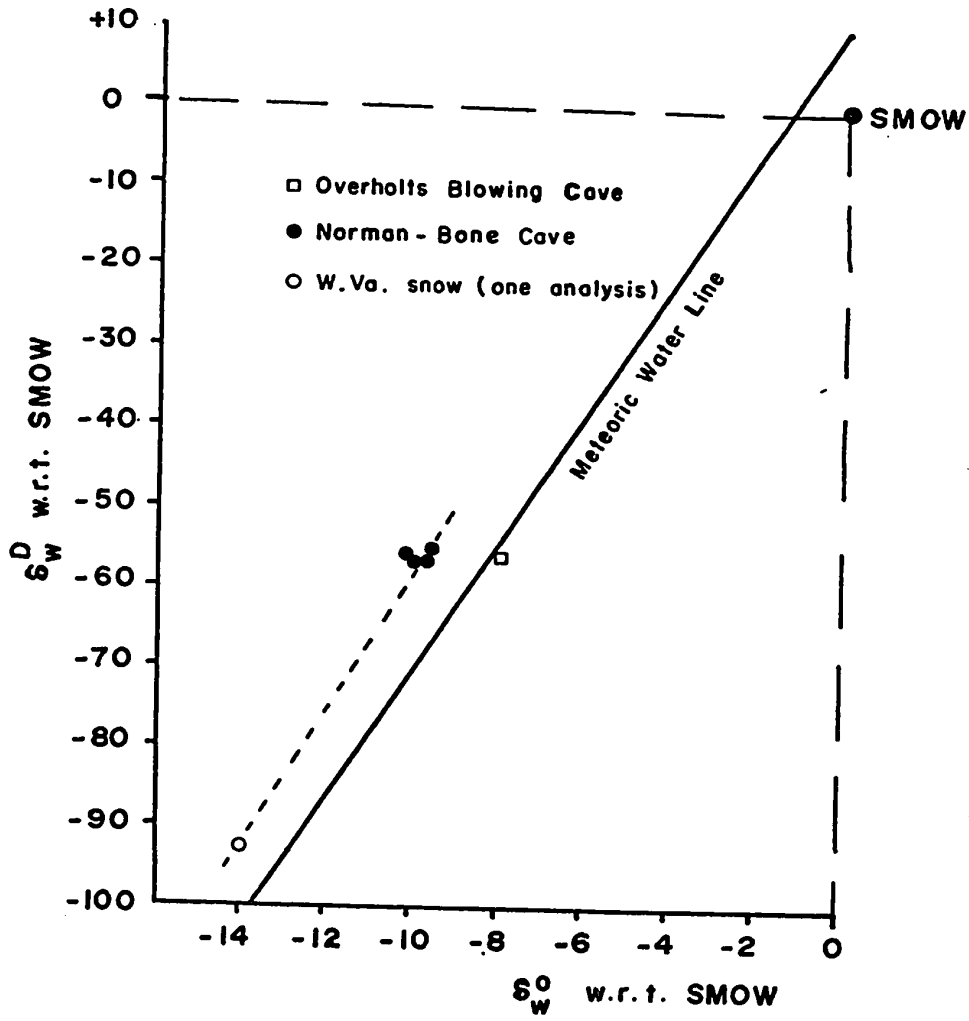


Figure 4.4 Relationship between δ_w^D and δ_w^O in West Virginia cave waters and one sample of snow.

4.11.7 δ_w^D and δ_{ct}^O in Recent Speleothems and Fluid Inclusions

A search for recent speleothems was undertaken to check the validity of this new method for isotopic thermometry. For the most recent speleothems temperatures of deposition calculated from δ_1^D and δ_{ct}^O should not only be uniform for one cave but they should be approximately equal to the present mean annual surface temperature. The tips of four stalactites were collected from the Norman-Bone Cave. Approximately 5 gm of $CaCO_3$ was considered to be a minimum sample weight. Drip-water was collected at each site; the isotopic composition of these four drip-waters are represented by the cluster of points on Figure 4.4.

The stalactites were judged to be recent because they were small and appeared to be actively growing. A dated, recent stalagmite (NB11) was available for analysis but no drip-water was collected at this site. NB11 was actively growing between 3600 and 2000 years B.P. In addition, an undated stalagmite inferred to be recent was collected from the Half-Way Room of Norman-Bone Cave (NBM-1).

From the fluid inclusion data and the oxygen isotopic composition of the calcite a temperature of deposition was calculated. The results are shown in Table 4.5. A number of points emerge from these results:

- 1) In only 2 out of 7 analyses is the isotopic temperature comparable to the measured cave temperature (NC6 and NBM-1).
- 2) The D/H ratio of the fluid inclusions is not comparable to the D/H ratio of the drip-waters.

Table 4.5

Stable Isotope Data for Recent Speleothems from Norman-Bone Cave

Sample	Date of Collection	δ_{dw}^O SMOW	δ_i^D SMOW	δ_i^O (calc) SMOW	δ_{dw}^O SMOW	δ_{ct}^O w.r.t P.D.B.	$T^{\circ}C$
NC4-b	04.20.72	-55.5	-59.7	- 8.71	-10.32	-5.70	6.3
NC5	04.20.72	-55.3	-64.2	- 9.27	- 9.67	-6.47	4.8
NC6	04.20.72	-56.4	-59.4	- 8.67	-10.13	-6.87	8.0
*NC7	04.20.72	-56.9	-39.3	- 6.16	- 9.93	-6.36	18.2
+NBM-1	-	-	-60.1	- 8.76	-	-7.87	12.0
*NB11-2	-	-	-74.2	-10.52	-	-7.02	1.7
*NB11-1	-	-	-34.0	- 5.50	-	-5.66	19.7

* Mass spectrometer results corrected for low signal voltage

+ Analysis by K. Hardcastle

3) δ_{ct}^O is not constant as would be expected if all the deposits were recent and deposited in isotopic equilibrium.

4) The inordinately high (NC7 and NB11-1) and low (NB11-2) isotopic temperatures are caused principally by large fluctuations in δ_i^D .

It is shown in Section 4.11.8 that the isotopic temperatures calculated for NC4-b and NC5 are probably acceptable. These temperatures are lower than present-day temperatures because the deposits are not recent but were probably formed during a cooler period and have only recently become active again.

From Table 4.3 the average isotopic composition of freshly deposited CaCO_3 is -6.95 ‰ (23.21 ‰ w.r.t. SMOW). The analyses reported in Table 4.2 are probably more representative of very recent deposits than those in Table 4.4 because for the former only approximately 0.5 gm of the most recent material deposited was collected for analysis. Approximately ten times as much material was required for a successful D/H analysis. Only when the oxygen isotopic composition of a speleothem approximates this average value can it be considered a very recent deposit. Deviations from the average are therefore controlled either by kinetic processes or by fluctuations of climate. Sample NC6 most closely resembles the present-day deposits both with respect to the isotopic composition of the calcite and the temperature of deposition. The only other non-dated sample that can be considered recent on the basis of its oxygen isotopic composition is NC7.

The results for NB11 are unacceptable because no such temperature fluctuations can be considered within the period that deposition

took place. Similarly, NC7 must be rejected because cave temperatures of 18°C are most unlikely. All three results are linked by a common factor: the quantity of water extracted from the samples was extremely low. A convenient explanation would be that water was lost during the pre-treatment of the samples but evaporative losses would leave the residual water enriched in deuterium and therefore cannot explain the "light" water extracted from NB11-2. A possible explanation of these results is the replacement of the primary inclusions with "light" or "heavy" water representative of winter and summer precipitation respectively. This possibility is explored further in Section 4.11.8.

The average δ_1^O as predicted from the Craig-Dansgaard relationship (and excluding the "anomalous" analyses, NC6, NB11-1 and -2) is -8.85 ‰ which is close to the average summer drip-water composition of -8.66 ‰ in the Norman-Bone Cave (Table 4.3). Evidently the April drip-waters, with an isotopic composition closer to that of atmospheric precipitation collected during the winter, are not potential fluid inclusions. These limited data are in agreement with the earlier statement that active deposition on speleothems takes place predominantly in the summer months. This is rather indirect support for the validity of the Craig-Dansgaard relationship for fluid inclusions.

4.11.8 δ_1^D and Temperature of Deposition of Fossil Speleothems

Stalagmite NB10 from Norman-Bone Cave appears to have been deposited in isotopic equilibrium and was one of the fossil speleothems chosen for analysis. The locations of the samples are shown in Figure 4.5,

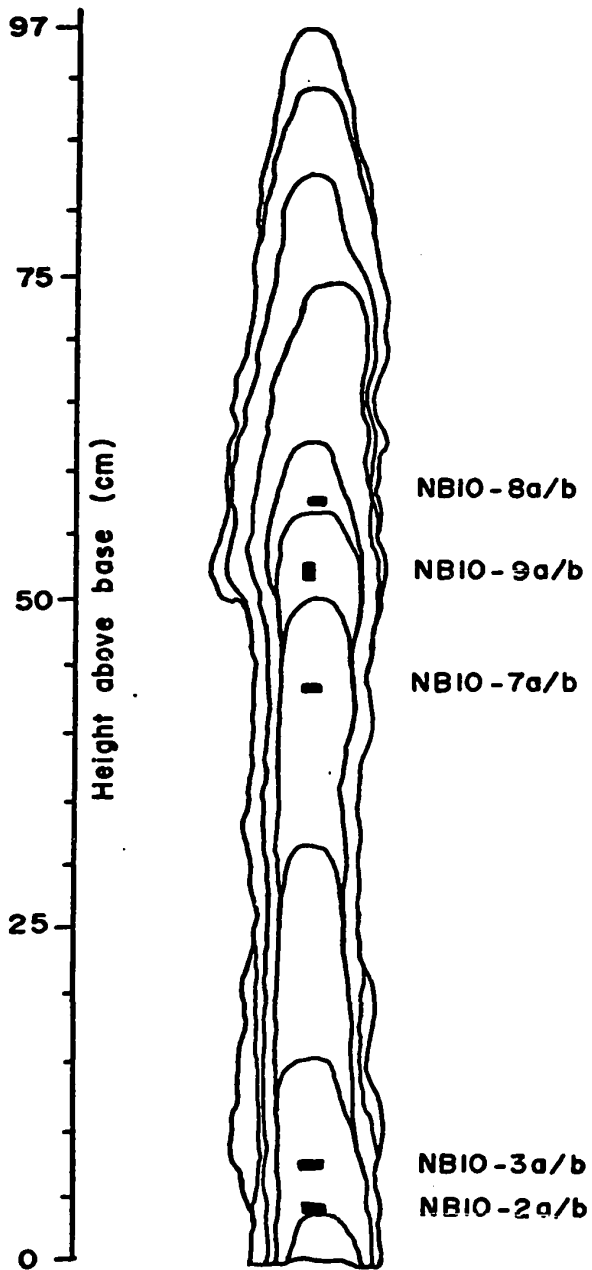


Figure 4.5 Location of samples removed from the Norman-Bone Cave stalagmite NB10 for fluid inclusion analysis.

Table 4.6

Stable Isotope Data for a Fossil Speleothem from Norman-Bone Cave

Sample	Average height above base (cm)	δ_i^D w.r.t. SMOW	δ_i^{18O} (calc) w.r.t. SMOW	δ_{ct}^{18O} w.r.t. SMOW	$T^\circ C$	Age
NB10-9a	59	-65.7	-9.46	24.22	1.69	173,000 \pm 5000
NB10-9b		-64.2	-9.27	24.12	2.77	
NB10-8a	53	-52.4	-7.80	24.01	9.24	-
NB10-8b		-55.3	-8.16	24.07	7.30	
NB10-7a	46	-60.5	-8.81	23.41	7.22	183,000 \pm 6000
NB10-7b		-62.5	-9.06	23.51	6.04	
NB10-3a	8	-66.1	-9.51	23.95	2.51	-
NB10-3b		-71.0	-10.10	24.00	-0.01	
NB10-2a	5	-70.0	-10.00	24.41	-1.00	200,000 \pm 7000
NB10-2b		-61.7	-8.96	24.16	3.84	

and the results are presented in Table 4.6. The results show that there is no relationship between the temperature of deposition and δ_{ct}^O , which is approximately constant, but in general the fluid inclusions become lighter as temperatures decrease.

A second fossil deposit from Grapevine Cave (GV2) was also analysed in detail. (The morphometry of both deposits is described in detail in Chapter 6). Figure 4.6 shows the location of each of the samples and the results of the analyses are shown in Table 4.7. In this deposit there is a 3 ‰ variation in δ_{ct}^O and little variation in δ_i^O . The general trend of results indicates that lower temperatures are characterised by lighter fluid inclusions and heavier δ_{ct}^O values. Some of the results are unacceptable: these include GV2-2b, GV2-3c and GV2-5a. GV2-2b may be an untrustworthy analysis because the extracted water was not completely converted to H₂, but the other analyses were considered trustworthy from the standpoint of hydrogen isotopic analysis. The negative temperatures of deposition are associated with the heaviest calcites and the lightest fluid inclusions.

It is certain that some of the calculated temperatures are too low and it is possible that the isotopic temperatures in general are slightly too low. However, a constant systematic error in the method cannot account for the discrepancies, because lower temperatures are more in error than higher temperatures. If it is assumed that the errors are not due to kinetic effects during the deposition of CaCO₃ or to widespread replacement of the primary inclusions (which should result in random rather than consistent low temperatures) then the error may be due to a change in the $\delta_w^D - \delta_w^O$ relationship. The work of

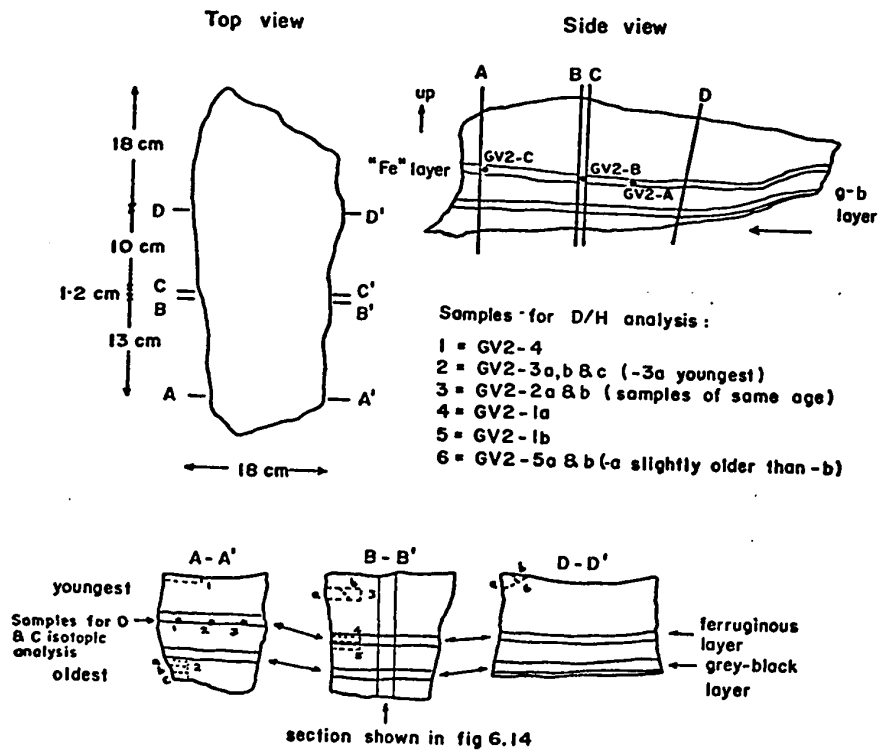


Figure 4.6. Sectioning and location of samples for stable isotopic analysis in the Grapevine Cave flowstone, GV2. (Figure 6.14 shows the stratigraphy in more detail).

Table 4.7

Stable Isotope Data for a Fossil Speleothem from Grapevine Cave

Sample	Average ht. above base* (cm)	% H ₂ O	δ_i^D		$\delta_i^{18}O$ (calc)		$\delta_{ct}^{18}O$ w.r.t. SMOW	T°C	Age years B.P.
			w.r.t. SMOW	w.r.t. SMOW	w.r.t. SMOW	w.r.t. SMOW			
GV2-5b	17.0	-	-62.5	-9.06	25.53	-1.50	} 60,400±2900		
GV2-5a	16.5	-	-62.1	-9.01	26.67	-5.24			
GV2-2a ⁺	15.0	0.18	-51.2	-7.65	26.43	0.46	} 70,200±3600		
GV2-2b ^{***}	15.0	0.23	-61.9	-8.99	26.80	-5.62			
GV2-1a ^{***}	6.0	0.24	-52.2	-7.78	24.29	7.98	97,200±3000		
GV2-1b ⁺	5.0	0.38	-56.6	-8.33	24.24	5.96	104,500±2700		
GV2-3a	3.0	-	-58.3	-8.54	26.40	-2.65	} 159,000±6000		
GV2-3b	2.0	-	-54.5	-8.06	24.20	7.22			
GV2-3c	1.0	-	-64.8	-9.35	26.25	-5.03			

* The height of each sample has been normalised to coincide with the scale on Figs 6.15 and 6.16.

** Incomplete conversion of H₂O → H₂

+ Analyses by K. Hardcastle

Moser and Stichler may be relevant here, for they showed that the $\delta_W^D - \delta_W^O$ relationship in aged snow is different from that in freshly deposited snow. If the isotopically heavy calcites do represent deposition during a cold period when mean annual temperatures approached zero degrees then a large proportion of the cave drip-water would be derived from snow melt. Their equation (4.22) predicts that δ_W^O will be isotopically heavier relative to the value obtained using the Craig-Dansgaard relationship. Isotopic temperatures which were formally negative do, in fact, become slightly positive when the Moser-Stichler relationship is used. This explanation is entirely speculative and, if proven correct, will complicate even further interpretation of the isotopic evidence from proglacial areas.

In Figure 4.7 all the data, both for recent and fossil speleothems are plotted as δ_i^D against the calculated (isotopic) temperature of deposition. A straight line has been fitted to the data from Norman-Bone Cave by the method of least squares. The slope of this line is 1.64 ± 0.21 ‰ per °C. Assuming $(d\delta_i^D)/(d\delta_i^O) = 8$, then the change in δ_i^O is 0.20 ± 0.03 ‰ per °C. This is comparable to the same value obtained experimentally for present-day precipitation (Figure 4.2) and is considerably less than the 0.67 ‰ per °C proposed by Dansgaard. Schiegl (1972) has shown that the temperature dependence of δ_W^D for Dutch precipitation is approximately 3.3 ‰ per °C (0.4 ‰ per °C for oxygen). This confirms that a universal value for the temperature dependence of the isotopic fractionation in precipitation is not valid.

The Grapevine Cave data show considerable scatter but if the

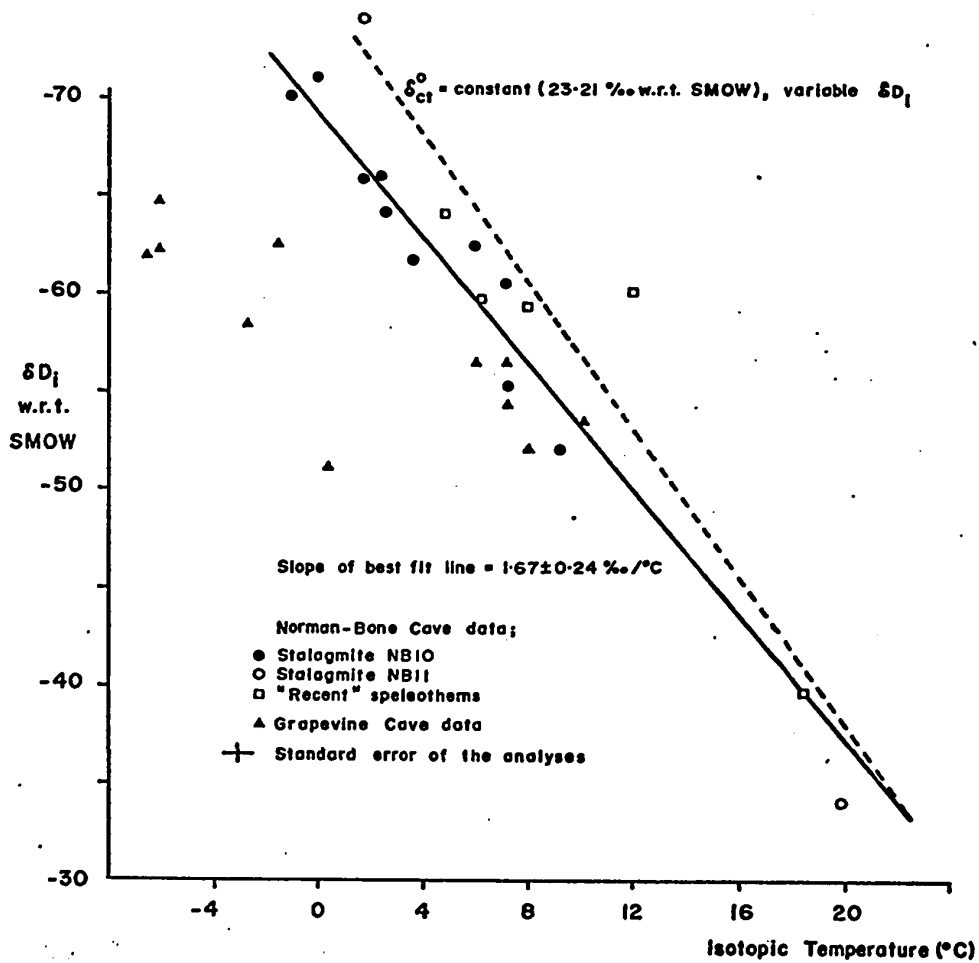


Figure 4.7. The relationship between δ_1^D (the D/H isotopic ratio in fluid inclusions) and the calculated isotopic temperature of deposition of recent and fossil speleothems. (The line is fitted to the NB10 data and the "recent" speleothem data only).

negative temperatures are discarded the remaining data points cannot be distinguished from the Norman-Bone data. This suggests that, at least during warm periods, parallel isotopic variations in the precipitation over these two caves occurred.

The slope of 0.2 ‰ per °C for the Norman-Bone data explains the relatively constant δ_{ct}^O values for NB10 samples. $CaCO_3$ deposited from water of constant isotopic composition is enriched in O^{18} by 0.24 ‰ per °C decrease in temperature. But the water is depleted in O^{18} by 0.2 ‰ per °C decrease in temperature, so the net effect is an enrichment of only 0.04 ‰ per °C in δ_{ct}^O . This does not explain the relatively large δ_{ct}^O variations observed in GV2 samples and suggests that the δ_1^O versus temperature of deposition relationship is not constant, as might be inferred from Figure 4.7.

An attempt is made to explain these observations in terms of climate change rather than non-equilibrium fractionation or random δ_w^O variations in Chapter 8 (Section 8.6). More evidence is collected in the following Chapters to show that in general a decrease in regional temperature is accompanied by the deposition of speleothems relatively enriched in O^{18} , as in GV2.

The best-fit line in Figure 4.7 when extrapolated to higher temperatures also fits (approximately) the data which were rejected previously as unacceptable (NB11-1,-2 and NC7). In a different situation, where limits could not be placed on temperature extremes, the data might be regarded as acceptable. Consequently the correlation between δ_1^D and temperature cannot be offered as a criterion for acceptable results.

This situation may be explained by replacement of the original fluid inclusions. The dashed line in Figure 4.7 illustrates how the calculated temperature of deposition will vary if the isotopic composition of the water changes whilst the isotopic composition of the CaCO_3 remains constant. The average $\delta_{\text{ct}}^{\text{O}}$ of freshly deposited recent CaCO_3 (23.21 ‰ w.r.t. SMOW) was chosen to show that the anomalous results could be explained by this phenomenon. The best-fit line to the speleothem data and this artificially constructed line converge at a temperature of 22°C, explaining the fit of the anomalous data to the best-fit line. The original fluid inclusions in NB11-2 were apparently replaced by isotopically light water typical of winter precipitation whilst in the case of NB11-1 and NC7 the inclusions were replaced by water more typical of summer precipitation.

Correct interpretation of the results of this study must rely upon the assumption that the original fluid inclusions have not been replaced at a later date by water of different isotopic composition. To help in this interpretation the isotopic composition of the CaCO_3 must be taken into account; if a relatively light CaCO_3 gives a low temperature of deposition (for example NB11-2) then the result must be considered suspect. The water content of the sample may also help in determining the usefulness of the result: it has already been noted that the anomalous results were associated with calcites containing very little included water.

The total variation in δ_i^{O} of the fluid inclusions analysed so far is surprisingly small considering that a wide range of climates is apparently encompassed by the samples analysed, which range in age

from 200,000 years to modern. This agrees with the results obtained by Stuiver (1968) in the Great Lakes Region but stands in direct contradiction to the predictions of Dansgaard. However, the primary fluid inclusions represent only the isotopic composition of water from which CaCO_3 was deposited and this is not necessarily a measure of mean annual meteoric precipitation. It has already been noted that the majority of speleothem deposition in West Virginia at present takes place during the summer, therefore, the isotopically lighter winter precipitation plays little part in determining the isotopic composition of recent fluid inclusions. This relationship between the "season" of CaCO_3 deposition and the isotopic composition of fluid inclusions is developed further in Chapter 8.

4.11.9 The Ability of Speleothems to Retain Fluid Inclusions

Because temperatures of deposition can only be obtained from speleothems that have retained the primary fluid inclusions in an isotopically unmodified form, an experiment was designed to determine under what conditions the included water is removed. It was considered particularly necessary to establish if leaving the samples under vacuum for up to 24 hours resulted in significant losses.

Ten cubes approximately 1.2 cm along each edge were cut from a section of flowstone from Grapevine Cave (section B-B' in Figure 4.6), weighed and then placed in a vacuum oven at room temperature. Figure 4.8 shows the position of each sample in relation to the growth layers and in relation to the isotopic analyses. The cubes were re-weighed at intervals to record weight loss under vacuum and at intervals the

Figure 4.8 Location of samples removed from Grapevine Cave Flowstone GV2 and heated under vacuum to measure water retention characteristics. (The location of samples removed for fluid inclusion analysis and isotopic temperature calculations is shown on the extreme right of the figure).

Sample No.				Isotopic Temp, °C	
▶	1	0.918*	0.261**	} GV2-5a - 5.24 GV2-5b - 1.50	
1" ▶	2	5.02	0.260		} GV2-2a 0.46 GV2-2b - 5.62
	3	5.65	0.305		
2" ▶	4	0.765	0.290		
	5	2.91	0.150		
	6	3.32	0.161		
4" ▶	7	3.01	0.206	} GV2-1a 5.96 GV2-1b 7.98	
5" ▶	8	1.75	0.301		
	9	1.55	0.262		
6" ▶	10	3.65	0.253	} GV2-3a - 2.65 GV2-3b 7.22 GV2-3c - 5.03	
7" ▶					

* % of total water removed between 4.5 and 24.5 hrs under vacuum at ambient temperature.

** total amount of water removed under the conditions of the experiment (in gms)

temperature of the oven was increased to a final temperature of 110°C. The progressive weight loss, which was presumed to be due to gradual evaporation of the fluid inclusions, is recorded in Table 4.8. The weight loss after 4.5 hours was attributed to the removal of the majority of the surface adsorbed water. The experiment was concluded after 116 hours when it was considered that the majority of the included water had been removed.

The results show that most of the included water is retained under vacuum at ambient temperatures so it can be reasonably assumed that the inclusions are isolated from the cave environment and are not lost or replaced under normal conditions. The water content is reasonably constant regardless of age and is comparable to the measured values reported in Table 4.7. However, small losses do occur between 4.5 and 20 hours which indicates that a correction for loss during outgassing should be applied to the measured δ_i^D . (The brief heating period immediately prior to crushing the sample is not expected to result in significant extra losses but clearly the heating episode should not be too long or too intense. In light of these results the heating step is probably best omitted). Water containing the light isotopes O^{16} and protium will be preferentially lost and the measured δ_i^D of the residual water will therefore be heavier than the original water.

An attempt can be made to correct for these losses if it is assumed that isotopic fractionation is controlled by the Rayleigh Distillation law. (N.B. There is no justification for assuming that all of the water removed by outgassing is primary included water).

Table 4.8

Loss of Water from Speleothem Samples when Heated Under Vacuum

Sample No. see Fig. 4.7	4.5 hrs at 20°C	20 hrs at 20°C	24 hrs at 60°C	24 hrs at 80°C	22 hrs at 100°C	20 hrs at 110°C
1	a) 0.000017	0.000152	0.003064	0.005714	0.004978	0.002561
	b) 0.00030	0.00240	0.0509	0.1422	0.2209	0.2614
	c) 0.115	0.92	17.9	54.5	84.5	100
2	a) 0.000815	0.000894	0.005332	0.008028	0.001796	0.001910
	b) 0.0118	0.0249	0.1025	0.2193	0.2441	0.2719
	c) 4.35	8.95	38.0	80.5	90.0	100
3	a) 0.000915	0.001108	0.006316	0.008689	0.001704	0.001791
	b) 0.0142	0.0315	0.1299	0.2652	0.2917	0.3196
	c) 4.45	9.85	40.5	83.0	91.2	100
4	a) 0.000115	0.000124	0.004098	0.007120	0.003402	0.001390
	b) 0.0021	0.0043	0.0780	0.2061	0.2673	0.2923
	c) 0.72	1.47	26.7	70.5	91.5	100
5	a) 0.000358	0.000270	0.002327	0.004163	0.001273	0.001228
	b) 0.0058	0.0102	0.0480	0.1157	0.1364	0.1564
	c) 3.7	6.52	30.7	74.0	87.5	100
6	a) 0.000096	0.000321	0.003273	0.004161	0.001542	0.001374
	b) 0.0016	0.0069	0.0448	0.1142	0.1399	0.1628
	c) 0.98	4.25	27.5	70.2	86.0	100
7	a) 0.000237	0.000390	0.002136	0.004453	0.004088	0.001805
	b) 0.0038	0.0100	0.0442	0.1156	0.1811	0.2100
	c) 1.8	4.77	21.0	55.0	86.5	100
8	a) 0.000163	0.000314	0.002412	0.005899	0.006860	0.002475
	b) 0.0027	0.0080	0.0485	0.1475	0.2626	0.3041
	c) 0.89	2.63	15.9	48.5	86.2	100
9	a) 0.000178	0.000198	0.001465	0.003982	0.005123	0.001977
	b) 0.0037	0.0077	0.0379	0.1199	0.2254	0.2661
	c) 1.4	2.89	14.3	45.0	84.5	100
10	a) 0.000481	0.000595	0.002506	0.006341	0.005325	0.001540
	b) 0.0074	0.0167	0.0555	0.1537	0.2362	0.2601
	c) 2.8	6.43	21.3	59.0	91.0	100

a) weight loss (gm)
b) cumulative weight loss
c) percent of total weight loss

The original isotopic composition of the fluid inclusions may be calculated from the equation:

$$R/R_0 = f^{(1-\alpha)}$$

where f = fraction of the initial liquid water remaining

α = fractionation factor

R = H_2O^{18}/H_2O^{16} ratio of the residual water

R_0 = H_2O^{18}/H_2O^{16} ratio of the water before distillation is initiated.

If fractionation is an equilibrium process then $\alpha^D = 1.080$ at 25°C. If kinetic fractionation effects are involved $\alpha^D = 1.11$.

Corrections have been evaluated assuming both equilibrium and kinetic processes in an attempt to assign limits to the expected error. Samples GV2-1a and GV2-2b have been chosen to illustrate the magnitude of the correction. These are shown in Table 4.9.

Loss of fluid inclusions prior to crushing therefore will give a calculated temperature of deposition higher than the actual temperature of deposition. When the loss is less than 1% the correction will be negligible. In light of these results, which were obtained after fluid inclusion analyses were completed, it is apparent that the period the sample is left under vacuum before crushing should be reduced. An optimum time should be determined by experiment. Also, the ability of representative samples to retain fluid inclusions should be determined before crushing is attempted.

Table 4.9
Isotopic Temperatures Corrected for Fluid Inclusion Loss

Sample	f	δ_i^D (meas)	δ_i^D (corr)		T ^o C		
			$\alpha=1.08$ (equil)	$\alpha=1.11$ (kin.)	meas.	corr with $\alpha=1.08$	corr with $\alpha=1.11$
GV2-2b	0.95	-61.9	-65.74	-67.18	-5.62	-7.27	-7.88
GV2-1b	0.97	-56.6	-58.89	-59.75	5.96	4.66	4.45

Conclusions

From the results presented so far a number of conclusions regarding the behaviour of stable isotopes in precipitation and during the deposition of CaCO₃ on speleothems can be noted.

1) Conditions favouring the deposition of CaCO₃ in isotopic equilibrium with cave waters are found in West Virginia caves. These conditions are not fully understood but slow rates of deposition in an unventilated, moist environment where concentration of CO₂ in the cave air is relatively high are probably important.

2) Freshly deposited (recent) calcites have an isotopic composition close to -6.95 ‰ w.r.t. P.D.B. (23.21 ‰ w.r.t. SMOW). Isotopic temperatures of deposition of fresh calcites when calculated from δ_{ct}^O and δ_w^O are slightly lower than measured mean annual surface temperatures (by about 2^oC).

3) More deposition of CaCO₃ on speleothems appears to take place during the warmer, summer months.

4) Primary fluid inclusions, representing fossil seepage waters, are potentially useful for interpreting oxygen isotopic variations in the CaCO_3 of speleothems. There are firm indications that regional cooling is accompanied by the deposition of isotopically heavier CaCO_3 .

5) If assumptions are made about the $\delta_w^D - \delta_w^O$ relationship, temperatures of deposition may be calculated. Temperatures are occasionally out of the range expected in West Virginia. The reason for these anomalous temperatures is not known but they may be due to replacement of the primary inclusions and/or a change in the $\delta_w^D - \delta_w^O$ relationship in response to climate changes.

6) From analyses of recent precipitation and fossil fluid inclusions, a 1°C decrease in regional temperature results in precipitation depleted by 0.2 to 0.3 ‰ in O^{18} .

7) Systematic errors introduced during the extraction of the inclusions or during the measurement of isotopic ratios may account for some of the anomalous results.

CHAPTER FIVE

RADIOCHEMICAL ANALYTICAL TECHNIQUES

5.1. Sample Preparation

Preparation and handling of samples was kept to a minimum. The interior portions of stalagmites were always used because the exterior of many of the stalagmites were often contaminated with clayey material. Based on the morphology of stalagmites it was found that a drill core whose diameter is about 2/3 that of a columnar stalagmite avoids contamination by younger layers deposited parallel to the surface of growth. Depending on the diameter of the stalagmite either a 2" or 1" drill was used to obtain sample cores. The cores were lightly etched in dilute acid to remove CaCO_3 slurry and possible contamination from the drill. Samples were then drilled out normal to the axis with a 1/8 " hand-drill for stable isotope analysis. To avoid contamination by rock dust from other samples the cores were not processed in the crushing laboratory but were broken into smaller fragments in a mortar, and then dissolved in cold 2N HNO_3 . Most samples were entirely soluble in the HNO_3 and gave a clear solution. When any insoluble residue was obtained it was filtered off and weighed. In only a few cases, notably the Grapevine flowstone analysis reported later, did the insoluble residue amount to more than 0.1%.

Flowstone samples offered more of an extraction problem. Since they were deposited as successive thin, horizontal layers, a single,

well-defined layer or a group of layers should ideally be sampled for analysis. However, in the flowstone sample collected from Grapevine Cave not only were there slight surface irregularities from layer to layer but also the block thinned out from one end to the other. The result was that attempts to obtain single layers by sawing parallel to the lamination resulted in saw cuts transecting growth layers, making it impossible to assign absolute ages to the successive layers. However, when it became important to know the age of a particular layer in the block a different technique was tried which enabled the entire layer to be sampled. A small handheld pneumatic drill was used to chip off small pieces of calcite until all of the layers of interest had been removed. This was quite a successful approach, but time consuming.

5.2. Analytical Considerations

The object of the chemical separations is to extract radiochemically pure uranium and thorium from the CaCO_3 samples. Both U and Th are mounted on stainless steel disks for α - counting and isotopic analysis. The isotopic ratios of interest are $\text{Th}^{230}/\text{U}^{234}$, $\text{U}^{234}/\text{U}^{238}$, and $\text{Th}^{230}/\text{Th}^{232}$. There are two considerations of prime interest when preparing uranium and thorium for isotopic analysis:

(1) The final preparation should not be contaminated with chemical impurities because these would be deposited on the planchet and thus constitute a "thick" source when counting. A sample thickness of more than approximately 100 micrograms/sq. cm. leads to attenuation of the α -particles and a tailing of the low energy side of a peak into adjacent peaks of lower energy. It is possible, but troublesome to

correct for this effect.

(2) The final preparations should also be radiochemically pure, i.e. free from radioisotope impurities with similar α - particle energies. Naturally occurring isotopes which fall in this category can be classed in two groups, namely those that interfere with the uranium spectrum and those that interfere with the thorium spectrum. Th^{232} , Th^{230} , Th^{228} , Ra^{226} , Po^{210} and Bi^{210} are isotopes of the first group, U^{234} , Ra^{226} , Po^{210} and Bi^{210} comprise the second group. Good resolution of the α -spectra will discriminate between certain of the impurity and sample peaks. Po^{210} has a very similar α -particle energy to both U^{232} and Th^{228} (see Figure 2.2) and cannot be easily detected as an impurity.

The extraction and purification of uranium and thorium is accomplished via a series of steps that are designed to discriminate against both chemical and radiochemical contamination. The details of the analytical techniques are described in Section 5.5. The following describes the procedure for obtaining radiochemical purity.

5.2.1. Separation of Thorium from Uranium

Anion exchange in a chloride medium effectively separates U^{6+} from Th^{4+} in 9M HCl (Kraus and Nelson, 1955). Uranium is retained on a strong base anion exchange resin whilst thorium is eluted by 9M HCl. The uranium eluate is further purified by thenoyltrifluoroacetone (TTA) extraction. Hyde and Tolmach (1955) have illustrated the pH dependence of extraction of U and Th from 0.2M TTA in benzene. At pH 1.0 100% of Th is extracted into the organic phase whilst less than 5% U is extracted. A combination of these two steps results in uranium completely free

of Th contamination. The pH dependence of TTA extraction of the radioelements of interest in this study is illustrated in Table 5.1 (Poskanzer and Foreman, 1961).

Table 5.1
pH for 10,90 and 100% Extraction of Elements in the Uranium
Decay Series into 0.2M TTA in benzene.

	10%	90%	100%
Th	0.2	0.6	1.2
Po	0.4	1.3	2.4
Bi	1.5	2.0	3.0
U	1.7	2.5	3.5
Pb	2.7	3.7	5.2
Ac	3.9	4.9	6.0

5.2.2. Separation of Radium-226 from Uranium and Thorium

Radium is discriminated against during the $\text{Fe}(\text{OH})_3$ precipitation step but a small amount of Ca and Ra is unavoidably occluded in the precipitate. A second precipitation was rarely carried out since radium is separated from uranium and thorium during the anion exchange steps. The alkaline earth elements are not extracted by anion exchange resins under any conditions. Radium is further discriminated against at the TTA extraction step since alkaline earths are not extracted by TTA at the low pH values used (Hageman, 1950).

5.2.3. Separation of Uranium and Thorium from Protactinium

Pa^{231} contamination would be evident in all but the most poorly

resolved spectra but it is worthwhile noting that the element is discriminated against in the analytical procedure.

Pa is adsorbed with U on an anion exchange resin in Cl^- form and is eluted along with U. However, Pa is quantitatively extracted into TTA at pH 1.0 so subsequent extractions of U at pH 3.0 produces a Pa-free sample.

5.2.4. Separation of Thorium from Bismuth and Polonium

Bismuth is incompletely adsorbed from Cl^- media onto an anion exchange column but Po is completely adsorbed (Kraus and Nelson, 1955). Under the conditions of U elution (0.1M HCl), Bi and Po are both incompletely eluted. After Cl^- exchange Th can be contaminated with Bi and U by Bi and Po. There is only slight adsorption of Bi on NO_3^- anion exchange resin. Bi and Th are difficult to separate by TTA. Thus the Th sample mount may be contaminated with a little Bi. Bi is not a problem itself but Po^{210} , the daughter of Bi^{210} does constitute a problem, as it has similar energy to Th^{228} . Po^{210} grows into equilibrium with a 138 day half-life so counting of the Th preparation immediately will result in minimum error, should slight Bi^{210} contamination occur. As a matter of course TTA extractions were always carried out immediately prior to counting.

5.2.5. Separation of Uranium from Bismuth and Polonium

Uranium is likely to be contaminated with Po and small amounts of Bi after the Cl^- anion exchange step. In the next step, TTA extraction at pH 1.0, about 70% of Po is extracted into the organic phase according to Hageman (1950). The remaining Po will be extracted at pH

3.0 along with U but will be volatilized during the flaming of the sample planchet. Since it is impossible to detect Po^{210} activity under the U^{232} tracer peak it would be useful to use a Po tracer to monitor Po contamination. (eg. Po^{208} , $t_{1/2} = 2.94$ years, $E_{\alpha} = 5.115$ MeV). The presence of Po^{210} is only detected by monitoring its decay ($t_{1/2} = 134.8$ days). A number of samples were counted a number of months after preparation and in no case was there a significant difference in U^{232} activity (Table 5.3).

Bi is extracted into TTA at the pH of U extraction, but again counting immediately after preparation minimises any error due to Po^{210} growth.

5.3. Reagents and Reagent Purity

All reagents used were ANALAR grade and water was deionised following distillation. The reagents used in quantity (HCl , HNO_3 , NH_4OH) were not entirely free of uranium and thorium but the degree of contamination was insignificant except at lowest levels of counting. Reagent blanks were monitored from time to time in runs spiked with $\text{U}^{232}/\text{Th}^{228}$ or Th^{227} and found to be reasonably constant if constant proportions of the reagents were used. The results of the reagent blank runs are listed in Table 5.2. These results are not true reagent blanks but the sum of the reagent blank activity and activity due to U^{232} spike tailing. This accounts for the apparent excess U^{234} (and Th^{230}) because the U^{232} tail intensity extends towards lower energies. If it is assumed that U^{232} tailing contributes very little to the U^{238} peak then the concentration of U in the quantity of reagents used in each

Table 5.2

Summary of Reagent Blank Analysis

	U^{238} c/min	U^{234} c/min	U^{232} c/min	Th^{232} c/min	Th^{230} c/min	Th^{228} c/min
<u>No spike</u>						
RB1	0.058	0.075	0.0375	-	-	-
RB2 ⁽¹⁾	0.026	0.039	0.075	-	-	-
RB3 ^{(1) (3)}	0.097	0.182	0.114	0.010	0.035	0.246
<u>U^{232}/Th^{228} Spike Added</u>						
RB4	0.061	0.015	-	-	-	-
RB5	0.070	0.110	-	0.055	0.092	-
RB6	0.043	0.072	-	0.023	0.066	-
RB7	0.044	0.077	-	0.040	0.066	-
RB8 ⁽³⁾	-	-	-	0.031	0.232	-
RB9	0.066	0.142	-	0.050	0.128	-
Average and Error (2)	0.057 ±0.006	0.083 ±0.021	0.06 ⁽⁴⁾	0.040 ±0.005	0.088 ±0.015	0.235 ⁽⁵⁾ ±0.025

(1) Reagent blank using same amount of reagents as used in water analyses.

(2) Average of RB4-RB9, normalized to uniform counting geometry and 100% yield. (N.B. analysis RB8 excluded)

(3) These values are not used in calculating average blank correction. Probably these blank runs were contaminated with some U and Th from a sample being processed at the same time.

(4) This activity is probably due to Po^{210} and not U^{232} .

(5) Average of Th^{228} activity in Th^{227} -spiked sample analyses; probably due to Ra^{223} and Th^{227} tail.

is approximately 0.3μ gms.

The only reagent used in varying quantities was HNO_3 . 250 ml aliquots of 8M HNO_3 were used to separate Th^{227} from Ac^{227} ; the thorium α - spectrum thus obtained never showed Th^{230} or Th^{232} activity. In addition, when VYCOR distilled HNO_3 was used in a blank-run (analysis RB9) there was no reduction in uranium or thorium activity. In fact the blanks were higher than usual. These results indicate that both U and Th are not derived from the HNO_3 and that it is acceptable to use varying amounts of the acid.

Similarly, the Th^{228} "blank" activity observed in Th^{227} -spiked runs is the sum of the Th^{227} tail and a small contribution due to Ra^{223} . The majority of this "blank" activity would be absent when a $\text{U}^{232}/\text{Th}^{228}$ spike (instead of Th^{227}) is used, consequently no correction (other than background activity) was subtracted from measured Th^{228} activities. Reagent blank analysis RB3 refutes the above statement but this is not considered to be a representative analysis.

The whole problem of reagent blank corrections might be avoided if specially purified reagents were used or if attempts were made to reduce the amounts of reagents used. It is possible that some contamination is from airborne particles and this error would be quite difficult to reduce unless special precautions were taken (e.g. work in a glove-box or dust free room). In this study a finite reagent blank was accepted and allowed for in the isotopic measurements.

5.4. Spike Preparations

5.4.1. U²³²/Th²²⁸ Spike Preparation and Calibration

In order to monitor chemical yields and to determine U and Th concentrations, a tracer, or spike, is added to the sample solution. Both Th and U chemical yields are required, so an ideal spike solution consists of a uranium isotope in equilibrium with its thorium daughter product. U²³² in equilibrium with daughter Th²²⁸ is generally used in this type of work because of their convenient α -particle energies. However, there are disadvantages to the use of this tracer combination. These are discussed in Section 5.9.

A U²³²/Th²²⁸ spike was obtained for this study from the Radiochemical Centre, Amersham, England. On diluting the spike for laboratory use disequilibrium was inadvertently introduced. The original spike was diluted with distilled water of near-neutral pH. This resulted in loss of Th²²⁸ from the solution, presumably as a result of hydrolysis and adsorption onto the walls of the container. (This problem was also encountered by Bender (1970) but to a lesser extent). When the disequilibrium was detected the solution was acidified to approximately 6N in HCl to avoid further Th²²⁸ losses. Since the Th²²⁸/U²³² activity ratio could no longer be assumed to be unity it was measured accurately and monitored at intervals to check that Th²²⁸ was growing towards equilibrium in the predicted way. The original spike solution was diluted to obtain a working solution with a U²³² activity of approximately 40 d.p.m./ml.

The spike calibration was carried out directly by evaporating a few drops of the spike solution onto a stainless steel disk and counting with a high resolution detector. The peaks due to U²³² + Th²²⁸ and

Ra²²⁴ were completely resolved. It was assumed that Ra²²⁴ was in equilibrium with Th²²⁸ so subtraction of the Ra²²⁴ activity from U²³² plus Th²²⁸ gave the U²³² activity. The ratio Ra²²⁴/U²³² (=Th²²⁸/U²³²) was measured to 1% precision and all measurements fell on the Th²²⁸/U²³² growth curve. A typical spectrum is shown in Figure 5.1.

5.4.2. Th²²⁷/U²³² Spike Preparation and Calibration

Th²²⁷ was "milked" from an Ac²²⁷ (t_{1/2}=22.0 years) stock solution by passing an aliquot of the Ac²²⁷/Th²²⁷ solution in 8M HNO₃ through an anion column in NO₃⁻ form. Th was retained and eluted with 0.1N HCl. U²³² was separated from Th²²⁸ daughter by passing a 9M HCl solution of the isotopes through a Cl⁻ form anion exchange column. U²³² is adsorbed and eluted with 0.1N HCl. For each run 5 ml of Ac²²⁷/Th²²⁷ and 1 ml U²³²/Th²²⁸ stock solutions were loaded onto the ion exchange columns and the eluates combined and added to the sample solution.

The first Th²²⁷/U²³² spike prepared was calibrated by assuming that the Th²³⁰/U²³⁴ ratio in a granite standard rock was unity. Samples G1 and G2¹ (Table 5.3) were spiked with Th²²⁷ and U²³²/Th²²⁸, and equation(5.1) used to calculate the spike activity ratios Th²²⁷/U²³² and Th²²⁸/U²³². It was also assumed that Th²³² and Th²²⁸ were in equilibrium in these samples. These assumptions appear reasonable because Rosh. et al. (1970) detected no isotopic fractionation in splits of the same rock sample. At the same time the Th²²⁸/U²³² activity ratio was measured. At the time of these experiments this was the only means available for cal-

¹Samples G1, G2, G3 and G4 were dissolved by Mr. J. Muysson, analytical geochemist with the Department of Geology.

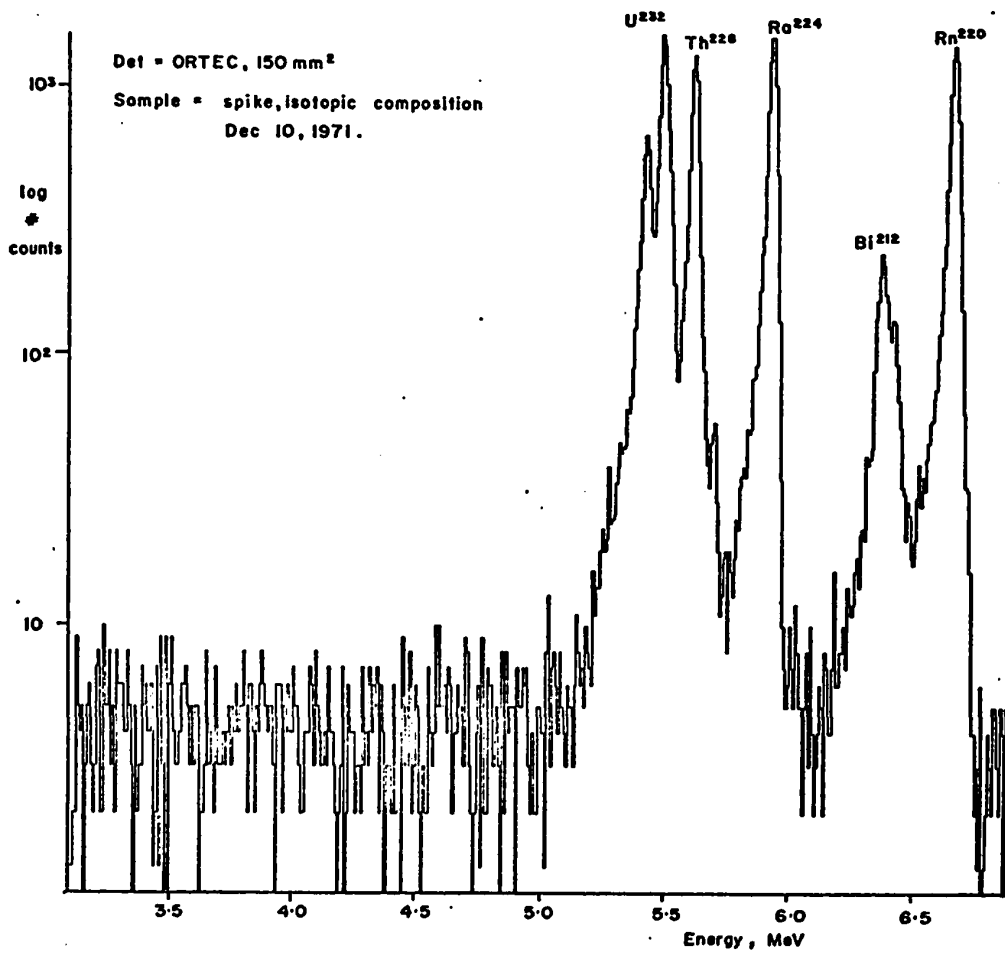


Figure 5.1 Alpha-particle energy spectrum of U²³²/Th²²⁸ spike.

Th²²⁸ is in secular equilibrium with its daughter products

Table 5.3

Analysis of Granite Standard ⁽¹⁾ and Calculation of Spike Ratios

Experiment	U p. p. m.	$\frac{U-234}{U-238}$	$\frac{U-238(2)}{U-232}$	$\frac{Th-230}{U-238}$	$\frac{Th-228}{U-232}$	$\frac{Th-227}{U-232}$
G1, t=0	19.0	1.01±0.01	1.29 ±0.015	-	0.59 ± 0.03 ⁽³⁾	3.69 ±0.07
t=120 days	-	1.04±0.03	1.32 ±0.02	-	-	-
t=150 days	-	1.03±0.015	1.35 ±0.02	-	0.57 ± 0.04 ⁽⁴⁾	-
G2	30.0	1.01±0.02	-	-	0.57 ± 0.025 ⁽³⁾	3.64 ±0.05
G3	20.5	1.02±0.011	-	1.03±.035	0.86 ⁽⁵⁾	-
G4	23.0	0.985±.017	-	0.98±0.04	0.86	-
average	24.9±5.2					

(1) Granite reference sample supplied by J. N. Rosholt (ref. J. N. Rosholt, Z. E. Peterman and A. J. Bartel, "U-Th-Pb and Rb-Sr ages in granite reference from S. W. Saskatchewan", Can. J. Earth Sciences, 7, (1), 1970). (U=23.36±0.19 p. p. m; Th= 81.97±0.92 p. p. m.)

(2) to check for Po²¹⁰ activity.

(3) calculated assuming Th²³⁰/U²³⁸ = 1.00.

(4) re-measured to check for Po²¹⁰ activity in the Th-spectrum; corrected for Th²²⁸ decay.

(5) Ratio measured by direct calibrations (see section 5.4)

Note: G1 and G2 are the spike calibration experiments. G3 and G4 represent true Th²³⁰/U²³⁸ isotopic analyses.

ibrating the spikes. This method is subject to a number of corrections and possible errors. First, Th^{227} has a 18.4 day half-life and so an appreciable amount decays during the analysis. The daughter product activity, Ra^{223} cannot be distinguished from the parent activity since both have similar energies. Correction for Ra^{223} can be made on a theoretical basis or by measuring the Po^{215} activity which should be the same as Ra^{223} since the short-lived Rn^{219} ($t_{1/2} = 3.9$ seconds) is the only intermediate isotope. However, theoretical and measured Po^{215} activities were quite different, probably due to Rn diffusion from the sample. Th^{227} activities were corrected by subtracting the theoretical Ra^{223} activity, (assuming Ra^{223} and Ra^{224} activity was zero when the Th mount was prepared for counting). Th^{227} also occurs naturally in the U^{235} decay chain which necessitates a small correction. A further correction must also be made for Ra^{224} which grows in under the Th^{227} peak. In addition to these considerations it must be assumed that Th^{227} is completely eluted from the column or that any losses during the elution of Th^{227} from the anion exchange columns are constant.

Considering the above comments the agreement between the duplicate analyses is very good. The error quoted is due to statistical uncertainties only. A spike ratio of 3.66 ± 0.06 was used in subsequent determinations.

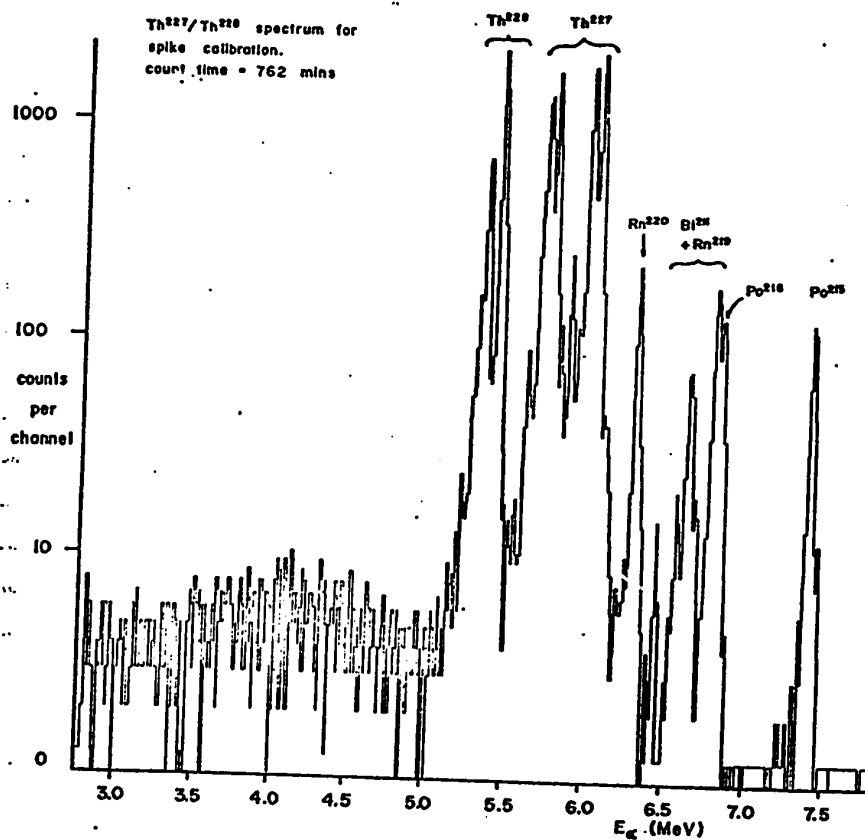
A second $\text{Th}^{227}/\text{U}^{232}$ spike mixture was calibrated by a more direct and accurate method. 1 ml each of the $\text{Ac}^{227}/\text{Th}^{227}$ and $\text{U}^{232}/\text{Th}^{228}$ solutions were mixed and evaporated to near dryness then the residue dissolved in 0.1N HNO_3 . The pH was kept less than 1.0 to avoid extraction of U^{232} . Extraction of Th is not quantitative at pH <1 but

this is immaterial. Thorium was extracted into 0.2M TTA in benzene. Uranium, radium and actinium remained in the aqueous phases. Quantitative extraction of thorium was not necessary since only the $\text{Th}^{227}/\text{Th}^{228}$ activity ratio was required. The $\text{Th}^{228}/\text{U}^{232}$ activity ratio was accurately known from direct calibration and therefore the $\text{Th}^{227}/\text{U}^{232}$ activity ratio was calculated. Corrections had to be applied for the growth of Ra^{223} and Ra^{224} under the Th^{227} peak but since counting was started immediately after separation of the thorium the corrections were small. A typical spectrum and calculation is shown in Figure 5.2. Reproducible results were obtained on three extractions, the average of which was 2.36 ± 0.02 . This ratio was used in subsequent analyses using Th^{227} tracer. An example of an age calculation using Th^{227} tracer is shown in Appendix II.

Both Th^{227} and U^{232} (which are combined and added to the sample solution) must be quantitatively eluted from the columns if this spike ratio is to be used in age determinations. Incomplete elutions, or any other losses before the mixture is added to the sample solution will introduce errors into the age determinations. For this reason a $\text{U}^{232}/\text{Th}^{228}$ spike is inherently more reliable if it is first established that common Th^{228} is not present.

5.5. Preparation and Use of Ion Exchange Columns

Dowex 1-X8 anion exchange resin was used in the chloride form for uranium/thorium separations and in the nitrate form for thorium purification. The columns were prepared by slurring approximately 10 grams dry resin/column with 9M HCl or 8M HNO_3 and allowing the coarser



sample calculation:

	c/min									
	Th ²²⁸	Th ²²⁷	Rn ²²⁰	Po ²¹⁸						
	12.390	35.652	1.123	0.650						
background	- 0.065	- 0.231								
	12.325	35.421								
Ra ²²⁶ , Ra ²²⁴	- 0.016	- 2.590								
(calculated)	12.309	32.831								
Th ²²⁷ tail	- 0.232	+ 0.232								
	12.077	33.063	→ 33.72 (corrected for decay)							
$U^{232} = 12.077 \times \left[\frac{U^{232}}{Th^{228}} \right]_{spike} = 12.077 \times 0.835 = 14.46 \text{ c/min}$										
<table border="1"> <tr> <td>Th²²⁷</td> <td>33.72</td> <td>2.33 ± 0.03</td> </tr> <tr> <td>U²³²</td> <td>14.46</td> <td></td> </tr> </table>					Th ²²⁷	33.72	2.33 ± 0.03	U ²³²	14.46	
Th ²²⁷	33.72	2.33 ± 0.03								
U ²³²	14.46									

Figure 5.2 Alpha-particle spectrum of Th²²⁸/Th²²⁷ mixture.

particles to settle before decanting off the fine particles in suspension. It was observed that if this preliminary separation was not carried out the columns were very slow. Two strong acid-weak acid washing cycles were completed before the columns were put to use.

Uranium-thorium mixtures in 9M HCl were fed onto the Cl^- form anion exchange columns and Th washed through with 200 mls 9M HCl. Uranium was eluted with 250 mls 0.1M HCl. Thorium mixtures were fed onto a NO_3^- form anion exchanger, cation impurities washed thorough with 250 mls 8M HNO_3 , and thorium eluted with 300 mls 0.1M HCl. The elution curves for U and Th are plotted in Figure 5.3. A further 300 mls of 0.1N HCl was run through each column before they were reconditioned with strong acid. This made sure any errors due to "tailing" effects were avoided.

5.6. Experimental Procedures

The extraction of U and Th from pure calcites presents few problems. Speleothems are quite free of solid impurities since these are mostly filtered out of ground waters during their passage through the limestone. Speleothems contaminated with particulate matters generally grow where open channels and rapid drip-rates are encountered. Because of analytical and stable-isotopic considerations these types were not used in the study. The elements that are precipitated when a sediment-free solution loses CO_2 (outgasses) are those which form stable carbonates from bicarbonate solution, eg. Ca, Sr, Fe, Mn. Many elements that are picked up in solution as a result of acid leaching in the soil zone eg. Si, Al, Na, K will remain in solution when CaCO_3 is precipitated. If evaporation played an important part in the process one would

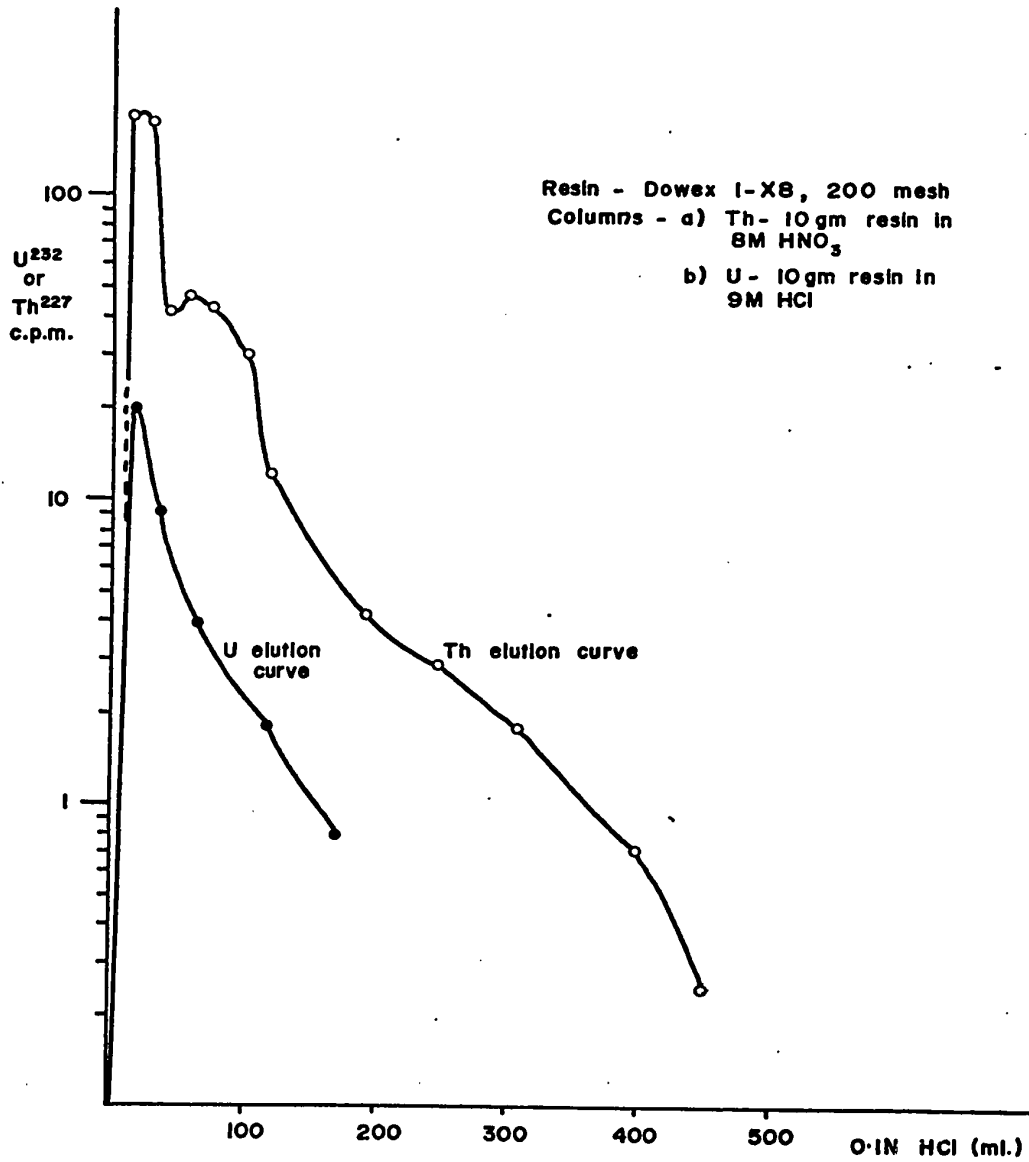


Figure 5.3 Elution of U and Th from Dowex anion exchange resin.

expect those elements to be precipitated also. Due to the rise in pH with outgassing, some precipitation of Fe, Al, and Si hydroxide gels could occur but does not appear to. Though appreciable dissolved silica is present in the ground water, no SiO_2 is ever detected in the precipitated carbonates.

Transition element impurities precipitated in the calcite include Mn and Fe (giving a red colouration). White (1971) has reported the presence of Ni (up to 500 p.p.m.) which imparts a green or yellow colouration. Mn, Ni, and Fe cause no problems since Fe is largely extracted with iso-propyl ether and Mn and Ni are not absorbed on either Cl^- or NO_3^- anion exchange resins.

5.6.1. Carbonate Analysis

CaCO_3 samples are dissolved in 2N HNO_3 and the solution spiked during the dissolution process. Where necessary the solutions are filtered before the addition of 300 mg Fe^{3+} carrier as FeCl_3 . The solution is mixed thoroughly and allowed to stand for a few hours to equilibrate; then heated to boiling. Fe(OH)_3 is precipitated by the addition of NH_4OH solution.

The precipitate is allowed to settle overnight, filtered off and washed free of ammonia with deionized water. The Fe(OH)_3 is then dissolved in 9M HCl and most of the iron removed with two iso-propyl ether extractions. The acid solution containing U and Th is heated to expel dissolved ether, then fed onto an anion exchange column conditioned with 9M HCl. Thorium is washed through the column with 9M HCl and uranium (and traces of Fe) eluted with 0.1N HCl.

The thorium-containing fraction is evaporated to dryness and converted to the nitrate form by addition of 5 ml 8M HNO_3 . This solution is fed onto an anion exchange column in nitrate form and alkaline earth impurities washed out with 8M HNO_3 . Thorium is eluted with 0.1N HCl. This solution is taken to dryness and the residue dissolved in 2 ml 0.1N HCl; then thorium is twice extracted with 2 ml portions of 0.25M TTA in benzene. The phases are allowed to separate completely, then the organic phase is transferred to a small beaker and the benzene slowly evaporated. The final few drops of solution are transferred to a polished steel disk, heated to just below the boiling point of the TTA/benzene solution. When all of the organic phase has evaporated the disk is flamed for about 30 seconds in a bunsen flame.

The uranium-containing eluant is evaporated to dryness and the residue dissolved in 2 ml 9M HCl. If any iron colouration (yellow-green) is apparent the iron is extracted with 5 ml iso-propyl ether; otherwise the solution is again evaporated and the residue dissolved in 2 ml of 0.1N HNO_3 . Th, Pa, and Po are extracted with 3 ml 0.25M TTA in benzene; then the pH of the aqueous phase is adjusted to 3.0 ± 0.2 and uranium is twice extracted with 2 ml portions of 0.25M TTA in benzene, If the amount of uranium extracted was appreciable, as indicated by strong yellow colouration in the organic layer, only one extraction is needed. If the colouration is very intense only a portion of the organic layer is evaporated to avoid a thick source. The organic phase is evaporated onto a steel disk and flamed for one minute. Strong heating ensures

that any remaining Po is volatilised.

5.6.2. Water Analyses

Three methods of concentrating U and Th from cave waters were examined. Two methods involved the co-precipitation and adsorption of the radioelements from large volumes of water by $\text{Fe}(\text{OH})_3$ and activated charcoal respectively. The third method involved the adsorption of the radioelements on $\text{Fe}(\text{OH})_3$ impregnated sponges following the method of Lal et al.(1963). This method of collection was considered to be potentially useful in small caves or passages which precluded the use of large containers.

$\text{Fe}(\text{OH})_3$ precipitation was carried out in 60 litre containers (polyethylene garbage containers) which were placed under drip sites and allowed to fill. Drip rates varied to a considerable extent and the containers would take from between 2 days to 4 weeks to fill. The water was first acidified; then approximately 1 gm of Fe^{3+} added as FeCl_3 . When uranium concentrations were required a U^{232} spike, separated from daughter Th^{228} , was added to the acidified solution. To ensure equilibrium the water was well stirred and left for a few minutes before addition of ammonia solution. The precipitate was allowed to settle overnight, then the supernatant siphoned off and the precipitate transferred to a 2 litre polyethylene bottle. This procedure allowed the container to be washed out and replaced under the same drip site for further analyses. Since precipitations were from a known volume, addition of U^{232} tracer allowed U concentrations to be measured.

It was observed that upon leaving the alkaline solution and

settled precipitate in place at the drip-site for a longer period of up to three weeks before discarding the supernatant more U was precipitated and up to three times as much U was concentrated in the $\text{Fe}(\text{OH})_3$. This procedure was adopted in the later stages of the work since accurate isotope ratios were of more interest than U concentrations (the measurement of which were precluded by this method).

The activated charcoal method of extracting uranium from water at pH 5 was unsuccessful when tried on U^{232} -spiked water. The method has been applied successfully by Nguyen and Lalou (1969) using wood charcoal fixed with hexamethylene tetramine at pH of 4.5 - 5.0. They report generally high yields ranging from 30% to 96%. Because of the failure of the initial experiments in West Virginia, the use of activated charcoal was dropped in favour of $\text{Fe}(\text{OH})_3$ scavenging.

The $\text{Fe}(\text{OH})_3$ impregnated sponges were used successfully but the efficiency of extraction was less than with the delayed settling technique described above. The large area $\text{Fe}(\text{OH})_3$ matrix had a great affinity for other elements as well as for uranium and subsequent clean chemical separations were difficult.

To summarize the extraction techniques, the best approach is probably to use a $\text{Fe}(\text{OH})_3$ scavenging step from a large volume of water, then to leave the container in situ while more uranium is scavenged. Inaccessible drip sites can be successfully sampled by placing a $\text{Fe}(\text{OH})_3$ impregnated natural sponge beneath the drip and leaving for long periods. (The open structure of the sponge also traps any sediment entering the cave so very mild acid solution of the $\text{Fe}(\text{OH})_3$ must be carried out to

avoid leaching of this sediment).

5.6.3. Laboratory Processing of Fe(OH)₃ Precipitates

The filtered Fe(OH)₃ precipitate is washed free of ammonia and dissolved in a minimum of dilute HCl. Generally a strong effervescence due to CO₂ release from co-precipitated CaCO₃ accompanies this step. The Fe solution is evaporated to dryness leaving an amorphous silica precipitate. This precipitate is washed with 3 x 10 ml portions of 9M HCl to remove iron and uranium: then most of the iron is removed by extraction with iso-propyl ether. The procedure followed is then the same as for the carbonate analysis.

The U and Th preparations are counted immediately after the flaming operations until the required statistical accuracy has been obtained.

5.7. Calculation of Isotope Ratios

All isotope ratios in the dissertation are expressed as activity ratios. Th²³⁰/U²³⁴ activity ratio is therefore simply the ratio of the number of disintegrations of Th²³⁰ recorded in the thorium spectrum divided by the number of disintegrations of U²³⁴ recorded in the uranium spectrum, the measured ratio being corrected to 100% chemical yield. Yield determinations are monitored by using U²³² and daughter Th²²⁸ spike of known activity ratio. U²³⁴/U²³⁸ ratios are measured directly from the uranium spectrum and Th²³⁰/U²³⁴ ratios are calculated from equation (5.1).

$$\left[\frac{\text{Th-230}}{\text{U-234}} \right]_s = \left[\frac{\text{Th-230}}{\text{U-234}} \right]_m \cdot \left[\frac{\text{Th-228}}{\text{U-232}} \right]_{\text{spike}} \cdot \left[\frac{\text{U-232}}{\text{Th-228}} \right]_m \dots \dots \dots (5.1)$$

where $\left[\frac{\text{Th-230}}{\text{U-234}} \right]_s$ is the isotope ratio in the sample

$\left[\frac{\text{Th-230}}{\text{U-234}} \right]_m$ is the isotope ratio measured from the spectra

$\left[\frac{\text{Th-228}}{\text{U-232}} \right]_{\text{spike}}$ is the isotope ratio of the spike

and $\left[\frac{\text{U-232}}{\text{Th-228}} \right]_m$ is the spike ratio measured from the spectra.

Some speleothems contain sufficiently large quantities of U that it is possible to measure accurately $\text{Th}^{227}/\text{Th}^{230}$ ($\cong \text{Pa}^{231}/\text{Th}^{230}$) activity ratios. Because the daughter products of Th^{228} mask this natural Th^{227} activity a $\text{U}^{232}/\text{Th}^{228}$ spike cannot be used to monitor yields. The sample solution was therefore split into two equal portions only one of which was spiked with $\text{U}^{232}/\text{Th}^{228}$. The other was spiked with Th^{228} - free U^{232} . The $\text{Th}^{227}/\text{Th}^{230}$ activity ratio was measured directly from the non-spiked Th spectrum. Only background and daughter Ra^{223} activity need be subtracted from the measured Th^{227} activity. This must then be corrected for decay as discussed in Section 5.4.2. A non-spiked Th spectrum is shown in Figure 5.4. The Th^{228} peak in this figure may in part be due to natural Th^{228} but the majority of the activity is due to Th^{228} which is slowly growing back into equilibrium with U^{232} . The corrected $\text{Th}^{227}/\text{Th}^{230}$ ratio and the $\text{U}^{234}/\text{U}^{238}$ ratio are then used to calculate the age of the sample from equation (2.7). This calculation relies upon the assumption that Pa^{231} activity in the sample is equivalent to Th^{227} act-

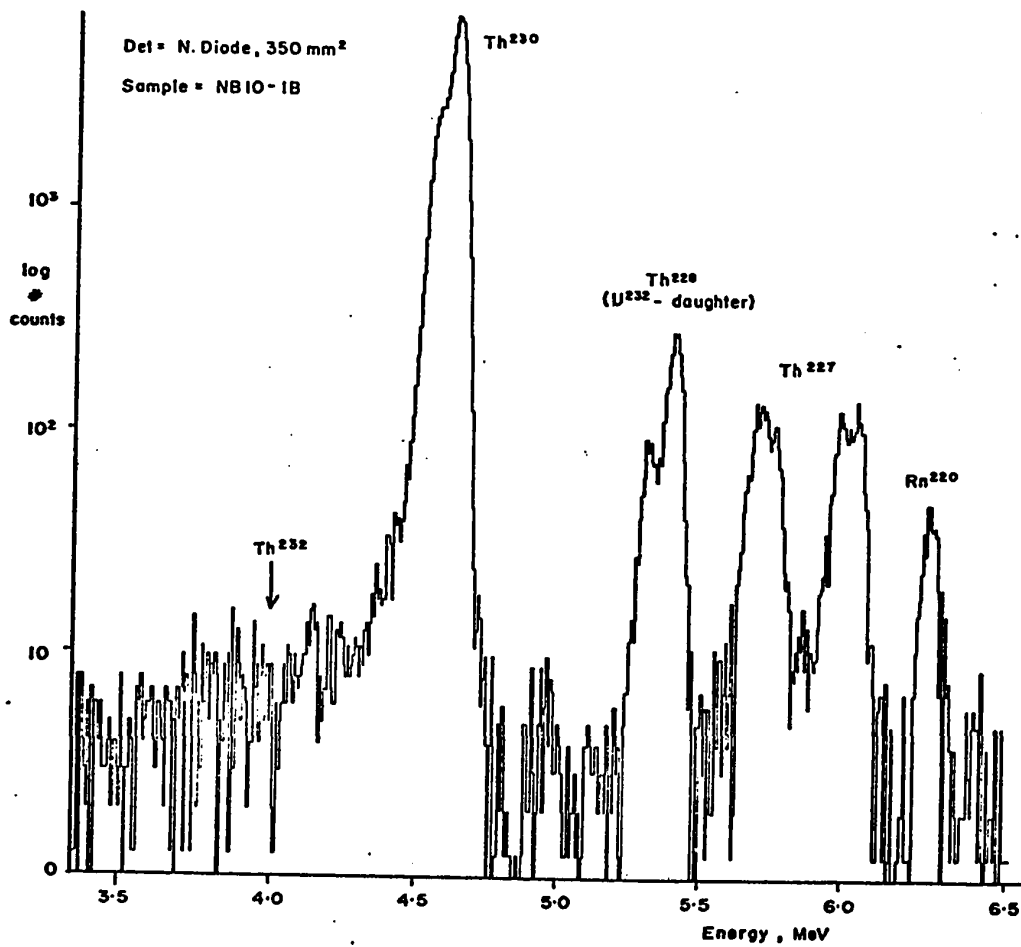


Figure 5.4 Thorium α - particle energy spectrum. (Th^{228} activity is from U^{232} and Th^{227} activity is derived from decay of U^{235} in the sample).

ivity. A $\text{Th}^{230}/\text{U}^{234}$ age was calculated for the spiked portion and the two ages compared.

5.8. Measurement of Uranium Concentrations

A calibration curve was constructed to measure uranium concentrations directly from the count rates recorded by the detector and analyser. Aliquots of a standard uranium solution (buffered to a pH of 3.0 - 3.5) and containing 12.3 micrograms/ml were extracted three times with 0.25 M TTA in benzene and the organic phase evaporated onto stainless steel disks. Care was taken to cover the same surface area of each planchet with the organic phase to ensure a uniform counting geometry and uranium distribution over the surface of the disk. The linear relationship (Figure 5.5) between count-rate and micrograms of uranium extracted is evidence for constant extraction efficiency and constant counting geometry. The slope of the two lines is simply a function of the geometry of the counting system which was kept constant. A second calibration curve was constructed when a new detector was obtained and the counting geometry changed. Again, a straight-line graph was obtained. Using these two calibration curves to calculate the U content of the standard granites a reasonable agreement between this method and the mass spectrometric method of Rosholt et al. (1970) is obtained (Table 5.3). The spread of results is greater using the α - spectrometric method which probably reflects inhomogeneity of the source mounts. Since accurate U analyses were not required for this work these results were considered acceptable.

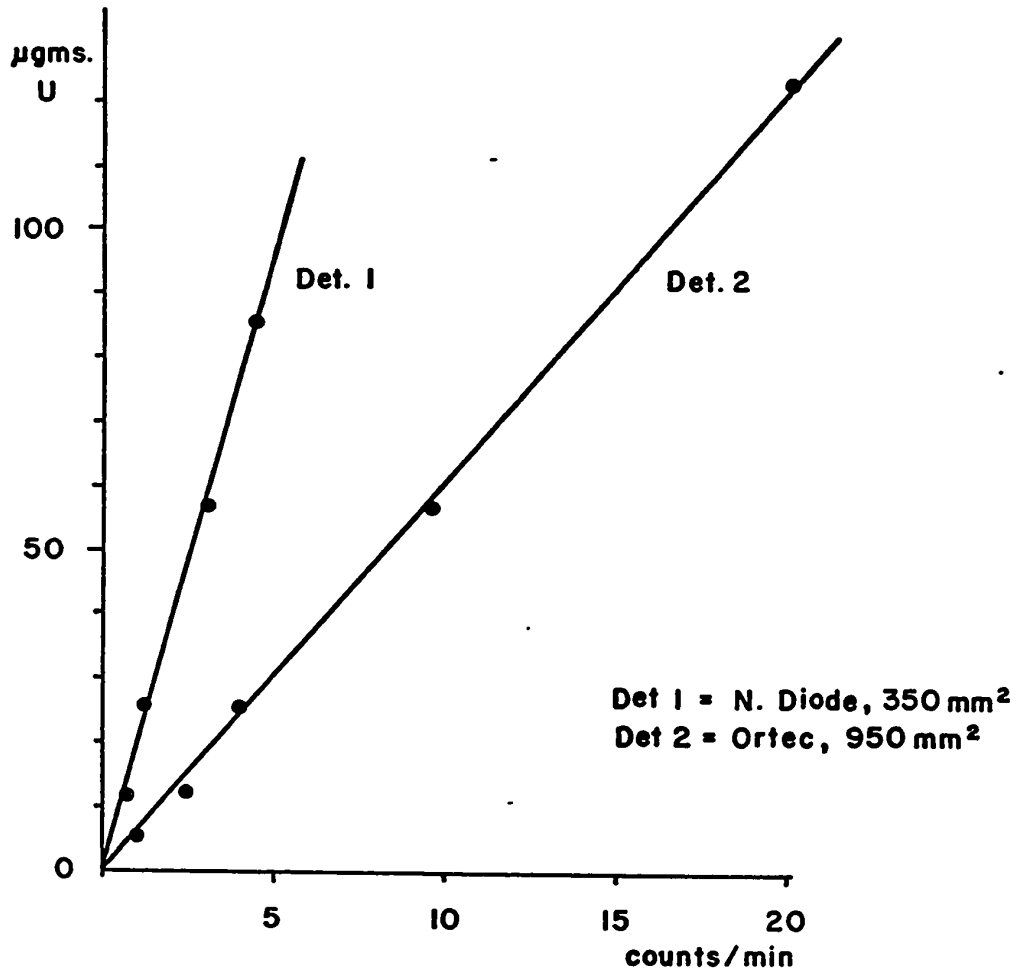


Figure 5.5 Calibration graph for calculating Uranium concentrations from count rates.

5.9 Alternative Spiking Procedures

Th^{228} is a naturally occurring isotope, therefore errors in age determinations using a $\text{U}^{232}/\text{Th}^{228}$ spike mixture will occur if an unknown proportion of natural Th^{228} contributes to the total Th^{228} peak intensity. Th^{232} should always be accompanied by an equilibrium amount of Th^{228} . Thus, small amounts of Th^{228} can be tolerated and corrected for in age determinations. However, appreciable Th^{232} -unsupported Th^{228} activity was observed in some active speleothems. Under these conditions a $\text{U}^{232}/\text{Th}^{228}$ spike cannot be used to monitor chemical yields.

A $\text{U}^{232}/\text{Th}^{227}$ spike mixture was used to check samples for natural Th^{228} activity. The α -particle energies of Th^{228} and Th^{227} are sufficiently different that peaks due to these two isotopes can be almost completely resolved. This method relies upon the fact that no excess natural Th^{227} is present in the sample. This seems reasonable because Th^{227} is a daughter of Pa^{231} and both isotopes are not normally present in waters (except as colloidal particles).

5.10 Precision, Accuracy and Sensitivity of the $\text{Th}^{230}/\text{U}^{234}$ Dating

Method

5.10.1 Precision and Accuracy

There are three possible sources of error which will effect both precision and accuracy of an assigned age. The first arises out of the experimental procedures and can be systematic or random. This type of error is assigned to :

(1) The introduction of U and Th via the reagents used or via fall-in.

(2) Contamination between samples during analysis (particularly during heating and evaporation steps).

(3) Incomplete removal of radiochemical impurities.

This type of error can be minimized by careful analytical work in a clean environment.

An attempt was made to evaluate the systematic errors by (a) monitoring U and Th concentrations in the reagents and (b) processing standard samples whose isotopes were known to be in secular equilibrium.

As shown in Table 5.3 a finite quantity of U and Th occurs in the reagents but when this is allowed for and when a small correction (0.3 to 0.5%) is made for detector contamination by α -recoil nuclei (mostly Th^{228} and daughters) the $\text{U}^{234}/\text{U}^{238}$ and $\text{Th}^{230}/\text{U}^{234}$ ratio of the standards is unity within the experimental error (Table 5.3, experiments G3 and G4). This enables the measured isotope ratio to be accepted with confidence as representing the true isotopic composition of the samples.

The second source of error that affects the precision of the determinations is due to the fact that radioactive decay is a statistical phenomenon and as such the activity of a radioisotope can only be measured to within certain limits which depend upon the number of disintegrations recorded. The expected standard deviation (σ) for x recorded disintegrations can be shown equal to \sqrt{x} if x is large and the counting time (T) is short compared to the half-life. When disintegration rates (x/T) are subtracted, multiplied or divided errors are propa-

gated.

i.e. for subtraction (or addition):

$$\sigma_{(x+y)} = \sqrt{\left(\frac{\sigma_x}{x}\right)^2 + \left(\frac{\sigma_y}{y}\right)^2} \dots\dots\dots(5.2)$$

for multiplication:

$$\sigma_{xy} = xy \sqrt{\left(\frac{\sigma_x}{x}\right)^2 + \left(\frac{\sigma_y}{y}\right)^2 + 2\frac{\sigma_{xy}^2}{xy}} \dots\dots\dots(5.3)$$

The covariance term (σ_{xy}) is usually small and can be neglected.

the standard deviation for division approximates to:

$$\sigma_{x/y} = \frac{x}{y} \sqrt{\left(\frac{\sigma_x}{x}\right)^2 + \left(\frac{\sigma_y}{y}\right)^2 - 2\frac{\sigma_{xy}^2}{xy}} \dots\dots\dots(5.4)$$

All errors in the study are quoted in terms of one standard deviation (1σ) i.e. there is a 66% chance that the true result falls between $\pm 1\sigma$ of the reported result.

A third source of error, and one for which no corrections are possible, arises from post-depositional migration of uranium and thorium within the carbonate lattice or from contact with waters which introduce further disequilibrium by the addition or leaching of radioelements from the lattice. Only detailed analyses can reveal these sources of errors. Concordant ages which agree with stratigraphic position are convincing evidence that closed-system conditions prevailed. There is, however, no certain check on the accuracy of ages unless all ages are verified by an independent method. This problem is discussed further in Chapter 6.

5.10.2 Sensitivity

The sensitivity of the dating methods depends primarily on the U content of the sample. The limit of detection was arbitrarily defined at four times the standard deviation of the reagent blank plus background activity. The limit of detection is therefore $4(b/T)^{1/2}$ (Komura and Sakano, 1964), where b = reagent blank and background count rate and T = count time. A typical count time is 2000 minutes, therefore the detection limit becomes approximately 0.03 c/min assuming $b = 0.1$ c/min (this is a typical blank and background count rate assuming 50% yield). If 0.03 c/min is assumed to be the limit of detection for Th^{230} activity then the lowest limit of the age determination can be expressed as:

$$0.03 = \frac{0.16}{2} \times (U) \times 0.5 \times (1 - e^{-\lambda_{230} T_{230}}) \dots \dots \dots (5.2)$$

where 0.16 is the count rate for 1 μgm U (using large area detector, CA-070-950-100, see section 5.11)

(U) is total amount of U in sample (μgm)

0.5 is assumed yield of U

λ_{230} is decay constant for Th^{230}

T_{230} is the lower age limit obtainable by the deficient ionium method.

If $\lambda_{230} T_{230}$ is $\ll 1$ equation 5.2 can be reduced to:

$$T_{230} = \frac{0.75}{\lambda_{230}(U)} = \frac{8.1 \times 10^4}{(U)} \text{ years}$$

The lower age limit obtainable with a 100 μgm sample of U would therefore be approximately 800 years. This could be improved upon by increased counting times, better chemical yields and lower background and reagent blank corrections.

5.11 Counting Equipment

The equipment used to detect, measure and resolve the activity of the U and Th isotopes of interest is shown schematically in Figure 5.6.

Of the two available methods to detect α -particles, namely the gridded ionization chamber and the surface-barrier semi-conductor detector the latter was chosen for use in this study. Advances in semi-conductor materials and fabrication have resulted in solid state detectors that have high resolution and reasonable efficiency. The ionization chamber is more efficient but has relatively poor resolution. Three detectors of different surface area and resolution were purchased to allow versatility in spectrum measurements.

The characteristics of the detectors are listed in Table 5.4.

Table 5.4.

Detector Characteristics

Manufacturer	Model No.	Surface Area mm ²	Resolution*
ORTEC	A.025-150-100	150	17.4 keV
NUCLEAR DIODE	L2-50-21	350	50 keV
ORTEC	CA-070-950-100	950	58 keV

* F.W.H.M. resolution at 5.5 MeV (Am-241)

The elements of detector theory are discussed by Thurber (1964). The detectors are used in a clean (cold-trapped) vacuum to prolong their useful life. Because of the proximity of the active source to the de-

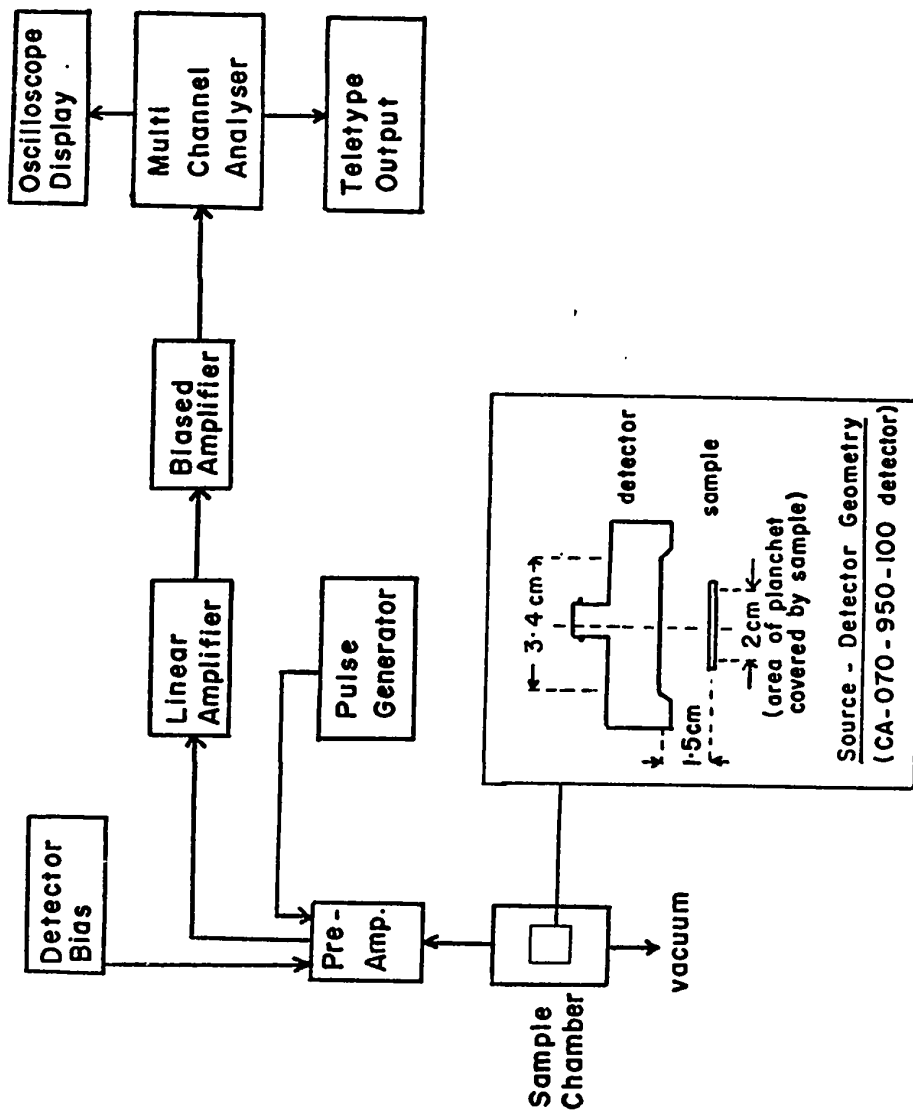


Figure 5.6 Schematic diagram of a particle spectrometer, showing in detail source-detector geometry.

detector surface the detector becomes contaminated by α -recoil nuclei. Detector contamination is troublesome but can be corrected for by frequent monitoring of background count rates. Thurber (1964) discusses possible ways of overcoming detector contamination but no attempt was made to overcome the problem in this study. Only when very low levels of counting are contemplated should attention be given to the problem of reducing contamination.

The spectrometer assemblage is one commonly used for high resolution α -spectrometry. The amplifier system provides a linear signal span of 0 - 10 volts which is the range of input voltage accepted by the multichannel analyser (MCA). The biased amplifier expands a certain portion of the range of the linear signal so the portion of interest in the α -spectrum can be expanded to fill the 512 channels of the MCA. The majority of the equipment was used as supplied by the manufacturer. The preamplifier, though, was slightly modified since it was supplied with a high (100 Megohm) resistor to ground which is too high for the small bias voltages applied to the detectors (50 volts) with the result that the voltage drop across the resistor was too high and the bias to the detector too low. A 3.0 Megohm resistor was placed in parallel with the 100 Megohm to reduce this resistance.

5.12. Data Processing

Data processing was by calculator in the early stages of the work but computer processing of the data was undertaken later to avoid error and to save time. Two programs were used, one to simply plot and sum the counts per spectrum and the other to compute isotope ratios,

ages and errors in both when the total counts had been subdivided manually into isotopic abundances. The program used to calculate isotope ratios etc. is described in Appendix II . To facilitate computer processing the MCA information was read out on punched tapes then converted to cards on the IBM (model 46) tape-to-card reader.

5.13. Leaching Experiments

An experiment was constructed to observe whether or not isotopic fractionation took place when carbonate was dissolved in the presence of detrital silicate particles using mild acid. 150 gms of a very pure flowstone sample (sample GV1, p.219) was mixed with 20 gms of a fine cave sediment from Bone Cave consisting mostly of clay and silt size particles. The carbonate was dissolved in cold 2N HCl, the solution spiked with U^{232}/Th^{228} , then the residue filtered off and the filtrate processed in the normal way. Only slight colouration in the filtrate was observed. At the same time an identical calcite sample was processed without the addition of the sediment. The results are shown in Table 5.5.

Table 5.5

Results of Leaching Experiment on Grapevine Flowstone GV1

sample	U p.p.m	U^{234}/U^{238}	Th^{230}/U^{234}	Th^{230}/Th^{232}	Age (yrs B.P.)
GV1-3 + clay	0.18	1.73 ± 0.05	0.35 ± 0.05	55	44,000 ± 5200
GV1-4 (pure calcite)	0.09	1.48 ± 0.07	0.42 ± 0.05	76	60,000 ± 7000

U is apparently leached from the sediment but rather surprisingly little Th^{232} or Th^{230} is leached. The result is that the "age" of the calcite mixed with sediment is 27% lower than the true age. The sediment was not analysed for U or Th.

The conclusions of this experiment are supported by the work of Thurber (1964) and Kaufman (1964). Thurber extracted U from a deep-sea core (consisting of 50% red clay and 50% carbonate) with hot conc. HCl and measured a $\text{U}^{234}/\text{U}^{238}$ activity ratio of 1.22 in the solution. The maximum value of this ratio if the core was modern could only be 1.15 (the modern value of sea water) indicating that some U^{234} was preferentially leached from the sediment. Kaufman also attempted some similar leaching experiments using a mixture of calcite and silicate. The results indicated that under mild acid conditions (cold 1N HNO_3) 93.5% of uranium is extracted and U^{234} is preferentially leached from the sediment but that only 63.2% of Th^{230} is extracted and only 58.3% of Th^{232} . Kaufman proposed that some of the carbonate Th is adsorbed on silicate particles and is only released when stronger acids are used.

Kaufman's results differ from the results of this study in that he found a finite amount of Th was removed by HNO_3 leaching. The $\text{Th}^{230}/\text{Th}^{232}$ ratio of Grapevine sample GV1-3 was lowered only slightly when dissolved with HCl in the presence of the silicate impurities. It may well be that HCl leaches less Th than HNO_3 or that the Bone Cave sediment contains very little Th^{232} or Th^{230} , but still the net result would be a lowering of the measured age because proportionally more U is leached than Th.

The proportion of sediment:carbonate was far higher in this

experiment (1:7.5 by weight) than in the remainder of the samples analysed. From this experiment it can be inferred that any contribution of U from sediment trapped in the calcite will tend to increase both the U^{234}/U^{238} ratio and the U concentration and result in a calculated age that is too low. The apparent lack of Th^{232} leaching does not preclude the fact that Th^{230} may be preferentially leached since it will occupy a radiation damaged uranium site. This would tend to produce high ages but the net effect actually observed is a lowering of the measured age, so ionium leaching is apparently less important than uranium leaching. In fact Kaufman's experiments show that Th^{230} from the sample is likely to be lost by adsorption on silicate particles at the pH of these experiments. This may account in part for the low Th yields measured in some of the extractions. This single experiment and the interesting result obtained was not followed up by more detailed experiments since very pure calcites were analysed most of the time and the problem of contamination from extraneous sediment sources was not a significant one.

CHAPTER SIX

RESULTS FROM WEST VIRGINIA

6.1 THE NORMAN-BONE CAVE

6.1.1 Stalagmites NB1 and NB10 - Two Fossil Deposits from Norman-Bone Cave

Stalagmite NB1, collected from the Half-Way Room, Norman Cave was deposited on breakdown close to the wall of the room. The total height of the columnar stalagmite was 96 cm of which 93.5 cm were removed for analysis. Average diameter near the base was 9-10 cm and near the top 6.4 - 7.6 cm. The surface of the stalagmite, including the top was dry and there was no indication that CaCO_3 was still being deposited. The source of feed solution, a tubular straw stalactite approximately 2 meters above the stalagmite, was one of a large number of small stalactites clustered around widely spaced ceiling joints. Two or three of the stalactites are active and recent, very pure stalagmites are being deposited beneath them. Sample NBM-1 was collected from one of these active sites.

The analysis of NB1 was almost complete when the decision to start stable isotope analysis was made and the prime material had been dissolved or was crushed ready for dissolution. Only age analysis was therefore carried out on NB1, which is unfortunate since deposition of this speleothem covered an interesting span of time. Figure 6.1 represents NB1 in cross section, showing the location of the samples, and Table 6.1 lists the results of the analyses. The analytical results are shown graphically in Figure 6.1.

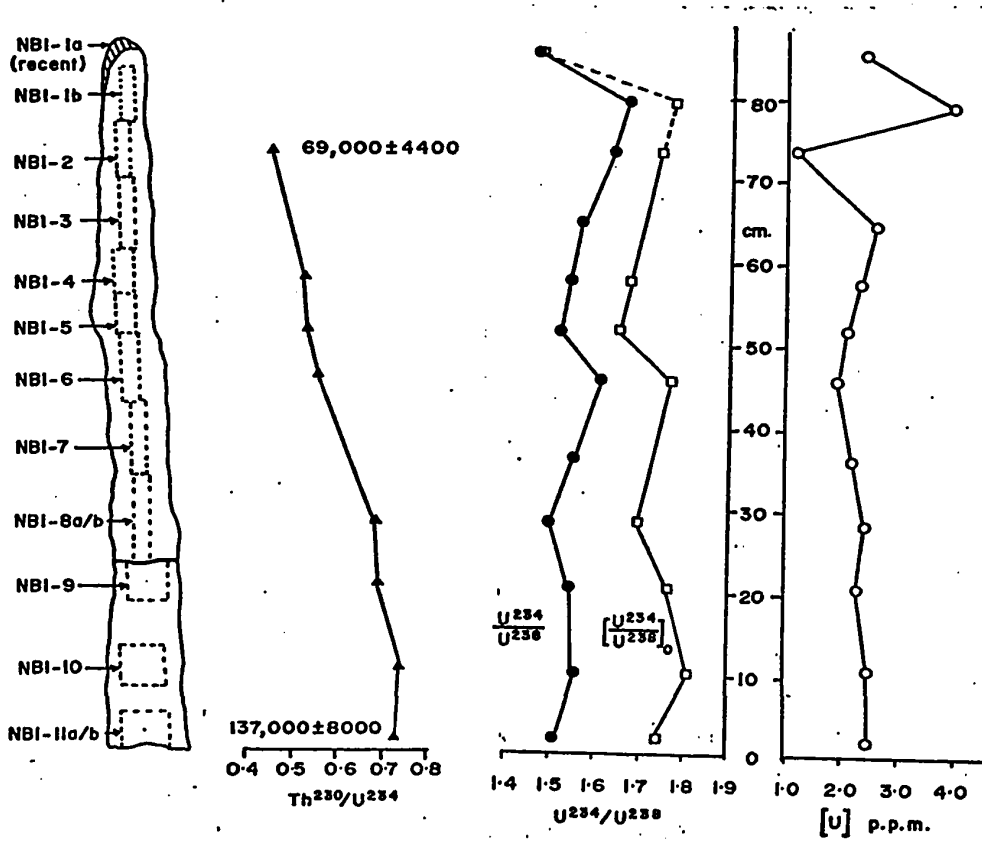


Figure 6.1. Uranium content, $\text{Th}^{230}/\text{U}^{234}$, and $\text{U}^{234}/\text{U}^{238}$ isotopic variations in stalagmite NBI, Norman-Bone Cave.

Table 6.1

Isotopic Analysis of Stalagmite NB1 (Norman-Bone Cave)

Sample	Average height above base (cm)	(U) p.p.m.	$\left[\frac{U-234}{U-238} \right]_0$	$\left[\frac{Th-230}{U-234} \right]$	$\left[\frac{Th-230}{Th-232} \right]$	Age (years B.P.)
NB1-1A	90	2.28	1.46±0.03	1.47±0.03	0.044±0.0005	1000
NB1-1B	80	3.85	1.67±0.02	-	-	4900 ± 100
NB1-2	73	1.04	1.61±0.03	1.74±0.05	0.475±0.021	90
NB1-3*	65	2.49	1.56±0.03	-	-	-
NB1-4	58	2.25	1.54±0.02	1.67±0.04	0.535±0.013	110
NB1-5	52.5	2.06	1.52±0.02	1.65±0.045	0.545±0.017	68
NB1-6	46	1.86	1.61±0.02	1.79±0.04	0.573±0.032	77
NB1-7	38	2.13	1.55±0.04	-	-	-
NB1-8A	28	2.40	1.49±0.015	1.69±0.02	0.692±0.0035	49
NB1-8B	28	1.53	1.50±0.02	-	-	-
NB1-9	20	2.24	1.54±0.02	1.77±0.05	0.697±0.040	60
NB1-10	9.5	2.43	1.56±0.01	1.81±0.02	0.749±0.005	38
NB1-11A	1.9	3.31	1.56±0.03	1.82±0.06	0.757±0.022	106
NB1-11B	1.9	2.43	1.51±0.02	1.73±0.04	0.735±0.025	287

* no spike added; $U^{238}/Po^{210} = 112$ ** Th^{227}/U^{232} spike used; zero Th^{228} confirmed.

Sections NB1-4 and NB1-6 were analysed using $\text{Th}^{227}/\text{U}^{232}$ spike in order to check for common Th^{228} . No Th^{228} activity above background was detected in these two sections. Section NB1-3 was split and one half of the sample processed without addition of spike to check for Po^{210} activity in either the U or Th spectrum; none was found. Sections NB1-11A and NB1-11B representing two halves of a 2" drill core gave acceptable results. The $\text{Th}^{227}/\text{U}^{232}$ spike mixture was added to NB1-11A and again no significant Th^{228} activity was observed.

The crown of the stalagmite readily broke away from the majority of the column. It was poorly cemented onto a weathered surface. This top section proved to be recent (NB1-1A), with a $\text{U}^{234}/\text{U}^{238}$ ratio appreciably lower than in the remainder of the stalagmite (i.e. ratios corrected for decay). None of the remainder of the column showed evidence of discontinuous growth. Growth appeared to be fairly regular at an average rate of $1.2 \text{ cm}/10^3$ years but this can be broken down to a period of more rapid growth between 137,000 and 119,000 years B.P. ($1.4 \text{ cm}/10^3$ years) and slower growth between 119,000 and 69,000 years B.P. ($1.0 \text{ cm}/10^3$ years). This supports the general contention (Franke, 1965) that stalagmites of regular diameter represent constant growth rates. Using a growth rate of $1 \text{ cm}/10^3$ years, deposition on NB1 must have stopped approximately 58,000 years B.P.

Stalagmite NB10, located in the same room and approximately 8 metres away from NB1 was one of two prominent broken stalagmites lying near the centre of the room. The other stalagmite, 2 metres long and 30.5 to 46 cm in diameter could not be removed from the cave for analysis. Both were oriented in a North-South direction and may have been toppled

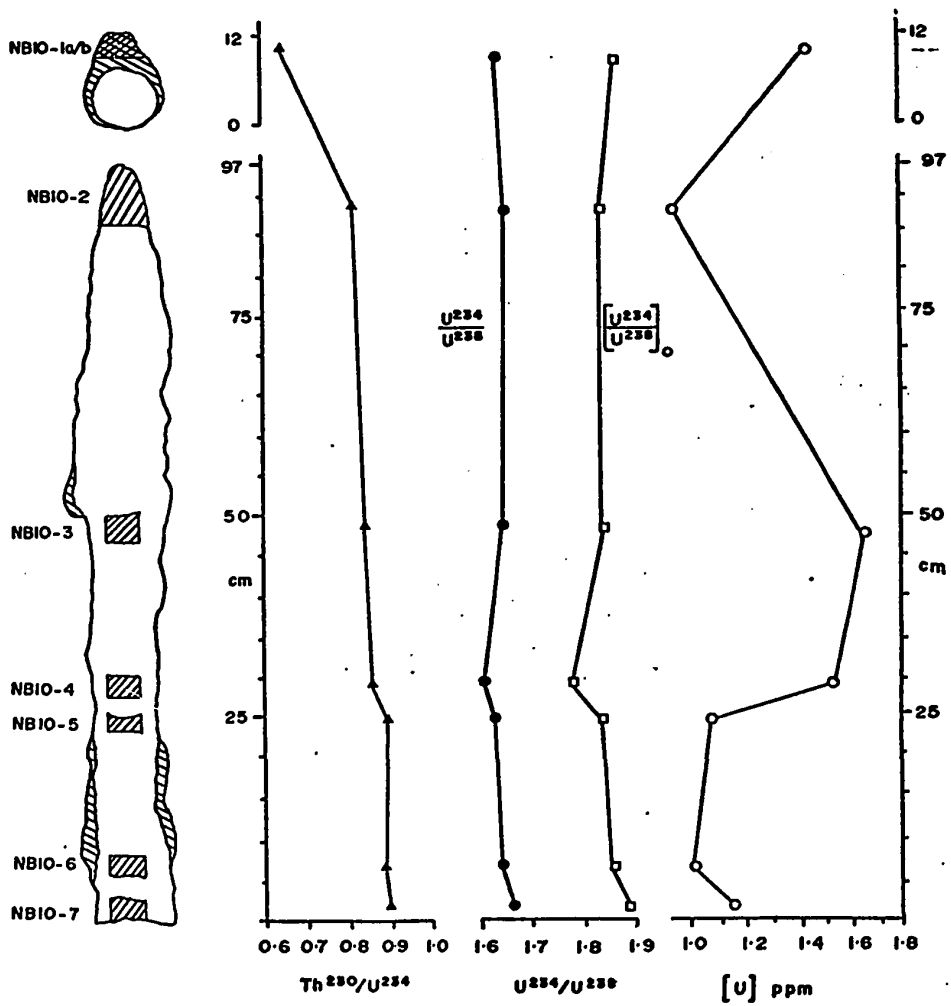


Figure 6.2. Uranium content, Th^{230}/U^{234} and U^{234}/U^{238} isotopic variations in stalagmite NB10, Norman-Bone Cave.

by earth tremors. The break near the base of NB10 was covered with a thin layer of CaCO_3 indicating that no further substantial deposition on the stalagmite would have occurred. Two nodular concretions formed on the broken stalagmite gave evidence of a later phase of deposition.

The reconstructed stalagmite stood .97 cm high. Its diameter at the base was 6.9 cm increasing to 12.7 cm approximately 66 cm above the base and then gradually decreasing towards the top. A cross-section is shown in Figure 6.2. Upon sectioning a number of prominent growth layers were revealed and, near the widest section, some voids which were attributed to slight resolution. Figure 6.3 is a photo of a typical longitudinal and cross-section of NB10 showing the later depositional phase. The location of the photographed section is shown in Figure 6.9. The CaCO_3 appeared to be mostly free of impurities. No major breaks in the depositional sequence were apparent.

Table 6.2 lists the results obtained for analysis of NB10. Locations of the samples are shown in Figure 6.2. The HNO_3 solution containing sample NB10-1 was split into two equal portions only one of which was "spiked" with $\text{U}^{232}\text{-Th}^{228}$ and processed in the usual manner. The remainder was processed without the spike to measure (a) any common Th^{228} activity and (b) Th^{227} activity (to enable a $\text{Pa}^{231}/\text{U}^{235}$ ratio to be calculated). No Th^{228} activity was measured. Using the measured $\text{Th}^{227}/\text{U}^{235}$ activity ratio an age of 115,000 years B.P. was calculated which compares favourably with the Th^{230} age of 105,000 years B.P. considering the errors involved in correcting Th^{227} activities (Chapter 5, section 5.4.2). In calculating the Th^{227} age it was assumed that Th^{227} is in equilibrium with Pa^{231} . Ac^{227} ($t_{1/2} = 21.7$ years) is the

Table 6.2

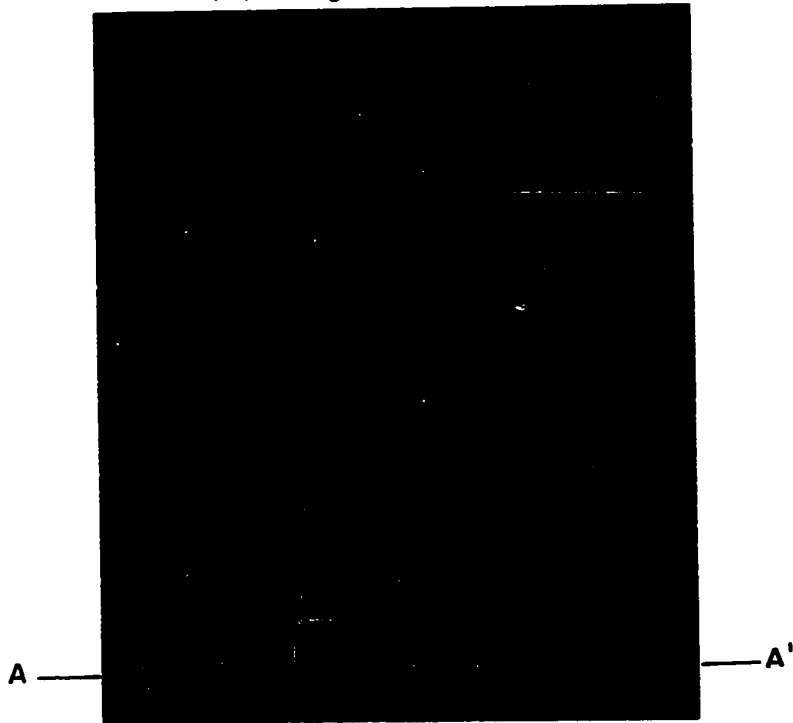
Isotopic Analysis of Stalagmite NB10 (Norman-Bone Cave)

Sample	Average height above base (cm)	(U) p.p.m.	$\left[\frac{U-234}{U-238} \right]_0$	$\left[\frac{Th-230}{U-234} \right]$	$\left[\frac{Th-230}{Th-232} \right]$	Age (years B.P.)	
NB10-1A	-	1.45	1.67±0.02	1.91±0.04	0.653±0.015	267	105,000 ± 4000
NB10-1B	-	-	1.66±0.02	-	-	295	115,000 ± 8000*
NB10-2	89	0.91	1.61±0.03	1.97±0.06	0.819±0.018	135	163,000 ± 6800
NB10-3	48	1.65	1.60±0.03	1.98±0.05	0.843±0.017	146	173,000 ± 6900
NB10-4	29	1.53	1.51±0.02	1.85±0.05	0.854±0.022	187	183,000 ± 9700
NB10-5	24	1.07	1.55±0.03	1.97±0.08	0.895±0.002	1000	203,000 ± 11300
NB10-6	6.5	.98	1.58±0.02	2.00±0.06	0.884±0.002	357	195,000 ± 10400
NB10-7	1.5	1.10	1.61±0.02	2.07±0.07	0.898±0.018	1000	199,000 ± 8800

* from Th^{227}/Th^{230} ratio.

Figure 6.3 Longitudinal section and cross-section of part of NB10. (A - A' is shown in Figure 6.5. The cross-section shows the later phase of deposition on the side of the fallen stalagmite).

(a) Longitudinal section



(b) Cross section

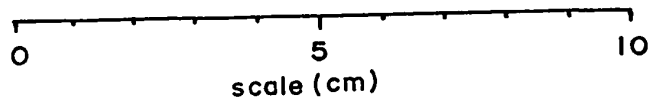
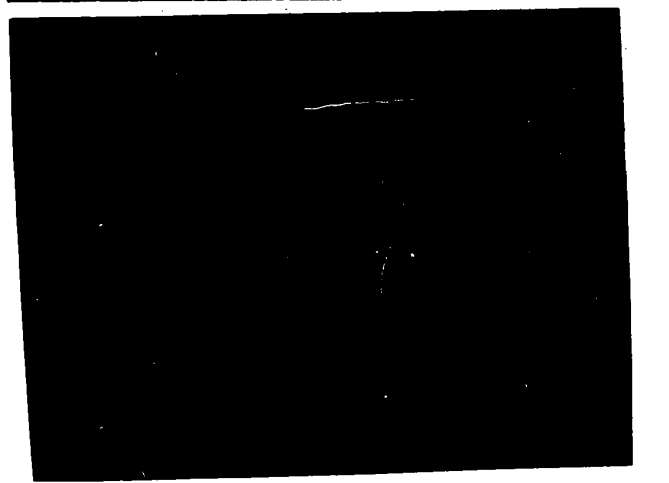


Figure 6.4 Results for NB1 and NB10 plotted as $\text{Th}^{230}/\text{U}^{234}$ against $\text{U}^{234}/\text{U}^{238}$ (the isochron graph described in Chapter 2). If $\text{U}^{234}/\text{U}^{238}$ ratio were constant at the time of deposition and the system remained closed, all points should lie on a single line parallel to the heavy lines.

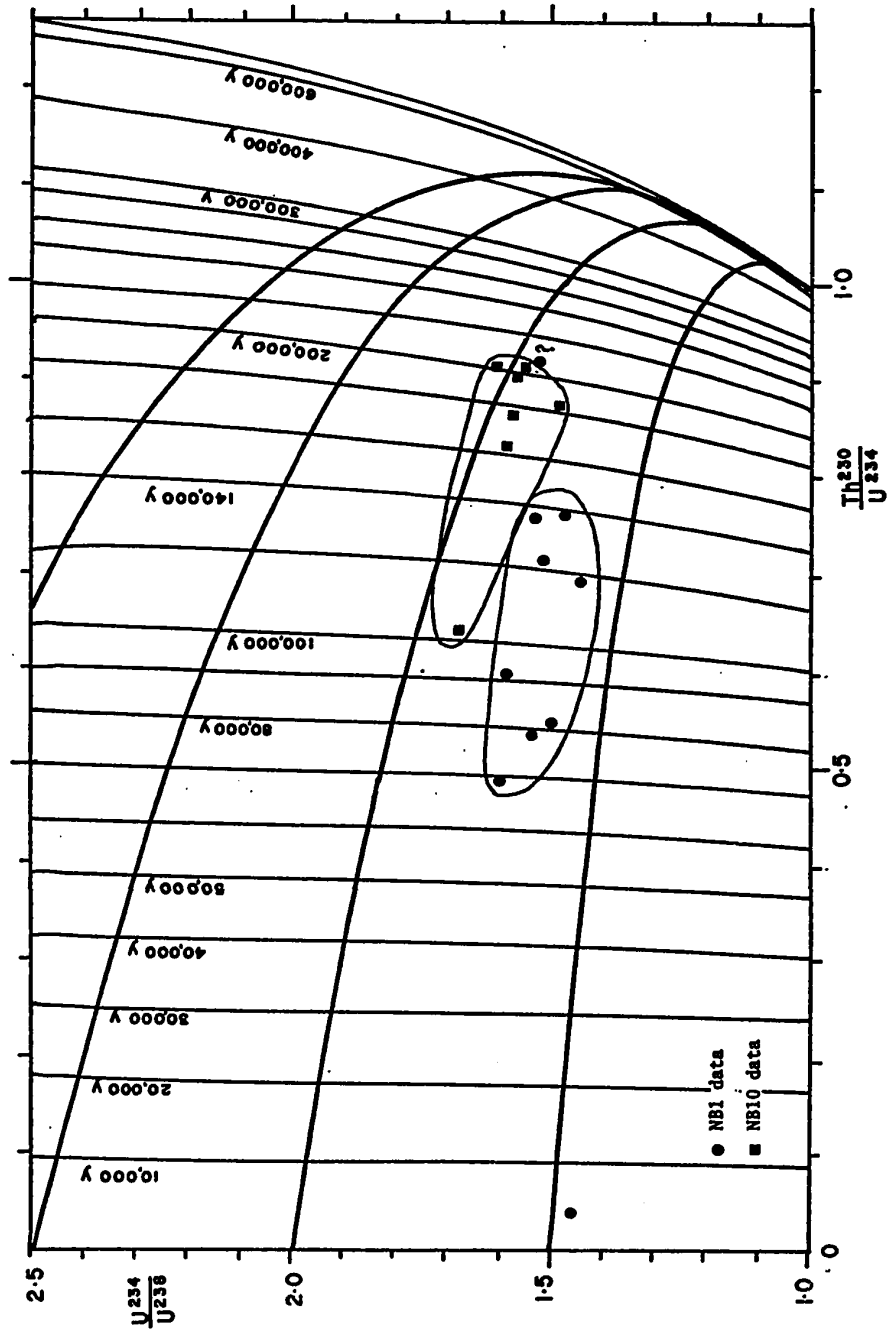



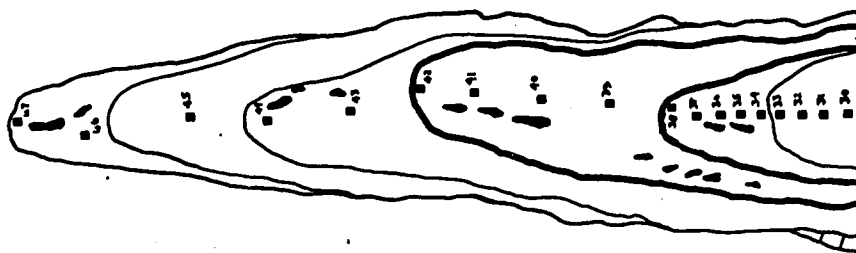
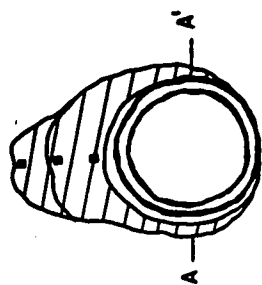
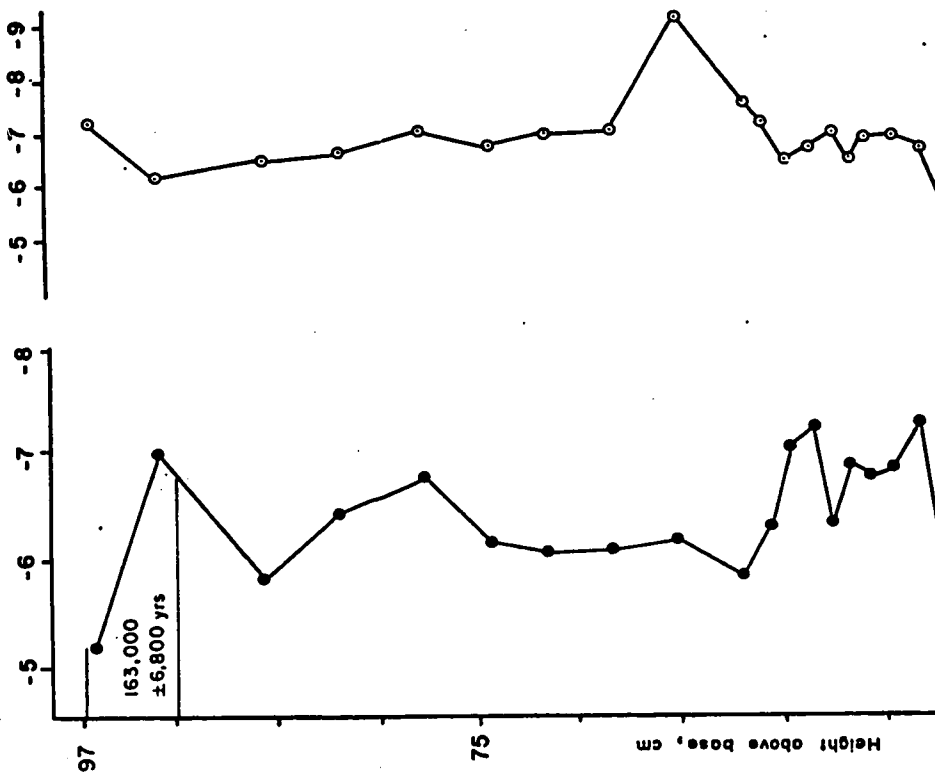
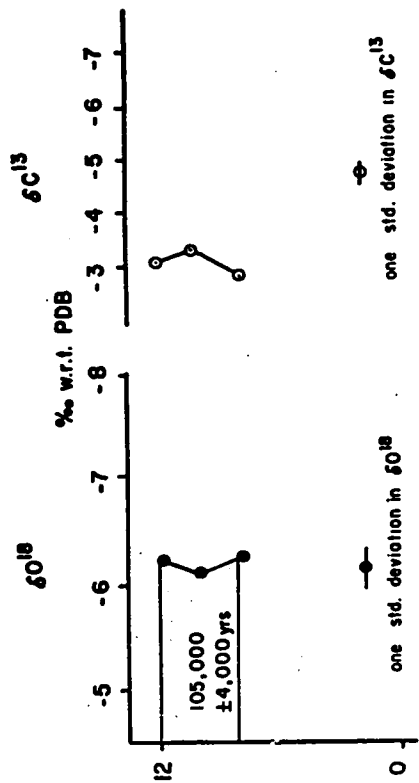
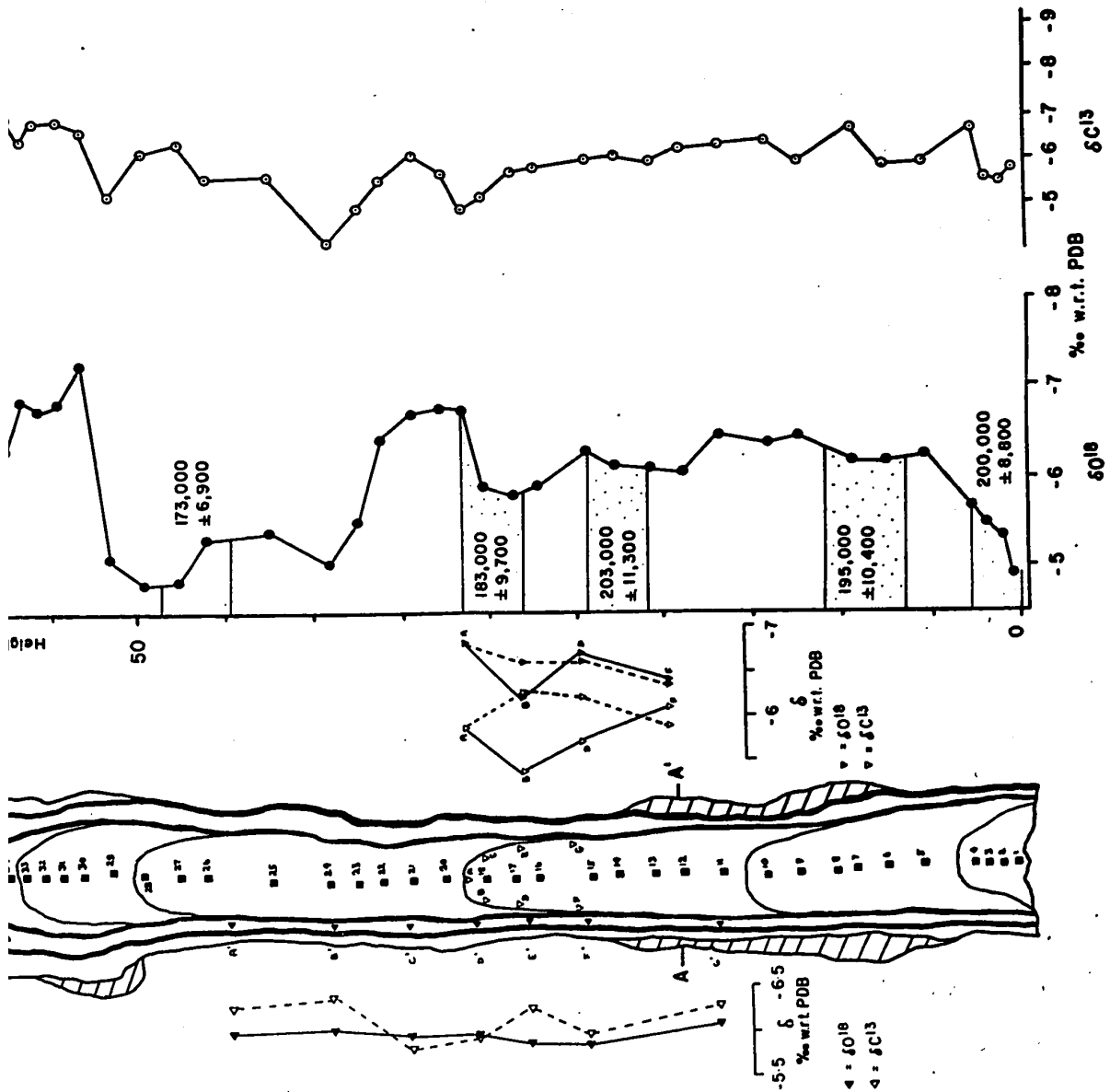


Figure 6.5 Oxygen and carbon isotope profile along the axis
of NB10.

-  = solution cavities
-  = secondary deposition after collapse
-  = sampling points





intermediate between Th^{227} and Pa^{231} and because it is relatively short-lived the assumption is quite reasonable. This age calculation also assumes that Pa^{231} activity was zero at the time of deposition. No check was made on this assumption for recent speleothems. However, thorium and protactinium are geochemically coherent and the fact that no initial thorium is present in speleothems supports the assumption that no initial protactinium is present.

The average rate of growth of this stalagmite was $2.5 \text{ cm}/10^3$ years. The older layers, formed between approximately 200,000 and 183,000 years B.P. were deposited at a rate of $1.7 \text{ cm}/10^3$ years. Between 183,000 and 173,000 years B.P. the rate was $2.1 \text{ cm}/10^3$ years. The youngest layers formed between 173,000 and 163,000 years B.P. were deposited at a faster rate of $4.1 \text{ cm}/10^3$ years.

Initial $\text{U}^{234}/\text{U}^{238}$ ratios, calculated from the age and measured $\text{U}^{234}/\text{U}^{238}$ are comparable to but slightly higher than those calculated from NB1. These results indicate that in this part of the cave at least, $\text{U}^{234}/\text{U}^{238}$ ratios are:

- a) constant at each drip site for a limited period of time.
- and b) similar between drip sites (though clearly distinguishable).

The results are plotted on the isochron graph in Figure 6.4 to illustrate this.

Both stalagmites NB1 and NB10 experienced a period of interrupted growth. When active deposition on NB10 was resumed (analysis NB10-1A/1B) the $\text{U}^{234}/\text{U}^{238}$ ratio remained unchanged whereas for NB1 (analysis NB1-1A) there was a distinct change in this ratio to a lower value.

Figure 6.5 is the oxygen and carbon isotope profile along the

axis of the stalagmite. Since numerous growth lines were clearly distinguishable oxygen isotope measurements along a single growth line were carried out to check that deposition was an equilibrium process. The general lack of correlation between δ_{ct}^C and δ_{ct}^O (Figure 4.1) and the constancy of δ_{ct}^O along a growth line was considered acceptable evidence that equilibrium deposition had taken place. This oxygen isotope profile is interpreted in terms of climate change in Chapter 8. At this point it can be noted that the lighter calcite layers were deposited during periods of warm climate.

6.1.2 NB2 and NB11 - Examples of Recent Deposits

Both of these stalagmites were considered to be recent. NB2 was still active when sampled but NB11 was inactive and dry. NB2 was growing on breakdown in a passage 7.5 metres above the present stream. NB11 was found at a higher level, approximately 16 metres above the stream but only 30 metres horizontally from NB2.

These stalagmites were sampled to measure present-day U^{234}/U^{238} ratios and to check the assumption that detrital Th is absent in modern stalagmites. Stalagmite NB2 was dissolved away in layers in an attempt to "strip" the growth layers in sequence. The parts of the stalagmite to be protected were masked; then it was inverted and placed in 1N HCl until the desired amount had been dissolved away. The procedure was repeated in fresh batches of acid and the masking progressively removed until all of the sample was dissolved. The technique was only partially successful because the stalagmite gradually became pointed instead of retaining its rounded shape. The changing geometry of the stalagmite is illustrated in

Figure 6.6(a).

The results of each analysis are discussed below and are collectively shown in Table 6.3.

NB2-1,2-2: No spike was added to the first two samples, NB2-1 and NB2-2. The Th^{228} activity therefore is natural and cannot be attributed to "common" Th, since Th^{232} activity is less than 0.1 cpm. Th^{230} activity was low, but because yields were not determined the actual Th^{230} content of the samples (and therefore the age) could not be calculated. It is interesting that the $\text{Th}^{230}/\text{Th}^{232}$ ratio (which is independent of yield) of the youngest section (NB2-1) is similar to that used by Kaufman and Broecker (1965) to correct for common Th. Little comment can be made on the $\text{Th}^{230}/\text{Th}^{232}$ ratios because of the relatively large uncertainty in background and blank corrections compared with the sample activity.

NB2-3: $\text{U}^{232}/\text{Th}^{228}$ spike was added on the assumption that short-lived Th^{228} or Ra^{228} would have decayed completely 1 cm or so below the surface of the deposit. This was not the case, however, and a Th^{228} activity of 27 cpm remains unaccounted for, assuming 100% recovery of the spike Th^{228} .

NB2-4: The Th^{228} content of this fourth layer could be attributed entirely to spike Th^{228} , but this is uncertain. Sample NB2-4 has less Th^{232} than the other layers, though the amount of detritus (which was very low in every layer) was not noticeably different).

NB2-5,6,7: Subsequent layers were spiked with $\text{Th}^{227}/\text{U}^{232}$ and the Th^{228} activities were attributed to reagent blank contamination plus Th^{227} tail.

Conclusions: The above results indicate that NB2 was deposited

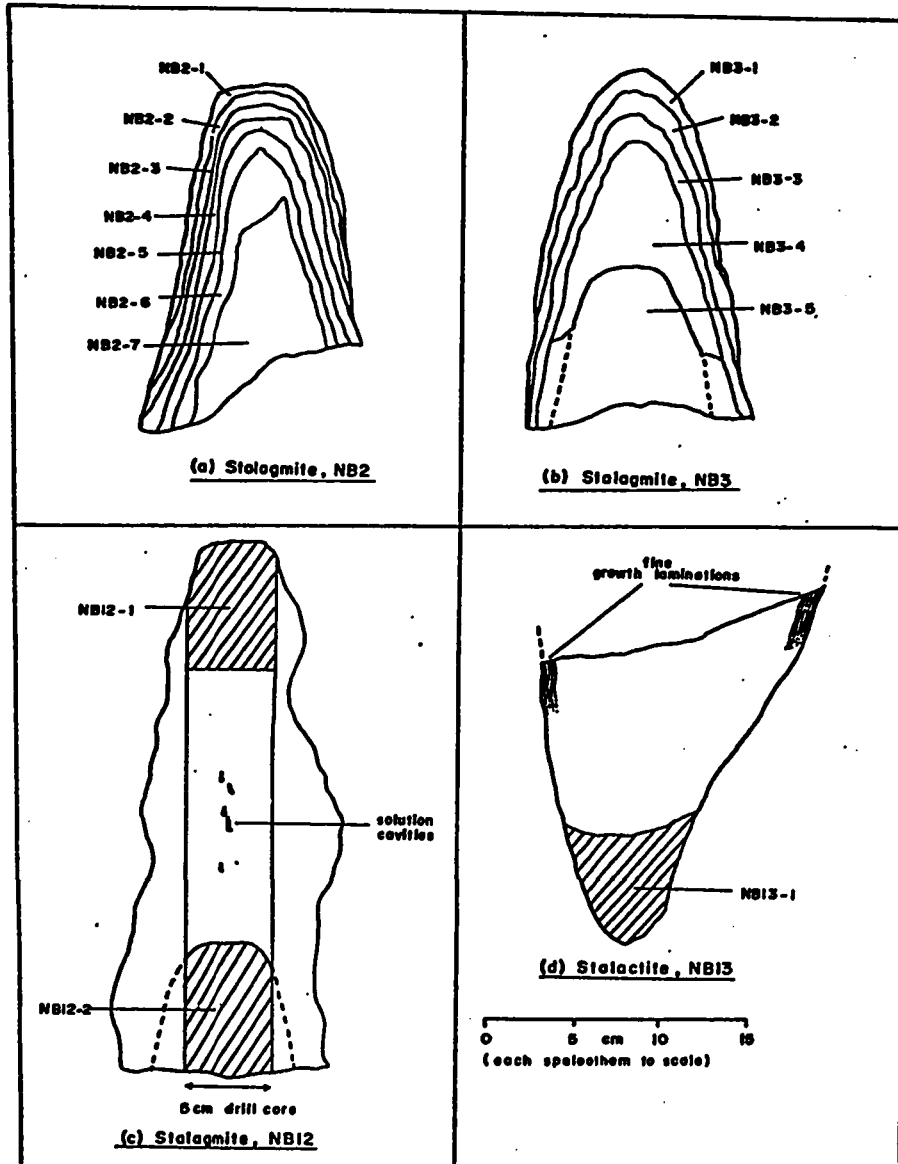


Figure 6.6 Location of analysed samples in speleothems NB2, NB3, NB12 and NB13, Norman-Bone Cave

within the last 5000 years and that over this relatively short period of time the U^{234}/U^{238} ratio in the cave waters was constant. The average value of 1.47 ± 0.06 is identical to that of NB1-1A (1.47 ± 0.03), another recent deposit from the same cave. The two sites were approximately 500 metres apart.

The results also show that Th^{232} -unsupported Th^{228} was present in the outer layers of this stalagmite. The distribution of Th^{228} was heterogeneous and apparently concentrated in a layer 1.3 to 1.9 cm below the surface of the deposit. This implies some sort of internal circulation and deposition within the stalagmite.

Gams (1965) has shown that water, under a pressure of 2 atmospheres, can be forced through a stalagmite. The flow-through time and rate of flow is dependent on the porosity of the deposit as expected. Some, presumably non-porous deposits, were impervious to water.

Cherdyntsev (1972, p.175) has also noted the presence of unsupported Th^{228} in cave travertines. The Th^{228}/Th^{232} ratio in one travertine was 15 ± 3 whilst in another it was > 30 . In young travertines Th^{228}/Th^{232} ratios as high as 67 were measured. Unsupported Th^{228} or parent Ra^{228} has also been identified in lacustrine carbonates (Kaufmann, 1964) in lake waters (Cherdyntsev, 1965) and in ocean waters (Moore, 1969; Cherry *et al.*, 1969; and Kaufmann, 1969). The disequilibrium between Th^{232} and Th^{228} has been attributed to extensive Ra^{228} migration. According to Cherdyntsev (1972, p.169) "... the enrichment of specimens in radiothorium (Th^{228}) does not render them unsuitable for U^{234} or ionium dating; the extensive migration of radium within travertine layers appears to be a normal effect." Of course, a U^{232}/Th^{228} spike

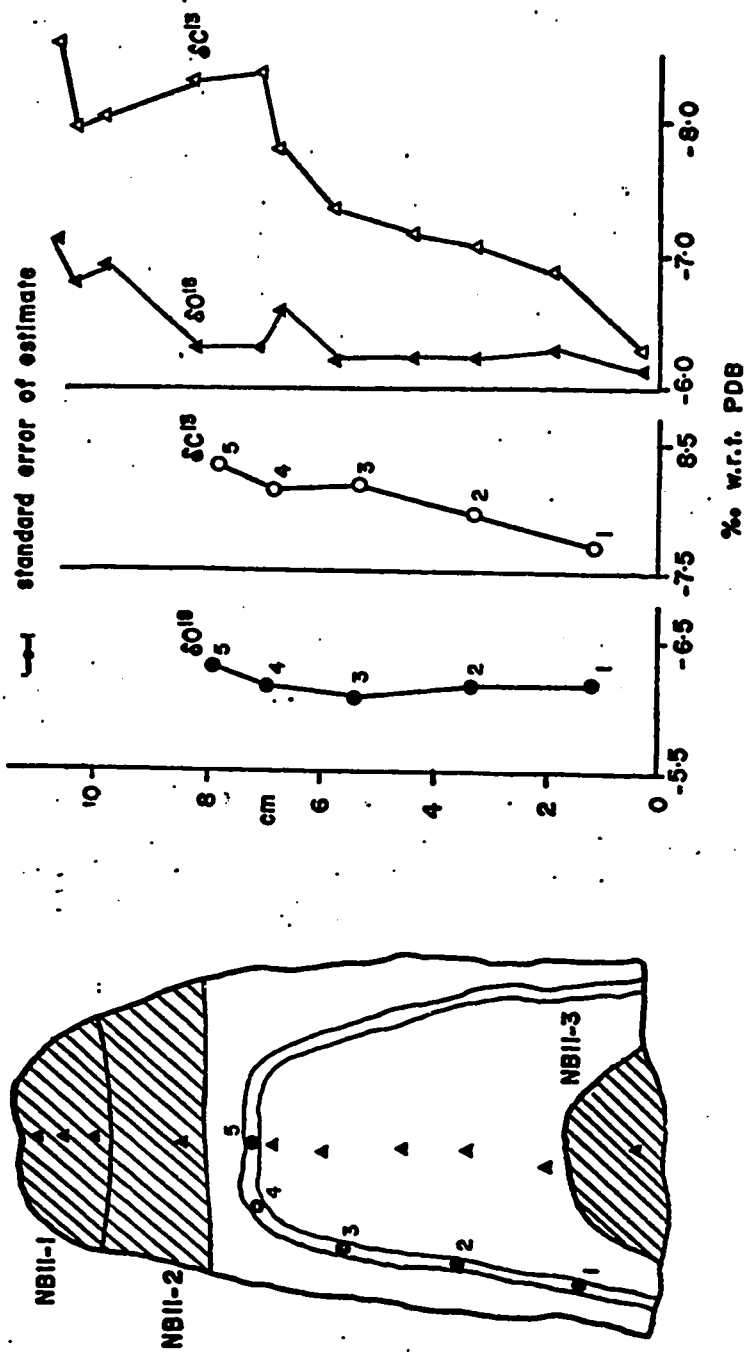


Figure 6.7 Oxygen and carbon isotopic variations along a single growth layer and along the axis of stalagmite NB11, Norman-Bone Cave

Table 6.3

Analysis of Stalagmites NB2 and NB11 (Norman-Bone Cave)

Sample	Weight loss (gm)	(U) p.p.m.	$\left[\frac{U-234}{U-238} \right]$	$\left[\frac{Th-230}{U-234} \right]$	$\left[\frac{Th-230}{Th-232} \right]$	Th-228 c.p.m.	$\left[\frac{Th-228}{Th-232} \right]$	Age (years B.P.)
NB2-1	79	-	1.48±0.04	-	1.70	7.760 ⁺	19.4	-
NB2-2	142	-	1.45±0.10	-	2.35	2.030 ⁺	4.5	-
NB2-3	118	0.65	1.49±0.07	-	2.16	30.250*	60.5	-
NB2-4	153	0.12	1.49±0.04	0.020±0.01	18.10	2.390*	-	2500 ± 1000
NB2-5	126	0.14	1.45±0.05	0.040±0.01	1.77	0.227**	-	4500 ± 1000
NB2-6	225	0.11	1.43±0.02	0.050±0.005	4.86	0.210**	-	5500 ± 500
NB2-7	410	0.35	<u>1.43±0.03</u>	0.030±0.003	4.86	0.242**	-	3000 ± 300
average			1.47±0.06					
NB11-1		1.82	2.42±0.035	0.0175±0.0010	>1000	-		2000 ± 100
NB11-2		1.60	2.43±0.040	0.0179±0.0013	>1000	-		2100 ± 100
NB11-3		1.88	2.44±0.050	0.0270±0.0015	30	0.190**		3500 ± 150

+ no spike added

* 5 mls Th²²⁸/U²³² spike used; maximum possible activity = 3.25 c/min (100% yield)** Th²²⁷/U²³² spike used; Th²²⁸ activity corrected to 100% yield.

mixture cannot be used as a tracer when this condition exists. Disequilibrium between Th^{232} and daughter Ra^{228} and Th^{228} is short-lived (six half-lives of $\text{Ra}^{228} = 40.2$ years) once a closed system is formed.

The Ra must be transported in solution along grain boundaries and cavities within the deposit and deposited as RaCO_3 , which is insoluble. Alternatively, the Ra may be introduced into the deposit via an exchange process. The $\text{U}^{234}/\text{U}^{238}$ ratio does not appear to be grossly affected by this process but the U concentration is highest in the layer showing the highest Th^{228} activity. This could be evidence for secondary U addition but the U distribution in speleothems is sufficiently inhomogenous (as shown in the results of this chapter) that this argument may be completely unjustified.

The movement of water within a speleothem will have a drastic effect on paleotemperature determinations from fluid inclusion analyses if these analyses include the "mobile" water. Because it is probably impossible to separate these two (isotopically inhomogenous) waters, no reliable temperature information can be expected from a deposit showing unsupported Ra^{228} or Th^{228} activity. Consequently, all speleothems that were considered suitable for stable isotope analysis were checked for excess Th^{228} activity.

Whereas the analysis of NB2 was quite problematic, analysis of NB11 yielded unambiguous results. The age of this deposit was comparable to that of NB2 but the $\text{U}^{234}/\text{U}^{238}$ ratio, though constant, was considerably higher and the U concentration was an order of magnitude higher. Very little "common" thorium was present. No Th^{228} activity was observed in the basal section analysed with $\text{U}^{232}/\text{Th}^{227}$ spike. An average growth rate

of $7.8 \text{ cm}/10^3$ years is calculated from the age data.

A further reason for sampling this stalagmite was to obtain recent $\delta_{\text{ct}}^{\text{O}}$ and $\delta_{\text{ct}}^{\text{C}}$ isotopic variations. A section through the stalagmite showed that the deposit contained one prominent growth layer. No relative change in $\delta_{\text{ct}}^{\text{O}}$ occurred along this growth layer suggesting that deposition was an equilibrium process. The stable isotope profile and the locations of the dated samples are shown in Figure 6.7. The axial isotopic analyses indicate a gradual decrease in $\delta_{\text{ct}}^{\text{C}}$ to lighter values nearer the top of the stalagmite and a sudden decrease in $\delta_{\text{ct}}^{\text{O}}$ about 2000 years B.P. to near modern values.

6.1.3 NB3 and NB12 - Fossil Deposits from Bone Cave

Stalagmite NB3 was collected in the dry section of Bone Cave. Though the stalagmite had been broken in some earlier event, its original growth position was located near roof level, 3.5 m above the floor of the passage. The outer layers of the stalagmite were weathered and crumbling; after scraping away some of this material hard crystalline calcite was uncovered below.

This surface texture could have been caused by inundation for a prolonged period which caused partial resolution of the outer surface. That the cave did experience flooding and massive filling with fine sediment is testified to by stratified residual pockets of partly lithified sediment near the roof of the present cave. The stalagmite may have been buried by sediment or submerged under water. Most other deposits in this part of the cave have the same appearance which suggests a similar history.

The stalagmite was dissolved in the same manner as NB2 and a succession of 5 layers were removed. NB3-4 and NB3-5 represent two quite different phases of growth. The stalagmite fractured cleanly around a growth discontinuity and analysis NB3-5 represents the isotopic composition of the oldest deposit. The results of these analyses are presented in Table 6.4. Figure 6.6b shows the changing geometry of the stalagmite. Only the first layer removed contained appreciable insoluble residue (0.85%); the inner layers were very pure and yielded extremely small quantities (<0.05%) of detritus. The greater-than-unity $\text{Th}^{230}/\text{U}^{234}$ ratio for layer NB3-3 and the associated low $\text{Th}^{230}/\text{Th}^{232}$ ratio indicates that Th was initially present. A graph of $\text{Th}^{230}/\text{U}^{234}$ versus $\text{Th}^{232}/\text{U}^{234}$ (Figure 6.8) extrapolated to $\text{Th}^{232}/\text{U}^{234} = 0$ indicates that in a Th^{232} -free sample Th^{230} would be close to isotopic equilibrium with U^{234} . The linear relationship indicates that the stalagmite was deposited over a short period of time and that the occluded Th had a constant initial $\text{Th}^{230}/\text{Th}^{232}$ ratio. The slope of the best fit line (0.93) gives this initial $\text{Th}^{230}/\text{Th}^{232}$ ratio. (The average $\text{Th}^{230}/\text{Th}^{232}$ ratio in the Earth's crust is approximately 0.8). This application of the isochron method originally proposed by Osmond et al (described in Chapter 2, p.46) indicates that NB3 is older than 300,000 years. Layers NB3-2 and NB3-3 were dated using the $\text{Th}^{227}/\text{U}^{232}$ spike mixture to check for "common" Th^{228} . No significant Th^{228} activity was observed in either Th spectrum.

Moving upward across the discontinuity (which represents an appreciable period of time because a weathering crust was able to form on the primitive stalagmite), $\text{U}^{234}/\text{U}^{238}$ ratios unexpectedly decrease from

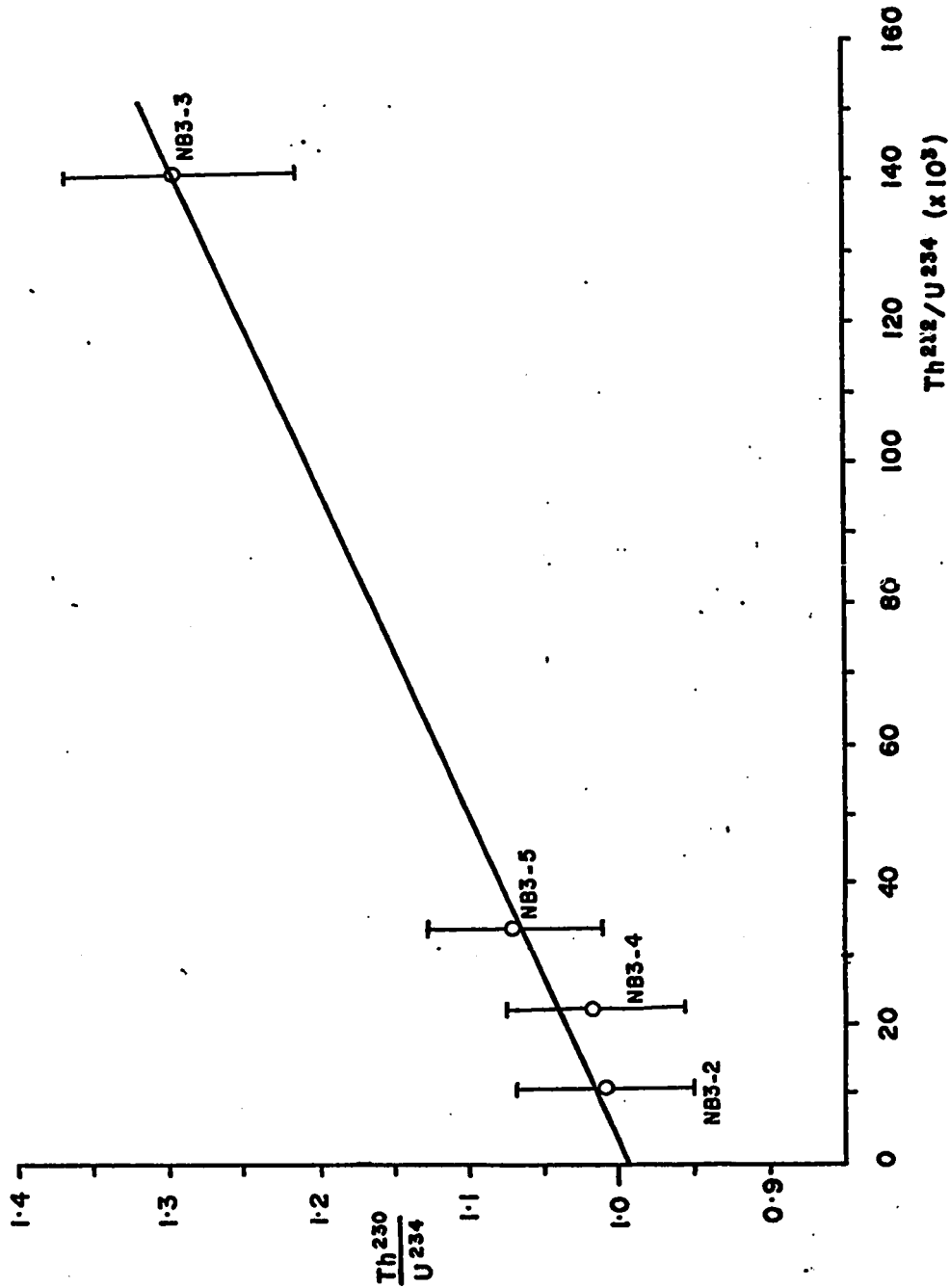


Figure 6.8 $\text{Th}^{230}/\text{U}^{234}$ plotted against $\text{Th}^{232}/\text{U}^{234}$ for stalagmite NB3. The straight-line relationship indicates that the excess Th^{230} can be attributed to a non-authigenic component of constant $\text{Th}^{230}/\text{Th}^{232}$ isotopic composition.

1.15 to 1.05. This indicates that the U isotopic composition of the parent water changed considerably or that U^{234} was leached from the sample. The constant U concentration across the hiatus would seem to preclude extensive leaching. Bone Cave water, based on one analysis, has a present-day U^{234}/U^{238} ratio of 1.45 ± 0.025 so the measured U^{234}/U^{238} ratios support the assumption that the stalagmite is at least 300,000 years old and possibly much older.

To reinforce the argument that Bone Cave contains deposits >300,000 years old another stalagmite (NB12) was collected about 50 metres away from the site of NB3. The surface of this deposit was fresher than that of NB3, though still completely dry, indicating that it might have been deposited after the episode of clastic infilling. Sampling was by means of a 5 cm diameter drill-core. It was subsequently cut along its length to observe the internal structure of the core. The internal structure of the stalagmite is shown in Figure 6.6c. A prominent hiatus was evident near the base of the core and the upper part of the core readily broke away from the lower part around the discontinuity. The upper portion of the stalagmite was a good example of single crystal growth since no grain boundaries could be seen. The top and base of the core were analysed; the results are incorporated into Table 6.4 for comparison with NB3. The Th yield for the basal analysis was virtually zero so only one Th^{230}/U^{234} ratio could be measured. (There was no obvious reason for the poor yield). The results are quite compatible with those obtained for NB3. As a further check on the reliability of the analysis, a Th^{227}/Th^{230} ratio was measured on the top section of the core. The near unity Th^{227}/Th^{230} ratio suggests an age of greater than

Table 6.4

Isotopic Analysis of Stalagmite NB3 and NB12 (Norman-Bone Cave)

Sample	(U) P.p.m.	$\left[\frac{U-234}{U-238}\right]_0$	$\left[\frac{Th-230}{U-234}\right]$	$\left[\frac{Th-230}{Th-232}\right]$	Age (years B.P.)	
NB3-1	-	1.19±0.05	>1.44	1.13±0.07	40	>300,000
NB3-2	0.25	1.06±0.02	>1.14	1.01±0.06*	91	>300,000
NB3-3	0.20	1.03±0.03	>1.07	1.29±0.08*	9.2	>300,000
NB3-4	0.27	1.05±0.025	>1.12	1.015±0.06	48	>300,000
NB3-5	0.28	1.15±0.03	>1.35	1.07±0.06	31	>300,000
NB12-1(top)	1.53	1.12±0.01	>1.38	1.02±0.017	213	>300,000**
NB12-2(base)	1.38	1.03±0.01	-	-	-	-
Bone Cave Water ⁺		1.45±0.025				

* Th^{227}/U^{232} spike used; no significant Th^{228} activity measured.

** $Th^{227}/Th^{230} = 0.95 \pm 0.07$, i.e. age $\geq 200,000$ years B.P.

+ sample collected approximately 60 meters from NB3

200,000 years. These results are discussed further in Section 8.1.2.

6.1.4 Stalagmite NB4 - Analysis of a Drill-core from the Butterscotch

Room

Stalagmite NB4 is located in the Butterscotch Room approximately 200 metres from the entrance to Norman Cave. The original deposit stood 1.6 m high but the top 50 cm section was broken and was lying at the base of the stalagmite. The break did not appear fresh and was possibly the result of some tectonic event. A number of large, broken deposits in the immediate area lend support to this assumption. NB4 is actually three columnar stalagmites that have coalesced to form one deposit as illustrated in Figure 6.9. The position of two 2.5 cm diameter drill cores removed from the middle stalagmite is shown. The upper part of the broken segment was removed from the cave and cut into 6 slab sections each 2.5 to 3.5 cm thick. The lower 4 sections contained a pure, coarse-grained calcite central portion about 7.6 cm in diameter and an outer layer of microcrystalline, porous calcite. These textural details are shown in Figure 6.10. The pure central portion was absent in the top two slab sections. These sections and textural changes in the drill core allowed partial interpretation of the internal stratigraphy of the stalagmite. The inferred stratigraphy is shown in Figure 6.9.

The results of the drill core analysis are listed in Table 6.5 and Figure 6.11. In general, the results were disappointing due to low U concentrations, and low Th yields. Consistent Th losses, as in this set of analyses, could be due to an interfering anion eg. PO_4^{3-} (derived from guano) which is known to interfere with anion exchange separations; or,

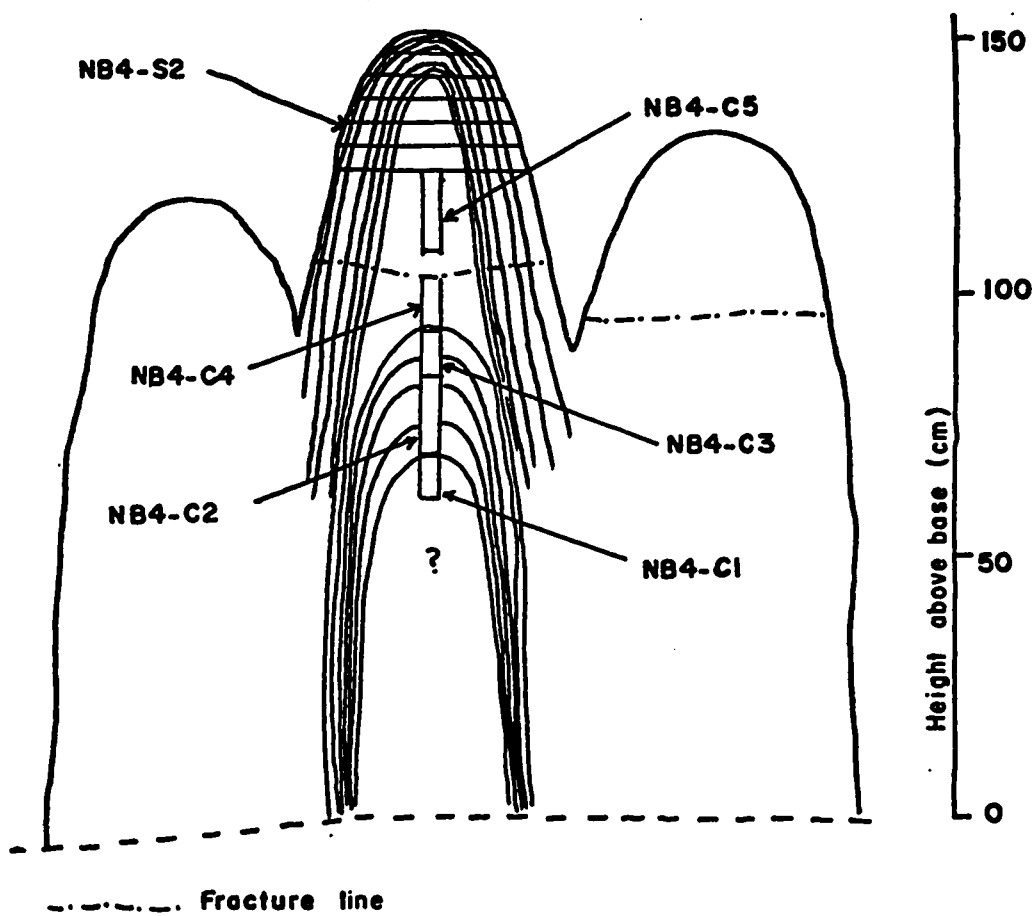


Figure 6.9 Longitudinal section through stalagmite NB4 showing location of the analysed samples. The stratigraphy is inferred from the drill-core and slab sections NB4-S1 to -S6.

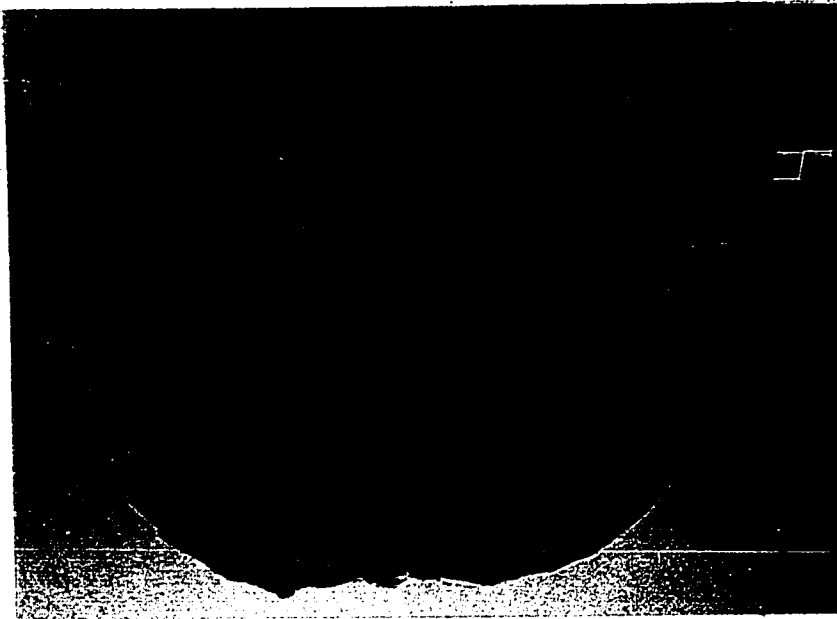
more likely, Th losses could be due to adsorption onto insoluble detrital particles.

The change in texture between core sections NB4-C3 and NB4-C4 suggests that deposition stopped between 103,000 years and 55-65,000 years ago. If deposition was continuous this results in an inordinately slow rate of accretion ($0.23 - 0.28 \text{ cm}/10^3 \text{ years}$). This is an order of magnitude different from that measured for other stalagmites from the same cave. On the basis of the $\text{Th}^{230}/\text{Th}^{232}$ ratio analysis NB4-C4 should be reliable but because of the low $\text{Th}^{230}/\text{Th}^{232}$ ratio in sample NB4-C5 the reported age will be too high. An attempt has been made to correct for this "common" Th^{230} by assuming that the original $\text{Th}^{230}/\text{Th}^{232}$ ratio was 1.7.

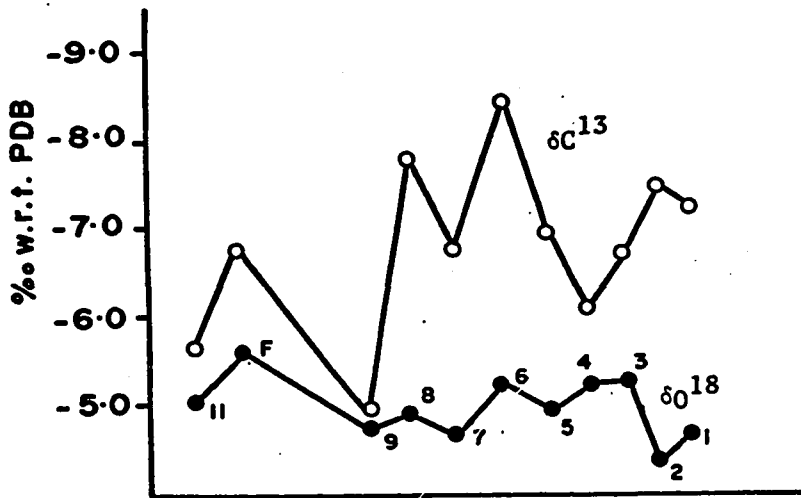
Detailed $\text{O}^{18}/\text{O}^{16}$ and $\text{C}^{13}/\text{C}^{12}$ isotope curves were constructed from the cored material and some analyses on the undated slab section (S2) were completed. Because of the low yields in the drill core analyses no attempt was made to date section S2, but a maximum age of 50-60,000 years can be assigned to the centre of this section. The interpretation of the oxygen isotope curve in Figure 6.11 is complicated by the apparent correlation between $\delta_{\text{ct}}^{\text{O}}$ and $\delta_{\text{ct}}^{\text{C}}$ in parts of the core. However, the $\delta_{\text{ct}}^{\text{O}}$ minimum recorded in section NB4-C3 and dated at $103,000 \pm 25,000$ years B.P. is not associated with a significant change in $\delta_{\text{ct}}^{\text{C}}$ and is correlative with the $\delta_{\text{ct}}^{\text{O}}$ minimum measured in the Grapevine flowstone, GV2 (described later). This suggests that, at least in this section of the core, paleo-climate change is being measured with the lighter calcites representing deposition during warmer climate.

Figure 6.10 shows the results of the stable isotope analyses for

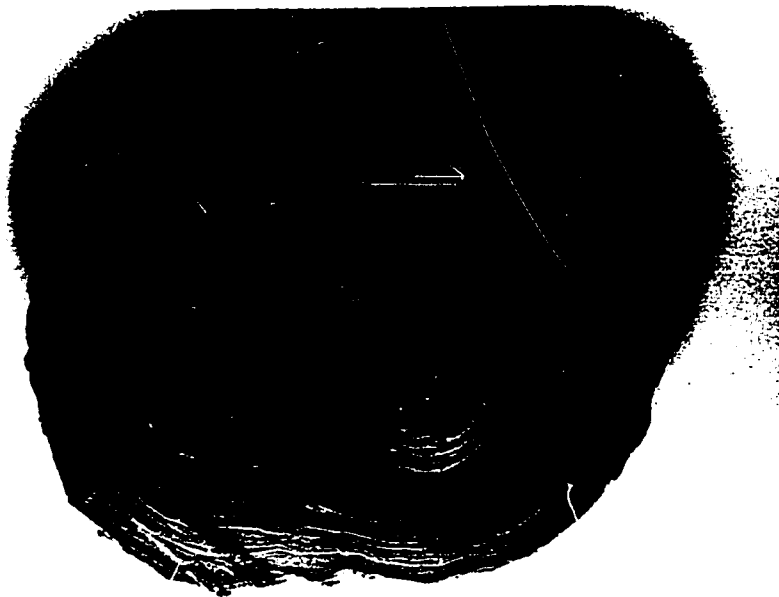
Figure 6.10 Cross-section and oxygen and carbon isotopic profile through the upper part of stalagmite NB4 (section NB4-S2) from the Butterscotch Room, Norman-Bone Cave.



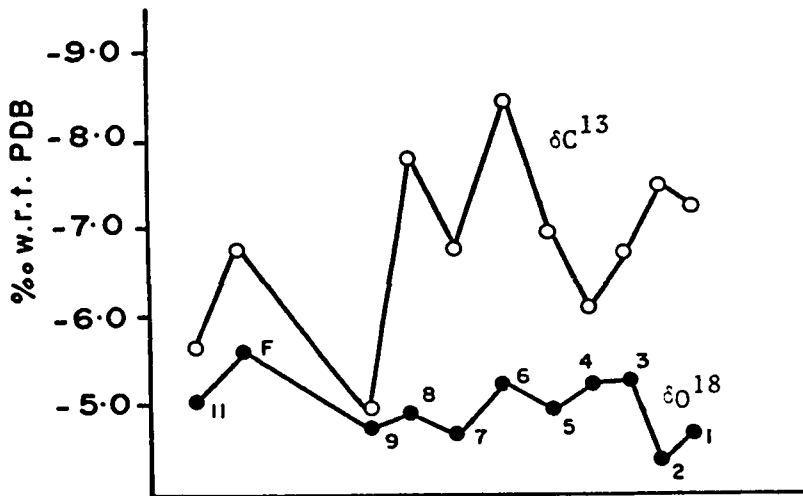
22.9 cm



	$\delta^{18}\text{O}$	$\delta^{13}\text{C}$
A	-5.69	-7.72
B	-5.36	-7.59
C	-5.63	-7.03
D	-5.48	-6.39
E	-5.26	-6.33
F	-5.49	-
G	-5.77	-7.21



22.9 cm



	δO^{18}	δC^{13}
A	-5.69	-7.72
B	-5.36	-7.59
C	-5.63	-7.03
D	-5.48	-6.39
E	-5.26	-6.33
F	-5.49	-
G	-5.77	-7.21

Table 6.5

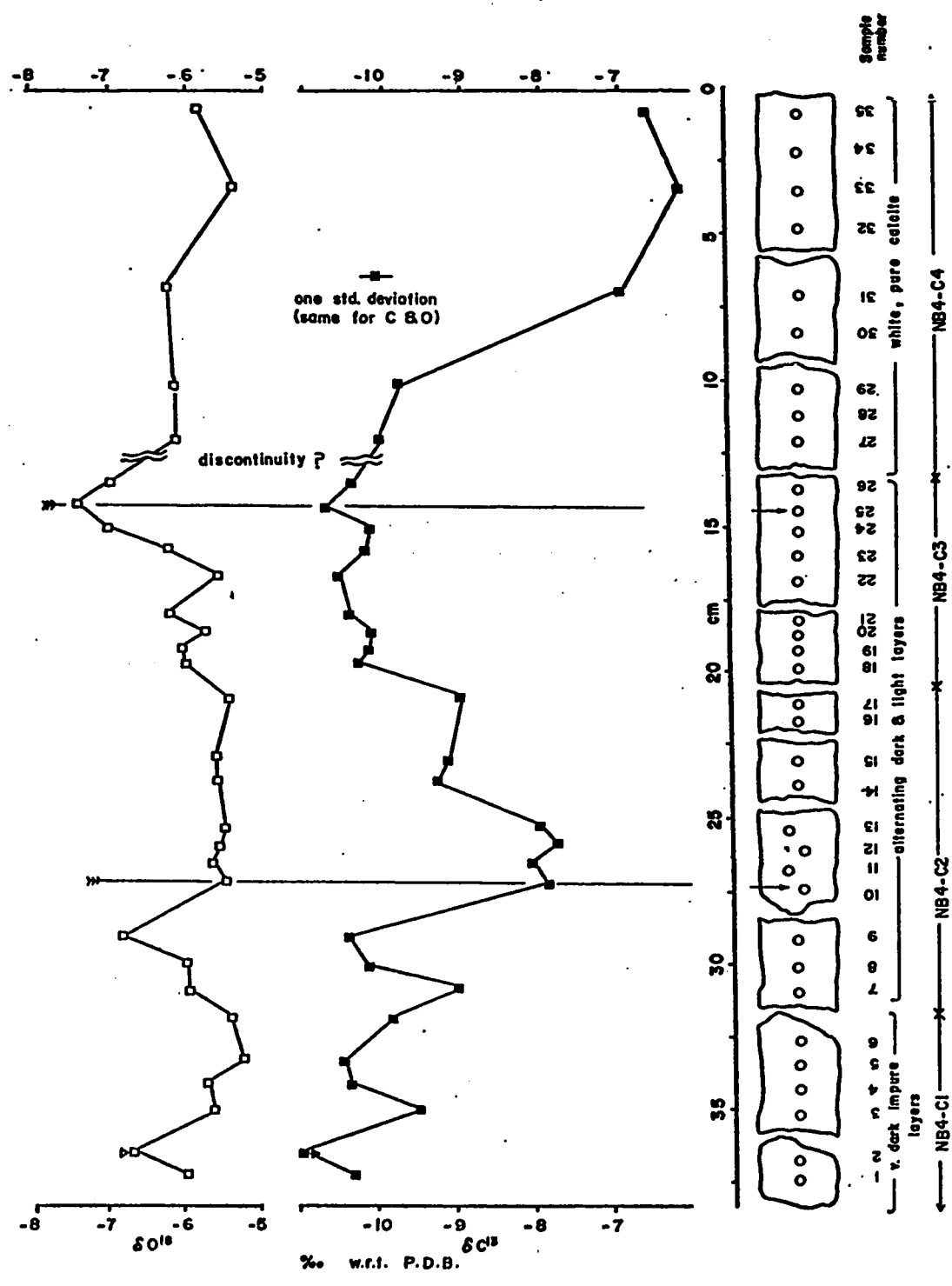
Analysis of Norman-Bone Drill Core NB4 and Stalactite NB13

Sample	Insoluble Residue	(U) p.p.m.	$\left[\frac{U-234}{U-238} \right]_0$	$\left[\frac{Th-230}{U-234} \right]$	$\left[\frac{Th-230}{Th-232} \right]$	Age (years B.P.)
NB4-C2	n.d.	0.12	1.35±0.10	-	-	-
NB4-C3	n.d.	0.24	1.33±0.04	1.45±0.09	0.636±0.096	103,500 ± 25200
NB4-C4	0.22%	0.43	1.19±0.04	1.22±0.05	0.394±0.033	53,000 ± 5700
NB4-C5	0.20%	0.23	1.56±0.06	1.68±0.08	0.465±0.037	64,900 ± 6700
					0.436±0.036	59,800 ± 6400**
NB13-1	n.d.	0.99	1.40±0.01	1.48±0.02	0.497±0.013	46.7
						71,000 ± 2500

* no Th yield

** corrected age assuming $\left[\frac{Th-230}{Th-232} \right]_0 = 1.7$ and addition was at time $t = 0$.

Figure 6.11 Oxygen and carbon isotopic profile along the
Norman-Bone Cave drill core, NB4.



the slab section S2. Many distinct layers can be observed and a traverse of one of those layers was completed to look for isotopic variations. Within the limits of experimental error no variation in δ_{ct}^o was observed which was considered support for equilibrium deposition. The darker layers are clearly more porous than the central portion, though distinct solution pockets are visible in the latter. The transition from light to dark calcite is accompanied by a sharp decrease in δ_{ct}^c but δ_{ct}^o is relatively constant. Taking the results of the drill core and slab together, it appears that there is an irregular increase in δ_{ct}^o from a value of -7.3 ‰ approximately 100,000 years ago to a value of -5.0 ‰ when deposition stopped. This indicates that deposition stopped after a period of cooling.

NB13, the tip of a stalactite curtain deposit, was analysed as part of the preliminary dating program. It was subsequently realised that this deposit would probably not give reliable climate information because it was located only 35 m. within the Norman Cave entrance and therefore within the range of diurnal temperature fluctuations. Only one apparently successful age determination was attempted and this is incorporated into Table 6.5 (because the nearest comparable deposit was NB4). The location of the sample is shown in Figure 6.6d. Deposition stopped approximately 72,000 years ago but, because the stalactite was 1.2 metres long, deposition must have started a considerable time before this. The initial U^{234}/U^{238} ratio is similar to NB4-C3 (deposited 103,000 \pm 25,000 years B.P.) and similar to the recent values of 1.47 measured for NB1 and NB2.

6.1.5 Stalagmites NB5 and NB9 - Two Neighbouring Deposits from the Butterscotch Room

These two stalagmites, deposited within 30 cm of each other, were chosen for analysis to determine if they were contemporaneous. It was hoped that oxygen isotopes would record identical secular variations in δ_{ct}^O . This would be strong evidence for interpretation of variations in δ_{ct}^O in terms of climate change.

NB5 stood 76 cm high and was of uniform diameter (7 cm). Only the lower section of NB9 was recovered and this was broken into a number of smaller sections which were strewn around the base of NB5. A photograph of these two stalagmites in pristine condition (taken by Thomas E. Wolfe circa 1965) shows that NB9 was approximately twice the height of NB5. Reconstruction of NB9 indicated that only the lower 70 cm section remained. This section was of the same uniform diameter as NB5.

NB5 was cut into 22 sections each approximately 3.5 cm thick and NB9 into 10 sections of varying thickness. Figure 6.12 indicates which sections were analysed. The results of these analyses are shown in Table 6.6. The analyses of the basal sections indicate that deposition started contemporaneously about 70,000 years B.P. However, in defiance of the laws of superposition, the upper layers appear to be older than the lower layers. The results, therefore, cannot be accepted. Because Th^{230}/Th^{232} ratios are relatively high the high ages cannot be explained by the introduction of detrital Th. These anomalous results are discussed further in Chapter 8.

Some stable isotope analyses were carried out concurrently with the age analyses. The samples were taken from the base of NB5, as shown

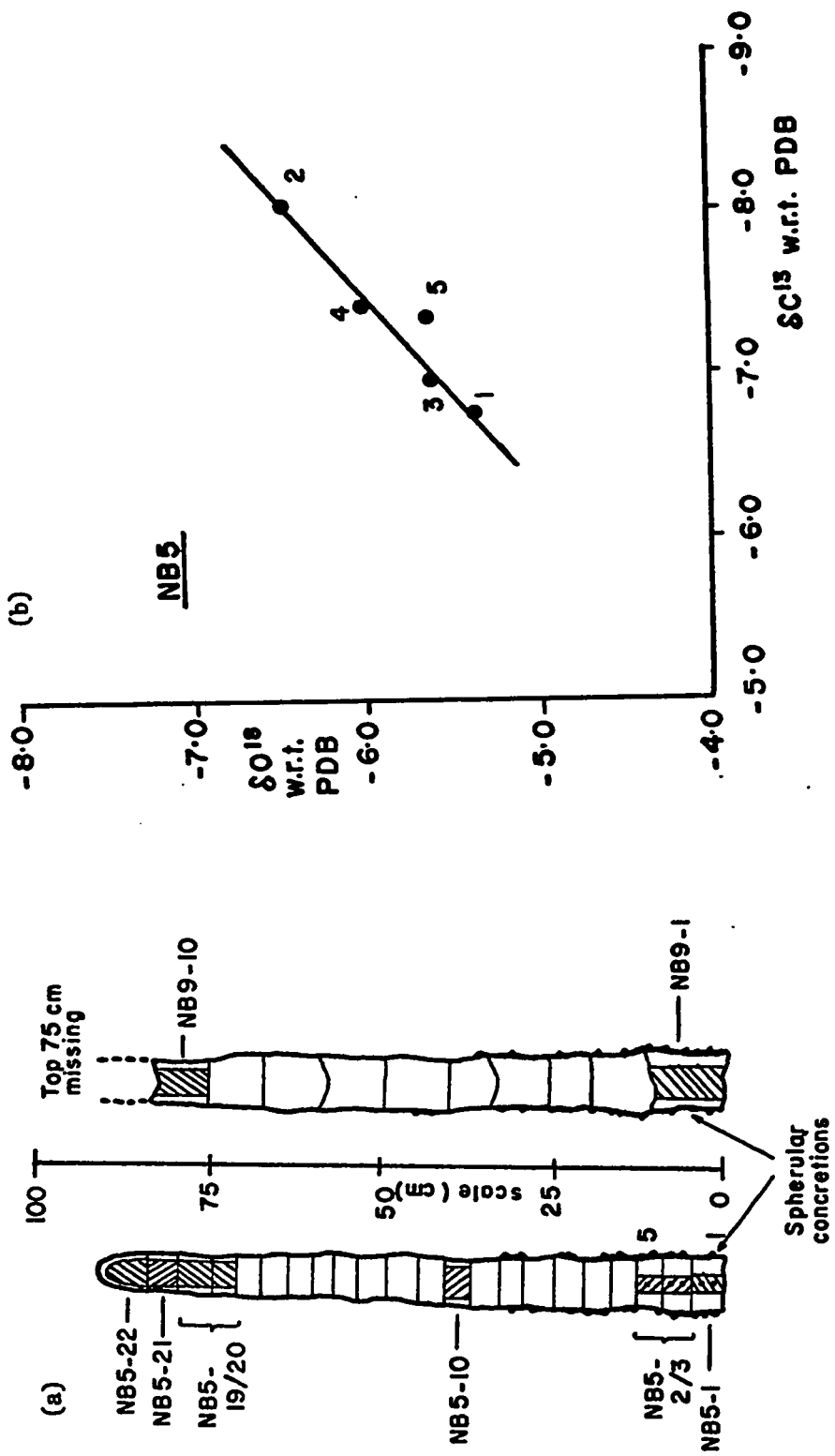


Figure 6.12 (a) Location of samples for age and stable isotopic analysis in stalagmites NB5 & NB9, Butterscotch Room, Norman Cave. (b) Relationship between $\delta_{\text{ct}}^{\text{O}}$ and $\delta_{\text{ct}}^{\text{C}}$ for samples from the base of NB5.

Table 6.6

Isotopic Analysis of Stalagmites NB5 and NB9 (Norman-Bone Cave)

Sample	Average height above base (cm)	(U) P.P.m.	$\frac{[U-234]}{[U-238]}$	$\frac{[U-234]}{[U-238]}$ _o	$\frac{[Th-230]}{[U-234]}$	$\frac{[Th-230]}{[Th-232]}$	Age (years B.P.)
NB5-1	3.0	-	1.63±0.04	1.75±0.06	0.504±0.02	43	72,000 ± 2500
NB5-2/3	10.0	-	1.58±0.03	1.72±0.05	0.494±0.032	54	70,000 ± 3000
NB5-10	39.0	0.29	1.615±0.09	1.753±0.13	0.505±0.030	29	72,400 ± 5900
NB5-19/20	75.0	0.37	1.678±0.03	2.012±0.05	0.786±0.013	550	143,300 ± 4600
NB5-21	82.0	0.23	1.99±0.045	2.408±0.08	0.737±0.015	26	124,000 ± 4200
NB5-22	86.5	0.24	2.15±0.11	2.56±0.19	0.678±0.040	63	108,000 ± 9900
NB9-1	5.0	0.63	1.49±0.02	1.60±0.04	0.48±0.02	56	68,000 ± 2700
NB9-10	80.0	0.39	1.85±0.02	2.53±0.10	0.955±0.03	97	212,400 ± 14700

in Figure 6.12a. Figure 6.12b shows a strong relationship between δ_{ct}^O and δ_{ct}^C with $\Delta_{ct}^O = 0.75 \Delta_{ct}^C$. This could indicate that kinetic factors determined the isotopic composition of the calcite but the relationship between Δ_{ct}^O and Δ_{ct}^C is not that predicted by Hendy. Because of the anomalous dating results no further stable isotope analyses were attempted.

6.2 GRAPEVINE CAVE

6.2.1. GV1 - An Ultra-Pure Flowstone Sample

This sample was a corner of a massive flowstone deposit covering breakdown. The outer surface of the flowstone was covered with a thin film of wet clay. The supply of water was enough to keep the surface of the deposit moist but not enough to allow significant deposition of $CaCO_3$. A sketch of the sample is shown in Figure 6.13. A prominent feature is the red layer just beneath the surface of the deposit. The remainder of the deposit is pure, white calcite which, when dissolved, left no insoluble residue.

The top of the flowstone proved to be recent. The presence of Th^{232} -unsupported Th^{228} in this layer indicates that some deposition is taking place. The middle part of the flowstone (10 cm beneath the surface) contained no significant Th^{228} activity.

A large amount of the sample (3 kgm) was available for analysis so the central portion of the block was crushed, sieved (to 200 mesh) and homogenised for triplicate analyses to check the dating method. The experiment was abandoned, however, when very low uranium concentrations were found. There is an order of magnitude difference between the U con-

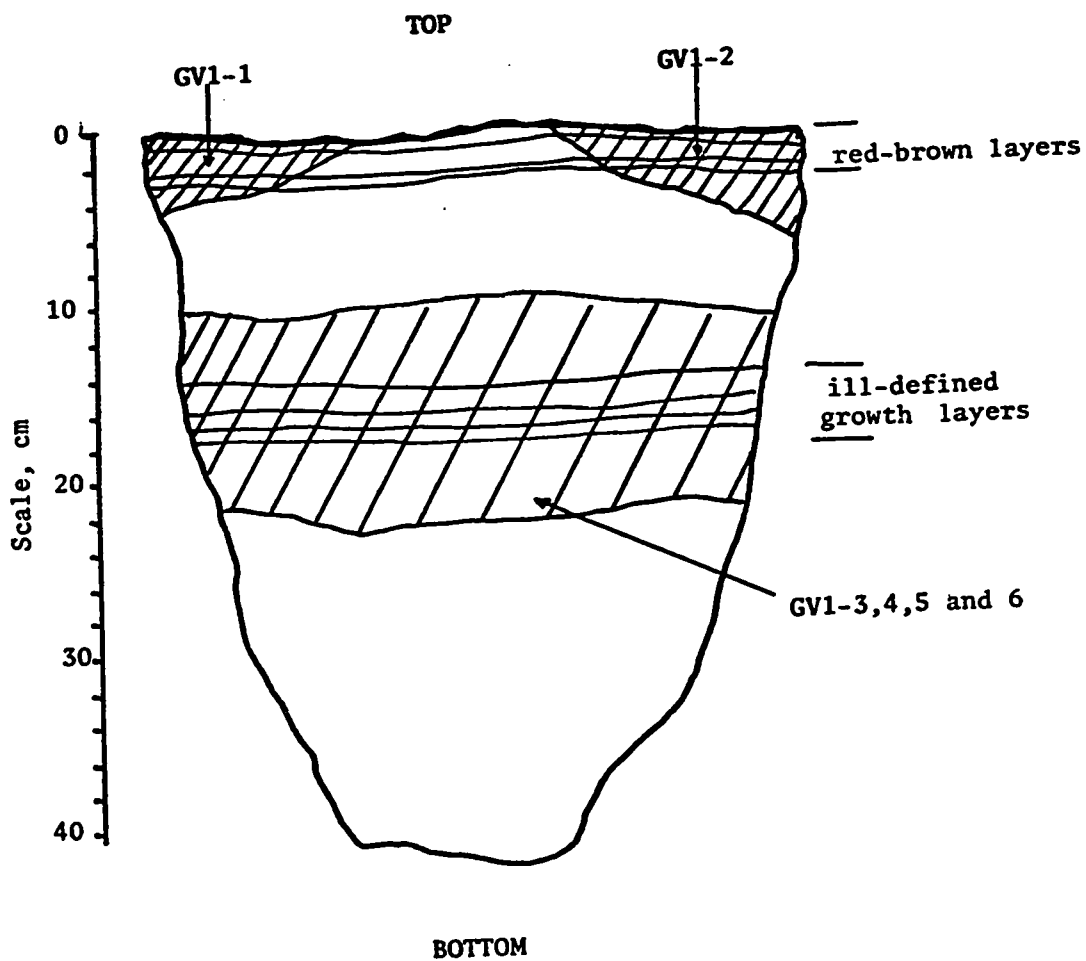


Figure 6.13 Cross-section through flowstone sample GV1, Grapevine Cave, showing location of analysed samples.

tent of the recent layer and the older layers. At the time of the analyses a small area, low efficiency detector was in use which would have prolonged the counting periods to excessive lengths. The results of the uranium analyses and one age determination are presented in Table 6.7.

6.2.2 GVC-1 - Analysis of a Drill Core from Grapevine Cave

Four 2.5 cm drill cores were obtained from Grapevine Cave. GVC-1, a horizontal drill core 43 cm long, cut across the growth layers of a massive stalagmite 3.5 metres in diameter and 6 metres high. The remaining drill cores, each about 27 cm long, were removed from smaller stalagmites. These cores, the locations of which are shown in Figure 3.4, were rejected due to their extremely low U contents (approximately 0.03 to 0.04 ppm) and insufficiency of material for accurate analysis.

The core which was analysed appeared similar in texture to the light brown, porous section of the Norman Cave drill core. The amount of insoluble residue was slightly greater than that measured in NB4, and probably sufficient to cause problems due to selective leaching of the sediment. The first (youngest) 7.5 cm section of GVC-1 was discarded because the calcite was extremely porous. The remaining four sections of the core were analysed for both U and Th but only U content and U^{234}/U^{238} ratios are reported in Table 6.7. The Th spectra were spoiled by appreciable tailing of the Th^{228} peaks which "swamped" the extremely small Th^{230} peaks. It was impossible to obtain Th^{230}/U^{234} ratios and Th^{230}/Th^{232} ratios. (This tailing was caused by incomplete chemical separations which resulted in relatively thick Th sources. A change in the extraction procedure to that described in Chapter 5 removed this problem).

Table 6.7
Isotopic Analysis of Flowstone GV1 and Drill Core GVC-1 (Gregovine Cave)

Sample	Depth of midpt. of sample from surface (cm)	(U) p.p.m.	$\frac{[U-234]}{[U-238]}$	$\frac{[U-234]}{[U-238]}_0$	$\frac{[Th-230]}{[U-234]}$	$\frac{[Th-230]}{[Th-232]}$	$\frac{Th-228}{c.p.m.}$	$\frac{[Th-228]}{[Th-232]}$	Age (years B.P.)
GV1-1	1.0	0.95	2.28 ± 0.03	$= 2.3$	0.09	>100	24.3	>100	<10,000(1)
GV1-2	1.3	-	2.48 ± 0.04	$= 2.5$	-	-	16.0	>100	-
GV1-2(2)	-	-	2.52 ± 0.03	-	-	-	-	-	-
GV1-4(3)	15	0.09	1.48 ± 0.07	1.52 ± 0.09	0.42 ± 0.05	76	-	-	$60,000 \pm 7000$
GV1-5	15	-	1.47 ± 0.07	-	-	56	0.29	1.1 ± 0.3	-
GV1-6	15	-	1.53 ± 0.07	-	-	107	0.52	1.3 ± 0.4	-
GVC1-1	3.8	-----discarded-----	-	-	-	-	-	-	-
GVC1-2	14	0.21	0.7 ± 0.1	-	-	-	-	-	-
GVC1-3	21.5	0.06	1.82 ± 0.11	-	-	-	-	-	-
GVC1-4	30	0.05	2.00 ± 0.06	-	-	-	-	-	-
GVC1-5	39.5	0.05	1.96 ± 0.08	-	-	-	-	-	-

(1) maximum age is approximately 10,000 years B.P. - this assumes 100% Th^{228} recovery.

(2) analysis by A. Kaufmann.

(3) GV1-4, GV1-5 and GV1-6 are analyses of identical material. No spike was added to GV1-5 and -6.

The amount of insoluble residue from GVC1-2, -3, -4, and -5 was 0.29%, 0.18%, 0.27%, and 0.32% respectively.

An interesting feature of the analyses is the low U^{234}/U^{238} ratio in GVC1-2. The older part of the core gives high U^{234}/U^{238} values more typical of other Grapevine Cave speleothems. The low U^{234}/U^{238} value reflects a drastic change in the isotopic composition of the cave water. Similar low U^{234}/U^{238} ratios for ground waters have been obtained, for example by Cherdyntsev, (1965) who measured a present-day value of 0.8.

In summary, though there are advantages to working with drill cores of massive deposits, there are also some serious disadvantages. These large deposits represent either long periods of slow growth or shorter periods of rapid growth. Deposits of the latter type are generally porous and contaminated with appreciable occluded detrital material. Both GVC-1 and NB4 represent this type and appear to be unsuitable for accurate dating. The former type were not encountered in this study.

6.2.3 GV2 - A Layered Flowstone Deposit

The exact location of this sample in the cave is uncertain because it was removed from the cave during trail-building operations.

The flowstone block (approximately 46 cm by 15 cm by 18 cm, see Figure 4.5 p.131) was deposited on sediment, some of which was cemented to its base. A cross-section through the narrowest part is shown in Figure 6.14. As discussed in Chapter 5, the sampling of this block posed problems and the first nine analyses were of slab-samples cut approximately parallel to the growth layers (GV2-1 to 7(a) and GV2-10). A further pair of analyses (GV2-8 and GV2-9) were undertaken

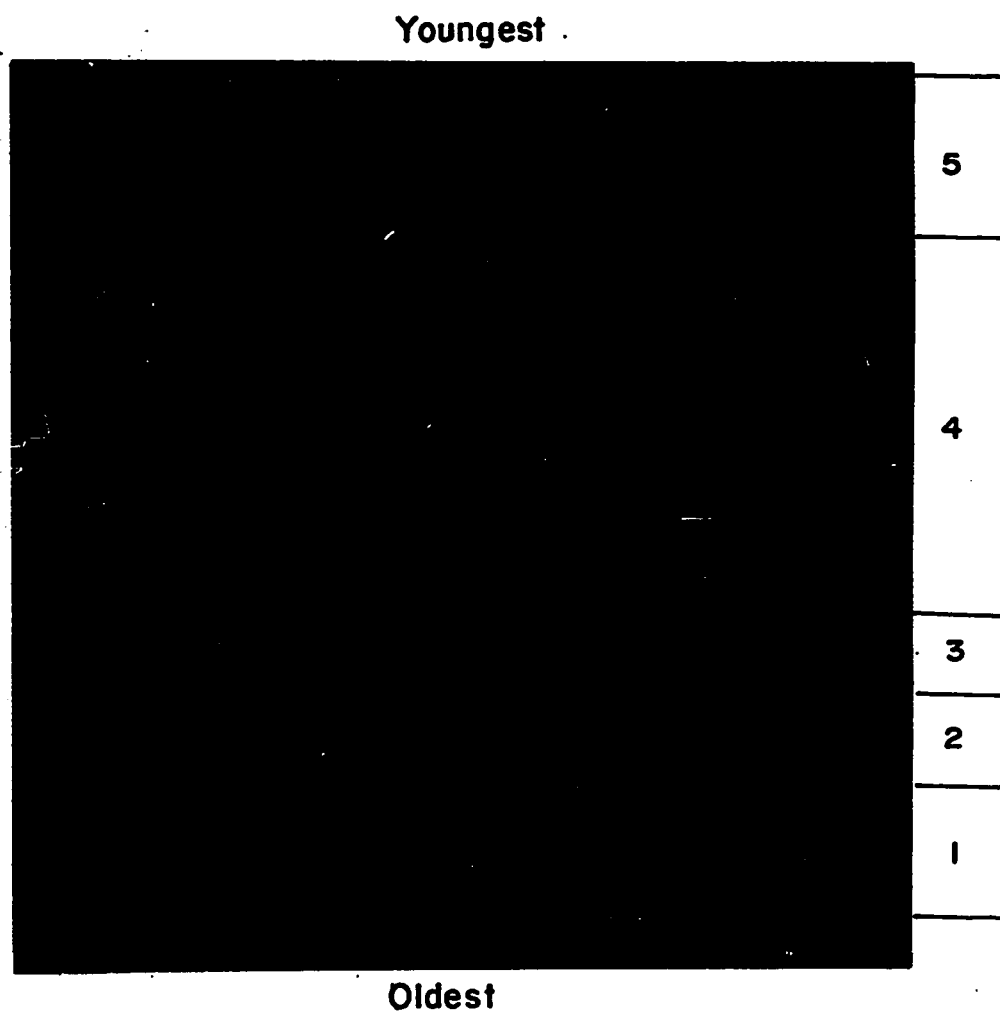


Figure 6.14 Cross-section through flowstone sample GV2, Grapevine Cave. (The numbered layers are described in the text).

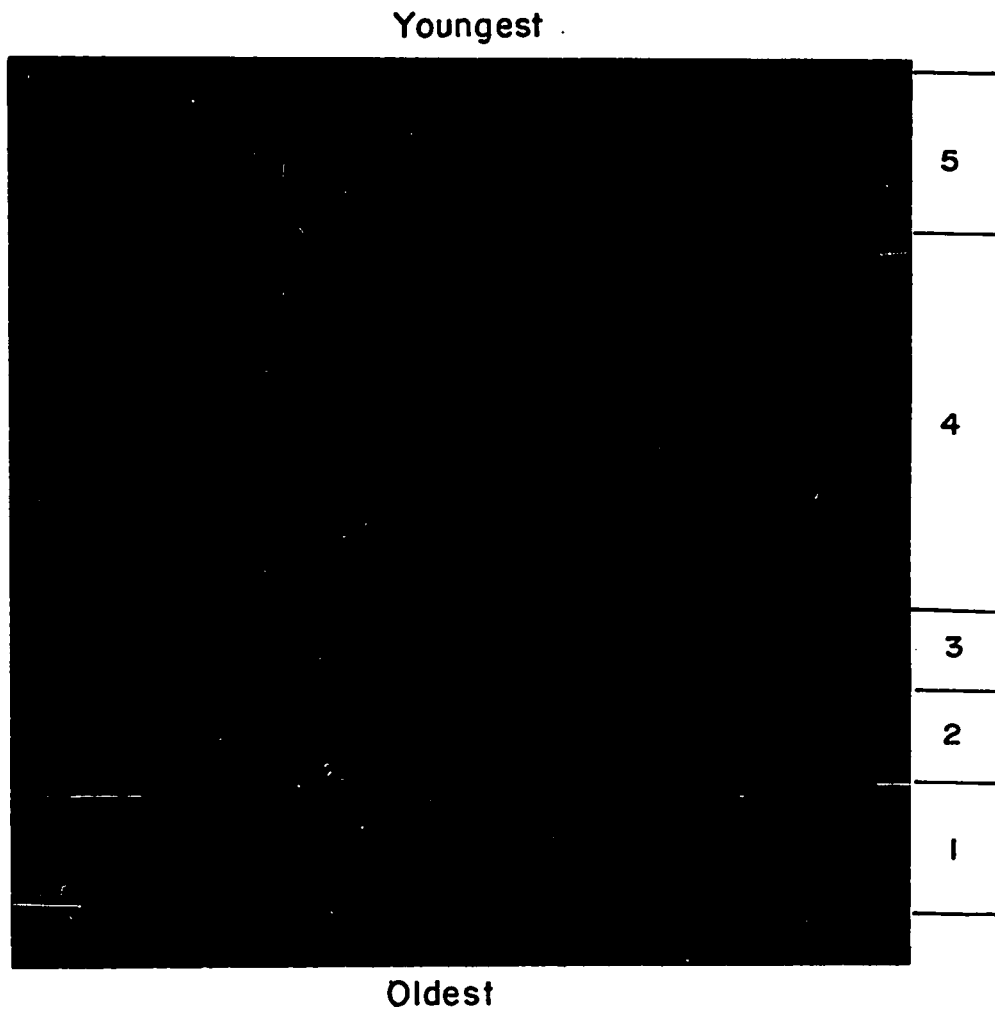


Figure 6.14 Cross-section through flowstone sample GV2, Grapevine Cave. (The numbered layers are described in the text).

to obtain better age control on the lower part of the flowstone.

These samples were obtained by chipping away the required layers with a small, pneumatic drill. The required layers can be accurately removed using this technique. However, some of the spalled calcite fragments are lost in the process and so, if losses are not constant, a sampling error may be introduced. The result of all these analyses are presented in Table 6.8. Figure 6.15 illustrates graphically the (radio) isotope variations from layer to layer and Figure 6.16 the stable isotope variations.

The sample was considered to contain evidence of at least five periods during which conditions of deposition changed considerably.

- (Oldest) Section 1. (GV2-10) Deposition of thin, well defined layers gradually darkening to a sharp transition at Section 2 where the layers become dark grey to black.
- Section 2. (GV2-8,9) Above the dark layers the calcite becomes gradually lighter and the layers are less well defined.
- Section 3. (GV2-7) Sharp transition to red-brown layers. Fe^{2+} and Mn^{2+} were identified in these layers. The colouration gradually fades into Section 4.
- Section 4. (GV2-3,4,5,6) Pure white calcite with some prominent layering and slight resolution.
- (Youngest) Section 5. (GV2-1,2) The boundary between section 4 and 5 is a zone of re-resolution. Above this zone the calcite is relatively porous and grey-coloured. The porosity decreases towards the top of the deposit where well-

defined growth layers are again apparent.

The average age of the lowest 2 cm section is 160,000 years whilst the layers immediately above are approximately 100,000 years old. The most plausible interpretation of these results is a short period of deposition during predominantly cold climate conditions about 160,000 years B.P. followed by a long hiatus in deposition until approximately 100,000 years B.P. This interpretation is compatible with the evidence from NB10 which indicates a period of rapid cooling about 160,000 years ago. Unfortunately, the warm interval recorded in sample GV2-3b (Table 4.7) was not detected in the earlier measurements along the section B-B' (Figure 4.5). Lighter δ_{ct}^o values of about -6.0 ‰ w.r.t. PDB should have been recorded near samples GV2-47 and -49. Experimental error could be involved but it is also possible that the closely spaced layers at the base of GV2 are so isotopically inhomogenous that more frequent sampling should have been attempted. The hiatus in deposition probably corresponds in part to the occurrence of the Illinoian glaciation.

Layers GV2-7,8 and 9 represent a period of rapid growth starting approximately 100,000 years ago. The ages obtained are not sufficiently accurate to assign a growth rate during this period. This corresponds to a δ_{ct}^o minimum shown in Figure 6.16 and to the deposition of trace quantities of Mn^{2+} (and possibly iron) which gives the flowstone its characteristic colouration. The colouration is similar to that observed at the top of the flowstone sample GV1 which was shown to be recent. In both cases the transition from white to red layers is quite abrupt. A climate change is possibly signified by this transition. Warm, humid climate would favour

Table 6.8

Analysis of GV2 Flowstone (Grapevine Cave)

Sample	Height of midpt. of sample above base (cm)	Insoluble Residue	U p.p.m.	$\left[\frac{U-234}{U-238}\right]_0$	$\left[\frac{U-234}{U-238}\right]_0$	$\left[\frac{Th-230}{U-234}\right]$	$\left[\frac{Th-230}{Th-232}\right]$	Age (years B.P.)
GV2-1	17.0	0.385	0.04	1.88±0.03	2.18±0.090	0.413±0.014	148	60,400 ± 2900
GV2-2	15.5	0.515	0.10	1.98±0.07	2.32±0.085	0.419±0.028	167	81,200 ± 6600
GV2-3	14.0	0.808	0.13	2.08±0.06	2.28±0.080	0.428±0.021	85	70,000 ± 3600
GV2-4	12.0	0.444	0.14	1.79±0.05	1.94±0.080	0.467±0.018	56	69,000 ± 2800
GV2-5	10.0	0.413	0.09	2.06±0.05	2.25±0.060	0.555±0.018	55	85,900 ± 3000
GV2-6	8.4	0.118	0.07	1.99±0.04	2.32±0.050	0.506±0.012	39	79,500 ± 2100
GV2-7	6.3	0.075	0.07	2.07±0.04	2.32±0.050	0.601±0.013	52	97,200 ± 2500
GV2-7a	5.1	-	0.08	2.01±0.03	-	-	-	-
GV2-8	4.5	0.091	0.11	2.18±0.04	2.55±0.060	0.619±0.012	247	104,500 ± 2700
GV2-9	3.1	-	0.08	1.93±0.04	2.21±0.070	0.594±0.017	44	96,000 ± 3900
GV2-10	1.2	0.248	0.17	2.04±0.04	2.60±0.100	0.816±0.022	126	159,000 ± 6900

7

Figure 6.15 U^{234}/U^{238} variations along Grapevine Cave flowstone GV2.

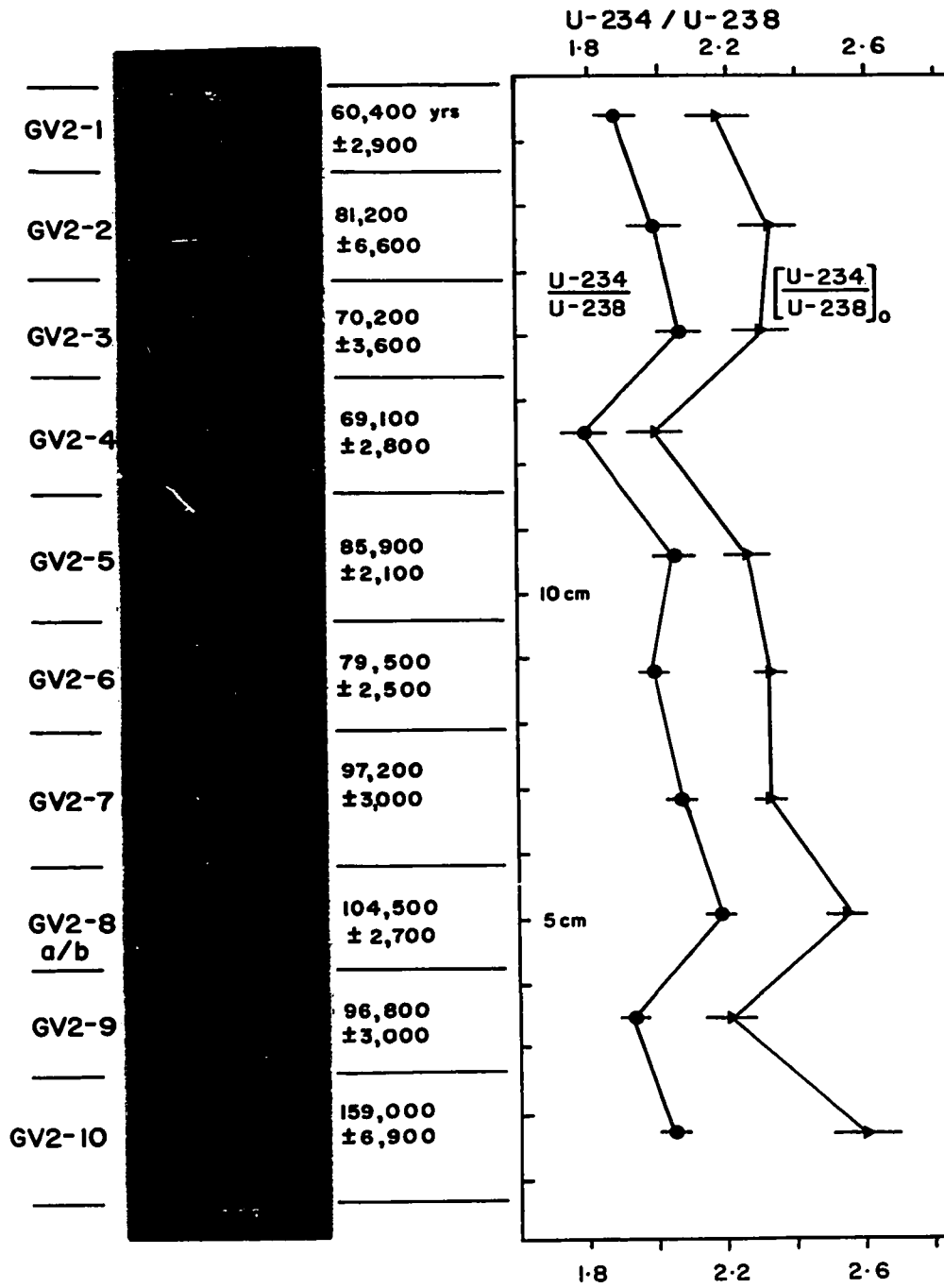
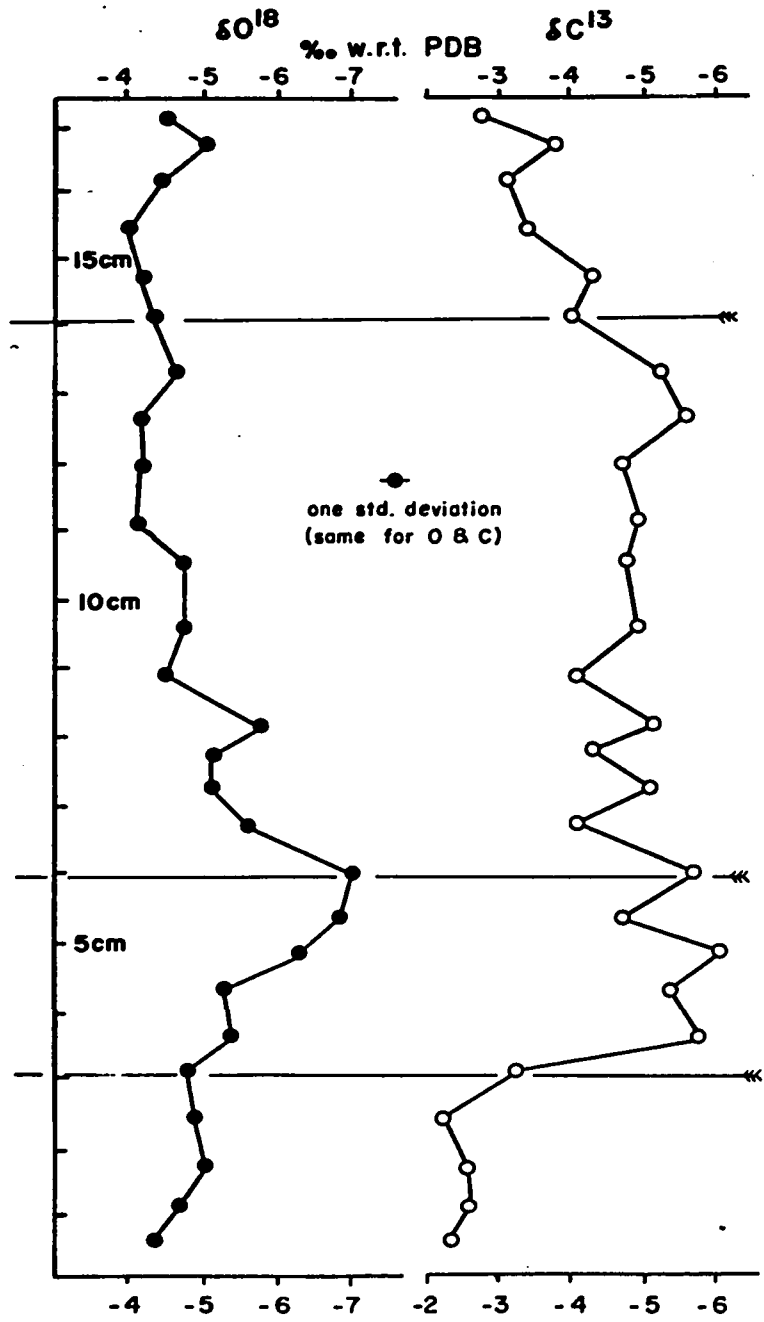


Figure 6.16 Oxygen and carbon isotopic variations along Grapevine
flowstone GV2. The lightest δ_{ct}^o values represent deposition
during a warm period between approximately 105,000 years
B.P. and 95,000 years B.P.

Sample
Number

- 1
- 3
- 5
- 7
- 9
- 11
- 13
- 15
- 17
- 19
- 21
- 23
- 25
- 27
- 28
- 29
- 31
- 33
- 35
- 37
- 39
- 41
- 43
- 45
- 47
- 49
- 51



the transport of Mn^{2+} in solution. This is because high biotic activity would be favoured by such conditions and high CO_2 production would leave the lower soil layers depleted in O_2 . Mn^{2+} is stable under these conditions. The water percolating through the soil layers, acidified by the high CO_2 content of the soil air, would be capable of leaching Mn^{2+} . Essentially the same argument was used by Galimov et al (see Chapter 4, p. 95) to explain the presence of ferruginous layers in stalagmites (though they do not discuss the oxidation state). It is interesting that lighter δ_{ct}^C values are associated with these manganiferous/ferruginous layers, indicating that δ_{ct}^C is a climatic variable also. This is discussed further in Chapter 8, section 8.6 .

The remaining layers represent a period of growth ending approximately 60,000 years ago. The average growth rate of these younger layers is $0.25 \text{ cm}/10^3 \text{ years}$ but this does not take into account possible removal of layers or cessation of growth. The anomalously high age for layer GV2-2 may be due to the preferential leaching of U from the deposit which would tend to increase the Th^{230}/U^{234} ratio. From the cross-section of the flowstone in Figure 6.14 it can be seen that this layer is more porous than the others and therefore more susceptible to leaching. Layer GV2-2 was deposited on a surface which was subjected to considerable re-solution. The solutional cavities and irregular surface can be seen in Figure 6.14. The period after 70,000 years B.P. and before 60,000 years B.P. therefore probably represents a very wet period when undersaturated waters entering the cave were capable of dissolving the flowstone. The other anomalous ages are not so pronounced and are probably due to the limitations of the sampling method.

The initial U^{234}/U^{238} ratios are reasonably constant and comparable to the ratio measured in GV1-1 and in the older layers of GV1-1. They are also the highest measured in West Virginia. However, the lower initial U^{234}/U^{238} ratio in GV1-4 (1.52 ± 0.09) again shows that this ratio can vary within a single speleothem. Until the reasons for these sharp changes are understood the decay of excess U^{234} cannot be used with certainty to date speleothems older than 300,000 years.

6.3 Correlation Between the Isotope Records of NB4 and GV2

Because of the poor age control on NB4 a comparison between this isotope record and that of GV2 cannot be confidently attempted. It was assumed that the core section NB4-C3 and GV2-7 were deposited over approximately the same interval of time. The measured isotopic variations are plotted in Figure 6.17. It can be seen that the intensity of the isotopic variations are quite similar indicating that the same climatic event was recorded in both caves. A time scale cannot be fitted to the older isotopic record in NB4 because the rate of deposition is not known, nor is it known if deposition was continuous. It has been assumed that the marked change in texture between NB4-C3 and NB4-C4 denotes a break in the deposition sequence.

One of the remaining two NB4 age determinations (NB4-C4 and NB5-C5) is clearly in error. The isotopic variations in section NB4-C4 and the undated section (NB4-S2) have been placed on a time scale assuming:

1) that age analysis NB4-C5 is in error. Non-authigenic Th^{230} may be contributing to the high Th^{230}/U^{234} ratio and the low Th^{230}/Th^{232} ratio supports this.

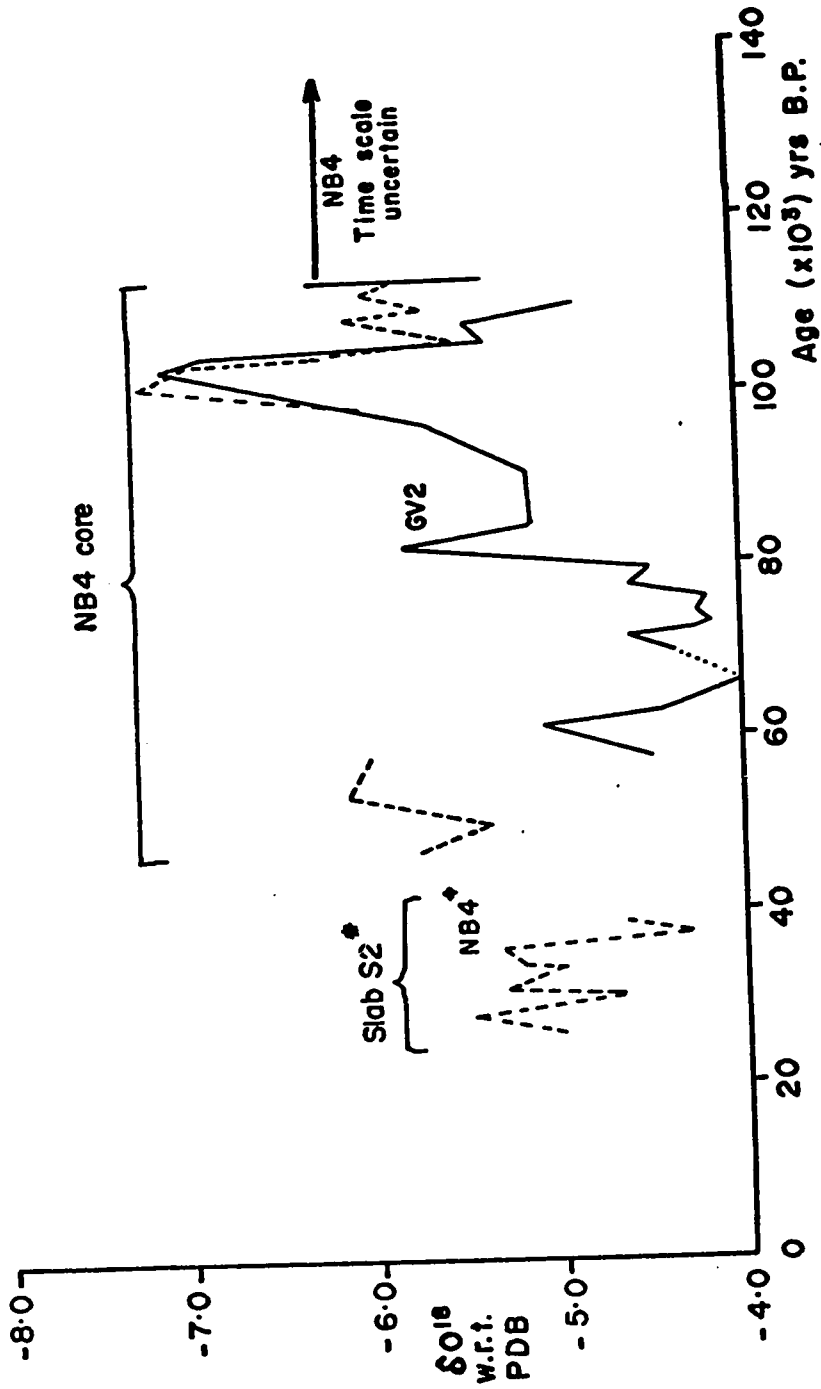


Figure 6.17 Oxygen isotopic variations in stalagmites NB4 and flowstone GV2, parts of which were deposited contemporaneously. (* Note: Time scale based on a constant growth rate of $1 \text{ cm}/10^3$ years between 25×10^3 & 55×10^3 years B.P.)

2) an average growth rate past NB4-C4 of $1 \text{ cm}/10^3 \text{ years}$. This rate is the average "cool period" growth rate for other Norman-Bone stalagmites NB1 and NB10. There is no evidence in this section of a depositional hiatus.

If this growth rate is assumed then it can be calculated that deposition conveniently stopped about 25,000 years ago, or at the beginning of the main Wisconsin cold period. Thus, if this interpretation is correct, the upper part of NB4 was deposited during the interstadial phase between the two Wisconsin glacial phases. A relatively warm period appears to be recorded near the beginning of this interstadial. It must be stressed that this interpretation is only tentative but if we are to distinguish between true climatic events and random isotopic fluctuations this type of correlation must be attempted.

6.4 Results of the Water Sampling Program

Table 6.9 lists the results of the water sampling program carried out over a period of 3 years. The first three waters collected were analysed for Th using Th^{234} as a tracer. The tracer was added back at the laboratory on the assumption that Th, if present in the cave waters would be precipitated quantitatively with NH_4OH (see Chapter 5, p 162). No Th alpha-activity was detected in any of the preparations confirming the assumption that Th-free waters enter the cave. No further Th analyses were attempted. These and subsequent waters were all analysed for $\text{U}^{234}/\text{U}^{238}$ ratio and U concentrations were measured at sites NBW-2 and NBW-4.

The modern stalagmites collected at or near the drip sites in no way reflect the average $\text{U}^{234}/\text{U}^{238}$ composition of modern waters. The

spread of present-day water isotopic composition is considerable except in the case of NBW-4 which was quite constant (1.68 ± 0.08) but different from a modern stalagmite situated only 30 cm from the drip site. It is quite possible that over a longer period of time or with more frequent sampling the isotopic composition of the various waters will average out to a value closer to that observed in stalagmites. (Only a few mgm of CaCO_3 would have been precipitated during the sampling period).

The results of this program indicate that variations in the $\text{U}^{234}/\text{U}^{238}$ ratio occur both over short periods of time and over small areal extents. The validity of using present-day $\text{U}^{234}/\text{U}^{238}$ ratios in speleothems to obtain ages by the decay of excess U^{234} is therefore open to grave doubts. If real differences exist between the $\text{U}^{234}/\text{U}^{238}$ ratios in the calcites and the waters from which they are precipitated these differences may reflect the fact that U^{4+} and U^{6+} both occur in solution as different chemical species. If oxidation of U^{4+} to U^{6+} in solution is incomplete then a wide range of $\text{U}^{4+}/\text{U}^{6+}$ ratios might be expected. The $\text{U}^{234}/\text{U}^{238}$ ratio in the two valence states should be different if account is taken of the fact that more $^{234}\text{U}^{6+}$ atoms will be leached in preference to $^{234}\text{U}^{4+}$ atoms. This is because a Th^{234} recoil atom is partially stripped of electrons during the decay process and $^{234}\text{U}^{6+}$ is produced. Kolodny and Kaplan (1970) verified this in a study of sea floor phosphorites. The $\text{U}^{234}/\text{U}^{238}$ ratio of U^{4+} in the mineral was consistently less than unity whilst the $\text{U}^{234}/\text{U}^{238}$ ratio in the U^{6+} was consistently greater than unity. Therefore, as the $\text{U}^{4+}/\text{U}^{6+}$ ratio in solution increases the $\text{U}^{234}/\text{U}^{238}$ ratio should decrease. From this rather simplified treatment it might be expect-

Table 6.9

 $^{234}\text{U}/^{238}\text{U}$ Ratios in Cave Waters

Date Collected	Huglis Cave	NBM-1	Norman-Bone Cave NBM-2	NBM-3	NBM-4	Grapevine Cave GVM-1	GVM-2	Crows Nest Spring
July '68								2.08±0.12
July '68								2.40±0.08
Aug. '68								2.00±0.10
Aug. '69								2.19±0.10
June '69	2.02±0.11				1.68±0.03			
Sept '69	2.25±0.13							
Nov. '69							2.08±0.10	
June '70		1.50±0.06	1.32±0.10			1.44±0.06	1.33±0.08	
July '70		2.25±0.07	1.35±0.09*		1.72±0.06*			
Nov. '70	1.91±0.16				1.77±0.07			
June '71		1.32±0.04		2.03±0.04	1.60±0.03			
July '71	1.77±0.05							
Sept '71				1.57±0.04				
average and st. dev.	1.91±0.25	1.69±0.44	1.33±0.1	1.80	1.66±0.08	1.44±0.06	1.70±0.1	2.16±0.18
$^{234}\text{U}/^{238}\text{U}$ in modern stal.	1.74±0.05	1.39±0.04	-	-	2.10±0.05	-	±2.4**	-

Norman-Bone Cave

NBM-1 = Site passage above streamway; NBM-2 = Butterscotch Room (near NBS and NBS); NBM = Butterscotch Room (near NBS); NBM-4 = Main (stream) passage.

Grapevine Cave

GVM-1 = Second room (furthest from entrance); GVM-2 = First (larger) room.

* 2.0 ml ^{232}U tracer added to bucket; (U)_{NBM-2} = 0.4 µg/litre, (U)_{NBM-4} = 0.2 µg/litre

** This is the average of GVM-1 and GVM-2, located about 30 metres from the drip-site.

ed that as the uranium content of the water increases the U^{234}/U^{238} ratio should decrease. This expectation does hold for the two West Virginia samples whose U concentrations were measured.

Because of the size (0.99\AA) and charge of the U^{4+} ion it would be accommodated more easily in the $CaCO_3$ lattice ($Ca^{++} = 0.95\text{\AA}$) than the UO_2^{2+} ion. Therefore, if the total amount of U in solution is not precipitated the U^{234}/U^{238} ratio in the $CaCO_3$ should be less than that in the water if U exists as U^{4+} and U^{6+} . The experimental evidence only supports this in two instances (Hughes Cave and NBW-1) indicating that this hypothesis is invalid or that insufficient measurements have been taken. It would be interesting to devise an experiment which would selectively remove U^{4+} or U^{6+} from the cave waters to check the above hypothesis. It would be possible to analyse speleothem samples for U^{4+} and U^{6+} using the method of Kolodny and Kaplan but this was not attempted in this study. Further comments are made about the relation between the U^{234}/U^{238} and U content of speleothems in Chapters 7 and 8.

6.5 Summary

The interpretation and significance of the results are discussed in detail in Chapter 8, but it may be useful at this point to summarize the characteristics of each speleothem and its suitability for U-series dating. This is attempted in Table 6.10 which is a compilation of the petrologic characteristics and the environment of deposition of each of the speleothems described in Sections 6.1 and 6.2.

Table 6.10

Summary of the Petrology and Environment of Deposition of Speleothems Chosen for Isotopic Analysis



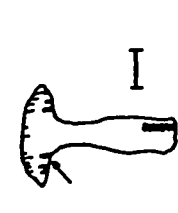
Sample	Passage Cross Section at Site	Comments	Suitable for Dating
NB1	 <p>Half-May Room Norman-Bone Cave</p>	<p><u>Description of site:</u> Room formed by collapse; breakdown substrate; dry; no perceptible air movement; one of many stalagmites.</p> <p><u>Description of sample:</u> Non-porous; holocrystalline; pure, white opaque calcite; detritus only on surface; smooth surface; some cavities caused by re-solution. (U) = 1.04 - 3.85 ppm</p>	Yes
NB2	 <p>Passage near present stream level Norman-Bone Cave</p>	<p><u>Description of site:</u> low wide passage; breakdown substrate; wet; slight air movement; single deposit.</p> <p><u>Description of sample:</u> Non-porous; holocrystalline; pure, white, opaque calcite (?); clean wet surface; very little occluded detritus. (U) = 0.11 - 0.65 ppm</p>	<p>No</p> <p>²³⁰Th/²³²Th 1) Low ²²⁸Th 2) Excess</p>
NB3	 <p>Fossil Exit Passage Bone Cave</p>	<p><u>Description of site:</u> Narrow, high passage; bedrock substrate; entire area of cave very dry; slight air movement; one of many deposits.</p> <p><u>Description of sample:</u> Non-porous; holocrystalline; creamy-white opaque calcite (?); eroded surface; detritus on surface; little occluded detritus; one prominent depositional hiatus; broken. (U) = 0.20 - 0.28 ppm</p>	<p>Yes (Except outer layer)</p>

Table 6.10 - continued


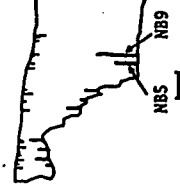

NB4	 <p data-bbox="609 1480 657 1648">Butterscotch Room Norman Cave</p>	<p data-bbox="365 871 641 1396"><u>Description of site:</u> wide, high room enlarged by collapse bedrock substrate; dry (entire area quite dry); no perceptible air movement; one of three large stalagmites in immediate area; top broken</p> <p data-bbox="365 1396 641 1396"><u>Description of sample:</u> broad, columnar stalagmite; variable texture, from creamy-white opaque calcite to dark brown; dark colours due to occluded detritus; surface of deposit rough; well-defined internal stratigraphy; very porous in parts.</p> <p data-bbox="365 1396 641 1396">(U) = 0.12 - 0.43 p.p.m.</p>	<p data-bbox="365 1396 641 1669">Inconclusive</p> <p data-bbox="365 1669 641 1669">1) possibility of U leaching</p> <p data-bbox="365 1669 641 1669">2) relatively high detrital component</p>
NBS 6 NB9	 <p data-bbox="933 1480 982 1648">Butterscotch Room Norman Cave</p>	<p data-bbox="673 871 950 871"><u>Comments apply to both NBS and NB9</u></p> <p data-bbox="673 871 950 1396"><u>Description of site:</u> wide, high room enlarged by collapse bedrock substrate; dry (entire area quite dry); no perceptible air movement; one of many stalagmites in area.</p> <p data-bbox="673 1396 950 1396"><u>Description of sample:</u> columnar stalagmite; uniform texture; holocrystalline; creamy-white opaque calcite; detritus on surface; nodular concretions on lower half of deposit; little internal stratigraphy; no occluded detritus</p> <p data-bbox="673 1396 950 1396">NOTE: top half of NB9 missing; remainder broken</p> <p data-bbox="673 1396 950 1396">NBS (U) = 0.23 - 0.37 ppm NB9 (U) = 0.39 - 0.63 ppm</p>	<p data-bbox="673 1396 950 1669">No</p> <p data-bbox="673 1669 950 1669">Stalagmites do not form a closed system</p>
NB10	 <p data-bbox="1177 1480 1226 1648">(both stalagmites broken) Half-Way Room, Bone Cave</p>	<p data-bbox="998 871 1274 1396"><u>Description of site:</u> Room formed by collapse; breakdown substrate; dry; no perceptible air movement; one of many stalagmites</p> <p data-bbox="998 1396 1274 1396"><u>Description of sample:</u> Non-porous; holocrystalline, translucent to opaque creamy-white calcite; small amount of detritus on surface; no occluded detritus; well-defined internal stratigraphy; irregular surface due to deposition after collapse.</p> <p data-bbox="998 1396 1274 1396">(U) = 0.91 - 1.65</p>	<p data-bbox="998 1396 1274 1669">Yes</p>

Table 6.10 - continued

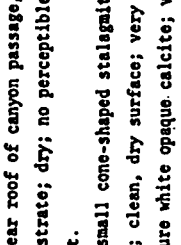
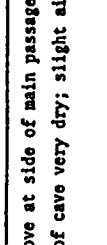
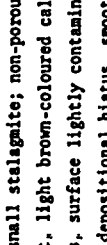
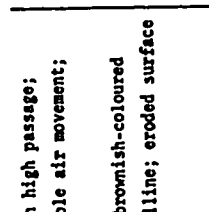
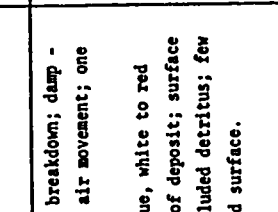
		Yes
<p>NB11</p>  <p>Fossil passage above stream, Bone Cave</p>	<p><u>Description of site:</u> near roof of canyon passage, lightly mud-covered bedrock substrate; dry; no perceptible air movement; single deposit.</p> <p><u>Description of sample:</u> small cone-shaped stalagmite; holocrystalline; non-porous; clean, dry surface; very smooth, regular surface; very pure white opaque calcite; very little occluded detritus; one prominent growth layer.</p> <p>(U) = 1.60 - 1.82 ppm</p>	<p>Yes</p>
<p>NB12</p>  <p>Fossil exit passage Bone Cave</p>	<p><u>Description of site:</u> alcove at side of main passage; bedrock substrate; entire area of cave very dry; slight air movement; single deposit.</p> <p><u>Description of sample:</u> small stalagmite; non-porous; holocrystalline; translucent, light brown-coloured calcite; little occluded detritus, surface lightly contaminated with detritus, one prominent depositional hiatus, smooth irregular surface; some cavities due to re-solution.</p> <p>(U) = 1.38 - 1.53 ppm</p>	<p>Yes</p>
<p>NB13</p>  <p>Entrance Room Norman Cave</p>	<p><u>Description of site:</u> wide, low passage, 30 m from entrance to Norman Cave, intermittently wet, one of a group of large deposits; within the range of diurnal temperature fluctuations; little air movement.</p> <p><u>Description of sample:</u> tip of large stalactitic curtain deposit; crumbly, sugary texture; creamy-white opaque calcite; prominent layering; some occluded detritus; slightly eroded surface.</p> <p>(U) = 0.99 ppm</p>	<p>Inconclusive Only one age determination</p>

Table 6.10 - continued

<p>GVC-1</p>  <p>Drill core, Grapevine Cave</p>	<p><u>Description of site:</u> large stalagmite in high passage; dry; deposition on bedrock; no perceptible air movement; one of many large deposits. <u>Description of sample:</u> porous, opaque, brownish-coloured calcite; some occluded detritus; crystalline; eroded surface (U) = 0.05 - 0.21 ppm</p>	<p>Inconclusive 1) low U 2) possibility of leaching or exchange</p>
<p>GV1</p>  <p>Grapevine Cave</p>	<p><u>Description of site:</u> thick flowstone on breakdown; damp - fed by occasional drips; no perceptible air movement; one of many deposits. <u>Description of sample:</u> non-porous, opaque, white to red calcite (?); prominent red band at top of deposit; surface covered with light film of clay; no occluded detritus; few prominent growth layers; slightly eroded surface. (U) = 0.09 - 0.95 ppm</p>	<p>Inconclusive 1) Th-228 in upper layers 2) possibility of U leaching or exchange</p>
<p>GV2</p>	<p><u>Description of site:</u> precise location of sample unknown; apparently deposited on slope and on sediment. <u>Description of sample:</u> texture varies from porous and opaque to non-porous, translucent calcite; prominent layering; colour of layers from grey-black to red; surface very fresh; some re-solution between layers; some occluded detritus. (U) = 0.04 - 0.13 ppm</p>	<p>Yes except for porous layers</p>

Note: Scale of each cross-section is shown by meter bar (—)

CHAPTER SEVEN
APPLICATION OF THE $\text{Th}^{230}/\text{U}^{234}$ DATING METHOD TO SPELEOTHEMS FROM
OTHER KARST AREAS

This chapter describes some speleothem analyses which were carried out to aid the regional interpretation of the karst areas involved. These analyses were mostly carried out after sufficiently encouraging results had been obtained from West Virginia to indicate that the ionium dating method worked. The chief criterion for accepting ages in this part of the study was internal consistency of results but when possible Th^{227} was measured and a $\text{Pa}^{231}/\text{U}^{235}$ age calculated.

The caves sampled were those near the Crowsnest Pass in the Southern Canadian Rockies, Alberta and in the Nahanni region, North West Territories. Most of the samples were collected by Dr. D.C. Ford. Samples from caves of the El Abra range near Ciudad Valles, S.L.P., Mexico were also collected.

7.1 The Crowsnest Pass Area

The Crowsnest Pass (elevation 4500 feet) is the southernmost pass in the Canadian Rockies. The Pass intersects a mountain range which trends approximately N-S, and which was formed by the Lewis thrust fault. The beds are a mixture of limestone, shale and dolomite. Caves are developed in the Palliser Formation of Upper Devonian age and in the Livingstone Formation of Mississippian age. The high altitude caves from which most of the samples were collected are relict and are being

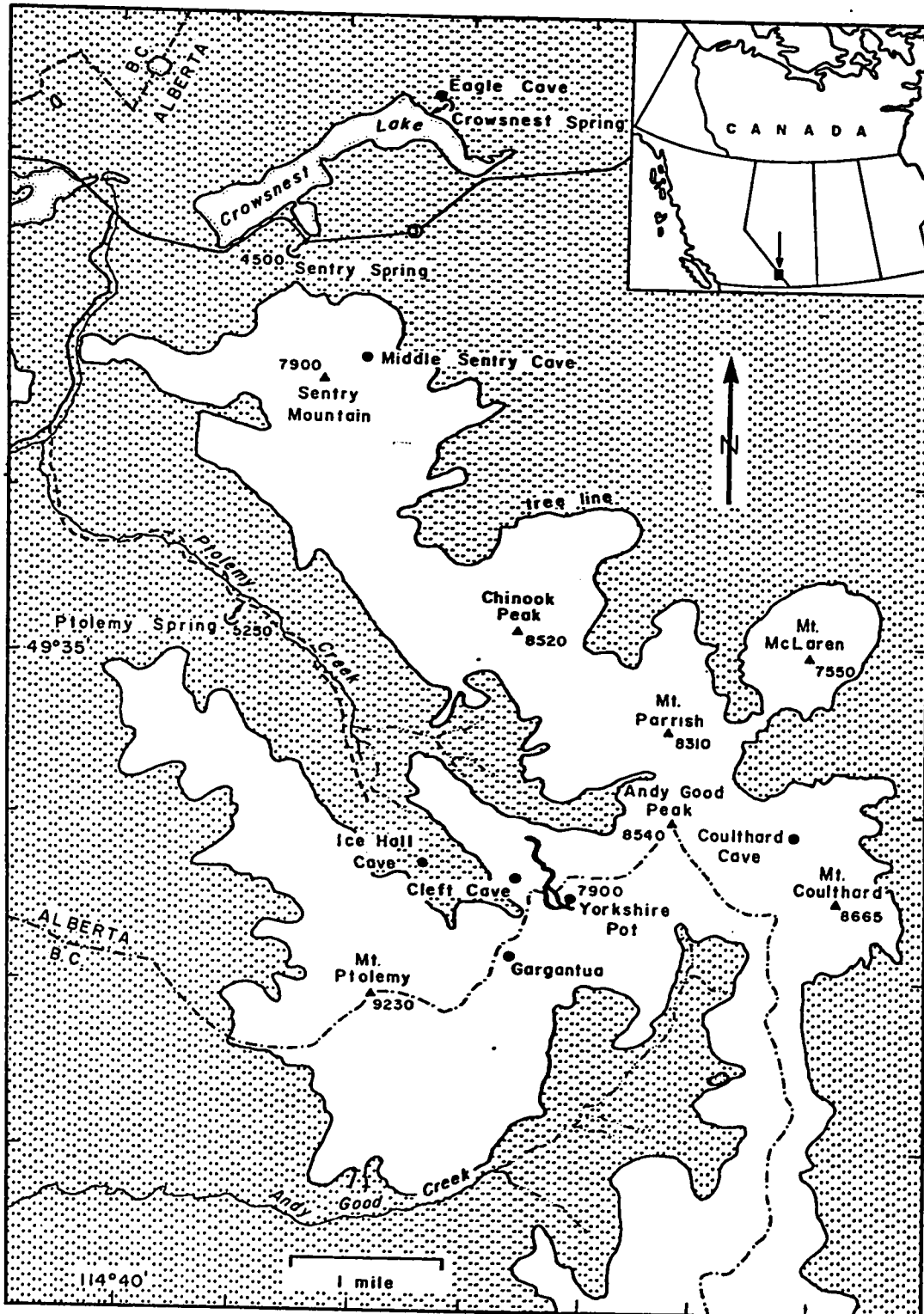
destroyed or filled in with debris. The locations of the caves sampled are shown in Figure 7.1. For a more detailed description of the area see Ford et al., (1972).

7.1.1 Description of the Samples

7.1.1.1 Coulthard Cave Stalagmite

This sample was part of a large irregular roof stalactite, 17.8 cm in diameter, which was broken and half-buried under angular limestone fragments. These fragments were released by frost shattering of the roof and walls. It is probable that this debris was the result of an extreme glacial climate and that the stalactite was formed during milder climate conditions. The stalactite consisted of numerous layers, some of which represented periods of no deposition when a weathering crust had formed. The layers parted at those surfaces quite readily. Most of the calcite was coloured deep red (with Mn^{2+}) but thin layers of white calcite were "sandwiched" between the manganiferous calcite layers. (Manganese was identified in this deposit by a spot test involving the oxidation of Mn^{2+} to Mn^{7+} and formation of the characteristic $KMnO_4$ colour). It is possible that Fe^{3+} also contributed to the calcite colouration. A sample from near the central channel i.e. the oldest layers and a sample of the outer layers were chosen for isotopic analysis. These two samples are separated by at least one prominent discontinuity.

Figure 7.1 Sketch map of the alpine karst area immediately south of the Crowsnest Pass, Southern Alberta, showing the location of the caves studied.



7.1.1.2 Middle Sentry Cave Flowstone

This sample was a flowstone fragment 15.2 cm thick. A section cut perpendicular to the growth layers revealed a series of well-defined laminations but no evidence of discontinuous growth or re-resolution. Unlike the Coulthard Cave sample the flowstone was free of manganese but tinted yellow-brown with fine detritus. Three samples MS1, MS2 and MS3 from the base, centre and top of the deposit respectively were analysed.

7.1.1.3 Eagle Cave Flowstone

The first flowstone deposit obtained from this cave was collected by Mr. G. McKechnan then of the University of Calgary. The precise location of the sample was not described. A second sample was collected by Dr. Ford after analysis of the first sample gave unexpected results. The flowstone is similar in appearance to the Coulthard sample. It is 3.8 cm thick, crystalline throughout and red coloured. Some layering is visible but no depositional hiatus is apparent within the flowstone layer. The upper and lower surface of the deposit was contaminated with clayey detritus but this was removed with an acid wash before analysis.

7.1.1.4 Yorkshire Pot Samples

A suite of samples was collected by the author from this cave but only one was analysed as part of the regional survey. A wide variety of relatively small stalagmites and stalactites are to be found in this cave ranging from ultra-pure white calcites to deep red-coloured deposits. The stalagmite chosen for analysis was one of many small broken ones, possibly the result of tectonic activity. It was 10 cm high, very

pure and had grown as a single crystal; the top 5 cm section was chosen for analysis.

7.1.1.5 Gargantua Cave Samples

A number of speleothems were collected from this cave by the author and Dr. D.C. Ford. Again, only one was chosen for analysis and this was a portion of a layered stalactite 7.3 cm in diameter and 10 cm long with a white central portion and a red coloured outer portion. The white central portion was drilled out of the sample and analysed.

7.1.2 Results

Table 7.1 is a summary of the results of this preliminary sampling programme. Little opportunity existed for sampling present-day drip-waters currently depositing calcite but the Crowsnest Spring, a large resurgence in the Crowsnest Pass, was taken as representative of present-day groundwater and a number of U^{234}/U^{238} analyses were carried out to obtain present-day values. These results are incorporated into Table 7.1.

It was confirmed that these deposits were suitable for dating. In most of the samples Th^{232} was almost entirely absent. Middle Sentry Cave is an exception. The presence of non-authigenic Th^{230} in speleothems of the Crowsnest Pass Area could not be checked for since a modern stalagmite was not available for analysis. However, none of the spring waters contained measurable Th^{230} or Th^{232} , and a stalagmite inferred to be "recent" from Castleguard Cave near the Columbia Icefields, Banff National Park, gave an age of 4300 ± 200 yrs (CG1 in Table 7.1). This is rather indirect evidence that initial Th^{230} in the Crowsnest region speleothems

Table 7.1

Analysis of Crowsnest Area Speleothems (Southern Alberta)

Sample	Cave	Insoluble Residue %	(U) p.p.m.	$\frac{[U-234]}{[U-238]}$	$\frac{[U-234]}{[U-228]}$	$\frac{[Th-230]}{[U-234]}$	$\frac{[Th-230]}{[Th-232]}$	Age
CT1	Coulthard Cave	-	0.23	1.00±0.02	1.01±0.03	0.862±0.026	99	235,000±19500
CT2	Coulthard Cave	-	0.25	1.07±0.02	1.16±0.06	0.925±0.029	162	296,000±32500
E1A	Eagle Cave	-	0.33	1.15±0.02	>1.40	0.976±0.026	304	>300,000
E1B	Eagle Cave	-	0.53	1.18±0.02	>1.40	1.06±0.027	300	>300,000
E2	Eagle Cave	-	0.28	1.40±0.02	1.70±0.06	0.869±0.026	46	198,000±13000
MS1	Middle Sentry	0.95	0.12	1.10±0.03	1.14±0.04	0.636±0.025 0.595±0.024	10	114,000±7000 102,500±6000*
MS2	Middle Sentry	0.14	0.07	1.07±0.04	1.12±0.06	0.818±0.032 0.808±0.032	24	197,000±17500 191,000±16500*
MS3	Middle Sentry	0.075		0.97±0.03	0.93±0.05	0.873±0.038	18	273,000±37000
YP1	Yorkshire Pot	-	3.13	1.21±0.015	1.32±0.03	0.756±0.028	402	178,000±10500
GAR1	Gargantua Cave	-	3.73	1.07±0.015	>1.21	0.993±0.016	141	>300,000
CG1	Castleguard Cave	-	3.19	1.21±0.014	1.22±0.014	0.034±0.001	64	4,000±200

* corrected for non-authigenic Th^{230} ; assumes $(Th^{230}/Th^{232})_0 = 1.7$

is insignificant.

$(U^{234}/U^{238})_0$ ratios of the speleothems are uniformly somewhat lower than those measured in West Virginia, though the Crowsnest Spring has a high present-day initial ratio. The flowstone sample collected from Eagle Cave by Dr. Ford (E2) situated 300 feet above the spring, gives a $(U^{234}/U^{238})_0$ ratio of 1.70 ± 0.06 . The sample of flowstone (E1) collected from Eagle Cave by G. McKechnan yielded an age of >300,000 years. The isotopic data for the two samples are not compatible because only one flowstone layer is present in the cave. No depositional hiatus was evident in the flowstone so it was assumed that the layer represented one depositional event. The entire thickness of each sample was used in the analyses so each analysis should have given the same age. However, the data for E1A and E1B are internally consistent. These results must remain unexplained at present because the relative locations of the samples are not known. These results offer quite a problem if geomorphic rates of erosion are considered. Since Eagle Cave must have been above the water table for deposition to have occurred and since the cave is at present 300 feet above the lake level, then the valley floor was lowered no more than 300 feet in a minimum of 300,000 years if the McKechnan sample is accepted as authentic and as yielding reliable ages. A maximum rate of $30.5 \text{ cm}/10^3$ years is calculated using these data and a maximum rate of $44 \text{ cm}/10^3$ years using the data of the second analysis (E2). These rates are much lower than those proposed by geomorphologists studying present-day erosion rates.

The Coulthard Cave analyses represent two distinct periods of

deposition. The Coulthard stalactite U^{234}/U^{238} ratios do not support a constant ratio in the percolation water at one drip site, but the Eagle Cave sample E1 and the upper part of the Middle Sentry Flowstone do support a reasonably constant U^{234}/U^{238} ratio at each drip site. However, none of these ratios are comparable to the high present-day ratio of the Crowsnest Spring.

The Middle Sentry Cave Flowstone was the only deposit found to contain detrital Th. The rather dubious assumption that $(Th^{230}/Th^{232})_0 = 1.7$ was made and the ages obtained corrected for non-authigenic Th^{230} . The possibility must be considered that in each analysis an incorrect age was measured. The insoluble residue may 1) contribute detrital U by leaching or 2) preferentially adsorb daughter Th^{230} released from the dissolution of the sample. The immense period of deposition (170,000 years maximum) is a little difficult to accept because deposition was apparently continuous and therefore a growth rate of $0.09 \text{ cm}/10^3 \text{ years}$ is calculated and deposition would have been continuous throughout at least one major glacial period (the Illinoian). However, since little is known of the rate of growth of alpine cave flowstone deposits and the manifestation of depositional hiatuses the ages should not be dismissed on these grounds, but should be accepted with caution.

The Yorkshire Pot stalagmite and Gargantua stalactite are single analyses and as such should also be cautiously accepted. As a general rule two or more ages for a single stalagmite should be determined and should be internally consistent. The Gargantua age determination does apparently confirm the fossil nature of this high cave.

7.2 The Nahanni Region, N.W.T.

A suite of speleothem samples was collected by Dr. D.C. Ford during a recent visit to the caves of the Nahanni region. Figure 7.2 shows the location of the caves sampled (Grotte Valerie and Trou Claudette). The results of some preliminary analyses are summarised in Table 7.2. On the basis of these results and the available geomorphic evidence Ford (in press) has attempted to interpret the tectonic history of the region. The caves contain numerous small deposits and some large flowstone deposits. Most are inactive but some speleothem deposition is currently taking place. The caves were inferred by Dr. Ford to be very old because they sit between 600 and 1400 feet above the river and are now mostly fossil. The measured ages of the samples supports this hypothesis. A supposedly modern sample was verified by the isotopic data as being very recent. The remaining deposits represent phases of deposition broadly comparable with some of those of the Southern Canadian Rockies.

One of the large flowstone deposits from Grotte Valerie was sampled and was seen to consist of at least two distinct flowstone layers which could be easily separated. The top of the outer layer had undergone solutional erosion. A stalactite from Trou Claudette had also undergone severe re-solution. According to the geomorphic evidence Ford (in press) inferred that this major phase of speleothem deposition was succeeded by an intense erosional phase then another minor depositional phase.

All of the samples except NGV-4 and NTC-1 were deeply coloured;

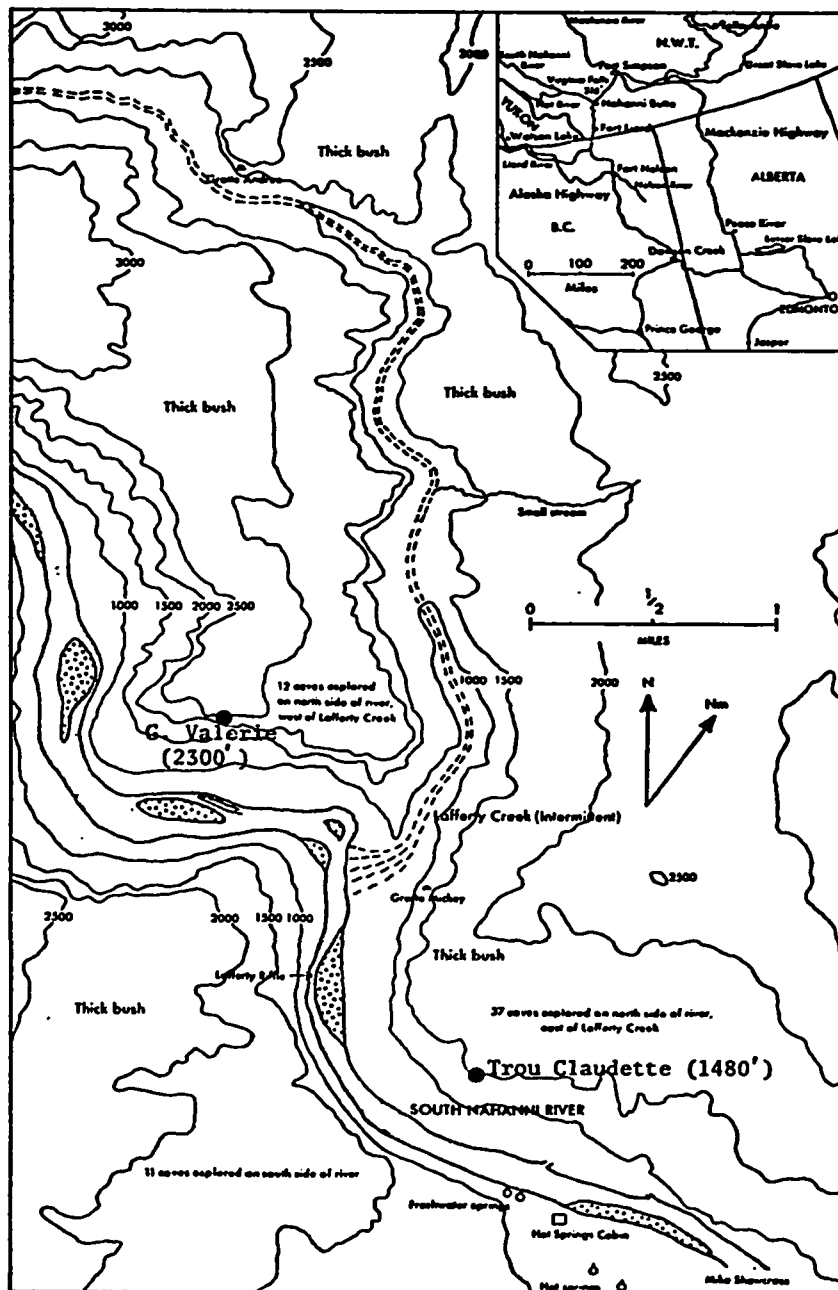


Figure 7.2 Map of the Nahanni Region Showing the Location of the two Caves Studied.

Table 7.2

Analysis of Speleothems from the Nahanni Region

Sample	(U) p.p.m.	$\left[\frac{U-234}{U-238}\right]$	$\left[\frac{U-234}{U-238}\right]_0$	$\left[\frac{Th-230}{U-234}\right]$	$\frac{Th-227}{Th-230}^*$	$\left[\frac{Th-230}{Th-232}\right]$	Age Years B.P.
NGV-1, base of inner sheath	4.31	0.98 ±0.01	0.96 ±0.02	0.975 ±0.085	1.0 ±0.1	>1000	290,000 ^{+∞} -50,000
NGV-2, base of outer sheath	17.9	1.01 ±0.005	1.017 ±0.006	0.84 ±0.03	-	450	200,000±20,000
NGV-3, top of outer sheath	12.9	1.045 ±0.006	1.082 ±0.007	0.85 ±0.025	1.04 ±0.06	300	217,000±17,000
NGV-4, modern, fallen stalac- tite, 30 cm long	32.6	0.97 ±0.01	-	0.01	-	26	<2,000
NTC-1, severely re-dissolved stalactite	7.6	0.99 ±0.01	-	0.96 ±0.02	-	250	275,000 ^{+75,000} -35,000

* Th-227/Th-230 ratio is expressed as a uranium equivalent ratio (=21.7 x activity ratio)

NGV = samples from Grotte Valerie, NTC = sample from Trou Claudette.

again the colouration was attributed to Mn^{2+} and Fe^{3+} . White and coloured calcite layers showed cyclic variation within the samples but the coloured layers were consistently thicker. These speleothems had very high U content, considering the average of all previous analyses. Because of the high uranium contents an attempt was made to obtain Pa^{231}/Th^{230} ages of two of the samples by measuring the Th^{227}/Th^{230} ratio. In both analyses the activity ratio was, within the limits of experimental error, equal to that predicted by secular equilibrium. This is good evidence that these stalagmites have remained a closed system since deposition. The age of the Trou Claudette sample was not checked by this means and, as a single analysis, must be cautiously accepted. The stalactite had suffered severe re-resolution but the portion analysed was massively crystalline and appeared to be unaltered.

The U^{234}/U^{238} isotope ratio of some of these samples are atypical in that the initial ratios appear to be less than unity. There is obviously no application here for the excess U^{234} dating method, and the near-unity ratio precludes the use of a deficient- U^{234} method. It is possible that in this situation a soluble uranium-containing mineral is being dissolved rather than leached by the acid karst waters. U^{4+} in an old mineral will have a U^{234}/U^{238} ratio less than 1.0. U^{4+} is not normally mobile (it is chemically similar to Th^{4+}) but if the mineral containing U were dissolved, U^{4+} may be released and oxidised to U^{6+} (as UO_2^{2+}) which is very soluble. Some U^{4+} may be transported to the cave depending on the kinetics of the oxidation process. This might explain the high U concentrations since U^{4+} ($r = .0.99\bar{8}$) and Ca^{2+} ($r =$

0.95Å) have similar ionic radii and U^{4+} will therefore be fairly easily accommodated in the $CaCO_3$ lattice. The UO_2^{2+} ion with its awkward shape is presumably less easily accommodated. This conclusion is supported by the study of Kolodny and Kaplan (1970) who showed that U^{4+} is preferentially incorporated into phosphorites (presumably substituting for the Ca^{2+} ion).

7.3 Periods of Speleothem Deposition in the Canadian Rockies and N.W.T.

In Figure 7.3 the measured ages of all the Western Canadian speleothems have been plotted in an attempt to identify widespread phases of deposition. The Middle Sentry Cave data has been omitted because of the doubtful analyses. An extensive period of non-deposition and, at least in the N.W.T., fluvial erosion within the caves (Ford, 1972) has been identified in Grotte Valerie and Coulthard Cave. It is assumed here that both caves recorded the same event. The remainder of the data can be split into at least two periods of deposition, one occurring before (from approximately 270,000 to >300,000 years) and one after (from 170,000 to 240,000 years) the erosional phase. It is quite possible that these phases will be sub-divided when more data is available.

It can be stated with some confidence that these speleothems date periods of interglacial climate. During periods of glacial climate it is quite unlikely that water can percolate into the caves because even now cave temperatures in the Crowsnest region are between 3 and 5°C and in the N.W.T. cave temperatures are close to 0°C. With a small drop in mean annual temperature water will freeze before entering the caves.

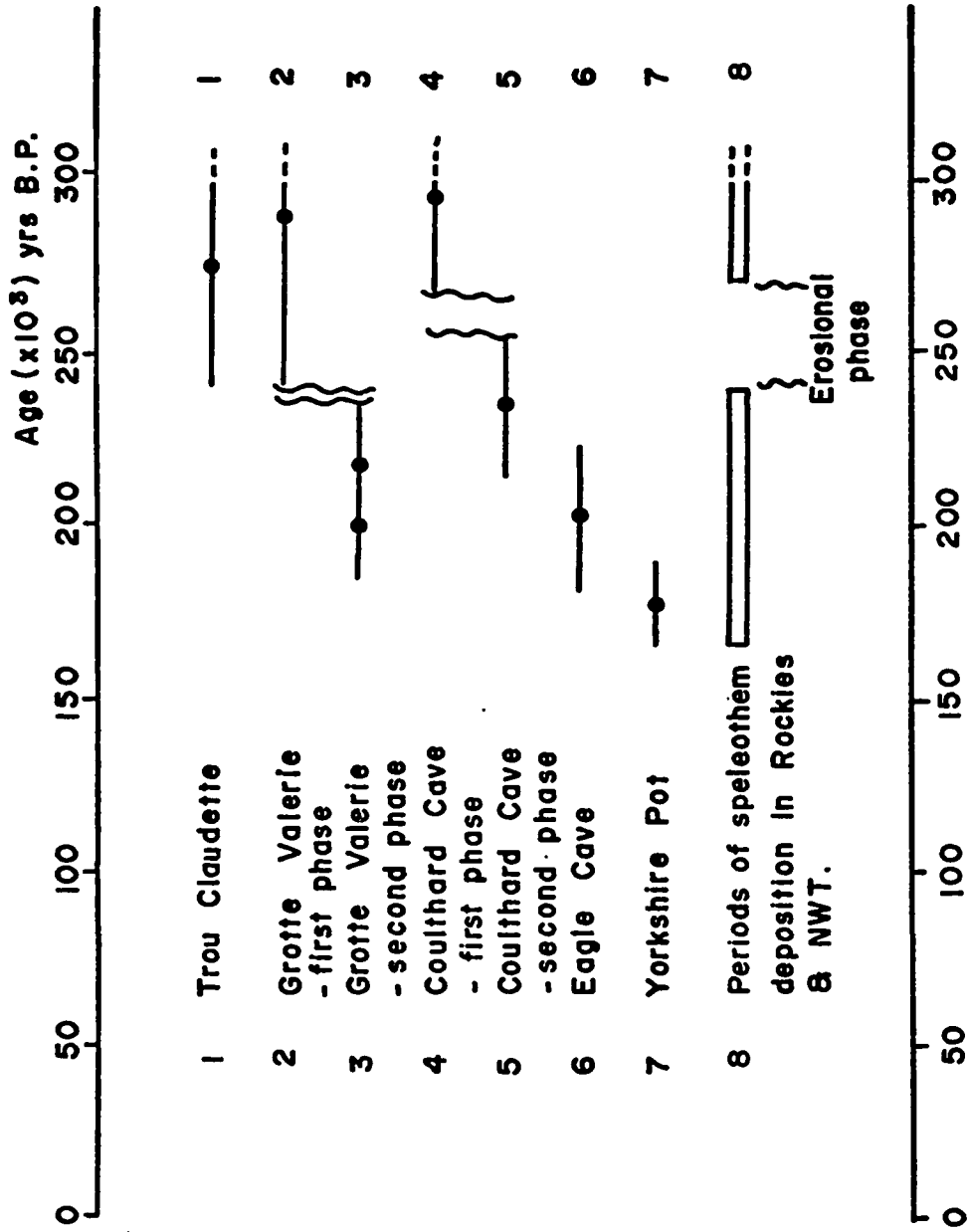


Figure 7.3 Approximate periods of speleothem deposition (equivalent to interglacials) in W. Canada.

(Note: this does not preclude all water entering the caves, only that water which enters the rock slowly and is in intimate contact with the rock will be frozen). Thus, interglacial conditions appear to have lasted from approximately 170,000 to 240,000 years B.P. and from 270,000 to >300,000 years B.P. These interglacial periods were probably interrupted by relatively short periods of cold climate.

There is little evidence for extensive speleothem deposition during the penultimate interglacial period (the Sangamon) especially in the N.W.T. This seems to indicate that Sangamonian climate was somewhat colder (or drier) in these regions than at present and during the previous interglacial period. This observation needs verification by further, more extensive sampling.

Some recent K-Ar ages of pumice and rhyolite flows have enabled limits to be placed on glacial/interglacial episodes in the Rocky Mountains of the U.S.A. (Richmond, 1970). These should be broadly comparable with equivalent episodes in the Canadian Rockies and N.W.T. An age of 290,000 years was obtained for a rhyolite pumice from Yellowstone National Park which covered a Sacagawea Ridge moraine (this glacial period is considered to be equivalent to the Illinoian of the mid-continental U.S.A.). Interglacial deposits representing the "Last Great Interglacial" lie between a pumice 180,000 years old and a rhyolite flow between 121,000 and 128,000 years old. The younger flow is overlain by glacial deposits. A earlier advance of the Sacagawea Ridge glacier may have taken place between 290,000 and 180,000 years B.P. These results are compatible with the glacial/interglacial episodes inferred from the speleothem data. The majority of the speleothems

appear to post-date the older Sacagawea Ridge glaciation and a second glacial advance is apparently confirmed by the erosional phase (Figure 7.3) approximately 250,000 years ago. The next interglacial period, based on the speleothem data appears to have started between 200,000 and 240,000 years ago, somewhat earlier than proposed by Richmond. However, the author does not disclose the nature of the deposits which underlie the 180,000 year old pumice, so the only firm conclusion that can be inferred from the K-Ar ages is that the Sacagawea Ridge interglacial (considered to be equivalent to the Sangamon) started between 290,000 and 180,000 years B.P.

At the moment insufficient data is available to permit detailed comparisons between the various regions, but such comparisons may offer valuable checks on both the K-Ar and U-series dating methods.

7.4 The Ciudad Valles Area, San Luis Potosi, Mexico

Ciudad Valles lies on the El Abra limestone range which is part of the Sierra Madre Oriental. The range runs north-south, roughly parallel to and 80 km inland from the east coast of Mexico. Many caves are developed in the pure El Abra limestone, some containing abundant speleothems. A stalagmite from Cueva de Tinaja was chosen for analysis. This sample was collected by John Fish, Dr. Ford, and the author during a visit to the El Abra caves in June 1971.

7.4.1. Tinaja Stalagmite, MT1

The stalagmite was of constant diameter (approximately 7.6 cm) and 78 cm long. It was deposited on sediments approximately 3 m above the cave floor. It had fallen over and broken in three pieces. A thin,

brown-black coating on the surface of the stalagmite and on the surface exposed when it fractured indicated that it had repeatedly been submerged by flood waters or even buried under further sediments and re-exposed. The two pieces were lightly cemented to the cave fill.

Each section was cut along its length and a large number of growth lines and cavities exposed. The growth lines were very closely and evenly spaced. They numbered approximately 10 per cm. Along the axis of the stalagmite were dozens of small solutional cavities some lined with the remains of calcareous organisms whilst others were filled with a black residue which was presumably soil washed down from above the cave. None of the cavities appeared to be interconnected. The whole stalagmite was tinted red. Part of the colour was attributed to Mn^{2+} which was positively identified by the permanganate spot test. The results of three analyses are reported in Table 7.3. The growth rate was approximately constant at $2 \text{ cm}/10^3 \text{ years}$ and is broadly comparable with rates in West Virginia during periods of warm climate. Based on this rate deposition started approximately 50,000 years B.P. The majority of this period corresponds to glacial conditions in the Northern Hemisphere so it is apparent that speleothem deposition is not significantly affected by glacial/interglacial climate changes.

It is interesting that the U^{234}/U^{238} ratio is approximately unity in this stalagmite; apparently no selective leaching of U^{234} has taken place above the cave. The uniform U^{234}/U^{238} ratio and the sequential ages obtained is strong evidence that the stalagmite remained a closed system despite localised re-solution in most parts of the stalagmite. Further analyses of Mexican cave samples would be very rewarding because

Table 7.3

Analysis of the Tinaja Stalagmite, Ciudad Valles, S.L.P., Mexico

Sample	Height above base (cm)	(U) p.p.m.	$\left[\frac{U-234}{U-238} \right]_0$	$\left[\frac{Th-230}{U-234} \right]$	$\left[\frac{Th-230}{Th-232} \right]$	Age Years B.P.	
MT-1	76	2.53	.963±.017	.962±.017	.073±.003	94	8200 ± 400
MT-2	52	2.37	.994±.011	.994±.012	.173±.004	87	20,600 ± 500
MT-3	20	1.99	.992±.017	.991±.021	.285±.004	70	37,000 ± 900

a continuous record of speleothem deposition and Pleistocene climate change may be recorded.

CHAPTER EIGHT

DISCUSSION OF THE EXPERIMENTAL RESULTS

8.1 Appraisal of the Dating Methods

The results of the dating study will be summarized in this section and the suitability of speleothems for U-series disequilibrium dating discussed.

8.1.1 Appraisal of the $\text{Th}^{230}/\text{U}^{234}$ Method (Deficient Ionium Method)

Two of the objects of this appraisal were:

1) to assess the reliability of the $\text{Th}^{230}/\text{U}^{234}$ dating method for speleothems and 2) to check the assumption that all Th^{230} extracted from a speleothem sample was authigenic.

The $\text{Th}^{230}/\text{U}^{234}$ ratio should increase exponentially from top to bottom of a stalagmite deposited at a constant rate. In this study no stalagmites were found which grew at a constant rate but, in general, $\text{Th}^{230}/\text{U}^{234}$ ratio in the stalagmites studied did increase in an irregular manner from top to bottom. The recent stalagmites analysed (NB2, NB11, NGV3, CG1) did contain no appreciable Th^{230} . NB2, however, contained measurable Th^{232} activity so it is probable that the majority of the measured Th^{230} activity was from non-authigenic Th. The small contribution of authigenic Th^{230} is due to low U content of the sample. Young speleothems cannot be accurately dated given these conditions. The detrital Th component would become less significant in older samples. The detrital Th component in NB11 was very low. This,

coupled with a high U content allowed accurate ages to be measured in spite of its youth. The internal consistency of the results for NB11 is strong support for the assumption that, given pure CaCO_3 , all of the Th^{230} is authigenic.

The possibility that the chemical treatment of the sample leaches Th (or U) from detrital particles (eg. resistate minerals, clays) must be considered. The experiments described in section 5.12 indicate that U is more easily leached from detrital material than Th when 1N HCl is used to dissolve the sample. U^{234} appears to be more easily leached than U^{238} which is to be expected because exactly the same happens in subaerial weathering. The extent of leaching will be a function of pH, eH, temperature, U/Th, U(IV)/U(VI) and the age of the sediment so it would be very difficult to predict the effect of leaching on the measured age of a sample. Under the conditions of the experiment described in section 5.12 leaching resulted in apparently young $\text{Th}^{230}/\text{U}^{234}$ ages. Consequently, only CaCO_3 containing very little (or preferably no) detritus, can be considered suitable material for $\text{Th}^{230}/\text{U}^{234}$ dating. Fortunately, this type of deposit is abundant in most caves.

A special circumstance must be considered when the absence of a Th^{232} peak in the Th alpha spectrum cannot be taken as sufficient indication that all Th^{230} is authigenic. This may occur when a resistate mineral rich in U but with a very low Th content is present as a detrital phase (eg. some zircons and apatites). The relative leaching effect would probably be $\text{U}^{234} > \text{U}^{238} > \text{Th}^{230}$. Leaching of this detrital component would result in a high measured $\text{U}^{234}/\text{U}^{238}$ ratio (which

would probably be attributed to changes in the U^{234}/U^{238} ratio in the parent waters when terrestrial carbonates are analysed) and a low Th^{230}/U^{234} ratio. This contamination would be impossible to detect and is further reason for analysing only pure carbonates.

8.1.2 Appraisal of the U^{234}/U^{238} Method (Excess U^{234} Method)

The appraisal of the excess U^{234} method to date speleothems remains inconclusive. Some analyses, in particular NB1, NB10 and GV2 indicate that U^{234}/U^{238} ratios in parent waters are reasonably constant over long periods of time. Other analyses indicate that wide variations at one site (NB4) can occur over a relatively short period of time and recent stalagmites (NB2 and NB11) in the same cave have constant, but quite different U^{234}/U^{238} ratios.

There appears to be no correlation between the U^{234}/U^{238} ratio in cave drip-waters and the U^{234}/U^{238} ratio in $CaCO_3$ deposited from these waters. This may simply reflect an insufficient number of water analyses but there remains the possibility that the uranium species in solution are different in isotopic abundance and composition than those deposited in the $CaCO_3$. This aspect deserves further investigation.

Clearly, the U^{234}/U^{238} dating method cannot be used unless there is some support for the assumption that the U^{234}/U^{238} ratio remained constant over the period of deposition and that this ratio can be estimated today. Figure 8.1(a) and (b) is a graphical summary of all initial U^{234}/U^{238} ratios versus time. The initial Grapevine cave ratios indicate that a decrease in this ratio occurred between

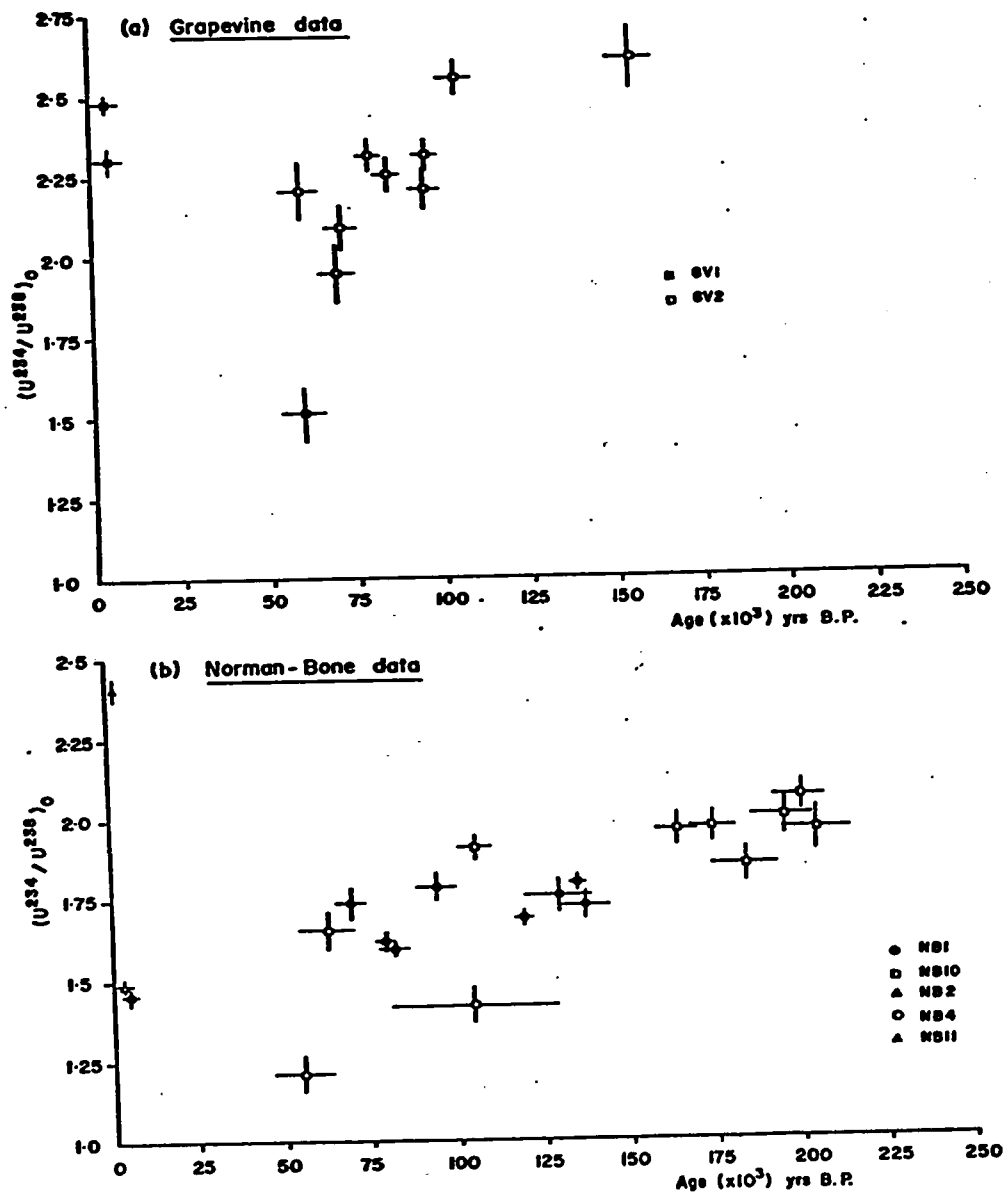


Figure 8.1 Initial $^{234}\text{U}/^{238}\text{U}$ ratios (calculated from the $\text{Th}^{230}/\text{U}^{234}$ age) of (a) Grapevine Cave samples and (b) Norman-Bone Cave samples, plotted against $\text{Th}^{230}/\text{U}^{234}$ age of the samples.

160,000 and 60,000 years B.P. The trend is apparent also in the Norman-Bone Cave data, and as is shown in the next section the lower initial U^{234}/U^{238} ratios are associated with lower U concentrations in the Norman-Bone speleothems. This may be due to a reduction in the amount of uranium available for leaching as soils become more mature and the thickness of limestone above the cave decreases. This does not bode well for the excess U^{234} dating method but from the West Virginia data available the initial U^{234}/U^{238} ratio can be estimated within wide limits. A lower limit for this ratio appears to be about 1.5, and this is close to the single value obtained for Bone Cave water. An upper limit for the same ratio appears to be about 2.5. The average initial ratio is therefore close to 2.0

Only two stalagmites (NB3 and NB12) in West Virginia were found for which the Th^{230}/U^{234} ratio was unity. The decay of excess- U^{234} cannot be applied to NB3 because the measured U^{234}/U^{238} variations increase from top to bottom of the stalagmite indicating that a change in the isotopic composition of the parent water occurred. However, an attempt can be made to assign an age limit to NB12. Using an initial ratio of 2.0 the age of the top is calculated to be 760,000 $\begin{matrix} +140,000 \\ -290,000 \end{matrix}$ years B.P. and the base is 1,250,000 $\begin{matrix} +160,000 \\ -280,000 \end{matrix}$ years old in agreement with a thorium age of >300,000 years. These calculations cannot be refined until initial ratios are known with more precision. Thompson (personal communication) used the decay of excess U^{234} to date a stalagmite from Blanchard Springs Cavern, Missouri.

An almost exponential decrease in U^{234}/U^{238} ratios along the length of the stalagmite was measured indicating both a constant growth rate and constant initial U^{234}/U^{238} ratio. Using an initial ratio of 1.56, the average of neighbouring drip-waters, ages of 800,000 \pm 48,000 years and 148,000 \pm 28,000 years were calculated for the base and top of the deposit respectively. A hiatus in deposition apparently occurred between approximately 400,000 and 500,000 years ago. When account is taken of this hiatus, an average growth rate of 0.1 cm/10³ years is calculated which is an order of magnitude lower than growth rates of West Virginia stalagmites of similar dimensions. Unfortunately the Th^{230}/U^{234} ratios showed no systematic variations from layer to layer and was attributed to open system conditions which did not, however, affect the U^{234}/U^{238} ratio.

8.1.3 Appraisal of the Th^{227}/Th^{230} (Pa^{231}/Th^{230}) Method

(Deficient Protactinium Method)

The Th^{227}/Th^{230} ratio, an independent measure of the age of a speleothem, relies upon the assumption that (a) Th^{227} activity is a direct measure of Pa^{231} activity and (b) no Pa^{231} was initially present in the sample. These assumptions were not rigorously tested but some preliminary analyses indicate that they are valid. In only a very few instances could the Th^{227} activity be measured because low U contents usually precluded accurate results. In the four samples for which the Th^{227}/Th^{230} age could be compared to the Th^{230}/U^{234} age (NB10-1b, NB12-2, NGV2 and NGV3) the results were compatible. This method will probably not be generally applicable to speleothem

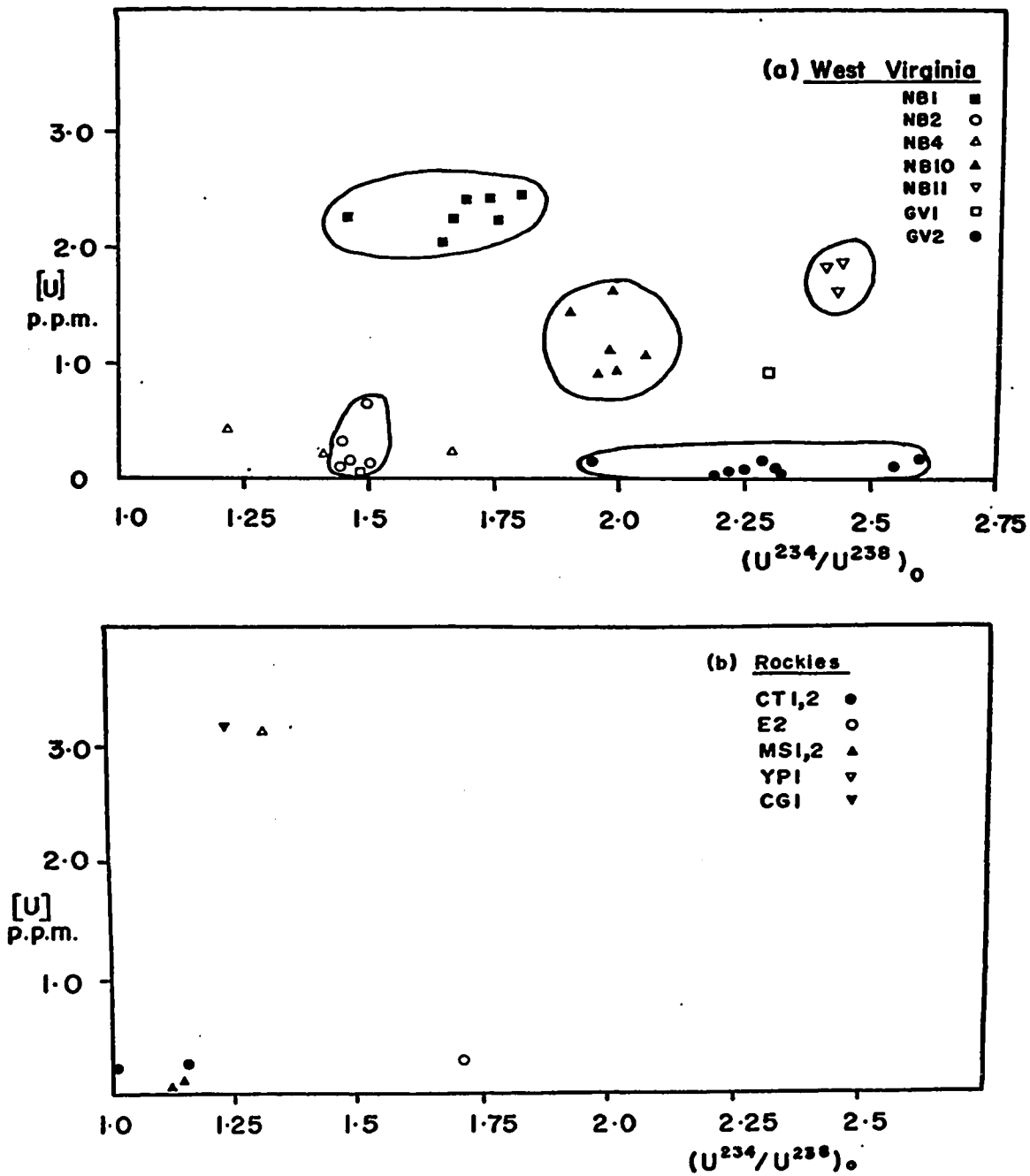


Figure 8.2 Initial U^{234}/U^{238} ratios (calculated from the Th^{230}/U^{234} age) plotted against U content of speleothems from (a) West Virginia and (b) the Canadian Rockies.

dating because of the very low levels of activity involved. When abundant amounts of sample with a U-content 2-3 p.p.m. are available accurate results should be obtainable and should offer a valuable check on the $\text{Th}^{230}/\text{U}^{234}$ age.

8.2 Relation Between Uranium Concentration and Initial $\text{U}^{234}/\text{U}^{238}$ Ratios in Speleothems

In Figure 8.2 (a) the uranium concentration (U) for each West Virginia sample is plotted against the initial $\text{U}^{234}/\text{U}^{238}$ ratio. The same parameters are plotted in Figure 8.2 (b) for the Rockies samples. In general, the (U) and $\text{U}^{234}/\text{U}^{238}$ of each speleothem varies over a quite narrow range, with the exception of NB4 and GV1.

Intuitively, one would expect the waters with lower (U) to exhibit the highest $\text{U}^{234}/\text{U}^{238}$ ratios because the effects of preferential leaching are gradually masked as uranium, of near unity $\text{U}^{234}/\text{U}^{238}$ ratio, is dissolved. If it is assumed that the distribution coefficient between carbonate and water is reasonably constant then the speleothem too should record a high $\text{U}^{234}/\text{U}^{238}$ ratio when the (U) is low. However, there is no clear negative correlation between (U) and $(\text{U}^{234}/\text{U}^{238})_0$ for the West Virginia speleothems. The chemical composition of the solute, the $\text{U}^{4+}/\text{U}^{6+}$ and U isotopic composition of the materials being leached will modify any simple general relationship between (U) and $(\text{U}^{234}/\text{U}^{238})_0$ in the parent waters of a given area. However, it does appear that the uranium content and uranium isotopic composition at each site within a cave is reasonably constant.

A wide range of (U) values at a single site, such as those observed for NB4 and GV1 may indicate that post-depositional leaching or assimilation of U has occurred. At this point, though, it would be premature to conclude that all West Virginia speleothems must show such constant U content and U isotopic composition. If this were shown to be the case then this relationship would be a valuable diagnostic tool in verifying the closed system assumption and in applying the excess U²³⁴ dating method.

8.3 Anomalous Results

Anomalous ages which could not be accounted for by statistical error were obtained for some speleothems from West Virginia. Those samples not showing internally consistent results (NB3, NB4, NB5, NB9 and part of GV2) can be divided into two groups: (a) those with low U content and/or an appreciable detrital component and (b) those with relatively high U content and/or no detrital component. The error in the former group may be attributed to systematic errors in the extraction procedure. For example, airborne contamination or leaching of occluded detritus could account for the discrepancies in NB3, NB4 and GV2-2. The error in (the latter) group (b) cannot be readily attributed to experimental error. This probably indicates that some assumptions basic to the principle of the dating method, are not satisfied by these samples. Stalagmites NB5 and NB9 definitely fall into this group. Both stalagmites were quite pure and little Th²³² activity was observed in the thorium spectrum, so a detrital Th²³⁰ component is ruled out. In this case,

therefore, the validity of the closed system assumption must be questioned.

Because the top of each stalagmite was apparently older than the base either U addition near the base could have occurred or U could have been leached from near the top. However, the relatively constant U concentrations in NB5, at least, do not support this unless the original U concentrations varied over a large range.

The relative ages of the upper sections of NB5 (NB5-19 to 22) are acceptable but the ages of the lower sections of NB5 (NB5-1 to -10) are unacceptable because they imply a very rapid rate of accretion. It has consistently been shown that this type of deposit grows slowly. It is possible that the two speleothems were partly submerged when water flooded the Butterscotch Room. This is supported by the fact that the nodular concretions on the surface of the lower part of each stalagmite are ususally found on deposits which have been (or are) submerged in waters saturated with CaCO_3 . It is possible that this water was able to permeate into each deposit causing the system to become open. The net effect of open system conditions apparently resulted in low measured ages due either to (a) net loss of Th^{230} or (b) net addition of U^{234} . With the available data it is not possible to distinguish between these two mechanisms.

Other anomalous speleothem ages reported by Rosholt and Antal (1962) and Cherdyntsev (1971) were attributed to U leaching but a low age determination precludes this (unless more Th^{230} than U^{234} is leached, which is unlikely). Some Th^{230} may be lost because

it will be present strictly as a recoil atom and therefore in a damaged site and susceptible to leaching. Both U^{234} and U^{238} will initially be in undamaged sites but with increasing age of the system more of the U^{234} atoms will occupy radiation damaged sites and will be susceptible to leaching. At the pH of cave waters (8.0-9.0) Th should be immobilised as the hydroxide but it is possible that the minute amounts of Th^{230} involved may be transported on the surface of colloidal-size particles. If leaching of U and Th from a deposit does occur it is possible that the U^{234}/U^{238} ratio will be a more reliable indication of age because little U-isotopic fractionation is expected in a young ($<10^5$ years) sample. This assumes that U^{234}/U^{238} ratios in the parent waters were relatively constant. If net addition of U takes place then no age information can be obtained.

The amount of leaching of U or Th that can take place inside a deposit should increase with its porosity. Consequently, it is essential that after deposition on a porous speleothem stops it should not subsequently come into contact with appreciable amounts of water, It is usually quite easy to check this requirement by examination of the surface of the deposit. Speleothems with irregular, eroded surfaces or those that show evidence of submersion should be avoided. When deposition on an old speleothem surface starts again by the normal processes of CO_2 loss from the drip water the underlying layers appear to be unaffected. This appears to be the case with NB1 and NB10.

Bearing the above comments in mind, it is interesting to

look at the anomalous results again. All of these results were obtained from speleothems that can be classified into two categories:

- 1) porous deposits or layers and
- 2) submerged deposits.

NB4 and GV2-2 fall into the first category and NB3, NB5 and NB9 into the second. Analysis NB4-C3 appears to be reliable in that the oxygen isotope record agrees with that of GV2, but this could be fortuitous. GVC-1, also a porous deposit, gave puzzling results. However, there still remains the possibility that some of the analyses are due to experimental error. Because of these uncertainties none of the above results are used in the following discussion. The Rockies samples and the Mexican samples all gave apparently acceptable ages. One of the Nahanni samples (NTC-1) did show evidence of an erosional phase so the measured age should be accepted with caution. None of the Rockies or Mexican samples were porous, but the Tinaja stalagmite did contain isolated "worm-holes".

8.4 Criteria for Reliable Speleothem Ages

Based on the results reported in Chapters 6 and 7, a speleothem must meet four criteria before measured ages can be regarded as acceptable.

- 1) The speleothem must contain no appreciable detrital material. As a general rule, speleothem samples containing <1% detritus should be rejected or care should be taken to ensure that no U or Th is leached from the detritus.

- 2) The internal stratigraphy of the speleothem must be preserved to show that no recrystallisation or re-resolution has taken place. No

recrystallised deposits were encountered in this study, but in regions where aragonite speleothems are formed (predominantly in warmer regions than West Virginia) inversion may occur. By analogy with marine carbonates and fresh-water molluscs, the process of recrystallisation in speleothems will result in U loss.

3) The speleothem should be impermeable, i.e. devoid of interconnected cavities. Small (<1 cc) isolated etch pits are evident in most speleothems but this small scale re-solution does not appear to affect U-series age determinations.

4) The surface of the speleothem should be well preserved and should show no signs of large-scale re-solution or submersion. Porous speleothems in particular should be avoided if they show evidence of the above effects.

8.5 Speleothem Deposition as an Indicator of Paleoclimate

It was assumed in Chapter 7 that speleothems deposited at high latitudes are interglacial in origin. There are indications that this is also true in West Virginia. Evidence is obtained by comparing phases of speleothem deposition with phases of coral deposition. The glacio-eustatic theory equates high sea-level with interglacial climate and low sea-level with glacial climate. Well defined periods of coral growth occurred on a world-wide basis during periods of high sea-level; therefore these fossil corals can be used to date periods of warm climate. Coral terraces, corresponding to a specific sea-level stand, can be dated in areas where tectonic uplift has raised the terrace above the present-day mean sea level. The rate of

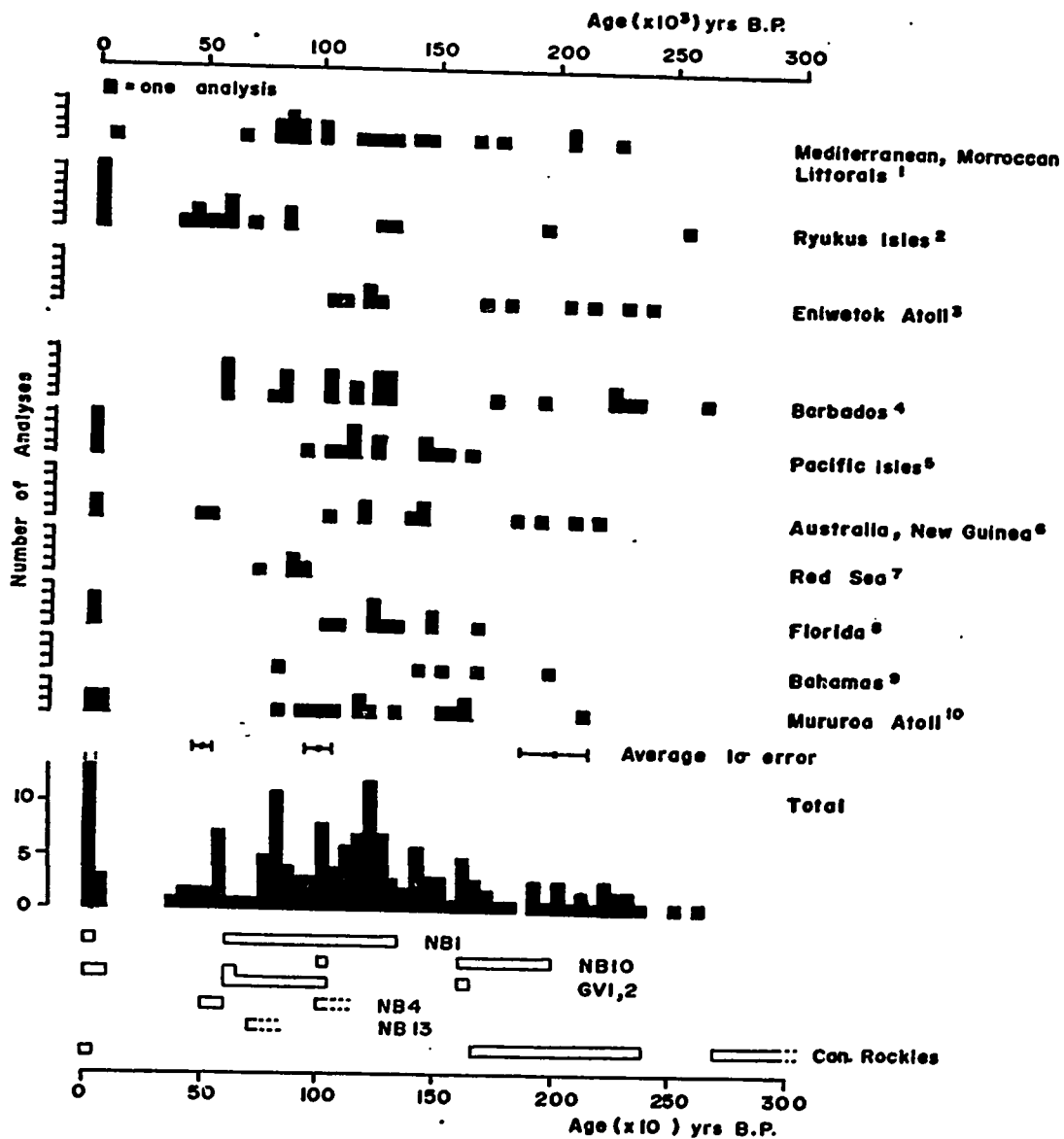
uplift must be sufficiently slow that true eustatic phenomena are recorded.

Corals that are preserved in the aragonitic form are mostly suitable for dating by the $\text{Th}^{230}/\text{U}^{234}$ method. The histograms in Figure 8.3 were compiled from published studies on coral dating. (Some ages obtained for oolites and marine molluscs from raised beaches are included because they give concordant $\text{Pa}^{231}/\text{Th}^{230}$ and $\text{Th}^{230}/\text{U}^{234}$ ages). The coral ages for the most part date high sea-level stands (the Ryukyus and New Guinea are in areas of rapid tectonic uplift and the 40,000 - 60,000 year old terraces actually date periods of relatively low sea level, but interglacial climate). Because of inaccuracies in the dating method the histogram is smoothed-out somewhat but accurate dating of corals from the Barbados suggests that the highest sea-level stands are relatively short-lived. For the last interglacial period these high stands are dated at $82,000 \pm 3000$, $105,000 \pm 5000$ and $125,000 \pm 6000$ years B.P. (Mesollela et. al., 1969). Only the oldest terrace was formed when sea level stood higher than at present (by approximately +2 to +6 meters). The younger terraces were formed when sea level stood approximately 10 - 13 meters below the present level. More recently, a $60,000 \pm 2000$ year old stand has been recognised in the Barbados by James et. al. (1971). A series of higher Barbados levels were formed between 170,000 and 230,000 years B.P.

The period between 60,000 and 125,000 years B.P. broadly correlates with the deposition of NB1. GV2 and parts of GV1, NB10, NB4 and NB13 were also deposited within this interval. NB1, GV2 and NB13

Figure 8.3 A comparison between periods of coral deposition and speleothem deposition.

1. Stearns and Thurber, 1967
2. Konishi et al., 1970
3. Barnes et al., 1956
4. Ku, 1968; Mesollela et al., 1969,
James et al., 1971
5. Veeh, 1966
6. Veeh and Chappell, 1970
7. Veeh and Geigengack, 1970
8. Osmond et al., 1965; Broecker and Thurber, 1965
9. Broecker and Thurber, 1965
10. Labeyrie et al., 1967b



became inactive between about 60,000 and 70,000 years ago. Therefore it seems a marked deterioration of climate occurred during this period. The period between 170,000 and 230,000 years B.P. broadly correlates with the deposition of NB10 and some of the Western Canadian speleothems.

The dearth of coral and speleothem ages between 10,000 and 30,000 years B.P. confirms that (a) this was a glacial period and (b) that speleothem deposition in West Virginia is interrupted during periods of cold climate. Mesollela et al. (1969) interpreted the dearth of coral ages in the Barbados between 130,000 and 170,000 years B.P. to represent the penultimate glacial phase. No speleothems have been found to be active during this period either.

This type of gross interruption of speleothem deposition can only be expected in regions where appreciable glacial/interglacial climate contrast is expected. It has been shown (Section 7.4.1) that in Mexico speleothem deposition was continuous throughout the coldest part of the Wisconsin glaciation. The search for a continuous isotopic climate record should therefore be conducted in a region of stable climate.

8.6 Interpretation of the Oxygen Isotopic Composition of West Virginia Speleothems

Oxygen isotopic abundances were measured in order to detect changes in the Late Pleistocene climate of West Virginia. As noted in Chapter 4, however, to interpret changes in δ_{ct}^O in terms of regional temperature changes, it is necessary to know the changes in the

isotopic composition of waters from which the CaCO_3 was deposited (δ_w^{O}). One may choose to assume that a decrease in temperature consistently depletes meteoric water in O^{18} by 0.7 ‰ per $^{\circ}\text{C}$, as predicted by Dansgaard (1964), but this leads to certain problems. The isotopic composition of modern speleothems (in the West Virginia sample area) is approximately -6.95 ‰ and according to the above assumption CaCO_3 deposited at lower temperatures should be more depleted in O^{18} due to the relatively small (0.24 ‰ per $^{\circ}\text{C}$) effect of temperature on the $\text{ct-H}_2\text{O}$ fractionation factor ($\alpha_{\text{ct-H}_2\text{O}}$). However, deposition of part of the Grapevine Cave flowstone (GV2) took place in a well-documented cooling period between 60,000 and 70,000 years B.P. (evidence for which is presented by Lamb and Woodroffe, 1970) and yet $\delta_{\text{ct}}^{\text{O}}$ increased relative to present $\delta_{\text{ct}}^{\text{O}}$ values. The fluid inclusion analyses and temperature calculations derived from them also indicate that in most cases a temperature decrease is accompanied by the deposition of CaCO_3 more enriched in O^{18} .

It appears that the effect of a decrease in temperature of deposition on the oxygen isotopic composition of speleothems is controlled principally by changes in $\alpha_{\text{ct-H}_2\text{O}}$. However, under certain circumstances it appears that waters entering a cave can become depleted in O^{18} sufficiently to offset the effect of temperature on $\alpha_{\text{ct-H}_2\text{O}}$. Under these circumstances little net change in $\delta_{\text{ct}}^{\text{O}}$ would occur. Parts of stalagmite NB10 show this effect.

If it is assumed that cave drip-waters tend to be enriched in O^{18} during summer months relative to winter months and that CaCO_3 is

deposited predominantly from the enriched waters, the observed isotopic variations can be explained. In fact it was shown in Chapter 4 (Sections 4.8 and 4.9) that modern CaCO_3 is deposited from waters isotopically similar to June and July meteoric precipitation. This is due to a combination of processes. First, the isotopic composition of meteoric precipitation falling as snow will be modified by isotopic fractionation during the process of sublimation. Moser and Stichler (1971) demonstrated that snow only 3 days old became enriched in deuterium by 19% (or approximately 2.4 ‰ in O^{18}) due to sublimation. In addition, much of the winter melt will be lost as surface run-off if the snow pack is impervious. Only a small proportion of the meteoric precipitation is expected to enter the ground-water system during winter, therefore, and that which does will be isotopically enriched in D and O^{18} relative to average winter precipitation and thus biased toward the isotopic composition of summer precipitation.

Second, it has been demonstrated that soil CO_2 levels are lower in winter than in summer (Pitty, 1966, Vilenskii, 1965) due to reduced biotic activity. According to Hendy (1969), if closed system conditions prevail the CO_2 content of the soil air must be maintained above about 1.25% Atm (at 10°C) for CaCO_3 deposition to occur when the percolating water meets the cave atmosphere (assumed to contain 0.03% Atm CO_2). Some measurements of soil CO_2 levels were taken in the vicinity of Norman-Bone Cave during the summer of 1971 using a Drager CO_2 sampler. These varied from 0.98 % Atm to 1.5% Atm with an average of 1.1% Atm (6 samples). If chemical equilibrium were established in

a closed system, CaCO_3 deposition would be marginal even in the summer months based on these measurements. It was hoped that $\delta_{\text{ct}}^{\text{C}}$ values could be used to establish whether the system was open or closed but the evidence was ambiguous. It remains to be shown whether dissolution of limestone in West Virginia takes place in an open or closed system.

It follows from the above arguments that as regional temperatures decrease and snow persists for longer periods each year, speleothem deposition will be from water which is progressively more biased (isotopically) toward summer precipitation. This summer precipitation will be depleted in O^{18} relative to present-day summer precipitation (by 0.7 ‰ according to Dansgaard). It can be argued, therefore, that little change in the isotopic composition of the water from which CaCO_3 is deposited will take place. For, as regional temperatures decrease, the isotopic composition of the water from which CaCO_3 is deposited will be progressively biased toward the mean July value. This mean July value will decrease as temperatures decrease. The two effects will tend to cancel each other and the net effect will be very little change in $\delta_{\text{w}}^{\text{O}}$ at any given drip site, leading to an increase in $\delta_{\text{ct}}^{\text{O}}$ due to the effect of falling temperature on $\alpha_{\text{ct-H}_2\text{O}}$.

An attempt is made to illustrate this argument in Figure 8.4. It is assumed that sinusoidal surface temperature variations of similar intensity to those at present occur as regional temperatures decrease. Cave temperatures are considered to be constant but variations in $\delta_{\text{w}}^{\text{O}}$ of drip-waters entering the cave will occur. These

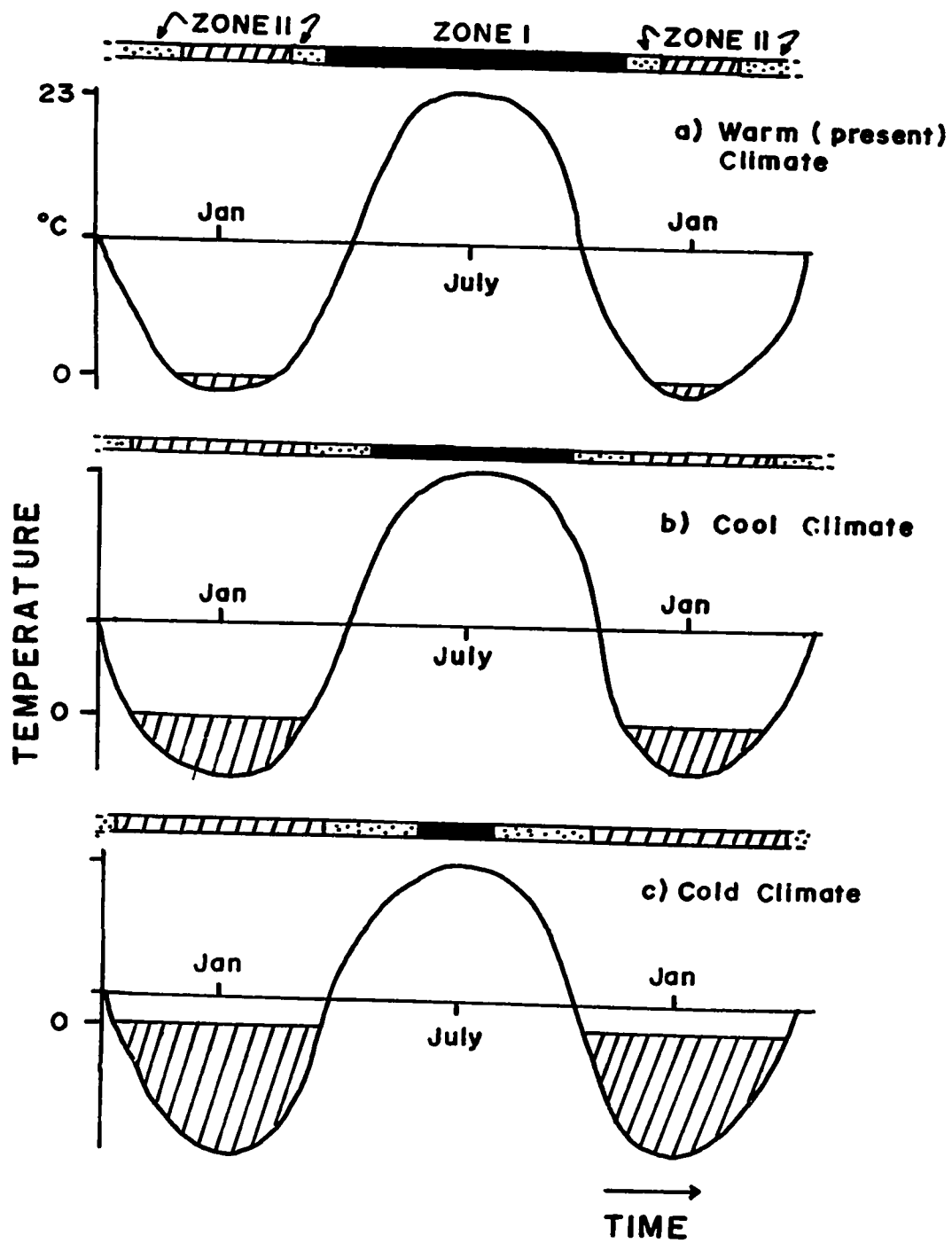


Figure 8.4 Schematic diagram showing the effect of decreasing mean annual temperatures on the seasonal periods of speleothem deposition.

variations will probably be damped and slightly out of phase with the surface variations by an amount which will depend on the residence time of water in the system. The hatched areas under each curve represent periods when waters which entered the ground subsequently deposited little or no CaCO_3 . The solid bars (zone I) indicate periods when speleothem deposition is favoured and the stippled extension (Zone II) to each bar represents periods of limited CaCO_3 deposition. It is necessary to assume that these latter periods increase in length at the expense of Zone I as regional temperatures decrease. The slow recovery of vegetation after a long winter and limited CO_2 production would validate this assumption. A complicating factor in the argument is the seasonal distribution of meteoric precipitation. If this varies as regional climate changes then the relatively simple model described above will be inadequate to describe the $\delta_{\text{ct}}^{\text{O}}$ changes. At the moment this potential complication cannot be assessed.

The above arguments assume that the vadose ground-water system is isotopically and chemically inhomogeneous and infer that flow-through times are relatively rapid. $\delta_{\text{w}}^{\text{O}}$ values for April and July/August drip-waters collected from Norman-Bone Cave support this. The average April drip-water has an isotopic composition of -10.0 ± 0.5 ‰ (4 samples, see Table 4.5) whilst the average July/August drip-water has an isotopic composition of -8.66 ± 0.16 ‰ (5 samples, see Table 4.3). Pitty (1966) demonstrated that 2 drip-sites only a few feet apart in Pooles' Cavern, Derbyshire were of completely

different chemical composition. This is evidence for the isotopic and chemical inhomogeneity of the ground water system. Drew (1968) has used dye to measure flow-through times for meteoric precipitation. He found the time taken for meteoric precipitation to reach a cave through 30 m of bed-rock was quite rapid (within a few days) when water sank into bare limestone but slower (2-3 weeks) when appreciable (30-60 cm) soil cover was present. The thickness and permeability of the soil apparently determines the residence time of vadose water in the system. This residence time will be quite variable from region to region, but in West Virginia, where the caves are relatively shallow and where soil thickness above the caves studied is quite thin, it is expected to be short.

It should be noted that the cave waters do not represent the average annual isotopic composition of meteoric precipitation because of the bias toward summer precipitation described above. It is possible that Dansgaard's Rayleigh Distillation Model does describe the changing isotopic abundance of meteoric precipitation but the temperature effect on δ_w^O of precipitation is irrelevant here; δ_w^O of drip water will vary with temperature in quite a different way than predicted by Dansgaard's model.

When these ideas are applied to other regions consideration must be given to seasonal variations of temperature, precipitation, run-off, ablation, soil and vegetation cover. In regions in which there have been no marked seasonal temperature changes, either now or during the glacial periods, then the model becomes irrelevant because no bias in the isotopic composition of drip waters is possible. In these regions

the former values of δ_w^O will still be difficult to infer unless the Dansgaard Model can be shown to be valid or unless precipitation is a single-stage condensation process of sea-water. Even so, variations in δ^O of the oceans must be taken into account.

8.6.1. Oxygen Isotopic Variations in Grapevine Cave Flowstone, GV2

Evidence is available to show that the lighter δ_{ct}^O values in GV2 are associated with $CaCO_3$ deposited during periods of warm climate. This is deduced from a comparison of the GV2 data with the precisely dated phases of coral deposition in the Barbados. The 60,000, 82,000 and 105,000 year old phases of coral deposition can be approximately correlated with the δ_{ct}^O minima in GV2 at 60,000, 80,000 and 100,000 years B.P. The warm period corresponding to the 125,000 year old high sea-level stand was not recorded in GV2. The most probable explanation of this is that deposition, once interrupted does not readily start again and a considerable period may elapse before the speleothem becomes active again. (NB1, NB4, and NB10 offer further demonstration of this). This may be due to $CaCO_3$ cementation of the orifice supplying water to the speleothem surface. In addition, flowstone can be supplied with water from several sources; therefore the period between 160,000 and 100,000 years B.P. could correspond to the interval between cutting-off of one supply and the opening-up of another.

Steinen et al. (1973) have recently shown that a eustatic low stand of sea level in the Barbados between 125,000 and 105,000 B.P. was associated with an intense glacial event. Part of this event is recorded in GV2 as heavy δ_{ct}^O values in sections GV2-8 and -9 dated at

about $100,000 \pm 3000$ years B.P. This indicates that deposition on GV2 started again during a cold period.

The range in oxygen isotopic composition of GV2 samples is 3.0 ‰ (from -4.0 ‰ to -7.0 ‰, see Figure 6.15). This represents a temperature change of 12.5°C if all the variation in $\delta_{\text{ct}}^{\text{O}}$ is attributed to changes in $\alpha_{\text{ct-H}_2\text{O}}$. Because a change of 12.5°C in cave temperature is unacceptable (present-day temperatures are close to 11°C) a slight change in $\delta_{\text{w}}^{\text{O}}$ to heavier values (compared to the present-day value) must be invoked to explain the total isotopic variation in $\delta_{\text{ct}}^{\text{O}}$.

In principle this can be checked by using the fluid inclusion analyses. At this point it is not known whether the data are reliable or not; especially since half of the GV2 samples gave negative temperatures of deposition. However, GV2-1a, -1b and -3b appear to be warm climate deposits and the average $\delta_{\text{i}}^{\text{O}}$ is -8.06 ‰. GV2-2a is a cold climate deposit but $\delta_{\text{i}}^{\text{O}}$ is -7.65 ‰ (Table 4.6). This supports the above argument and if, as is suspected, the estimated temperature of deposition of GV2-2a is too low the true $\delta_{\text{i}}^{\text{O}}$ of the water from which it was deposited must have been even heavier. More fluid inclusion analyses are required to check the validity of this argument.

In summary, the $\delta_{\text{ct}}^{\text{O}}$ profile of GV2 appears to reflect temperature changes directly, with lighter $\delta_{\text{ct}}^{\text{O}}$ values representing deposition at higher temperatures. $\delta_{\text{ct}}^{\text{O}}$ does not vary linearly with temperature because of small, indeterminate variations in $\delta_{\text{w}}^{\text{O}}$; therefore only general temperature variations are recorded.

8.6.2 Oxygen Isotopic Variations in Norman-Bone Cave Speleothems

Certain similarities between the NB10 and GV2 data exist. For example, when the isotopic temperature of deposition of Grapevine and Norman-Bone Cave samples is approximately equal, and equal to the present-day (isotopic) temperature, δ_i^O is approximately the same. This is illustrated in Table 8.1

Table 8.1
Isotopic Temperature of Deposition and δ_i^O of Warm Climate Speleothems

Sample	Temp. of Deposition (°C)	δ_i^O ‰ w.r.t. SMOW	Age yrs B.P.
average modern stal.*	9.55	-8.40	-
GV1	10.3	-7.95	?
GV2-1a	8.0	-7.78	104,000
NB10-8a	9.2	-7.80	170,000 (approx)
NB10-8b	7.3	-8.16	170,000 "
GV2-3b	7.2	-8.06	160,000
Average	8.6	-8.03	

* from Table 4.3 and including NC6 and NBM-1

These results indicate that, given the present climatic conditions, factors governing the isotopic composition of cave waters have been relatively constant over the last 170,000 years. In

particular it can be noted that NB10-8b and GV2-3b deposited within about 10,000 years of each other show almost identical isotopic variations.

However, interpretation of the Norman-Bone Cave data, in particular NB10, presents a problem if the same arguments are used as in the Grapevine Cave example above. As noted in Chapter 4 (Section 4.11.8) fluid inclusions in NB10 are depleted in O^{18} relative to the present when regional temperatures are low, in contrast to the Grapevine Cave situation. The change in δ_i^O with temperature ($0.21 \text{ } ^\circ/\text{oo}$ per $^\circ\text{C}$) almost exactly cancels the effect of temperature on $\alpha_{\text{ct-H}_2\text{O}}$ ($0.24 \text{ } ^\circ/\text{oo}$ per $^\circ\text{C}$) with the result that little net change in δ_{ct}^O should be observed as regional temperatures change. However, δ_{ct}^O values along the axis of NB10 vary over a range of $2.7 \text{ } ^\circ/\text{oo}$ (from $-4.7 \text{ } ^\circ/\text{oo}$ to $-7.4 \text{ } ^\circ/\text{oo}$, Figure 6.4) which is somewhat similar to the range of isotopic variations in GV2. The fluid inclusion - δ_{ct}^O data, indicating little change in δ_{ct}^O with temperature, are incompatible with the observed large excursions in δ_{ct}^O along the axis of NB10.

At first sight it would appear that either non-equilibrium deposition of parts of, or the whole of NB10 took place, or that the fluid inclusion data used to calculate temperatures of deposition is unreliable.

A further alternative explanation was sought because at least parts of NB10 were shown to have been deposited in equilibrium and the fluid inclusion data were internally consistent. If it is assumed that during extremely cold periods mean July temperatures were lowered

sufficiently that the mean isotopic composition of July precipitation resembled the isotopic composition of present-day late winter and spring precipitation, then the NB10 data can be explained. The average temperature of deposition of the cold climate samples (NB10-2a/b, NB10-3a/b and NB10-9a/b, Table 4.5) is 1.6°C and $\delta_i^{\circ} = -9.5$ ‰ (compared with 8.6°C and -8.03 ‰ respectively for warm climate samples). Therefore as average annual temperatures decrease it appears that δ_w° of drip-water at first remains constant (the Grapevine situation) and then δ_w° becomes lighter as temperatures decrease further. Because speleothem deposition stops during prolonged periods of cold climate the latter process will not often be recorded.

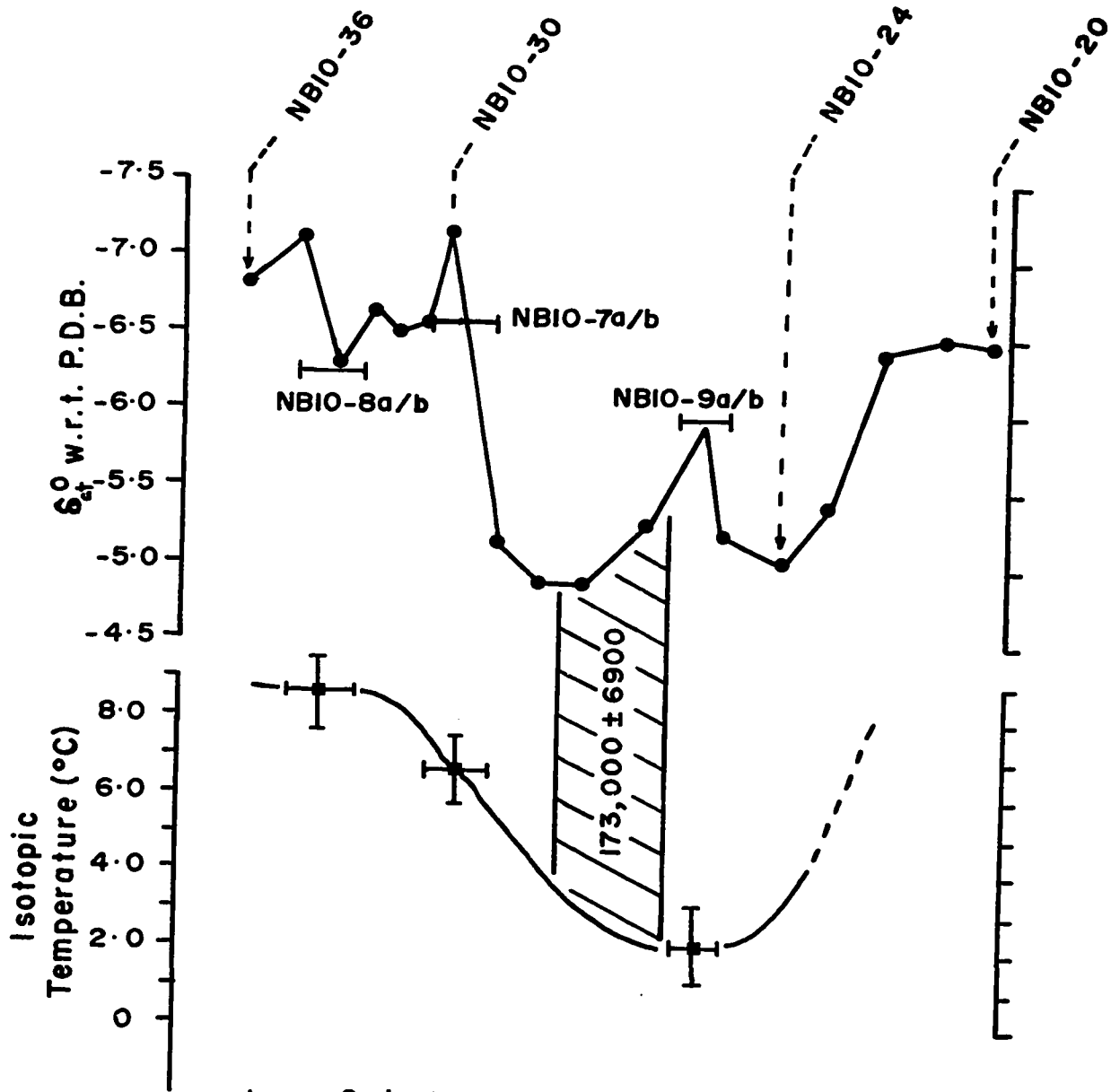
This rather complicated situation may be recorded in NB10 between about 185,000 and 170,000 years B.P. The relevant part of the isotopic curve is reproduced in Figure 8.5 (from Figure 6.5). The curve can be considered in three sections, starting with the oldest stable isotope sample NB10-20.

1) NB10-20 to NB10-24. This was a period of regional climatic cooling which resulted in the deposition of CaCO_3 progressively more enriched in O^{18} (the Grapevine situation described in Section 8.6.1).

2) NB10-24 to NB10-9a/b. This was a period of continued climatic cooling which culminated in extremely cold regional temperatures ($1-2^{\circ}\text{C}$) about 175,000 years B.P. CaCO_3 became depleted in O^{18} relative to the cool-climate sample (NB10-24) because water entering the cave became sufficiently depleted in O^{18} that the effect of a further decrease in temperature on $\alpha_{\text{ct-H}_2\text{O}}$ was negligible. (The

7

Figure 8.5 Variations in δ_{ct}^O and isotopic temperatures calculated from the fluid inclusion data for part of NB10. (Note the "w"-shape of the upper curve between analyses NB10-30 and NB10-24). Refer to Figure 6.5 for location of samples NB10-20 to NB10-36. NB10-7a/b, -8a/b and -9a/b refer to samples for D/H analysis. (see Table 4.6, p.129). Age increases from L to R.



— O-isotopic composition of samples from which fluid inclusions were extracted.

frequency of sampling along the axis of NB10 was not sufficient to record the δ_{ct}^o minimum, but fortunately the sample for fluid inclusion analysis did record this minimum temperature).

3) NB10-9a/b to NB10-30. This was a period of regional warming which resulted in the isotopic variations from NB10-20 to NB10-9a/b being reproduced in reverse. Rising temperatures resulted first in an increase in δ_{ct}^o (due principally to an increase in δ_w^o) then a decrease in δ_{ct}^o to near-modern values (due principally to the effect of temperature on α_{ct-H_2O}).

If this explanation is correct then a single, intense period of climatic cooling should always be accompanied by such a "w"-shaped δ_{ct}^o curve. It may be useful to bear this in mind during future investigations.

The above arguments imply that no simple relationship between δ_i^o (or δ_{ct}^o) and temperature of deposition exists. However, an apparently linear relationship between δ_i^o and isotopic temperature of deposition was shown to exist for Norman-Bone Cave samples (Figure 4.6). If the recently deposited speleothems and the NB10 samples are considered as two separate groups though, the same linear relationship cannot be fitted to both groups. The linear relationship for NB10 is apparently an artifact which arose because only warm and very cold-climate samples were analysed. This demonstrates that limited sampling can sometimes lead to erroneous conclusions. Further fluid inclusion analyses are required to verify the proposed explanations.

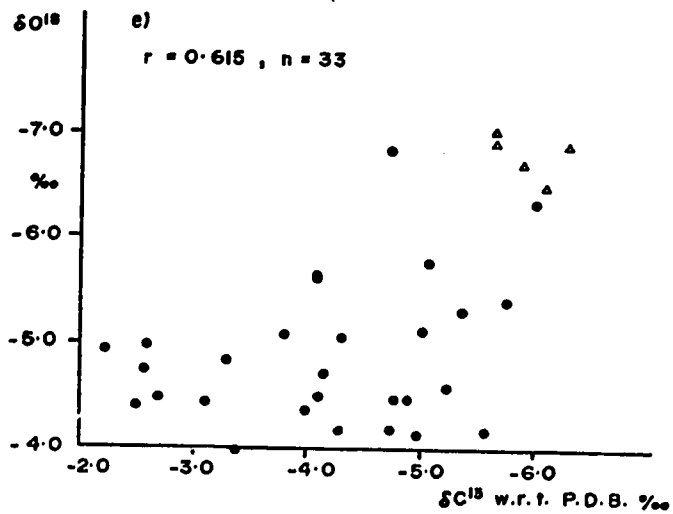
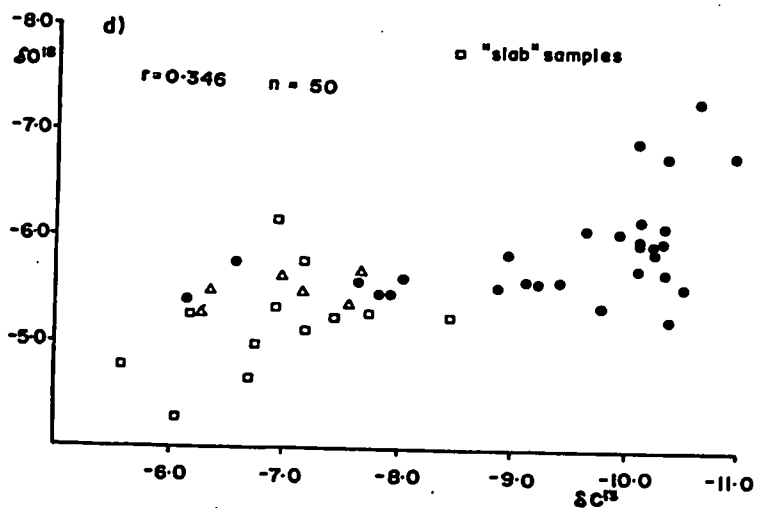
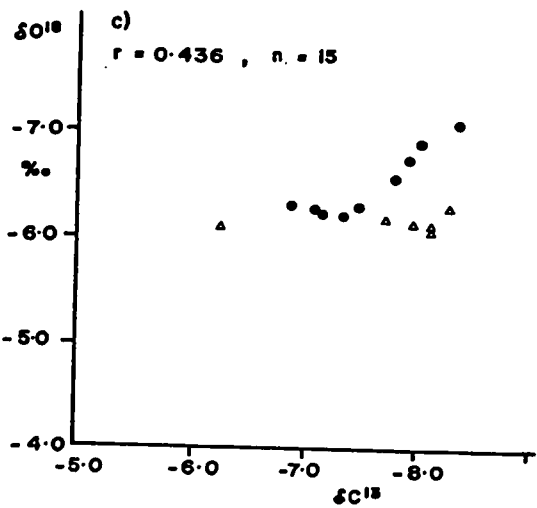
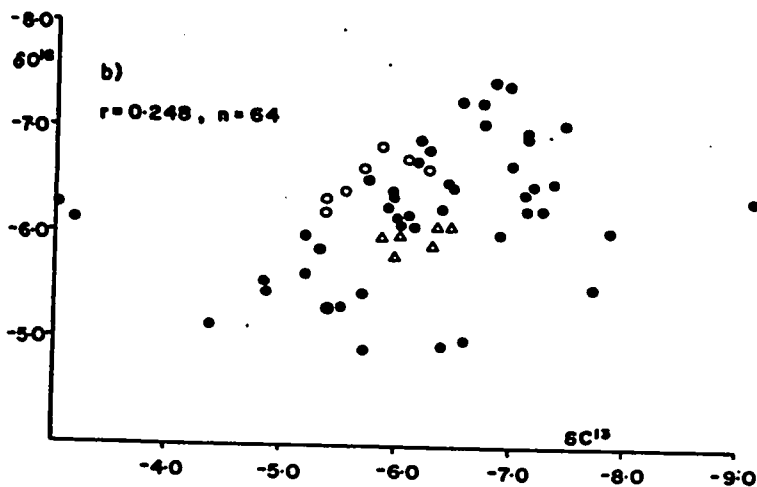
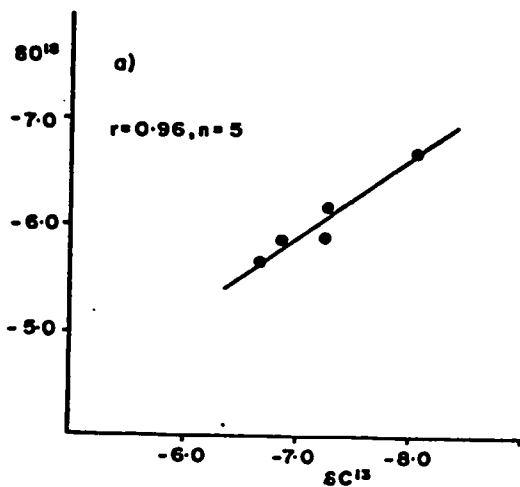
In summary, stalagmite NB10 appears to record a period of

very cold climate between about 170,000 and 180,000 years B.P. Deposition started and stopped during periods of warming and cooling respectively. Warm periods are recorded at about 183,000, 170,000 and 165,000 years B.P. The more pronounced δ_{ct}^O minima record periods of warm climate but due to the complicated relationship between temperature and the isotopic composition of water depositing $CaCO_3$, smaller δ_{ct}^O minima can apparently record periods of cold climate. In general, therefore, δ_{ct}^O values alone should not be used to interpret climate change but should be combined with fluid inclusion data or other paleoclimate data to establish the relationship between changes in δ_{ct}^O and changes in regional temperatures.

8.7 Carbon Isotopic Variations in West Virginia Speleothems

The carbon isotopic composition of the speleothems ranges from -2.2 ‰ (GV2) to -10.9 ‰ (NB4) w.r.t. P.D.B. δ_{ct}^O is plotted against δ_{ct}^C for speleothems NB4, NB5, NB10, NB11 and GV2 in Figure 8.6. Correlation coefficients were calculated and the percentage probability that the coefficients could have occurred by chance is 0.1% for NB5 and GV2, 1% for NB4, 5% for NB10 and >5% for NB11 (though NB11 axial samples show a better correlation). On average, therefore, there is a positive correlation between δ_{ct}^O and δ_{ct}^C . This correlation can be explained in terms other than non-equilibrium deposition, which should result in a much stronger correlation between δ_{ct}^O and δ_{ct}^C across growth layers than is observed. δ_{ct}^O and δ_{ct}^C variations along growth layers are also plotted in Figure 8.6 and the correlation required

Figure 8.6 δ_{ct}^o plotted against δ_{ct}^c for samples from stalagmites NB4, NB5, NB10 and NB11. (Norman-Bone Cave) and GV2 (Grapevine Cave). The correlation coefficient between δ_{ct}^o and δ_{ct}^c (r) is calculated for each speleothem.



- Axial samples
 - △ from around one growth ring
-
- a) Norman - Bone Cave stalagmite, NB5
 - b) " " NB10
 - c) " " NB11
 - d) " " NB4
 - e) Grapevine Cave flowstone, GV2
- N.B. all measurements w.r.t. P.D.B. (‰)

by non-equilibrium deposition is not observed.

Variations in δ_{ct}^c can be caused by variations of δ^c in the soil and atmospheric CO_2 or by changes in the rate at which $CaCO_3$ is precipitated from solutions entering the cave. Temperature changes have a negligible direct effect on the CO_2 - $CaCO_3$ fractionation factor ($\alpha_{CO_2-CaCO_3}$). If the biologic activity within the soil layer is reduced considerably, a proportionately larger amount of atmospheric CO_2 (with $\delta^c = -7.0$ to -8.0 ‰) will participate in the dissolution of the limestone. The HCO_3^- in solution will be proportionately heavier (as will the $CaCO_3$ precipitated in isotopic equilibrium with the HCO_3^-). Also, as the soil pCO_2 decreases, the relative effect of partial exchange of dissolved bicarbonate ions with limestone probably increases. This situation is most likely to be encountered during periods of cold climate when it has been shown (Section 8.6) that $CaCO_3$ is enriched in O^{18} . Long-term climate changes may therefore result in the deposition of $CaCO_3$ which is enriched in both C^{13} and O^{18} . However, soil CO_2 levels are in general an order of magnitude or more higher than atmospheric CO_2 concentrations and therefore a large decrease in biotic activity is required for the atmospheric CO_2 component (above process) to become significant. Under these conditions speleothem growth rate would either be very slow or zero. Another effect which would tend to increase δ_{ct}^c is the exchange between cave atmospheric CO_2 and dissolved HCO_3^- at the site of deposition. During periods of low biotic activity, the contribution to cave air CO_2 of light carbon outgassed from drip water would be lessened; therefore

δ^C of cave air CO_2 would approach that of atmospheric CO_2 and such CO_2 , exchanging with dripwater HCO_3^- would tend to increase δ_{ct}^C of the deposit.

This situation has been treated quantitatively by Hendy (1969). He showed that a combined Rayleigh Distillation Process and isotopic exchange between aqueous CO_2 and CO_2 of the cave air will produce CaCO_3 with δ^C between -12 and 0 ‰. This assumes dissolution of limestone ($\delta_{\text{1st}}^C = +1$ ‰ w.r.t. P.D.B.) by a solution containing soil CO_2 ($\delta_{\text{CO}_2}^C = -24$ ‰ w.r.t. P.D.B.) in a closed system, and neglects post-dissolution exchange between HCO_3^- and rock, which would lead to even higher δ^C . It is probable that the second process described, that of isotopic exchange with the cave atmosphere, will be the dominant one during periods of cold climate. Galimov *et al.* (1965), Labeyrie *et al.* (1967a) and Geyh (1969) also noted that changes in δ_{ct}^C were apparently influenced by climate changes.

8.8 The Late Pleistocene Climate Record Inferred from Phases of Speleothem Deposition and Oxygen Isotopic Abundances

In this section the results from the Rockies, N.W.T. and West Virginia are combined in an attempt to reconstruct late Pleistocene climate changes in North America. It is assumed that speleothems are deposited predominantly during interglacial and interstadial periods though it is recognised that non-climatic effects can affect speleothem deposition. However, if a number of speleothems in a given region become active or fossil at the same time this is considered good evidence for climate change. The terms "interglacial" and "glacial"

as used here simply mean periods of widespread speleothem growth and zero growth respectively. Speleothem growth can apparently occur at temperatures as low as 1-2 °C, therefore a combination of factors such as low temperatures, sparse precipitation and vegetation probably contribute to the cessation of speleothem growth. The "glacials" are not therefore strictly periods of cold climate. Conversely, "interglacials" are not strictly periods of warm climate. They are mostly periods of warm, moist climate but cold periods of short duration can be accommodated within an "interglacial".

The phases of speleothem deposition and the oxygen isotopic curves for West Virginia, the Canadian Rockies and N.W.T. are summarised in Figure 8.7. Based on the fact that GV2, NB1 and NB13 became inactive between approximately 60,000 and 70,000 years ago, and on the isotopic evidence for GV2, it is concluded that this represented a period of rapidly cooling climate. This period is generally accepted as the start of the early Wisconsin glaciation (see references in Lamb and Woodroffe, 1970) which was followed by a series of alternating cold and warm periods and then by the main (classical) Wisconsin glaciation. The upper section of NB4 was probably deposited during the interstadial phase between the early and classical Wisconsin glacial phases.

The penultimate glacial period, or Illinoian, apparently reached its maximum extent between about 160,000 and 135,000 years B.P. Growth of both GV2 and NB10 was interrupted 160,000 years ago and growth of NB1 started approximately 135,000 years ago. It is possible that growth

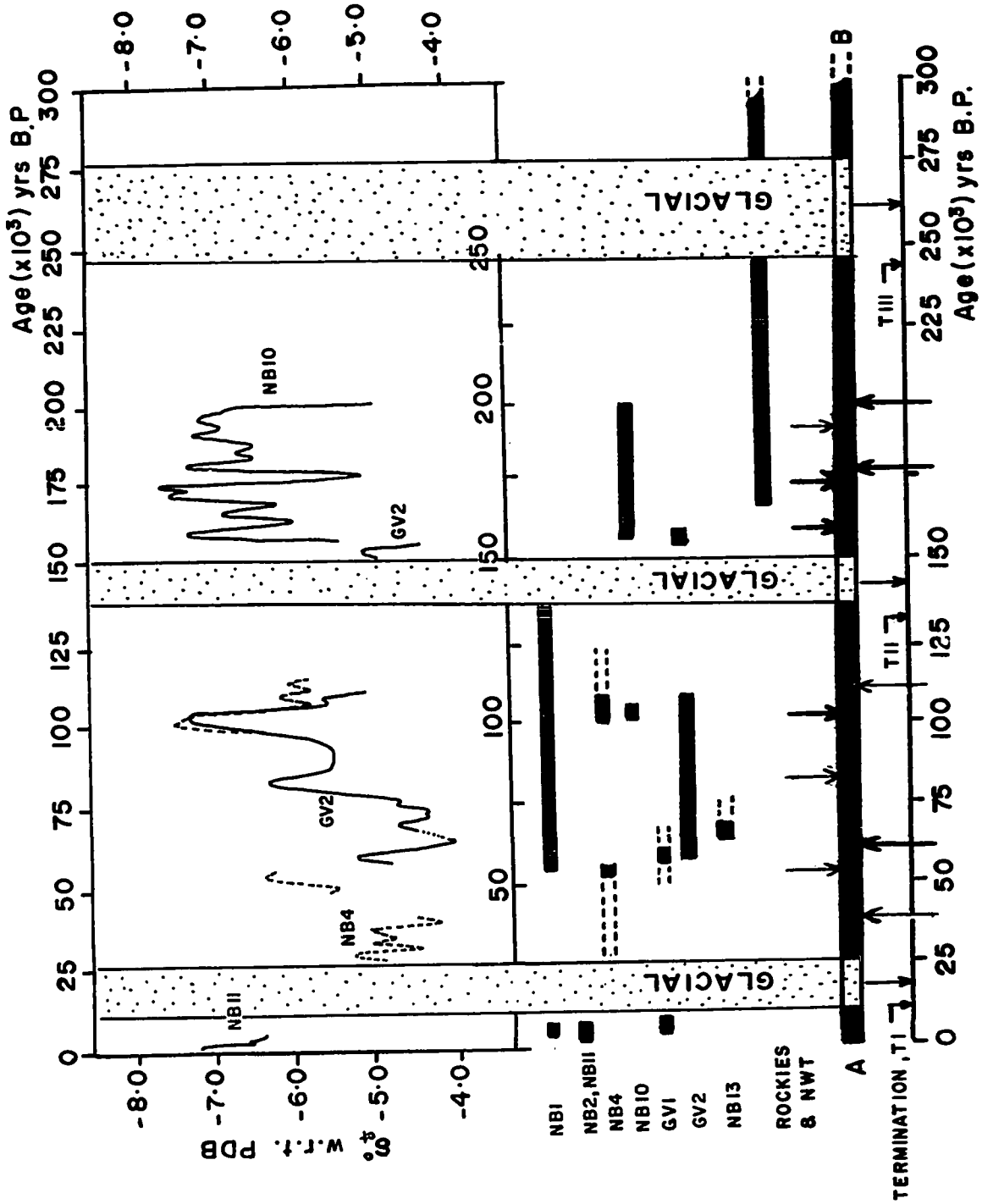
Figure 8.7 Summary of the speleothem data and a time scale for Late Pleistocene climatic events based on these data.

Explanation: The solid sections of bar AB represent generalised periods of speleothem deposition which occur during moist, cool to warm climatic conditions. The stippled areas represent extremely cold climatic conditions when zero speleothem deposition occurs.

The upper (6) arrows represent the δ_{ct}^O minima or temperature maxima; the thick arrows represent the warmest periods, the thin arrows periods of cooler climate.

The lower (5) arrows represent the δ_{ct}^O maxima or temperature minima; again, the thick arrows represent the coldest periods, the thin arrows periods of slightly warmer climate.

The Terminations (T1, T11, T111) of Broecker and van Donk are shown below the bar AB. These correlate with the end of a major glacial period.



of NB10 followed a glacial period approximately 200,000 years ago but in both the Rockies (Eagle Cave and Coulthard Cave) and the N.W.T. (Grotte Valerie, second speleothem phase) extensive speleothem deposition took place between 240,000 and 200,000 years B.P. Speleothem deposition at these latitudes should definitely have been interrupted by a prolonged glacial period, therefore it is assumed that the δ_{ct}^o maxima in NB10 represent short but intense periods of cooling within an interglacial period which lasted from approximately 240,000 to 160,000 years B.P. A further glacial phase (the Kansan?) is indicated by cessation of deposition in both the Rockies and N.W.T. from approximately 270,000 to 240,000 years B.P. These periods of speleothem deposition are summarised in Table 8.2. and an attempt is made to correlate these with the classical North American interglacial stages. The correlation becomes less precise as the age increases.

In Figure 8.7 the approximate mid point of the inferred glacial periods is compared to the so-called Terminations in the deep-sea record of Broecker and van Donk (1970). These Terminations are the mid-point of the rapid warming following a glacial maximum and should post-date the mid-point of the glacial periods. When this is considered the two sets of data agree quite well. The data also agrees with the age of the Marklines of Kukla (1970), the terrestrial equivalent of a Termination. The length of a glacial cycle appears to be about 110,000 to 130,000 years and is about the same for the last two cycles.

Table 8.2

Late Pleistocene Climate and Chronology Based on $\delta^{18}O_{ct}$ and Periods of Speleothem Deposition

Speleothem Growth (years B.P.)	No Speleothem Growth (years B.P.)	$\delta^{18}O_{ct}$ minima* (warm climate)	$\delta^{18}O_{ct}$ maxima* (cold climate)	North American Stages
60,000 - 135,000		60,000 - 65,000 (cool?)	65,000 - 70,000	
		75,000 - 80,000		Sangamon
		95,000 - 105,000		
	135,000 - 160,000		105,000 - 110,000	Illinoian
		160,000 - 165,000		
		168,000 - 172,000		
160,000 - 240,000		180,000 - 195,000	172,000 - 180,000	Yarmouth
	240,000 - 270,000		195,000 - 200,000	Kansan?
270,000 - ?				Aftonian?

* Based on the GV2 and NB10 records

8.9 Comparison of the Speleothem Isotopic Record with Other Isotopic Records

Any comparison made between sedimentary sequences must rely on an accurate time scale for each sequence or the less satisfactory "marker" horizons which allow certain levels to be correlated. No such stratigraphic horizons are present in speleothems with the exceptions of man-made soot layers which have been identified in stalagmites of Czechoslovakia (Petranek and Poubra, 1951). Shillat (1969) suggested that a fall of volcanic ash above a cave results in characteristic colouration within stalagmite and flowstone layers. If this is correct and if these layers can be correlated with known volcanic activity then these layers can be used as "marker" horizons.

At present, therefore, correlations must rely upon the assumption that the time scales are correct. In Sections 8.9.1 to 8.9.3 attempts are made to correlate the West Virginia speleothem record with the speleothem record from Southern France and with deep-sea records as well as that of the Greenland ice. However, controversy surrounds the time scale for deep-sea cores and the time scale for accumulation of ice, based on the physical laws of ice flow, is potentially subject to considerable error as the age increases. No detailed correlations have been attempted because of these uncertainties.

8.9.1 The Aven d'Orgnac Stalagmites of Southern France

Detailed isotopic curves have been measured for a recent (Labeyrie et al., 1967a) and fossil (Duplessey et al., 1971) stalagmite

from Aven d'Orgnac in the Ardeche province of Southern France. Recent Orgnac stalagmites have an average oxygen isotopic composition of approximately -5.85 ‰ (Labeyrie et al., 1967a, Duplessey et al., 1969). The fossil stalagmite dated by the deficient ionium method has an isotopic composition varying from -4.38 ‰ to -6.31 ‰ and was deposited between 130,000 and 90,000 years B.P. The oxygen isotope profile measured along the axis of the stalagmite is compared with that of GV2 in Figure 8.8. Duplessey et al. interpret the lighter δ_{ct}^O values to represent deposition in a cold climate and therefore the period between 92,000 and 97,000 years B.P. is considered to be a period of glacial advance. Duplessey et al. assume that water becomes progressively lighter as temperature decreases and that this effect outweighs the O^{18} -enrichment of the $CaCO_3$ due to a temperature decrease. They conclude that $CaCO_3$ is expected to become progressively lighter as the temperature decreases. This interpretation stems from the use of Dansgaard's theory which predicts that a regional temperature decrease of $1^\circ C$ will result in atmospheric precipitation depleted by 0.69 ‰ in O^{18} . This interpretation is not supported by the experimental evidence because:

- 1) recent stalagmites precipitated at $12.6^\circ C$ have an isotopic composition close to -5.9 ‰ which is comparable with the isotopic composition of the carbonate deposited between 92,000 and 97,000 years ago. Therefore the climate during this period is more likely to have been similar to the present climate.

- 2) The published measurements on drip-water oxygen isotopic

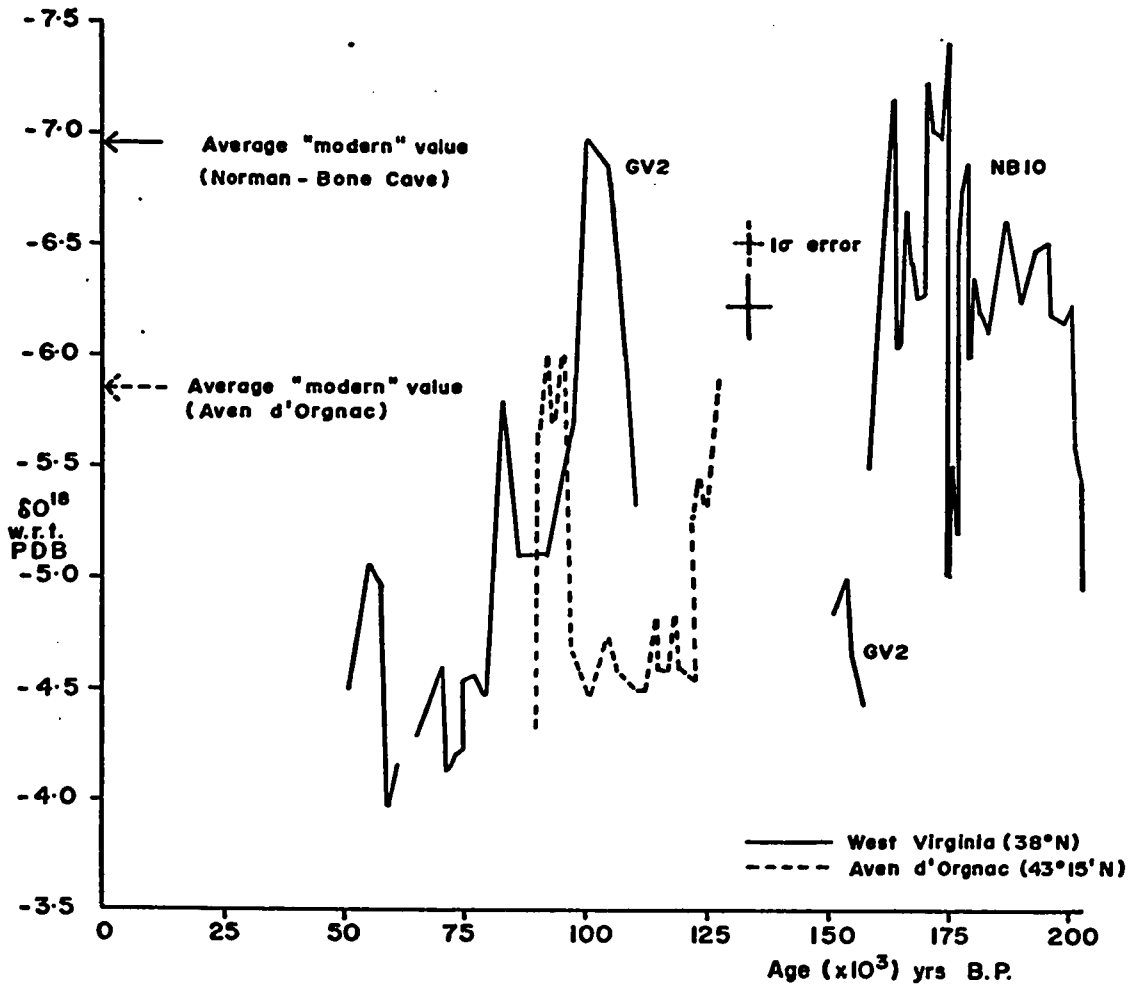


Figure 8.8 A comparison between the speleothem oxygen isotopic records for West Virginia and Southern France (Ardeche Province) between 60,000 and 130,000 years B.P.

composition do not support use of the Dansgaard theory. Based on the measurements of Duplessey et al. (1969) an enrichment factor of 0.14 ‰ per °C is calculated. Further published analyses by Duplessey et al. (1971) indicate a value of close to 0.3 ‰ per °C.

3) The rate of growth of the fossil stalagmite was greater between 100,000 and 92,000 years ago ($14.5 \text{ cm}/10^3 \text{ yr}$) than between 120,000 and 100,000 years ago ($3.2 \text{ cm}/10^3 \text{ yr}$) when climate was supposed to be warmer. The rate of growth was very rapid ($60 \text{ cm}/10^3 \text{ yr}$) when the lightest carbonate was deposited. Franke and Geyh (1971) showed that the rate of growth of speleothems in Central Germany is greater during periods of warm climate. Emiliani (1971) has also argued against the interpretation of Duplessey et al. on the grounds that the effect of temperature on the isotopic composition of atmospheric precipitation has been overestimated. In addition, Emiliani's interpretation of the data results in approximate agreement between his published paleoclimate curves obtained from isotopic analysis of foraminifera and the Orgnac stalagmite record.

If this interpretation is correct, and assuming that the isotopic variations are recording climate changes, then between 130,000 and 125,000 years B.P. a period of cooling led into a prolonged cold period lasting between approximately 125,000 and 97,000 years B.P. A pronounced but short-lived amelioration of climate occurred between 95,000 and 92,000 years B.P.; then deposition stopped after a short cooling period. This interpretation agrees in general with the interpretation of the isotopic evidence from Grapevine Cave (GV2). The

same short-lived warm period is recorded in both speleothems; the slight displacement in time of occurrence may be real or it may be attributable to experimental error. Because of the milder climate at Aven d'Orgnac, speleothem deposition was apparently continuous throughout this period of cold climate.

8.9.2 The Isotopic Record in Deep-Sea Sediments

The CaCO_3 of planktonic foraminifera also records both the oxygen isotopic composition of the water and temperature, if deposition is an equilibrium process. Assuming no post-depositional changes occur in these organisms, the constant "rain" of debris to the ocean floor buries the carbonate shells and preserves the climate record. Changes in the oxygen isotopic composition of the oceans and changes in temperature are both climatically controlled; therefore the change in temperature of deposition cannot be uniquely determined. Attempts have been made to estimate the change in isotopic composition of the oceans. The storage of O^{18} -deficient water in the Pleistocene ice-sheets resulted in tropical ocean waters enriched in O^{18} with respect to the present oceans. Emiliani (1970) estimates a maximum enrichment of 0.5 ‰ in δ_w^{O} of the ocean water. When allowance is made for this enrichment the temperature of the equatorial Atlantic during the last glacial age is calculated to be approximately 5°C cooler than at present. The accuracy of the correction for this isotopic enrichment depends upon a reliable estimate for the volume and isotopic composition of excess glacial ice and for the volume of the oceans.

Ice and water volumes are reasonably well known but the isotopic composition of the excess glacial ice is difficult to estimate. Emiliani proposes a value of near -9 ‰ on the grounds that much of the snow would have fallen at middle latitudes and would not have undergone extensive fractionation. Dansgaard and Tauber (1969) propose a value of -30 ‰ for the isotopic composition of the excess glacial ice. This is based on the average isotopic composition of Greenland and Antarctic ice. Using this value a change in the isotopic composition of the tropical ocean surface waters of $+1.2$ ‰ is calculated for the last glacial cycle. This value is significantly different to that estimated by Emiliani and accounts for 70% of the observed isotopic variation in foraminifera. Dansgaard & Tauber and Broecker & van Donk subscribe to the view that $\delta^{18}\text{O}$ of foraminifera records chiefly the amount of excess glacial ice on the Continents. The overall interpretation of the isotopic record in deep-sea sediments is not affected by this controversy, which at the moment is still unresolved.

The foraminifera themselves are not readily dated because of their small size, though attempts have been made to date them directly (Holmes, 1964) using the decay of excess Th^{230} . The non-carbonate sediment is generally dated by the $\text{Pa}^{231}/\text{Th}^{230}$ method and the assumption is made that the foraminiferal tests included in the sediment are of the same age. In addition to the analytical uncertainties discussed in Section 2.4, the actions of marine burrowing organisms introduce further uncertainties due to mixing of sediments of different ages. Despite these problems an isotopic "temperature" curve has been

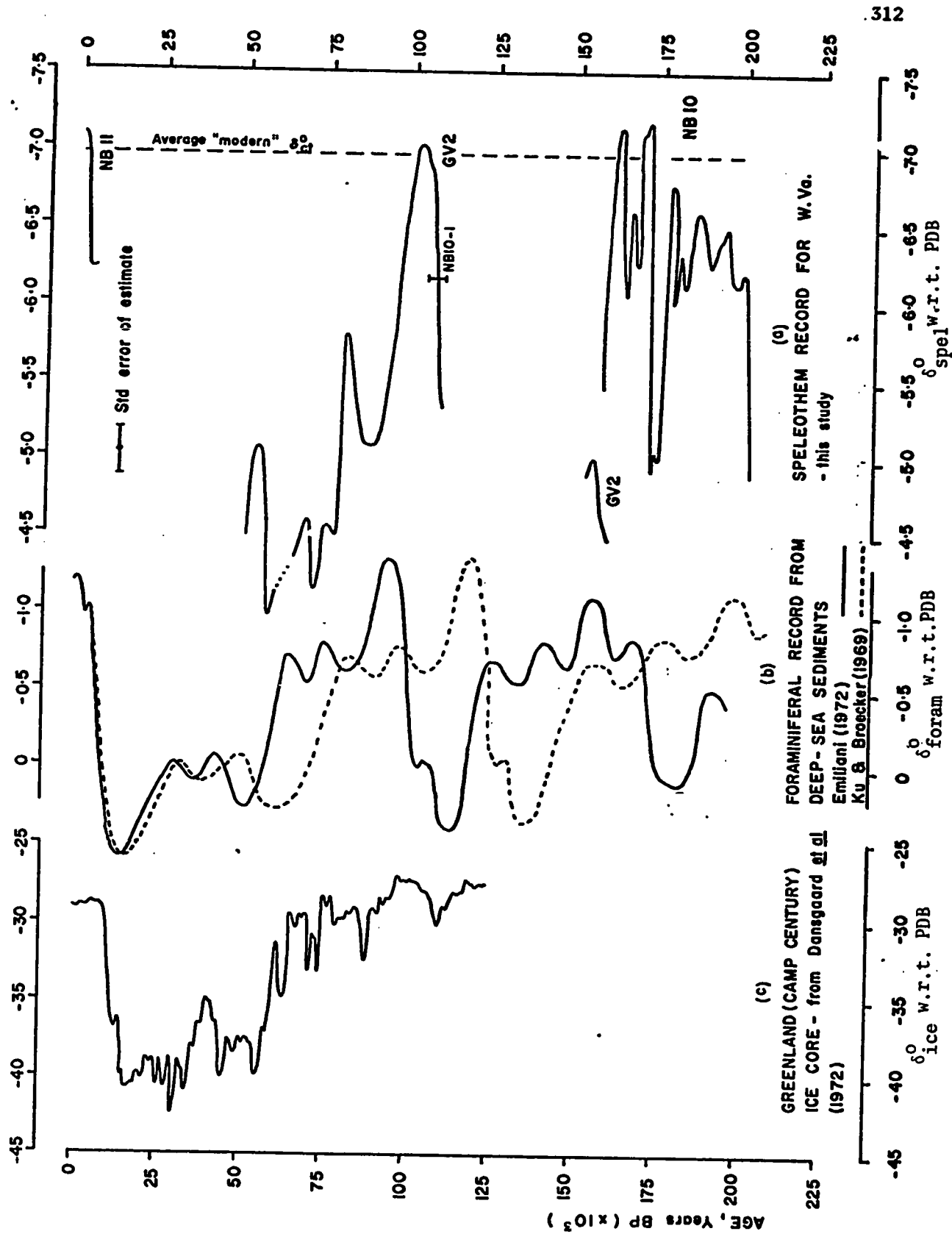
calculated, principally by Emiliani (1955, 1966, 1970, 1972), part of which is shown in Figure 8.8b (solid line). The same curve (which is generalised from Caribbean and Equatorial Atlantic deep-sea core data) is plotted using the expanded time scale of Broecker and Ku (dashed line).

The lightest $\delta_{\text{foram}}^{\circ}$ values represent periods of warmest climate which, in addition to recent times, occurred 100,000 (or 125,000) and 156,000 (or 205,000) years B.P. Conversely, the heaviest $\delta_{\text{foram}}^{\circ}$ values represent the coldest periods and those occurred 20,000 (or 25,000), 120,000 (or 150,000) and 180,000 (or 225,000) years ago.

The isotopic profiles in NB11, GV2 and NB10 were chosen for comparison with the deep sea profiles. There is no perfect correlation between the two records regardless of which time scale is used but there is a striking similarity between Emiliani's curve and the GV2 curve.

The main objection to Emiliani's curve is that it does not recognise the highest sea-level stand at 125,000 years B.P. as representing the warmest part of the Sangamon interglacial. However, the expanded time scale of Broecker and Ku does not allow for a glacial event between 125,000 and 105,000 years B.P. (recognised by Steinen et al in the Barbados) nor does it allow for a relatively high sea-level stand at 60,000 years B.P. (recognised by James et al in the Barbados). It is possible that the entire increase in $\delta_{\text{foram}}^{\circ}$ between 125,000 and 110,000 years B.P. (on the expanded scale) is due to an increase in δ_w° of the ocean surface waters in response to the preferential removal of O^{16} to expanding

Figure 8.9 A comparison between (a) the speleothem record for West Virginia, (b) the planktonic foraminiferal record from tropical deep-sea cores and (c) the ice record from Greenland.



Continental glaciers. However, if this were the case the $\delta_{\text{foram}}^{\text{O}}$ curve should also record the 60,000 year high sea-level stand.

Stalagmite NB1 was apparently continuously active between about 135,000 and 60,000 years B.P., therefore the intensity of the cold period between 125,000 and 105,000 years B.P. was probably not as severe as during the main Wisconsin. However, the $\delta_{\text{foram}}^{\text{O}}$ curve of Emiliani indicates that temperatures (or the amount of excess glacial ice) 20,000 and 110,000 years B.P. were quite similar.

The similarity between the NB10 record and the $\delta_{\text{foram}}^{\text{O}}$ curve of Emiliani is less pronounced but the $\delta_{\text{ct}}^{\text{O}}$ minimum in NB10 at about 170,000 years B.P. could correlate with the $\delta_{\text{foram}}^{\text{O}}$ minimum at about 160,000 years B.P. The cold period recorded in NB10 between 170,000 and 185,000 years B.P. could correlate with the cold event at 185,000 years B.P. recorded in the deep-sea sediments. According to Emiliani though, interglacial conditions should have lasted until about 120,000 years B.P., but both NB10 and GV2 became inactive about 160,000 years B.P. This was interpreted as the onset of a glacial period. The curve of Broecker and van Donk does record the onset of a glacial period about 160,000 years B.P. but not the extremely cold event recorded in NB10 about 175,000 years B.P.

As noted in section 8.8, when periods of speleothem deposition alone are considered, the data support the expanded time scale of Broecker and Ku. When the isotopic data alone are considered, there appears to be more support for the shorter time scale of Emiliani. The speleothem data, therefore, does little to help resolve this controversy surrounding the absolute age of deep-sea sediments. However, it is the opinion of this author that more emphasis should be placed on the periods of

speleothem deposition than the isotopic data. This is because the relative magnitude of δ_{ct}^o maxima and minima are not reliable indicators of minimum and maximum temperatures and therefore cannot be directly correlated with the maxima and minima of the δ_{foram}^o curve, whereas zero speleothem growth almost certainly indicates periods of prolonged cold climate. As more peaks are added to the spectra of climate change, correlation between different records becomes more tenuous unless the relative intensity of the isotope peaks can be used to "Fingerprint" each spectrum. Further speleothem studies may help resolve the problem and may eventually lead to a very detailed terrestrial isotope record.

8.9.3. The Isotope Record in the Greenland Ice

Dansgaard et al (1971) have measured a very detailed δ^o curve on a long ice core from Greenland. If it is assumed that snow becomes progressively depleted in O^{18} as the temperature gradient increases between the point of evaporation and the point of precipitation then inferences can be made about climate change. Problems are encountered when attempts are made to assign a time scale to this isotopic record. The older ice layers cannot be dated by any of the radiometric methods. Consequently, Dansgaard et al. applied the laws of glacier-flow dynamics to calculate the age at various depths. The older layers are compressed so that the 50,000 year period representing the last interglacial is contained within the bottom 30 meters of the 1390 metre long ice core. The age uncertainties involved, therefore, become larger toward the base of the core. The O^{18}/O^{16} profile is plotted in Figure 8.5(c) to allow comparison between it and the speleothem and deep-sea record.

Again, only broad comparisons can be made because of the tentative nature of the time scale. There is no evidence for the cold period between 125,000 and 105,000 years B.P., but from the present to 105,000 B.P. tropical and polar climate changes appear to be broadly synchronous. The ice record is not at variance with the speleothem record in W.Va. except for the fact that the relative amplitudes of the peaks are different. (also the cold period immediately prior to 105,000 yrs. B.P. is not recorded).

8. 10. Considerations for Future Research

The results obtained in this study are sufficiently encouraging that the search for a complete speleothem record should be continued. Speleothems potentially offer one of the best materials for high-resolution Middle to Late Pleistocene paleoclimate analysis. To overcome the limitation imposed on this study by the apparent cessation of speleothem deposition during the coldest part of a glacial cycle, speleothems from caves at lower latitudes should be studied. The "ideal" speleothem will:

- (1) Have a high U content, and will be pure (ie free of detrital material) and impervious to water.
- (2) Be continuously deposited during glacial/interglacial climate changes.
- (3) Be deposited rapidly enough for short-term climate changes to be resolved.
- (4) Be deposited (in equilibrium) from waters with an average oxygen isotopic composition equal to the mean annual value for meteoric precipitation, a readily measured parameter.

- (5) Be deposited in an environment where past changes in δ_w^O of meteoric precipitation can be evaluated.

The ideal" speleothem will possibly be located in a cave on a tropical island where changes in δ_w^O of meteoric precipitation are controlled only by the change in δ_w^O of the ocean surface water. If reliable fluid inclusion data is obtained from the speleothem, difficulties in assigning a change to δ_w^O of the oceanic surface waters due to Continental glacierisation may be resolved. A perennially thriving plant cover on a tropical soil will ensure continuous CO_2 production and continuous $CaCO_3$ deposition on the speleothem surface. However, care should be taken to check for kinetic effects introduced by evaporation of both surface water and sub-surface drips. A high cave temperature will favour evaporation of drip waters. Also, a high cave temperature, according to Moore (1956), will favour the deposition of aragonitic speleothems. Subsequent inversion is possible which will result in U and Th migration. However, old speleothems preserved in the aragonitic form may be suitable for dating by the U-He method. This would offer a useful check on Th^{230}/U^{234} ages and, in particular, U^{234}/U^{238} ages.

The majority of the age determinations in this study rely solely on the Th^{230}/U^{234} dating method. The credibility of future speleothem research would be greatly enhanced if attempts were made to measure Th^{230}/U^{234} and Pa^{231}/U^{235} ages on numerous samples, rather than the few attempted in this study. Dating would be restricted to speleothems with a high (> 2-3 ppm) U content; however, this type of deposit appears to be more widespread than might be inferred from the literature review.

8.10.1 Geomorphic Rates from Speleothem Age-Data

The minimum age of a cave passage or level can be obtained by searching for the oldest speleothem deposits in the passage. In principle, CaCO_3 deposition can start as soon as percolating water enters an air-filled void. In practise certain factors (for example, unfavourable climatic conditions or roof collapse) might cause the deposition of CaCO_3 to be delayed. The draining of a cave passage is controlled by lowering of the master valley. Changes in the amount of regional precipitation would cause the water table to fluctuate and this movement will probably be superimposed on the unidirectional movement due to valley lowering. Little net deposition is expected during periods when the water table fluctuates, therefore continuous speleothem deposition probably dates the permanent abandonment of the passage by phreatic waters.

Furthermore, in horizontal or near-horizontal strata, distinct levels of cave passages are often observed when an entrenching river is temporarily stabilised at base level. A series of such geomorphic events leaves distinct terrace levels and a 3-dimensional network of passages with progressively younger speleothems in the lower levels. These geomorphic events, which may be related to climate change or tectonic activity, can therefore be dated. Because speleothem deposition began probably after the event, the oldest speleothems will give a minimum age for the event. To apply this type of study to the measurement of the rates of geomorphic processes accurate correlation of terrace levels and cave levels is necessary. The sequence of geomorphic events must also be correctly inferred from the field evidence. Most geomorphologists would welcome reasonably accurate data on the rates at which fluvial and glacial erosion occur.

REFERENCES

- AMIN, B.S., O.P. Kharkar and D. Lal, 1966, Cosmogenic Be¹⁰ and Al²⁶ in marine sediments. *Deep Sea Res.*, v.13 (5), p.805-824
- ARMSTRONG, R.L., W. Hamilton and G.H. Denton, 1968, **Glaciation in Taylor Valley, Antarctica, older than 2.7 million years.** *Science*, v. 159, p.187
- ATTREE, R.W., M.J. Cabell, R.L. Cushing and J.J. Pieron, 1962, A calorimetric determination of the half-life of Th²³⁰ and consequent revision of its neutron capture cross-section. *Can. J. Phys.*, v.40, p.194
- BARNES, J.W., E.J. Lang and H.A. Potratz, 1956, Ratio of ionium to uranium in coral limestone, *Science*, v.124, p.175-176
- BENDER, M.M., 1968, Mass spectrometric studies of C¹³ variations in corn and other grasses. *Radiocarbon*, v.10, p.468-472
- BENDER, M.L., 1970, Helium-uranium dating of corals, Ph.D. Dissertation, Columbia University, New York
- BERGGREN, W.A., J.D. Phillips, A. Bertels and D. Wall, 1967, Late Pliocene and Pleistocene stratigraphy in deep sea cores from the south central North Atlantic. *Nature*, v.216, p.253-254
- BIGELEISEN, J., M.L. Perlman and H.C. Prosser, 1952, Conversion of hydrogenic materials to hydrogen for isotopic analysis. *Anal. Chem.*, v.24, p.1356-57
- BLANCHARD, R.L., 1963, Uranium decay series disequilibrium in age determination of marine calcium carbonates. Ph.D. Dissertation, Washington University

- BLANCHARD, R.L., U^{234}/U^{238} ratio in coastal marine waters and calcium carbonates. *J. Geophys. Res.*, v.70, p.4055
- BONATTI, E., D.E. Fisher, O. Joensuu, and H.S. Rydell, 1971, Post depositional mobility of some transition elements, phosphorous, uranium and thorium in deep sea sediments. *Geochim. Cosmochim. Acta*, v.35 (2), p.189
- BRITO, U. and C. Lalou, 1969, Dommages crees dans les cristaux de calcite par les irradiations. *Earth Planet. Sci. Lett.*, v.6, p.155-160
- BROECKER, W.S., 1963, A preliminary evaluation of uranium series inequilibrium as a tool for absolute age measurement on marine carbonates. *J. Geophys. Res.*, v.68, p.2817
- BROECKER, W.S. AND T.L. Ku, 1969, Caribbean cores P6304-8 and P6304-9: New analysis of absolute chronology. *Science*, v.166, p.404
- BROECKER, W.S., E.A. Olsen and P.C. Orr, 1960, Radiocarbon measurements and annual rings in cave formations. *Nature* v.185, p.93-94
- BROECKER, W.S., and D.L. Thurber, 1965, Uranium-series dating of corals and oolites from Bahaman and Florida Key limestones. *Science*, v.149, p.58-60
- BROECKER, W.S., D.L. Thurber, J. Goddard, T.L. Ku, R.K. Matthews and K.J. Mesollella, 1968. Milankovitch hypothesis supported by precise dating of coral reefs and deep-sea sediments. *Science* v.159, p.297-300.
- BROECKER, W.S. and J. van Donk, 1970, Insolation changes, ice volumes, and the O^{18} record in deep-sea cores. *Rev. Geophys. Space Phys.*, v.8, p.169-198.
- BROECKER, W.S. and W. Walton, 1959, The geochemistry of C^{14} in freshwater systems. *Geochim. Cosmochim. Acta*, v.16, p.15-34
- CHALOV, P.I., T.V. Tuzova and Ye.A. Amin, 1964, The U^{234}/U^{238} ratio in natural waters and its use in nuclear geochronology. *Geochem. Int.*, v.1 (1), p.402-408

- CHALOV, P.I., K.I. Merkulova and T.V. Tuzova, 1966, U^{234}/U^{238} ratio in water and bottom sediments of the Aral Sea and the absolute age of the basin. *Geochem. Int.*, v.3 (1), p.1149
- CHALOV, P.I., N.A. Svetlichnaya and T.V. Tuzova, 1970, U^{234}/U^{238} in the waters and bottom sediments of Lake Balkash and the age of the lake. *Geochem. Int.*, v.7 (4), p.604
- CHERDYNTSEV, V.V., 1955, in Transactions of the Third Session of the Commission for Determining the Absolute Age of Geological Formations, (in Russian), Moscow, Izdatel stvo Akad. Nauk. SSSR, p.175
- CHERDYNTSEV, V.V., 1971, Uranium-234. Israel Program for Scientific Translations, Monson, Jerusalem, 308 pp.
- CHERDYNTSEV, V.V., I.V. Kazachevskii, and E.A. Kuz'mina, 1963, Isotopic composition of uranium and thorium in the supergene zone. *Geochem. Int.*, v.3, p.271-283
- CHERDYNTSEV, V.V., I.V. Kazachevskii and E.A. Kuz'mina, 1965, Dating of Pleistocene carbonate formations by the thorium and uranium isotopes. *Geochem. Int.*, v.2, p.794-801
- CHERRY, R.D., I.H. Geriche and L.V. Shannon, 1969, Thorium-228 in marine plankton and sea water. *Earth Planet. Sci.Lett.*, v.16, p.451-456
- CLARK, G.M., 1968, Sorted patterned ground: New Appalachian localities south of the glacial border. *Science*, v.161, p.355-356.
- CLAYTON, R.N., 1959, Oxygen isotope fractionation in the system $CaCO_3-H_2O$. *J. Chem. Phys.*, v.30, p.1246-50
- COX, D.D., 1968, A late-glacial pollen record from the West Virginia-Maryland border. *Castanea*, v.33, p.137-149
- CRAIG, A.J., 1969, Vegetational history of the Shenandoah Valley, Virginia. *Geol. Soc. Amer.*, Spec. Paper 123, in Schum and Bradley (Editors), U. S. Contributions to Quaternary Research, p.283-296

CRAIG, H., 1953, The geochemistry of stable carbon isotopes. *Geochim. Cosmochim. Acta*, v.3, p.53

CRAIG, H., 1961, Isotopic variations in meteoric waters. *Science*, v.133, p.1702-1703

CRAIG, H., 1961, Standards for reporting concentrations of D and O¹⁸ in natural waters. *Science*, v.133, p.1833-34

CRAIG, H., 1965, The measurement of oxygen isotope paleotemperatures. in E. Tongiorgi (Editor), *Stable Isotopes and Paleotemperatures*, Proc. Spoleto Conf., CNR Lab. Geol., Pisa, p.161

CROPLEY, J.B., 1965, Influence of surface conditions on temperatures in large cave systems. *Nat. Speleol. Soc., Bull.*, No.1, p.1-10

CURRY, R.R., 1966, Glaciation about 3,000,000 years ago in the Sierra Nevada. *Science*, v.154, p.770

CURTIS, G.H., and J.F. Evernden, 1962, Age of basalt underlying bed I, Olduvai. *Nature*, v.194, p.611

DALRYMPLE, G.B., 1968, Potassium argon dating in Pleistocene correlation. in R.B. Morrison and H.E. Wright, Jr. (Editors), *Means of Correlation of Quaternary Successions*, v.8, Proc. VII Congress INQUA, 1965, University of Utah Press, p.175-194

DANSGAARD, W., 1964, Stable isotopes in precipitation. *Tellus*, v.4 p.436-468

DANSGAARD, W., S.J. Johnsen, J. Møller, and C.C. Langway, Jr., 1969, One thousand centuries of climatic record from Camp Century on the Greenland ice sheet. *Science*, v.166, p.377

DANSGAARD, W., and H. Tauber, 1969, Glacier oxygen-18 content and Pleistocene ocean temperatures. *Science*, v.166, p.499

- DAVIES, W.E., 1960, Meteorological observations in Martens Cave, West Virginia, Nat. Speleol. Soc., Bull., v.22, Part 2, p.92-100
- DREW, D.P., 1968, Tracing percolation waters in karst areas. Cave Res. Group Gt. Brit., Trans., v.10 (2), p.107-114
- DUPLESSY, J.C., J. Labeyrie, C. Lalou and H.V. Nguyen, 1970, Continental climatic variations between 130,000 and 90,000 years B.P. Nature, v.226, p.
- DUPLESSY, J.C., J. Labeyrie, C. Lalou and H.V. Nguyen, 1971, La mesure des variations climatiques continentales-Application a la periode comprise entre 130.000 et 90.000 ans B.P., Quaternary Res., v.1 (2), p.162
- DUPLESSY, J.C., C. Lalou and A.E. Gomes de Azevedo, 1969, Etude des conditions de concrecionnement dans les Grottes au moyen des isotopes stables de l'oxygene et du carbone. Acad. Sci., C.R., Ser. D, v.268, p.2327-2330
- EMILIANI, C., 1955, Pleistocene temperatures. J. Geol., v.63, p.538-78
- EMILIANI, C., 1966, Paleotemperature analysis of the Caribbean cores P 6304-8 and P 6304-9 and a generalized paleotemperature curve for the last 425,000 years. J. Geol. v.74 (6), p.109-126
- EMILIANI, C., 1970, Pleistocene paleotemperatures. Science, v.168, p.822-825
- EMILIANI, C., 1971, The last interglacial; paleotemperatures and chronology. Science, v.171, p.571-573
- EMILIANI, C., 1972, Quaternary paleotemperatures and the duration of the high temperature intervals. Science, v.178, p.398-400
- ENOCH, H. and S. Dasberg, 1971, The occurrence of high CO₂ concentrations in soil air. Geoderma, v.6 (1), p.17-23

- EPSTEIN, S, R. Buchsbaum, H.A. Lowenstaum and H.C. Urey, 1953, Revised carbonate-water isotopic temperature scale. Geol. Soc. Amer., Bull., v.64, p.1315-1326
- EPSTEIN, S., and T. Mayeda, 1953, Variations in O^{18} content of waters from natural sources. Geochim. Cosmochim. Acta, v.27 (4), p.213-224
- ERICSON, D.B., M. Ewing, G. Wollin and B.C. Heezen, 1961, Atlantic deep-sea sediment cores. Geol. Soc. Amer., Bull., v.72, p.193-286
- ERICSON, D.B. and G. Wollin, 1964, The deep and the past, Knopf, New York, 292 pp.
- EVERNDEN, J.F. and G.H. Curtis, 1965, The potassium-argon dating of late Cenozoic rocks in East Africa and Italy. Current Anthropology, v.6 (4), p.343
- EVERNDEN, J.F., D.E. Savage, G.H. Curtis and G.T. James, 1964, Potassium-argon dates and the Cenozoic mammalian chronology of North America. Amer. J. Sci., v.262, p.145
- FANALE, F.P. and O.A. Schaeffer, 1965, The helium-uranium ratios for Pleistocene high sea level stand. J. Geophys. Res., v.71, p.3319
- FANTIDIS, J., and D.H. Ehhalt, 1970, Variations of the carbon and oxygen isotopic composition in stalagmites and stalactites: evidence of non-equilibrium isotopic fractionation. Earth Planet. Sci. Lett., v.10, p.136-144
- FLEISCHER, R.L., L.S.B. Leaky, P.B. Price and R.M. Walker, 1965, Fission track dating of Bed I, Olduvai Gorge. Science, v.148, p.72
- FLINT, R.F., 1971, Glacial and Quaternary geology. Wiley, New York, 892 pp.
- FORD, D.C., (in press) Development of the canyons of the South Nahanni River, N.W.T. Can. J. Earth Sci.

- FORD, D.C., P. Thompson and H.P. Schwarcz, 1972, Dating cave calcite deposits by the uranium disequilibrium method: some preliminary results from Crowsnest Pass, Alberta. in E. Yatsu and A. Falconer (Editors), Research Methods in Pleistocene geomorphology. Proc., 2nd Guelph Symposium in Geomorphology, University of Guelph, p.247-56
- FORNACA-RINALDI, G., 1968, Il metodo $\text{Th}^{230}/\text{U}^{238}$ per la datazione di stalattiti e stalagmiti. Bollettino Di Geofisica Teorica Ed Applicata, v.10, (37), p.3-14
- FORNACA-RINALDI, G., C. Panichi and E. Tongiorgi, 1968, Some causes of the variations of the isotopic composition of carbon and oxygen in cave concretions. Earth Planet. Sci. Lett., v.4, p.321-324
- FRANKE, H.W., 1965a, The theory behind stalagmite shapes. Stud. Spel., v.1, Parts 2-3, p.89-95
- FRANKE, H.W., 1965b, Das Wachstum der Tropfsteine. in Proc. 4th International Congress of Speleology, Yugoslavia, v.3, p.97-103
- FRANKE, H.W. and M.A. Geyh, 1971, Radiokohlenstoffanalysen an Tropfsteinen. Umschau, v.3, p.91-92
- GALIMOV, E.M., 1966, Carbon isotopes of soil CO_2 . Geochem. Int., v.3, (1), p.889-897
- GALIMOV, E.M., V.A. Grinenko and I.M. Gubkin, 1965, Effect of leaching under surface conditions on the isotopic composition of carbon in secondary calcite. Geochem. Int., v.2 (1), p.79-82
- GAMS, I., 1968, Versuch einer Klassifikation der Tropfsteinformen in der Grotte von Postojna, in Proc. 4th Int. Congress Spel., Yugoslavia, 1965, v.3, p.117-126
- GEYH, M.A., 1970, Isotopenphysikalische Untersuchungen an Kalksinter, ihre Bedeutung für die ^{14}C -Altersbestimmung von Grundwasser und die Erforschung des Paläoklimas. Geologisches Jahrbuch, v.88, p.149-158

- HAGEMAN, F.T., 1950, The isolation of actinium. J. Amer. Chem. Soc., v.72, p.768
- HARMON, R.S., 1971a, The application of stable carbon isotope studies to karst research. Part I: Background and theory. Caves and Karst, v.13 (3), p.17-28
- HARMON, R.S., 1971b, The application of stable carbon isotope studies to karst research. Part II: An example from Central Pennsylvania. Caves and Karst, v.13 (4), p.29-36
- HAY, R.L., 1967, Revised stratigraphy of Olduvai Gorge. in W.W. Bishop and J.D. Clark (Editors), Background to Evolution in Africa, University of Chicago Press, Chicago, p.221
- HENDY, C.H., 1969, The isotopic geochemistry of speleothems and its application to the study of past climates. Ph.D. Dissertation, Victoria University, Wellington, New Zealand
- HENDY, C.H., 1970, The use of C^{14} in the study of cave processes. in I.U. Olssen (Editor), Radiocarbon Variations and Absolute Chronology, Proc. 12th Nobel Symposium, Uppsala, 1969, Wiley Interscience Div., New York
- HENDY, C.H., 1971, The isotopic geochemistry of speleothems - I. The calculation of the effects of different modes of formation on the isotopic composition of speleothems and their applicability as paleoclimate indicators. Geochim. Cosmochim. Acta, v.35, p.801-824
- HOLLAND, H.D., T.U. Kirsipu, T.J. Heubner and U.M. Oxburgh, 1964, On some aspects of the chemical evolution of cave waters. J. Geol., v.72 (1), p.36-67
- HOLMES, C.W., 1968, Th^{230}/Th^{232} (Ionium-thorium) dating of deep-sea foraminiferal ooze. in R.B. Morrison and H.E. Wright, Jr. (Editors), Means of Correlation of Quaternary Successions, Proc. VII Congress INQUA, v.8, 1965, University of Utah Press, p.207-241

- HYDE, E.K, 1949, Determination of the half-life of ionium. Natl. Nucl. Energy Series, Div. III, 14b, Transuranic elements Pt. II, p.1435
- HYDE, E.K. and J. Tolmach, 1955, T.T.A. extraction of dilute solutions of thorium nitrate and uranyl nitrate. ANL-4248, U.S. Atomic Energy Commission
- ISAAC, G.L., 1969, Studies of early culture in East Africa. World Archaeology, v.1 (1), p.1
- ISABAEV, E.N., E. Usatov and V.V. Cherdyntsev, 1960, The isotopic composition of uranium in natural minerals. Radiokhimiya, v.2, p.94
- JAMES, N.P., E.W. Mountjoy and A. Omura, 1971, An early Wisconsin reef terrace at Barbados, W.I. and its climatic implications. Geol. Soc. Amer., Bull., v.82 (7), p.2011-17
- JOHNSEN, S.J., W. Dansgaard, H.B. Clausen and C.C. Langway, 1972, Oxygen isotope profiles through the Antarctic and Greenland ice sheets. Nature, v.235, p.429-468
- KAUFMAN, A., 1964, Th²³⁰/U²³⁴ dating of carbonates from Lakes Lahontan and Bonneville. Ph.D. Dissertation, Columbia University, New York
- KAUFMAN, A., 1969, The thorium-232 concentration of surface ocean water. Geochim. Cosmochim. Acta, v.33, p.717
- KAUFMAN, A., 1971, U-series dating of Dead Sea Basin carbonates. Geochim. Cosmochim. Acta, v.35, (12), p.1269-1281
- KAUFMAN, A., and W.S. Broecker, 1965, Comparison of Th²³⁰ and C¹⁴ ages for carbonate materials from Lakes Lahontan and Bonneville. J. Geophys. Res., v.70, p.4039
- KAUFMAN, A., W.S. Broecker, T.L. Ku and D.L. Thurber, 1971, The status of U-series methods of mollusk dating. Geochim. Cosmochim. Acta, v.35 (11), p.1155

- KAUFMAN, M.I., H.S. Rydell and J.K. Osmond, 1969, U^{234}/U^{238} disequilibrium as an aid to hydrologic study of the Floridan aquifer. *J. Hydrol.*, v.9, p.374-386
- KEELING, C.D., 1958, The concentration and isotopic abundances of atmospheric carbon dioxide in rural areas. *Geochim. Cosmochim. Acta*, v.13, p.322-334
- KEELING, C.D., 1961, The concentration and isotopic abundance of CO_2 in rural and marine air. *Geochim. Cosmochim. Acta*, v.24, p.277-298
- KIGOSHI, K., 1971, Alpha-recoil thorium-234: Dissolution into water and the uranium-234/uranium-238 disequilibrium in nature. *Science*, v.173, p.49
- KIRBY, H.W., 1961, Calorimetric determination of the half-life of protactinium. *J. Inorg. Nucl. Chem.*, v.18, p.8
- KOCZY, F.F., 1954, Radioactive elements in ocean waters and sediments. *Geochemical balance in the Hydrosphere*. in H. Faul (Editor), *Nuclear Geology*, John Wiley and Sons, New York, p.120-127
- KOIDE, M., and E.D. Goldberg, 1965, Uranium-234/uranium-238 ratios in sea water. in M. Sears (Editor), *Progress in Oceanography*, v.3, Pergamon Press, London, p.173
- KOLODNY, Y., and I.R. Kaplan, 1970, Uranium isotopes in sea-floor phosphorites. *Geochim. Cosmochim. Acta*, v.34, p.3-24
- KOMURA, K., and M. Sakanoue, 1967, Studies on the dating methods for Quaternary samples by natural alpha-radioactive nuclides. *Sci. Rep. Kanazawa Univ.*, v.12 (1), p.21
- KONISHI, K., A. Omura and T. Kimura, 1968, U^{234}/Th^{230} dating of some late Quaternary coralline limestones from Southern Taiwan (Formosa). *Geology and Palaeontology of Southeast Asia*, V, p.211-224

KONISHI, K., S.O. Schlanger and A. Omura, 1970, Neotectonic rates in the Central Ryukyu Islands derived from Th²³⁰ coral ages. *Marine Geol.* v.9, p.225-240

KRAUS, K.A. and F. Nelson, 1956, Anion exchange studies of the fission products. in *Proc. Int. Conf., Peaceful Uses of Atom. Energy, Geneva, 1955*, v.7, P/837, p.113-125

KRONFELD, J., 1971, Hydrologic investigations and the significance of U²³⁴/U²³⁸ disequilibrium in the ground waters of Central Texas. in *Development of Remote Methods for Obtaining Soil Information and Location of Construction Materials Using Gamma Ray Signitures for Project THEMIS, Semi-annual report to U.S. Army Engineer, Dept. of Geology, Rice University, Houston, Texas*

KU, T.L., 1968, Protactinium-231 method for dating corals from Barbados Island. *J. Geophys. Res.*, v.73 (6), p.2271

KU, T.L. and W.S. Broecker, 1967, Uranium, thorium and protactinium in a manganese nodule. *Earth Planet. Sci. Lett.*, v.2, p.317-320

KUKLA, J., 1970, Correlations between loesses and deep-sea sediments. *Geologiska Foreningen i Stockholm Forhandlingar*, v.92 (2), p.148-176

LABEYRIE, J., J.C. Duplessy, G. Delibrias and R. Letolle, 1967a, Etude des temperatures des climats anciens, par la mesure de l'oxygen-18 du carbone-13 et du carbone-14 dans les concretions des cavernes. in *Symposium of Radio-active Dating and Methods of Low Level Counting, Proc. of IAEA Symposium, Monaco, 1967, SM-87/5*, p.153-160

LABEYRIE, J., C. Lalou and G. Delibrias, 1967b, Etude des transgressions marines sur an atoll du Pacifique par les methodes du carbone-14 et du rapport uranium-234/thorium-230. in *Symposium of Radioactive Dating and Methods of Low Level Counting, Proc. of IAEA Symposium, Monaco, 1967, SM-87/71*, p.349-357

- LAL, D., 1963, On the investigations of geophysical processes using cosmic ray produced radioactivity. in J. Geiss and E.D. Goldberg (Editors), Earth Science and Meteoritics, North Holland Publishing Co., Amsterdam, p.115-140
- LAL, D., J.R. Arnold and B.L.K. Somayajulu, 1964, A method for the extraction of trace elements from sea water. Geochim. Cosmochim. Acta., V.28, p.1111-1117
- LAMB, H.H. and A. Woodroffe, 1970, Atmospheric circulation during the last ice age. Quaternary Res., v.1, p.29-58
- MATTHEWS, W.H. and G.H. Curtis, 1966, Date of the Pliocene-Pleistocene boundary in New Zealand. Nature, v.212, p.979
- MCCREA, J.M., 1950, On the isotopic chemistry of carbonates and a paleotemperature scale. J. Chem. Phys., v.18, p.849-857
- MCDUGALL, I., and H. Wensink, 1966, Paleomagnetism and geochronology of the Pliocene-Pleistocene lavas in Iceland. Earth Planet. Sci. Lett., v.1, p.232
- MERRILL, J.R., E.F.X. Lyden, M. Honda and J.R. Arnold, 1960, The sedimentary geochemistry of the beryllium isotopes. Geochim. Cosmochim. Acta, v.18, p.108
- MESOLELLA, K.J., R.K. Matthews, W.S. Broecker and D.L. Thurber, 1969, The astronomical theory of climatic change: Barbados data. J. Geol., v.77, p.250-274
- MICHALEK, D.D., 1969, Fanlike features and related periglacial phenomena of the Southern Blue Ridge. Ph.D. Dissertation, University of North Carolina
- MIYAKE, Y., Y. Sugimura and T. Uchida, 1966, Ratio U^{234}/U^{238} and the uranium concentration in sea water in the Western North Pacific. J. Geophys. Res., v.71, p.3083

- MO, T., B.C. O'Brien and A.D. Suttle, 1970, Uranium: further investigations of uranium content of Caribbean cores P6304-8 and P6304-9. *Earth Planet. Sci. Lett.*, v.10, p.175
- MOORE, G.W., 1956, Aragonite speleothems as indicators of paleotemperature. *Amer. J. Sci.*, v.254, p.746-753
- MOORE, G.W., 1962, The growth of stalactites. *Nat. Speleol. Soc., Bull.*, v.24, p.98-99
- MOORE, G.W. and Brother G. Nicholas, 1964, *Speleology (the study of caves)*. Heath & Co., Boston, 120 pp.
- MOORE, W.S., 1969, Measurement of Ra^{228} and Th^{228} in sea water. *J. Geophys. Res.*, v.74, p.694
- MOSER, H. and W. Stichler, 1970, Deuterium measurement on snow samples from the Alps. in *Isotope Hydrology 1970, Proc. of an IAEA Symposium, Vienna, IAEA-SM-129/4*, p.43-57
- MUNNICH, K.O. and J.C. Vogel, 1959, C^{14} -altersbestimmung von süßwasser-Kalkablagerungen. *Naturwiss.*, v.46, p.169
- NIR, A., 1964, On the interpretation of tritium age measurements of ground water. *J. Geophys. Res.*, v.69 (12), p.2589-2595
- NGUYEN, H.V. and C. Lalou, 1969, Détermination simultanée du rapport isotopique $^{234}\text{U}/^{238}\text{U}$ et de la teneur en uranium-238 dans les eaux naturelles. *Radiochim. Acta.*, v.12 (13), p.156-160
- OLSEN, I.U., 1970, Radiocarbon variations and absolute chronology. *Proc. 12th Nobel Symposium, Uppsala, 1969, Wiley Interscience Div., New York*, 652 pp.
- OMURA, A. and K. Konishi, 1970, Evaluation of apparent ionium ages of some hermatypic corals. *Geol. Soc. Japan, J.*, v.8, p.391-397

- O'NEIL, J.R., R.N. Clayton and T. Mayeda, 1969, Oxygen isotope fractionation in divalent metal carbonates. *J. Chem. Phys.*, v.30 (12), p.5547-5558
- OSMOND, J.K., J.R. Carpenter and H.L. Windom, 1965, $\text{Th}^{230}/\text{U}^{234}$ age of the Pleistocene corals and oolites of Florida. *J. Geophys. Res.*, v.70 (8), p.1843-1847
- OSMOND, J.K., J.P. May and W.F. Tanner, 1970, Age of the Cape Kennedy barrier and lagoon complex. *J. Geophys. Res.*, v.75, p.469-479
- OSMOND, J.K., H.S. Rydell and M.I. Kaufman, 1968, Uranium disequilibrium in groundwater: an isotope dilution approach in hydrologic investigations. *Science*, v.162, p.997-999
- PETRANEK, J., and Z. Pouba, 1951, Dating of the development of the Domica Cave. Based on the study of the dark zones in the travertine formations. *Sbornik Ustredniho ustavu geologickeho Venovany k Sedesatinam Profesora Dr. Radima Kettnera, XVIII*, p.245-72 (in Czech. with an English summary)
- PILKEY, O.H. and H.G. Goodell, 1964, Comparison of the composition of fossil and recent mollusk shells. *Geol. Soc. Amer., Bull.*, v.75, p.217-228
- PITTY, A.F., 1966, An approach to the study of karst water. *Occasional Papers in Geography No. 5*, University of Hull, England
- PRICE, P.H. and E.T. Heck, 1939, West Virginia Geological Survey, Greenbrier County, Published by U.S.G.S.
- POSKANZER, A.M. and B.M. Foreman, Jr., 1961, A summary of TTA extraction coefficients. *J. Inorg. Nuc. Chem.*, v.16, p.323-336
- RICHMOND, G.M., 1970, Comparison of the Quaternary stratigraphy of the Alps and Rocky Mountains. *Quaternary Res.*, v.1, p.3-28

- RIGHTMIRE, C.T. and B.B Hanshaw, 1971, Relationship between the carbon isotopic composition of soil CO₂ and dissolved carbonate species in ground water (Abstract). Amer. Geophys. Union Trans., v.52, p.366
- RONA, E., and C. Emiliani, 1969, Absolute dating of Caribbean cores P6304-8 and P6304-9. Science, v.163, p.66-68
- ROQUES, H., 1969, A review of present-day problems in the physical chemistry of carbonates in solution. Cave Res. Group Gt. Brit., Trans., v.11,(3), p.139
- ROSHOLT, J.N., Jr., 1957, Quantitative radiochemical methods for the determination of the sources of natural radioactivity. Anal. Chem., v.29, p.1398
- ROSHOLT, J.N., Jr. and P.S. Antal, 1962, Evaluation of the Pa²³¹/U-Th²³⁰/U method for dating Pleistocene carbonate rocks. Geol. Survey Research, Prof. Paper 209, E108-E111
- ROSHOLT, J.N., Jr., C. Emiliani, J. Geiss, F.F. Koczy and P.J. Wangersky, 1961, Absolute dating of deep-sea cores by the Pa²³¹/Th²³⁰ method. J. Geol., v.69 (2), p.162
- RUTHERFORD, J.M., 1971, Factors affecting cavern development in the Great Savannah, West Virginia. Caves Karst, v.13 (6), p.48 (abstract)
- SACKETT, W.M., 1958, Ionium-uranium ratios in marine deposited CaCO₃ and related materials. Ph.D. Dissertation, Washington University
- SACKETT, W.M., 1966, Manganese nodules: Th²³⁰: Pa²³¹ ratios. Science, v.154, p.646-647
- SAVAGE, D.E. and G.H. Curtis, 1970, The Villafranchian stage - age and its radiometric dating. Geol. Soc. Amer., Spec. Paper 124, p.207
- SCHAEFFER, O.A., 1967, Direct dating of fossils by the He-U method. in Radioactive Dating and Methods of Low Level Counting, Proc. IAEA Symposium, Vienna, 1967, SM87-60, p.395-402

- SCHAEFFER, O.A. and R. Davis, 1958, Cl^{36} in nature. New York Acad. Sci. Ann., v.62, p.105
- SCHILLAT, B., 1969, Volcanic ash horizons in layered dripstone and cave sediments. Caves Karst, v.11 (6), p.41-48
- SCHLANGER, S.O., W.M. Sackett and H.A. Potratz, 1963, Dating of carbonate rocks by ionium and uranium ratios. U.S.Geol. Surv., Prof. Paper 260-BB, p.1053-1066
- SCHWARCZ, H.P., 1971, Conversion of mass spectrometric data for C, O, S. Technical Memo-71-7, Dept. of Geology, McMaster University
- SHOTTON, F.W., 1967, The problems and contributions of methods of absolute dating within the Pleistocene period. Geol. Soc. Lond., J., v.122, p.357-383
- SOMAYAJULA, B.L.K. and E.D. Goldberg, 1966, Thorium and uranium isotopes in sea water and sediments. Earth Planet. Sci. Lett., v.1, p.102-106
- STEARNS, C.E. and D.L. Thurber, 1967, Th^{230}/U^{234} dates of late Pleistocene marine fossils from the Mediterranean and Moroccan littorals. Prog. in Oceanography, v.4, p.293-305
- STEINEN, P.S., R.S. Harrison and R.K. Matthews, 1973, Eustatic low stand of sea level between 125,000 and 105,000 years B.P.: evidence from the subsurface of Barbados, West Indies. Geol. Soc. Amer., Bull., v.84, p.63-70
- STUIVER, M., 1968, Oxygen-18 content of atmospheric precipitation during the last 11,000 years in the Great Lakes Region. Science, v.162, p.994-997
- SZABO, B.J. and J.N. Rosholt, 1969, Uranium-series dating of Pleistocene molluscan shells from Southern California - an open system model. J. Geophys. Res., v.74 (12), p.3253-3260

- TARUTANI, T, R.N. Clayton and T. Mayeda, 1969, The effect of polymorphism and magnesium substitution on oxygen isotope fractionation between calcium carbonate and water. *Geochim. Cosmochim. Acta*, v.33, p.987-996
- THURBER, D.L., 1962, Anomalous U^{234}/U^{238} in nature. *J. Geophys. Res.*, v.67, p.4518-4520
- THURBER, D.L., 1964, Natural variation in the ratio U^{234}/U^{238} and an investigation of the potential of U^{234} for Pleistocene chronology. Ph.D. Dissertation, Columbia University
- THURBER, D.L., W.S. Broecker, R.L. Blanchard and H.A. Potratz, 1965, Uranium-series ages of coral from Pacific atolls. *Science*, v.149, p.55-58
- UREY, H.C., 1947, The thermodynamic properties of isotopic substances. *J. Chem. Soc.*, p.562
- UREY, H.C. C. McKinney and J. McCrea, 1948, Method for measurement of Paleotemperatures. *Geol. Soc. Amer., Bull.*, v.59, p.1359
- VEEH, H.H., 1966, Th^{230}/U^{238} and U^{234}/U^{238} ages of Pleistocene high sea level stand. *J. Geophys. Res.*, v.71 (14), p.3379-3386
- VEEH, H.H. and J. Chappell, 1970, Astronomical theory of climate change: support from New Guinea. *Science*, v.167, p.862-865
- VEEH, H.H. and R. Geigengack, 1970, Uranium-series ages of corals from the Red Sea. *Nature*, v.226, p.155-156
- VILENSKII, D.G., 1957, *Soil Science*. 3rd Edition, trans. by A. Birron, and Z.S. Cole (1963). Israel Program for Scientific Translations, Monson, Jerusalem
- VOGEL, J.C. and D. Ehhalt, 1963, Use of carbon isotopes in ground water. *in* *Radioisotopes in Hydrology*, Proc. Int. Symposium, IAEA, Vienna, p.380

WARWICK, G.T., 1962, Cave formations and deposits. in C.H.D. Cullingford (Editor), British Caving, Routledge and Kegan Paul Ltd., London, p.83-119

WELLS, A.W., 1971, Cave calcite. Stud. Spel., v.2, (3-4) p.129-148

WENDT, I., 1968, Fractionation of carbon isotopes and temperature dependence in the system CO_2 -gas- CO_2 in solution and HCO_3^- - CO_2 in solution. Earth Planet. Sci. Lett., v.4, p.64-68

WHITE, W.B. and J.J. Van Gundy, 1971, Geological reconnaissance of Timpanogos Cave, Utah. Paper presented at the 28th Nat. Spel. Soc. Conf., Blacksburg, Va., 1971

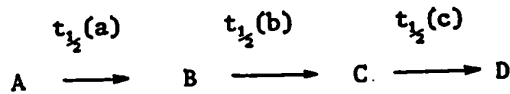
WOLFE, T.E., Sedimentation in three selected karst basins along the Allegheny Front of S.E. West Virginia. Ph.D. Dissertation, McMaster University, Hamilton (to be submitted).

ZEUNER, F.E., 1959, The Pleistocene Period, Hutchison, London, pp447.

APPENDIX I

DERIVATION OF THE TH ²³⁰/U ²³⁴ AGE RELATIONSHIP

Consider the sequential decay of an isotope A to daughters B, C and D.



$t_{1/2}(a)$ is the half-life of isotope A.

$t_{1/2}(b)$ is the half-life of isotope B.

$t_{1/2}(c)$ is the half-life of isotope C.

Let N_a^0, N_a = number of atoms of A at time t=0 and time t respectively.
 N_b^0, N_b = number of atoms of B at time t=0 and time t respectively.
 N_c^0, N_c = number of atoms of C at time t=0 and time t respectively.

then $\frac{dN_a}{dt} = -\lambda_a N_a$ where $\lambda_a = \frac{0.693}{t_{1/2}(a)}$

$$\frac{dN_b}{dt} = \lambda_a N_a - \lambda_b N_b \quad \text{where } \lambda_b = \frac{0.693}{t_{1/2}(b)}$$

and $\frac{dN_c}{dt} = \lambda_b N_b - \lambda_c N_c$ where $\lambda_c = \frac{0.693}{t_{1/2}(c)}$

The equation for radioactive decay gives:

$$N_a = N_a^0 e^{-\lambda_a t}$$

Therefore $\frac{dN_b}{dt} + \lambda_b N_b = \lambda_a N_a^0 e^{-\lambda_a t}$ (1)

multiply through by $e^{\lambda_b t}$ and rearrange:

$$\frac{d(N_b e^{\lambda_b t})}{dt} = \lambda_a N_a^0 e^{-(\lambda_a - \lambda_b)t}$$

integration gives

$$N_b \cdot e^{\lambda_b t} = \frac{\lambda_a}{\lambda_b - \lambda_a} \cdot N_a^0 \cdot e^{-(\lambda_a - \lambda_b)t} + K \quad \dots\dots\dots(2)$$

to find K put $t=0$; $N_b = N_b^0$ at $t=0$

$$\text{then} \quad K = N_b^0 - \frac{\lambda_a}{\lambda_b - \lambda_a} \cdot N_a^0 \quad \dots\dots\dots(3)$$

from (2) and (3)

$$N_b = \frac{\lambda_a}{\lambda_b - \lambda_a} \cdot N_a^0 \cdot (e^{-\lambda_a t} - e^{-\lambda_b t}) + N_b^0 \cdot e^{-\lambda_b t} \quad \dots\dots\dots(4)$$

when $A = U^{238}$ and $B = U^{234}$

$$e^{-\lambda_a t} = 1 \quad \text{and} \quad (\lambda_b - \lambda_a) = \lambda_b$$

$$\text{then} \quad N_b \lambda_b = \lambda_a N_a^0 \cdot (1 - e^{-\lambda_b t}) + N_b^0 \lambda_b \cdot e^{-\lambda_b t}$$

rearranging:

$$\left[\frac{N_b \lambda_b}{N_a^0 \lambda_a} - 1 \right] = \left[\frac{\lambda_b N_b^0}{\lambda_a N_a^0} - 1 \right] \cdot e^{-\lambda_b t}$$

since activity $\propto \frac{dN}{dt} \propto \lambda N$

$$\text{then} \quad \left(\frac{[U^{234}]}{[U^{238}]} - 1 \right) = \left(\frac{[U^{234}]_0}{[U^{238}]_0} - 1 \right) \cdot e^{-\lambda_{234} t}$$

$\left[\frac{U^{234}}{U^{238}} \right]$ is the activity ratio at time t

$\left[\frac{U^{234}}{U^{238}} \right]_0$ is the activity ratio at time $t=0$.

$$\text{now, } \lambda_b N_b = \frac{dN_c}{dt} + \lambda_c N_c$$

substituting for N_b in (4)

$$\frac{dN_c}{dt} + \lambda_c N_c = \lambda_b \left\{ \frac{\lambda_a}{\lambda_b - \lambda_a} \cdot N_a^0 (e^{-\lambda_a t} - e^{-\lambda_b t}) + N_b^0 e^{-\lambda_b t} \right\}$$

multiplying by $e^{\lambda_c t}$ and rearranging gives:

$$\begin{aligned} \frac{d(e^{\lambda_c t} N_c)}{dt} &= \frac{\lambda_a \lambda_b}{\lambda_b - \lambda_a} \cdot N_a^0 e^{-(\lambda_a - \lambda_c)t} - \frac{\lambda_a \lambda_b}{\lambda_b - \lambda_a} N_a^0 e^{-(\lambda_b - \lambda_c)t} \\ &\quad + \lambda_b N_b^0 e^{-(\lambda_b - \lambda_c)t} \end{aligned}$$

integration gives:

$$\begin{aligned} e^{\lambda_c t} N_c &= \frac{\lambda_a \lambda_b}{(\lambda_b - \lambda_a)(\lambda_c - \lambda_a)} \cdot N_a^0 e^{-(\lambda_a - \lambda_c)t} - \frac{\lambda_a \lambda_b N_a^0 e^{-(\lambda_b - \lambda_c)t}}{(\lambda_b - \lambda_a)(\lambda_c - \lambda_b)} \\ &\quad + \frac{\lambda_b N_b^0 e^{-(\lambda_b - \lambda_c)t}}{(\lambda_c - \lambda_b)} + K \end{aligned}$$

when $A = U^{238}$, $B = U^{234}$ and $C = Th^{230}$

$$\lambda_b - \lambda_a = \lambda_b \quad \text{and} \quad \lambda_c - \lambda_a = \lambda_c$$

also at $t=0$, $N_c = 0$ (i.e. no initial Th^{230} present)

therefore:

$$K = \frac{\lambda_a \lambda_b N_a^0}{(\lambda_b - \lambda_c)(\lambda_c - \lambda_a)} + \frac{\lambda_a \lambda_b}{(\lambda_b - \lambda_c)(\lambda_c - \lambda_b)} N_a^0 - \frac{\lambda_b N_b^0}{\lambda_c - \lambda_b}$$

substituting for K and rearranging:

$$N_c = \frac{\lambda_a N_a^0}{\lambda_c} (e^{-\lambda_a t} - e^{-\lambda_c t}) - \frac{\lambda_a N_a^0}{\lambda_c - \lambda_b} (e^{-\lambda_b t} - e^{-\lambda_c t}) \\ + \frac{\lambda_b N_b^0}{\lambda_c - \lambda_b} (e^{-\lambda_b t} - e^{-\lambda_c t})$$

for $t < 10^6$ yrs., $e^{-\lambda_a t} \approx 1$

therefore:

$$N_c \lambda_c = \lambda_a N_a^0 \cdot \left[(1 - e^{-\lambda_c t}) - \frac{\lambda_c}{\lambda_c - \lambda_b} (e^{-\lambda_b t} - e^{-\lambda_c t}) \right] \\ + \frac{\lambda_b N_b^0}{\lambda_a N_a^0} \cdot \frac{\lambda_c}{\lambda_c - \lambda_b} (e^{-\lambda_b t} - e^{-\lambda_c t})$$

but $\left[\frac{N_b \lambda_b}{N_a \lambda_a} - 1 \right] = \left[\frac{N_b \lambda_b}{N_a \lambda_a} - 1 \right] \cdot e^{\lambda_b t}$

therefore:

$$N_c \lambda_c = \lambda_a N_a^0 \cdot \left[(1 - e^{-\lambda_c t}) - \frac{\lambda_c}{\lambda_c - \lambda_b} \cdot \left(\frac{N_b \lambda_b}{N_a \lambda_a} - 1 \right) e^{\lambda_b t} \cdot (e^{-\lambda_b t} - e^{-\lambda_c t}) \right] \\ = \lambda_a N_a^0 \cdot \left[(1 - e^{-\lambda_c t}) - \frac{\lambda_c}{\lambda_c - \lambda_b} \cdot \left(\frac{N_b \lambda_b}{N_a \lambda_a} - 1 \right) (1 - e^{-(\lambda_c - \lambda_b)t}) \right]$$

activity $\propto \frac{dN}{dt} \propto \lambda N$

therefore: $\lambda_c N_c = \text{Th}^{230}$ activity at time t

$\lambda_a N_a^0 = U^{238}$ activity at time t=0 (= activity at time t)

$\frac{\lambda_b N_b}{\lambda_a N_a} = \frac{U^{234}}{U^{238}}$ activity ratio at time t.

therefore:

$$\frac{\text{Th}^{230}}{U^{238}} = (1 - e^{-\lambda_{230}t}) - \frac{\lambda_{230}}{\lambda_{230} - \lambda_{234}} \cdot \left(\frac{U^{234}}{U^{238}} - 1 \right) (1 - e^{-(\lambda_{230} - \lambda_{234})t})$$

multiplying by U^{238}/U^{234} gives

$$\frac{\text{Th}^{230}}{U^{234}} = \frac{(1 - e^{-\lambda_{230}t})}{U^{234}/U^{238}} - \frac{\lambda_{230}}{\lambda_{230} - \lambda_{234}} \left(1 - \frac{U^{234}}{U^{238}} \right) (1 - e^{-(\lambda_{230} - \lambda_{234})t})$$

APPENDIX II

U DATE II - A PROGRAM TO CALCULATE U-Th ISOTOPE RATIOS, $\text{Th}^{230}/\text{U}^{234}$ AGES AND ERRORS

This program, written in FORTRAN IV, is designed to calculate $\text{Th}^{230}/\text{U}^{234}$, $\text{U}^{234}/\text{U}^{238}$ and $\text{Th}^{230}/\text{Th}^{232}$ isotope ratios from uncorrected Th^{230} , Th^{232} , U^{238} and U^{234} count rates. Raw count rates are corrected for contributions due to background and U-Th contamination of the reagents. From the $\text{Th}^{230}/\text{U}^{234}$ ratio an age is calculated and then used to calculate the initial $\text{U}^{234}/\text{U}^{238}$ ratio, $(\text{U}^{234}/\text{U}^{238})_0$. The $\text{Th}^{230}/\text{U}^{234}$ age is calculated using an iterative method. An estimate of the age (t_0) is used to calculate t^* , the true age of the sample by the Newton method of successive approximations. This method states that if $F(x) = 0$ then

$$t_{n+1} = t_n - \frac{F(t_n)}{F'(t_n)}$$

where t_n = the nth iterative step

$$F(t) = - \frac{\text{Th-230}}{\text{U-234}} + (1 - e^{-\lambda_{230}t}) \frac{\text{U-238}}{\text{U-234}} + \frac{\lambda_{230}}{\lambda_{230} - \lambda_{234}} \left(1 - \frac{\text{U-238}}{\text{U-234}}\right) \cdot (1 - e^{-(\lambda_{230} - \lambda_{234})t})$$

$$\text{and } F'(t) = \frac{\text{U-238}}{\text{U-234}} \lambda_{230} e^{-\lambda_{230}t} + \lambda_{230} \left(1 - \frac{\text{U-238}}{\text{U-234}}\right) (1 - e^{-(\lambda_{230} - \lambda_{234})t})$$

$F'(x)$ is the derivative of $F(x)$.

$$\text{When } \frac{t_{n+1} - t_n}{t_{n+1}} < 0.001$$

$$t_{n+1} = t^*$$

$(U^{234}/U^{238})_0$ is calculated from the Th^{230}/U^{234} age and the measured U^{234}/U^{238} ratio.

Uranium concentrations are calculated using the calibration curve shown in Chapter 5 (Figure 5.5). If 5.0 mls Th^{228}/U^{232} spike with a U^{232} activity of 4.64 c/min are added then in terms of the program language

$$(U) = \frac{TN1 * 4.64 * 5.0}{TN3 * 0.17 * WEIGHT}$$

where

(U) = uranium concentration

TN1 = corrected U^{238} count rate

TN3 = corrected U^{232} count rate

0.17 = count rate for 1 μ gm U. (Det 2, Figure 5.5, p.170)

WEIGHT = weight of sample dissolved

This accounts for the factor 136.5 (B) in the program. This factor is constant for a given source-detector geometry and spike activity.

The program allows for the use of either a Th^{228}/U^{232} spike or a Th^{227}/U^{232} spike mixture. The decay of Th^{228} or Th^{227} during the experiment is corrected for. If Th^{227} is used as a tracer, allowance is made for the growth of Ra^{223} during the counting period. (It is assumed that Ra^{223} starts to grow into equilibrium with Th^{227} at

the same time as the counting period starts, therefore the final Th extraction into TTA must be completed immediately prior to starting the thorium count. Th^{227} derived from decay of U^{235} is corrected for by using the total Th^{227} activity (corrected for decay) to compute an approximate age for the sample then this age is used to compute an approximate age for the sample then this age is used to compute a $\text{Th}^{227}/\text{U}^{235}$ ratio. The natural Th^{227} activity is then subtracted from the total Th^{227} activity and a second age calculated. This iterative procedure is repeated until two consecutive age determinations differ by less than 0.1%.

Two examples of the input and computer output are listed on pages 351 and 352.

```

C
C          PROGRAM CORRECTS RAW COUNT RATE DATA AND COMPUTES TH-230/U-234
C          U-234/U-238 AND TH-230/TH-232 ISOTOPE RATIOS. THE AGE AND
C          ERROR IN THE AGE IS CALCULATED FROM TH-230/U-234 AND U-234/U-238
C          RATIOS
C          N1=U-238 COUNT RATE
C          N2=U-234 COUNT RATE
C          N3=U-232 COUNT RATE
C          N4=TH-232 COUNT RATE
C          N5=TH-230 COUNT RATE
C          N6=TH-228 OR TH-227 COUNT RATE
C          SPIKE = TH-228/U-232 OR TH-227/U-232 ACTIVITY RATIO IN SPIKE
C          CNTU = ACCUMULATION TIME FOR U SPECTRUM (MINS)
C          CNTT = ACCUMULATION TIME FOR TH SPECTRUM (MINS)
C          WEIGHT = WT OF SAMPLE IN GMS
C          DCTH = DELAY BETWEEN COUNTING TH-227 AND SEPARATION FROM AC-227 (MINS)
C          DECT = DELAY BETWEEN COUNTING TH-228 AND SEPARATION FROM U-232 (DAYS)
C          B1 = COUNTER BACKGROUND CORRECTION FOR U-238 AND TH-232
C          B2 = COUNTER BACKGROUND CORRECTION FOR U-234 AND TH-230
C          B3 = COUNTER BACKGROUND CORRECTION FOR U-232 AND TH-228
C          B4 = COUNTER BACKGROUND CORRECTION FOR TH-227
C          B5 = MULTIPLICATION FACTOR TO ALLOW FOR VARIATIONS IN AMOUNT
C              OF SPIKE USED
C          B = MULTIPLICATION FACTOR TO COMPUTE U CONCENTRATION FROM
C          U-238 COUNT RATES
C          *****
C          REAL N1,N2,N3,N4,N5,N6,N12,N52,N36,N54,NT52,N21,NN6,LAM7,LAM3
100  READ(5,199)IU,ITH
199  FORMAT(2I1)
      IF(IU.EQ.0)GO TO 101
      IF(IU.EQ.1)GO TO 200
101  READ(5,102)TITLE,TGS,CNTU,CNTT,SPIKE,WEIGHT,DECT,DCTH
102  FORMAT(A8,7E10.0)
      IF(EOF(5))999,997
997  CONTINUE
103  READ(5,104)N1,N2,N3,N4,N5,N6
104  FORMAT(6F10.0)
105  READ(5,106)B1,B2,B3,B4,B,B5
106  FORMAT(6F10.4)
      TAPPX=0.0
      NLOOP=0
      TN3=N3-B3
C          *****
C          YU = PERCENT YIELD OF URANIUM
C          ACTIVITY OF 5.0 ML 232 SPIKE = 24.17 C/M
C          *****
C          YU=100.*TN3/(24.17*B5)
C          *****
C          CORRECTION FOR U REAGENT BLANK
C          U-238 = 0.0568 C/M
C          U-234 = 0.0832 C/M
C          *****
C          TRB1=0.0568*YU/100.
C          TRB2=0.0832*YU/100.
C          TN1=N1-B1-TRB1
C          TN2=N2-B2-TRB2
C          IF(ITH.EQ.0)GO TO 107
C          IF(ITH.EQ.1) GO TO 108
107  SN6=N6-B3-N4

```

```

C
C
C
C
*****
CORRECTION FOR TH-228 DECAY
*****
THALF8=9.94E-4
TN6=SN6*EXP(THALF8*DECT)
YT=(100.*TN6)/(24.17*SPIKE*B5)
GO TO 109
108 NN6=(N6-B4)*CNTT
C
C
C
C
*****
CORRECTION FOR TH-227 DECAY AND RA-223 GROWTH
TN6=COUNT RATE FOR TH-227 CORRECTED FOR DECAY
TN7=CALCULATED COUNT RATE FOR RA-223
NN6=TOTAL NO COUNTS FOR TH-227+RA-223
*****
LAM7=2.6448E-5
LAM3=4.2113E-5
XA=EXP(LAM7*DCTH)
XB=1.0/LAM7
XC=(EXP(-LAM7*CNTT))/LAM7
XD=(EXP(-LAM3*CNTT))/LAM3
XF=1.0/LAM3
TN6=XA*(NN6/(XB-XC+1.688*(XD-XC-XF+XB)))
TN7=(TN6*1.688*(XD-XC-XF+XB))/CNTT
YT=(100.*TN6)/(24.17*SPIKE*B5)
109 CONTINUE
C
C
C
C
*****
CORRECTION FOR TH REAGENT BLANK
TH-232 = 0.0398 C/M
TH-230 = 0.0880 C/M
*****
TRB4=0.0398*YT/100.
TRB5=0.088*YT/100.
TN4=N4-B1-TRB4
IF(TN4.LT.1.E-20)TN4=1.E-20
TN5=N5-B2-TRB5
C
C
C
*****
PERCENT CORRECTION OF TOTAL COUNTS FOR BLANK AND B'GROUND
*****
BN1=B1+TRB1
BN2=B2+TRB2
BN3=B3
BN4=B1+TRB4
BN5=B2+TRB5
BN6=B3
P1=100.*BN1/ N1
P2=100.*BN2/ N2
P3=100.*BN3/ N3
P4=100.*BN4/ N4
P5=100.*BN5/ N5
P6=100.*BN6/ N6
CONCU=(B*TN1)/(TN3*WEIGHT)
C
C
C
C
*****
CALCULATION OF ISOTOPE RATIOS AND ERRORS IN THESE RATIOS
DUE TO STATISTICAL ERRORS IN THE COUNT RATE
N12 = MEASURED U-234/U-238 ISOTOPE RATIO
N52 = MEASURED TH-230/U-234 ISOTOPE RATIO

```

```

C      N54 = MEASURED TH-230/TH-232 ISOTOPE RATIO
C      N36 = MEASURED U-232/TH-228 ISOTOPE RATIO
C      NT52 = ACTUAL TH-230/U-234 ISOTOPE RATIO
N12=TN2/TN1
N52=TN5/TN2
N54=TN5/TN4
N36=TN3/TN6
NT52=N52*N36*SPIKE
C      ERR1 = ERROR IN U-238 COUNT RATE ETC.
ERR1=SQRT(TN1/CNTU)
ERR2=SQRT(TN2/CNTU)
ERR3=SQRT(TN3/CNTU)
ERR4=SQRT(TN4/CNTT)
ERR5=SQRT(TN5/CNTT)
ERR6=SQRT(TN6/CNTT)
C      BR1= ERROR IN U-238 REAGENT BLANK CORRECTION ETC.
BR1=0.0056
BR2=0.0212
BR4=0.0047
BR5=0.0146
C      ER1 = TOTAL ERROR IN U-238 ETC.
ER1=SQRT((ERR1*ERR1)+(BR1*BR1))
ER2=SQRT((ERR2*ERR2)+(BR2*BR2))
ER3=ERR3
ER4=SQRT((ERR4*ERR4)+(BR4*BR4))
ER5=SQRT((ERR5*ERR5)+(BR5*BR5))
ER6=ERR6
ER12=(TN2/TN1)*SQRT(ER1*ER1/(TN1*TN1)+ER2*ER2/(TN2*TN2))
ER52=(TN5/TN2)*SQRT(ER5*ER5/(TN5*TN5)+ER2*ER2/(TN2*TN2))
ER36=(TN3/TN6)*SQRT(ER3*ER3/(TN3*TN3)+ER6*ER6/(TN6*TN6))
ERT52= NT52*SQRT(ER52*ER52/(N52*N52)+ER36*ER36/(N36*N36))
IF(ITH.LT.1.0)GO TO 110
C      ER7 = ERROR IN U-232/TH-227 SPIKE RATIO
ER7=0.06
ERRT52=SQRT((ERT52*ERT52)+(ER7*ER7))
ERRT52=ERT52
TN6OLD=TN6
110 CONTINUE
NT52=(TN5*TN3*SPIKE)/(TN2*TN6)
IF(NT52.LT.1.0)GO TO 112
C      *****
C      TTN1 = U-238 CORRECTED FOR 100 PERCENT YIELD
C      TN35 = U-235 (1/21.7 TIMES U-238 ACTIVITY)
C      TNN6 = TH-227 ASSUMING 100 PERCENT YIELD
C      *****
111 TTN1=TN1*100./YU
TN35=TTN1/21.7
TNN6=TN35*YT/100.
TN6=TN6OLD-TNN6
P7=100.*TNN6/TN6
NT52=(TN5*TN3*SPIKE)/(TN2*TN6)
IF(NT52.LT.1.0)GO TO 112
THALF4=2.795E-6
RU0=((N12)-1.0)*EXP(THALF4*300000.)+1.0
GO TO 116
112 R52=NT52

```

```

C      T=TGS
      CALL THDATE(R52,N12,T,TN1,TN2)
C      *****
C      SUBROUTINE THDATE SOLVES AGE EQUATION BY AN ITERITIVE METHOD
C      *****
      IF(ITH.LT.1) GO TO 115
      TTN1=TN1*100./YU
      TTN6=TTN1*(1.-EXP(2.133E-5*T))/21.7
      TNN6=TTN6*YT/100.
      IF(ABS((TAPPX-T)/T).LT.0.0005) GO TO 115
      TN6=TN6OLD-TNN6
      P7=100.*TNN6/TN6
      NLOOP=NLOOP+1
      TAPPX=T
      IF(NLOOP.GT.10)GO TO 113
      GO TO 110
113  WRITE(6,114)
114  FORMAT(* NO CONVERGENCE *)
115  TL=TGS
      R52=NT52-ERT52
      CALL THDATE(R52,N12,TL,TN1,TN2)
      TU=TGS
      R52=NT52+ERT52
      CALL THDATE(R52,N12,TU,TN1,TN2)
      TA=ABS((TU-TL)/2.0)
      I=(T+50.)/100.
      T=I*100
      I=(TA+50.)/100.
      TA=I*100
      CALL UDATE(N12,RU0,T)
C      *****
C      SUBROUTINE UDATE COMPUTES INITIAL U-234/U-238 RATIOS
C      FROM MEASURED U-234/U-238 AND CALCULATED AGE (T)
C      *****
      R12=N12+ER12
      CALL UDATE(R12,RU0U,TU)
      R12=N12-ER12
      CALL UDATE(R12,RU0L,TL)
      RU0A=ABS((RU0U-RU0L)/2.0)
116  U238= 7HU-238 =
      U234= 7HU-234 =
      U232=7HU-232 =
      TH227=8HTH-227 =
      TH228=8HTH-228 =
      TH230=8HTH-230 =
      TH232=8HTH-232 =
      CM=5HC/MIN
      ER=7HERROR =
      PC=7HPERCENT
      IF(ITH.EQ.1) TH228=TH227
117  WRITE(6,118)
118  FORMAT(1H1)
      WRITE(6,119) TITLE,WEIGHT
119  FORMAT(* SAMPLE NO. = *,A10,5X,* SAMPLE WT. = *,F5.1, 1X,* GMS*)
      WRITE(6,120)
120  FORMAT(1H )

```

C

348

```
IF(ITH.EQ.1) GO TO 121
GO TO 123
121 WRITE(6,122)
122 FORMAT(* TH-227/U-232 SPIKE USED *)
123 WRITE(6,124)
124 FORMAT(* RAW DATA*)
WRITE(6,125)CNTU,CNTT
125 FORMAT(* U COUNT TIME = *,F5.0,1X,* MIN*,5X,* TH COUNT TIME = *,F
25.0,1X,* MIN*)
WRITE(6,126) U238, N1,CM, TH232, N4,CM
WRITE(6,126) U234, N2,CM, TH230, N5,CM
WRITE(6,126) U232, N3,CM, TH228, N6,CM
126 FORMAT(1X,A7,F8.3,2X,A3,5X,A8,F8.3,2X,A3)
WRITE(6,127)
127 FORMAT(20H *****)
WRITE(6,128)
128 FORMAT(* BACKGROUND AND REAGENT BLANK*)
WRITE(6,129)
129 FORMAT(*
ERROR ERROR*)
WRITE(6,130) U238,BN1,BR1,CM,TH232,BN4,BR4,CM
WRITE(6,130) U234,BN2,BR2,CM,TH230,BN5,BR5,CM
WRITE(6,130) U232,BN3,BR3,CM,TH228,BN6,BR6,CM
130 FORMAT(1X,A7,F8.3,2X,F4.3,1X,A3,5X,A8,F8.3,2X,F4.3,1X,A3)
WRITE(6,127)
WRITE(6,131)
131 FORMAT(* CORRECTED DATA*)
WRITE(6,129)
WRITE(6,132) U238,TN1,ER1,CM,TH232,TN4,ER4,CM
WRITE(6,132) U234,TN2,ER2,CM,TH230,TN5,ER5,CM
WRITE(6,132) U232,TN3,ER3,CM,TH228,TN6,ER6,CM
132 FORMAT(1X,A7,F8.3,2X,F4.3,1X,A3,5X,A8,F8.3,2X,F4.3,1X,A3)
WRITE(6,127)
WRITE(6,133)
133 FORMAT(* CORRECTIONS DUE TO BACKGROUND AND REAGENT BLANKS*)
WRITE(6,134)U238,P1,PC,TH232,P4,PC
WRITE(6,134)U234,P2,PC,TH230,P5,PC
WRITE(6,134)U232,P3,PC,TH228,P6,PC
134 FORMAT(1X,A7,F4.1,2X,A7,8X,A8,F4.1,2X,A7)
WRITE(6,120)
WRITE(6,127)
WRITE(6,135)CONCU
135 FORMAT(* URANIUM CONCENTRATION =*,F6.2,2X,* P.P.M.*)
WRITE(6,136)YU
136 FORMAT(* CHEMICAL YIELD OF URANIUM =*,F6.2,2X,* PERCENT*)
WRITE(6,137)YT
137 FORMAT(* CHEMICAL YIELD OF THORIUM =*,F6.2,2X,* PERCENT*)
WRITE(6,138)SPIKE
138 FORMAT(* SPIKE RATIO =*,F6.3)
WRITE(6,127)
IF(NT52.GE.1.0)GO TO 162
IF(ITH.EQ.1)GO TO 146
WRITE(6,139)
139 FORMAT(*
ERROR ERROR*
2)
WRITE(6,140 )N12,ER12,RU0,RU0A
140 FORMAT(* U-234/U-238 = *,F5.3,2X,F4.3,2X,* (U-234/U-238) ) = *,F5.3
```

```

C
      2,2X,F4.3)
      IF(N54.GT.999)GO TO 142
      WRITE(6,141 )NT52,ERT52,N54
141   FORMAT(* TH-230/U-234= *,F5.3,2X,F4.3,3X,* TH-230/TH/232 = *,F5.1)
      GO TO 144
142   WRITE(6,143 )NT52,ERT52,N54
143   FORMAT(* TH-230/U-234 = *,F5.3,2X,F4.3,3X,* TH-230/TH-232 = )1000*
2)
144   WRITE(6,145 )T,TA
145   FORMAT(* THORIUM AGE =*,F7.0,1X,F6.0,1X,* YEARS*)
      WRITE(6,127)
      GO TO 100
146   WRITE(6,147)
147   FORMAT(1H )
      WRITE(6,148)
148   FORMAT(20H *****)
149   FORMAT(* CORRECTIONS FOR TH-227 DECAY AND RA-223 GROWTH *)
      WRITE(6,150) N6,CM
150   FORMAT(* MEASURED TH-227 ACTIVITY = *,F7.3,1X,A3)
      WRITE(6,151)TN7,CM
151   FORMAT(* CALCULATED RA-223 ACTIVITY = *,F7.3,1X,A3)
      WRITE(6,152)TN6,CM
152   FORMAT(* CORRECTED TH-227 ACTIVITY = *,F7.3,1X,A3)
      WRITE(6,153 )TNN6,CM
153   FORMAT(* COMMON TH-227 = *,F7.3,1X,A3)
      WRITE(6,147)
      WRITE(6,148)
      IF(NT52.GE.1.0)GO TO 162
      WRITE(6,155)
155   FORMAT(*                               ERROR                               ERROR*
2)
      WRITE(6,156 )N12,ER12,RU0,RUOA
156   FORMAT(* U-234/U-238 = *,F5.3,2X,F4.3,2X,* (U-234/U-238)0 = *,F5.3
2,2X,F4.3)
      IF(N54.GT.999)GO TO 158
      WRITE(6,157 )NT52,ERT52,N54
157   FORMAT(* TH-230/U-234= *,F5.3,2X,F4.3,3X,* TH-230/TH/232 = *,F5.1)
      GO TO 160
158   WRITE(6,159 )NT52,ERT52,N54
159   FORMAT(* TH-230/U-234 = *,F5.3,2X,F4.3,3X,* TH-230/TH-232 = )1000*
2)
160   WRITE(6,161 )T,TA
161   FORMAT(* THORIUM AGE =*,F7.0,1X,F6.0,1X,* YEARS*)
      WRITE(6,148)
      GO TO 100
162   WRITE(6,1621)N12,ER12,RUO
1621  FORMAT(* U-234/U-238 = *,F5.3,2X,* ERROR= *,F5.4,4X,* INITIAL U-23
24/U-238 = *,F5.3,2X,* MINIMUM*')
      WRITE(6,163 )NT52,ERT52,N54
163   FORMAT(* TH-230/U-234= *,F5.3,2X,* ERROR= *,F5.4,4X,* TH-230/TH-23
22 = *,F5.1)
      WRITE(6,164)
164   FORMAT(* AGE IS ) 300,000 YEARS B.P.*)
      GO TO 100
200   READ(5,201)TITLE,CNTU,WEIGHT,N1,N2,N3
01   FORMAT(A8,5E10.0)

```



```

C
202  READ(5,202)B1,B2,B3,B
      FORMAT(4F10.4)
      TN1=N1-B1
      TN2=N2-B2
      TN3=N3-B3
      ER1=SQRT(TN1/CNTU)
      ER2=SQRT(TN2/CNTU)
      ER3=SQRT(TN3/CNTU)
      N21=TN2/TN1
      ER12=N21*SQRT(ER1*ER1/(TN1*TN1)+ER2*ER2/(TN2*TN2))
      CONCU=(B*TN1)/(TN3*WEIGHT)
      U238=7HU-238 =
      U234=7HU-234 =
      U232=7HU-232 =
      CM=3HC/M
      ER=7HERROR =
203  WRITE(6,203)
      FORMAT(1H1)
      WRITE(6,204)TITLE,WEIGHT
04   FORMAT(*SAMPLE NUMBER = *,A10,5X,* SAMPLE WEIGHT = *,F5.1,2X,* GMS
      2*)
      WRITE(6,120)
      WRITE(6,205)U238,TN1,CM,ER,ER1,CM
      WRITE(6,205)U234,TN2,CM,ER,ER2,CM
      WRITE(6,205)U232,TN3,CM,ER,ER3,CM
205  FORMAT(1X,A7,F7.4,2X,A3,5X,A7 ,F5.4,2X,A3)
      WRITE(6,120)
      WRITE(6,127)
      WRITE(6,206)CONCU
206  FORMAT(* URANIUM CONCENTRATION = *,F6.2,2X,* P.P.M.*)
      WRITE(6,207)N12,ER12
07   FORMAT(* U-234/U-238=*,F5.3,6X,* ERROR=*,F5.4)
      GO TO 100
999  STOP
      END
      SUBROUTINE THDATE(NT52,N12,TGS,TN1,TN2)
      REAL NT52,N12,TN1,TN2
      THALF0=9.23E-6
      THALF4=2.79E-6
      RLR=THALF0/(THALF0-THALF4)
      TN=TN2/TN1
10   ERLA=EXP(-THALF0*TGS)
      ERLB=EXP(-(THALF0-THALF4)*TGS)
      FUNC=- (NT52)+(1.0-ERLA)/TN+RLR*(1.0-1.0/TN)*(1.0-ERLB)
      DERIV=THALF0*ERLA/TN+THALF0*(1.0-1.0/TN)*ERLB
      DH=FUNC/DERIV
      TGS=TGS-DH
      IF(ABS(DH/TGS).GT.0.001)GO TO 10
      RETURN
      END
      SUBROUTINE UDATE(N12,RUO,T)
      REAL N12
      THALF4=2.79E-6
      RUO=((N12)-1.0)*EXP(THALF4*T)+1.0
      RETURN
      END

```

EXAMPLE - INPUT

1						
NB1-1B	5000.	793.	1250.	7.32	125.	
4.52	6.66	2.214	0.011	0.256	5.590	185'
0.005	0.051	0.053	0.160	136.5	1.	

EXAMPLE - OUTPUT

SAMPLE NO. = NB1-1B SAMPLE WT. = 125.0 GMS

TH-227/U-232 SPIKE USED

RAW DATA

U COUNT TIME = 793. MIN	TH COUNT TIME = 1250. MIN
U-238 = 4.520 C/M	TH-232 = .011 C/M
U-234 = 6.660 C/M	TH-230 = .256 C/M
U-232 = 2.214 C/M	TH-227 = 5.590 C/M

BACKGROUND AND REAGENT BLANK

	ERROR		ERROR
U-238 = .010	.006 C/M	TH-232 = .007	.005 C/M
U-234 = .058	.021 C/M	TH-230 = .055	.015 C/M
U-232 = .053	1 C/M	TH-227 = .053	1 C/M

CORRECTED DATA

	ERROR		ERROR
U-238 = 4.510	.076 C/M	TH-232 = .004	.005 C/M
U-234 = 6.602	.094 C/M	TH-230 = .201	.019 C/M
U-232 = 2.161	.052 C/M	TH-227 = 8.897	.084 C/M

CORRECTIONS DUE TO BACKGROUND AND REAGENT BLANKS

U-238 = .2 PERCENT	TH-232 = 63.6 PERCENT
U-234 = .9 PERCENT	TH-230 = 21.6 PERCENT
U-232 = 2.4 PERCENT	TH-227 = .9 PERCENT

URANIUM CONCENTRATION	= 2.28	P.P.M.
CHEMICAL YIELD OF URANIUM	= 8.94	PERCENT
CHEMICAL YIELD OF THORIUM	= 5.02	PERCENT
SPIKE RATIO	= 7.320	

MEASURED TH-227 ACTIVITY	= 5.590 C/M
CALCULATED RA-223 ACTIVITY	= .143 C/M
CORRECTED TH-227 ACTIVITY	= 8.897 C/M
COMMON TH-227	= .016 C/M

U-234/U-238 = 1.464	.032	(U-234/U-238)0 = 1.472	.034
TH-230/U-234 = .054	.005	TH-230/TH/232 = 50.1	
THORIUM AGE = 6000.	600.	YEARS	

EXAMPLE - INPUT

NC-1	80000.	1415.	2784.	0.795	300.	40.
14.29	20.00	6.609	0.11	4.264	2.289	
0.009	0.064	0.073		136.5	1.	

EXAMPLE - OUTPUT

SAMPLE NO. = NC-1

SAMPLE WT. = 300.0 GMS

RAW DATA

U COUNT TIME = 1415.	MIN	TH COUNT TIME = 2784.	MIN
U-238 = 14.290	C/M	TH-232 = .110	C/M
U-234 = 20.000	C/M	TH-230 = 4.264	C/M
U-232 = 6.609	C/M	TH-228 = 2.289	C/M

BACKGROUND AND REAGENT BLANK

	ERROR			ERROR	
U-238 = .024	.006	C/M	TH-232 = .014	.005	C/M
U-234 = .086	.021	C/M	TH-230 = .074	.015	C/M
U-232 = .073	I	C/M	TH-228 = .073	I	C/M

CORRECTED DATA

	ERROR			ERROR	
U-238 = 14.266	.101	C/M	TH-232 = .096	.008	C/M
U-234 = 19.914	.121	C/M	TH-230 = 4.190	.041	C/M
U-232 = 6.536	.068	C/M	TH-228 = 2.191	.028	C/M

CORRECTIONS DUE TO BACKGROUND AND REAGENT BLANKS

U-238 = .2 PERCENT	TH-232 = 12.3 PERCENT
U-234 = .4 PERCENT	TH-230 = 1.7 PERCENT
U-232 = 1.1 PERCENT	TH-228 = 3.2 PERCENT

URANIUM CONCENTRATION	= .99	P.P.M.
CHEMICAL YIELD OF URANIUM	= 27.04	PERCENT
CHEMICAL YIELD OF THORIUM	= 11.40	PERCENT
SPIKE RATIO	= .795	

U-234/U-238 = 1.396	.013	(U-234/U-238) ¹⁰ = 1.484	.019
TH-230/U-234 = .499	.010	TH-230/TH-232 = 43.4	
THORIUM AGE = 72100.	2000.	YEARS	

CD TOT 0050